

Bangor University

DOCTOR OF PHILOSOPHY

A molecular study on the adaption and response of plants to windy habitats

Bennett, Rhona Marie

Award date:
2008

Awarding institution:
Bangor University

[Link to publication](#)

General rights

Copyright and moral rights for the publications made accessible in the public portal are retained by the authors and/or other copyright owners and it is a condition of accessing publications that users recognise and abide by the legal requirements associated with these rights.

- Users may download and print one copy of any publication from the public portal for the purpose of private study or research.
- You may not further distribute the material or use it for any profit-making activity or commercial gain
- You may freely distribute the URL identifying the publication in the public portal ?

Take down policy

If you believe that this document breaches copyright please contact us providing details, and we will remove access to the work immediately and investigate your claim.

Download date: 10. Apr. 2024

A Molecular Study on the Adaptation & Response of Plants to Windy Habitats

Rhona Marie Bennett

**A thesis submitted to Bangor University in candidature for the degree
of Doctor of Philosophy**

**Bangor University, Wales
2008**



Abstract

Mechanical stress in plants may be created in nature by wind, rain, and through contact with animals. Wind stressed plants are typically physiologically dwarfed; characteristics include shorter (and often thicker) stems, reduced leaf surface area and changes in leaf angle. Growth responses to other mechanical stresses are similar, with exception to vibration stress, which may promote growth. This study shows that subjecting *Arabidopsis* plants to wind stress under experimental conditions results in the expected dwarfing of plants with respect to an unstressed control. In contrast, subjecting *Arabidopsis* seedlings to vibration stress promotes growth.

RT-PCR was used to look at gene expression in tissues sampled from plants subjected to wind and other mechanical stresses. Candidate wind/mechanical stress genes; genes encoding plant cell wall proteins, genes involved in lignin biosynthesis and those encoding cell signalling pathway intermediates were found to be differentially expressed in plants subjected to these stresses. Transgenic constructs for gene silencing of selected candidate wind/mechanical stress genes by RNA interference (RNAi) were designed with a view to analyzing the role of these genes in the response and adaptation of plants to wind stress. RNAi constructs targeting Expansin 3, Cellulose synthase 3, Touch gene 4, Cinnamoyl CoA reductase 2, and the Cinnamoyl CoA reductase family of *Arabidopsis* were generated. *Arabidopsis* plants were transformed with these constructs; the phenotypes of the resulting transgenic lines and expression of the targeted wind/mechanical stress genes in these lines under mechanical stress are detailed.

Contents

Declaration	i
Abstract	ii
Contents	iii
List of Figures	xiii
List of Tables	xviii
Abbreviations	xx
IUPAC codes	xxi
Acknowledgments	xxii
1. Introduction	1
1.1 Introduction	1
1.2 Defining Wind and Mechanical stresses	2
1.3 Growth and developmental effects of wind stress on plants	2
1.4 Plant Hardening	6
1.5 Mechanoperception	9
1.6 Signal Transduction of plant responses to wind and mechanical stresses	12
1.7 Biophysical properties pertaining to the response and adaptation to wind and mechanical stresses	14
a) Acid-growth & Turgor	15
b) Expansins and Xyloglucan endotransglycosylases	17
c) Plant cell wall proteins	18
d) Secondary growth	19
1.8 The role of plant growth regulators in the response to wind/mechanical stresses	20
1.9 The experimental approach	23
1.10 Aims	25
2. Materials & Methods	26
2.1 General Materials & Methods	26
2.1.1 General chemicals, consumables and equipment	26
2.1.2 Preparation of solutions	27
2.1.3 Commonly used buffers	27

2.1.4 Phenol: Chloroform solutions	27
2.1.5 Growth media and antibiotic supplements	27
2.1.6 Oxidative stress assay solutions	28
2.1.7 RNA extraction buffers	29
2.1.8 Formaldehyde gel solutions	29
2.1.9 Agarose gel electrophoresis	29
2.1.10 Minipreparation of plasmid DNA	30
2.1.11 Southern blotting and hybridization	30
2.1.12 Radioactive labeling of DNA probes	31
2.1.13 Extraction of plant genomic DNA	31
2.2 Plant Materials and Growth Conditions	32
2.2.1 Plant material	32
2.2.2 Propagation of plant material	32
a) Sterilizing <i>A.thaliana</i> seed	32
b) Plate-based germination of <i>A.thaliana</i> seed	33
c) Soil-based growth of <i>A.thaliana</i> seed	33
2.2.3 Phenotypic analysis of <i>Arabidopsis</i> plants	34
a) Plate-based phenotypic analysis of <i>Arabidopsis</i> plants	34
b) Soil-based phenotypic analysis of <i>Arabidopsis</i> plants	34
2.2.4 Subjecting plants to wind and mechanical stresses	37
a) Vibration stress (in seedlings)	37
b) Seismic stress	37
c) Gravity stimulation	37
d) Wind stress	38
e) Thigmic stress	38
f) Vibration stress (in plants)	38
2.3 Oxidative stress assays	39
2.3.1 Detection of hydrogen peroxide by the DAB-uptake method	39
2.3.2 Monitoring Peroxidase activity by use of Guaiacol	39
2.3.3 Monitoring peroxidase activity involved in the lignification process using Syringaldazine	40
2.3.4 Bradford Assay for protein determination	40
2.4 Analysis of Gene Expression	41
2.4.1 RNA Extraction	41

2.4.2 Estimation of RNA concentration	41
2.4.3 Denaturing formaldehyde agarose gel electrophoresis	42
2.4.4 RT-PCR analysis of gene expression	42
2.4.5 Polymerase Chain Reaction	43
2.4.6 Agarose gel electrophoresis	43
2.5 Cloning Techniques	44
2.5.1 Purification of PCR products and DNA	44
2.5.2 Estimation of DNA concentration	44
2.5.3 Extraction of plasmid DNA	45
a) Miniprep of plasmid DNA	45
b) Purification of small amounts of high quality plasmid DNA using Qiagen Qiaprep Mini kit	45
c) Purification of large amounts of high quality plasmid DNA using Qiagen Midi kit	45
2.5.4 Restriction enzyme digests	46
2.5.5 Electroelution & purification of DNA bands from agarose gels	46
2.5.6 Ligation of plasmid and insert DNA	47
2.5.7 Transformation of competent <i>E.coli</i> cells	47
a) Preparation of competent <i>E.coli</i> cells	47
b) Transformation of competent <i>E.coli</i> cells	48
2.5.8 Colony PCR to screen transformants	48
2.5.9 Storage of bacteria as Glycerol stocks	48
2.6 Generation of Transgenic Plants	49
2.6.1 Tri-parental mating of <i>Agrobacterium tumefaciens</i>	49
2.6.2 DNA extraction from <i>Agrobacterium tumefaciens</i>	49
2.6.3 Southern blotting and hybridization to screen transformants	50
a) Capillary transfer of DNA to nylon membranes	50
b) DNA hybridization	52
c) Radioactive labeling of DNA probes	52
d) Imaging	52
2.6.4 <i>Arabidopsis</i> plant transformation by the floral dip method	53
2.6.5 Selection of transgenic <i>Arabidopsis thaliana</i> plants	53
2.6.6. Extraction of plant genomic DNA	54

3. Phenotypic analysis of <i>Arabidopsis</i> plants subjected to	55
Wind and mechanical stresses	
3.1 Introduction	55
3.1.1 Simulating wind/mechanical stresses	55
a) Wind stress	55
b) Vibration stress	56
c) Seismic stress	57
d) Thigmic stress	57
3.1.2 Phenotypic analysis of <i>Arabidopsis</i> plants	58
3.2 Phenotypic analysis of <i>Arabidopsis</i> seedlings subjected to mechanical stresses	59
3.2.1 Vibration stress	59
a) Hypocotyl elongation in seedlings subjected to vibration stress	59
b) Root elongation in seedlings subjected to vibration stress	59
3.2.2 Seismic stress	62
a) Hypocotyl elongation in seedlings subjected to seismic stress	62
b) Root elongation in seedlings subjected to seismic stress	62
3.2.3 Gravity stimulation	62
a) Hypocotyl elongation in seedlings subjected to gravity stimulation	63
b) Root elongation in seedlings subjected to gravity stimulation	63
3.2.4 Discussion	66
3.3 Phenotypic analysis of <i>Arabidopsis</i> plants subjected to wind stress	67
3.4 Phenotypic analysis of <i>Arabidopsis</i> plants subjected to thigmic stress	68
3.5 Phenotypic analysis of <i>Arabidopsis</i> plants subjected to vibration stress	68
3.6 Discussion	73
3.7 Summary	74

4. Oxidative stress in plants subjected to wind and mechanical stresses	75
4.1 Introduction	75
4.1.1. The role of active oxygen species in plant development and defense pathways	75
4.1.2. Evidence for an oxidative burst in response to mechanical stress	76
4.2 The induction of active oxygen species & peroxidase activity in <i>Arabidopsis</i> seedlings subjected to vibration stress	77
a) Localization of H ₂ O ₂ synthesis in seedlings subjected to vibration stress	78
b) Soluble peroxidase activity in seedlings subjected to vibration stress	78
c) Lignin pathway specific soluble peroxidase activity in seedlings subjected to vibration stress	78
d) Discussion	78
4.3 The induction of active oxygen species & peroxidase activity in <i>Arabidopsis</i> plants subjected to wind stress	81
a) Localization of H ₂ O ₂ synthesis in plants subjected to wind stress	82
b) Soluble peroxidase activity in plants subjected to wind stress	82
c) Lignin pathway specific soluble peroxidase activity in plants subjected to wind stress	82
d) Discussion	83
4.4 Monitoring of active oxygen species in <i>Arabidopsis</i> plants subjected to vibration stress	86
a) Localization of H ₂ O ₂ synthesis in plants subjected to vibration stress	86
b) Soluble peroxidase activity in plants subjected to vibration stress	86
c) Lignin pathway specific soluble peroxidase activity in plants subjected to vibration stress	87
d) Discussion	87
4.5 Summary	89
5. Expression of candidate wind/mechanical stress genes in plants subjected to wind and mechanical stresses	90
5.1 Introduction	90
5.2 Candidate wind/mechanical stress genes	90
5.2.1 Expansin (EXP3)	91

5.2.2 Phenylalanine ammonia lyase (PAL1) and Cinnamoyl coenzyme A reductase (CCR2)	91
5.2.3 Cellulose synthase (CESA 3)	91
5.2.4 Arabinogalactan protein (AGP 3)	92
5.2.5 Glycine rich protein 6 (GRP6)	92
5.3 RT-PCR primers for candidate wind/ mechanical stress genes	94
5.4 Analysis of gene expression of candidate wind/mechanical stress genes in <i>Arabidopsis</i> seedlings & plants	96
5.4.1 Analysis of gene expression of candidate wind/mechanical stress genes in seedlings subjected to vibration stress	96
5.4.2 Analysis of gene expression of candidate wind/mechanical stress genes in plants subjected to wind stress	101
5.4.3 Summary of gene expression	105
5.5 Identification of common regulatory elements in the promoters of co-expressed genes	107
5.5.1 Detection of common motifs in the promoters of co-expressed genes	107
5.5.2 Characterization of promoter motifs found in co expressed genes	108
5.6 Summary	114
6. Expression of the extensin EXT1 gene in plants subjected to wind and mechanical stresses	115
6.1 Introduction	115
6.1.1 Synthesis of extensins	115
6.1.2 The <i>Arabidopsis</i> EXT1 gene: developmental regulation and induction by mechanical stresses	116
a) Expression of EXT1 during development	116
b) Expression of EXT1 in response to mechanical stress	116
6.1.3 Phenotypic changes in a transgenic <i>Arabidopsis</i> line over-expressing the EXT1 gene	117
6.2 Expression of EXT1 in wild-type seedlings and plants subjected to wind and other mechanical stresses	118
6.2.1 Analysis of EXT1 expression in seedlings subjected to vibration stress	119

6.2.2	Analysis of EXT1 expression in plants subjected to wind stress	120
6.2.3	Discussion	121
a)	Up-regulation of expression in seedlings subjected to vibration stress immediately after the cessation of stress	121
b)	EXT1 expression is not induced in the rosette leaves or inflorescence stems of <i>Arabidopsis</i> plants subjected to wind stress	121
6.3	Analysis of the <i>cis</i> promoter region of the EXT1 gene	122
6.4	Analysis of CaMV: atEXT1, over-expressing extensin subjected to wind and mechanical stresses	125
6.4.1	Phenotypic analysis of CaMV: atEXT1 seedlings subjected to vibration stress	125
a)	Root elongation in extensin over-expressing seedlings subjected to vibration stress	125
b)	Hypocotyl elongation in extensin over-expressing seedlings subjected to vibration stress	125
6.4.2	Phenotypic analysis of CaMV: atEXT1 transgenic plants over-expressing extensin subjected to wind stress	127
6.4.3	Discussion	129
a)	Root elongation of CaMV: atEXT1 seedlings is inhibited even under limited mechanical stress	129
b)	Over-expression of EXT1 limits the promotion of hypocotyl elongation that is induced by vibration stress	129
c)	Phenotype of plants over-expressing EXT1 subjected to wind stress	130
6.5	Summary	131
7.	RNA interference strategy	132
7.1	Introduction	132
7.1.1	Considerations for successful gene silencing by RNAi in plants	132
7.1.2	Generic vectors for Gene silencing by RNAi in plants	133
7.1.3	Estimation of off-target silencing during RNAi	134
7.2	Strategy for silencing of candidate wind stress genes using RNAi	135
7.2.1	Construct design	135

7.2.2 General cloning strategy	138
7.2.3 Generating PCR fragments for candidate wind stress genes with cohesive ends	138
7.2.4 Sub-cloning PCR fragments from candidate wind stress genes into pBluescriptIISK (pSKII)	142
7.2.5 Cloning of fragments into the RNAi vector in the sense and antisense orientations.	143
7.2.6 Cloning EcoRI fragment from RNAi + Sense + Antisense vector into the binary vector pBIN19	149
7.2.7 Transformation of <i>Agrobacterium tumefaciens</i> with the binary construct	152
7.2.8 Transformation of <i>Arabidopsis</i> plants	152
7.3 Summary	155
8. Phenotypic and gene expression analyses of RNAi transgenic lines subjected to mechanical stress	156
8.1 Introduction	156
8.2 Strategy for identification of transgenic lines	156
8.3 TCH4 RNAi transgenic lines	161
8.3.1 T ₁ generation TCH4 RNAi transgenic lines	161
a) Selection of T ₁ transgenic seedlings on media supplemented with Kanamycin	161
b) Phenotypic analysis of T ₁ generation	161
c) Assaying genomic DNA from T ₁ transgenic plants for the presence of an intact transgene	162
8.3.2 T ₂ generation TCH4 RNAi transgenic lines	164
a) Selection of T ₂ transgenic seedlings on media supplemented with Kanamycin	164
b) Gene expression analysis of transgenic lines by RT-PCR	164
c) Phenotypic analysis of T ₂ seedlings subjected to vibration stress	166

8.4	Expansin 3 RNAi transgenics	167
8.4.1	T ₁ generation of EXP3 RNAi transgenic lines	167
	a) Selection of T ₁ transgenic seedlings on media supplemented with Kanamycin	167
	b) Phenotypic analysis of T ₁ generation	167
	c) Assaying genomic DNA from T ₁ plants for the presence of an intact transgene	169
8.4.2	T ₂ generation of EXP3 RNAi transgenic lines	171
	a) Selection of T ₂ transgenic seedlings on media supplemented with Kanamycin	171
	b) Gene expression analysis of transgenic lines by RT-PCR	171
	c) Phenotypic analysis of T ₂ seedlings subjected to vibration stress	173
8.5	CCR2 and CCR family RNAi transgenics	174
8.5.1	T ₁ generation of CCR family (CCRF) RNAi transgenic lines	174
8.5.2	T ₁ generation of CCR2 RNAi transgenic lines	175
	a) Selection of T ₁ transgenic seedlings on media supplemented with Kanamycin	175
	b) Phenotypic analysis of T ₁ generation	175
	c) Assaying genomic DNA from T ₁ plants for the presence of an intact transgene	175
8.6	CESA 3 RNAi transgenics	177
8.7	Discussion	177
	a) Transformation efficiency using the simplified floral-dip method	177
	b) Plants from the first transgenic generation showed altered phenotypes	178
	c) Gene expression of T ₂ transgenic lines subjected to vibration stress	178
8.8	Summary	180

9. Concluding remarks and Future work	181
9.1 Phenotypic analysis of <i>Arabidopsis</i> plants subjected to wind/mechanical stresses	181
9.2 Generation of active oxygen species in <i>Arabidopsis</i> plants subjected to wind stress	181
9.3 Expression of candidate wind/mechanical stress genes in plants subjected to wind and mechanical stresses	182
9.4 Silencing of expression of candidate wind/mechanical stress genes	183
 Appendix A: Data from assays for the detection of soluble peroxidase activity.	 185
Appendix B: Characterization of the gene sequences for each candidate wind/mechanical stress gene.	189
Appendix C: Candidate gene fragments amplified for generation of the RNAi constructs.	200
Appendix D: Efficient siRNAs predicted by siRNA Scan for the final RNAi constructs.	205
 References	 210

List of Figures

Figure 1.1: Thigmonastic responses of the Venus fly-trap.	8
Figure 1.2: Prospective models for perception of mechanical stresses.	11
Figure 1.3: The cell wall and processes involved in cell growth.	16
Figure 2.1: Blotting apparatus for capillary transfer of DNA to nylon membranes.	51
Figure 3.1: Growth stages where vibration stress was applied.	58
Figure 3.2: Hypocotyl elongation at 14-days old of <i>Arabidopsis</i> Col seedlings subjected to vibration stress.	60
Figure 3.3: Hypocotyl elongation at 14-days old of <i>Arabidopsis</i> Ws seedlings subjected to vibration stress.	60
Figure 3.4: Hypocotyl elongation at 14-days old of <i>Arabidopsis</i> Col seedlings subjected to increasing intensities of vibration stress.	61
Figure 3.5: Root elongation at 14-days old of <i>Arabidopsis</i> Ws seedlings subjected to vibration stress.	61
Figure 3.6: Hypocotyl elongation at 14-days old of <i>Arabidopsis</i> Col seedlings subjected to seismic stress.	64
Figure 3.7: Root elongation at 14-days old of <i>Arabidopsis</i> Col seedlings subjected to seismic stress.	64
Figure 3.8: Hypocotyl elongation at 14-days old of <i>Arabidopsis</i> Ws seedlings subjected to gravity stimulation.	65
Figure 3.9: Root elongation at 14-days old of <i>Arabidopsis</i> Ws seedlings subjected to gravity stimulation.	65
Figure 3.10: Comparison of hypocotyl elongation at 14-days old in <i>Arabidopsis</i> Ws seedlings subjected to mechanical stresses.	66
Figure 3.11: Phenotypic analysis of <i>Arabidopsis</i> Col plants subjected to wind stress.	69
Figure 3.12: Phenotypic analysis of <i>Arabidopsis</i> Ws plants subjected to wind stress.	70
Figure 3.13: Phenotypic analysis of <i>Arabidopsis</i> Col plants subjected to thigmic stress.	71

Figure 3.14: Phenotypic analysis of <i>Arabidopsis</i> Ws plants subjected to vibration stress.	72
Figure 4.1: Soluble peroxidase activity in seedlings subjected to vibration stress.	80
Figure 4.2: Detection of Hydrogen peroxide in wind and mechanically stressed plants as determined by the DAB-uptake method.	84
Figure 4.3: Soluble peroxidase activity in the rosette leaves of wind stressed plants.	85
Figure 4.4: Soluble peroxidase activity in the rosette leaves of vibrated plants.	88
Figure 5.1: Expression of candidate wind stress genes immediately after cessation of stress in seedlings subjected to vibration stress.	99
Figure 5.2: Expression of candidate wind stress genes at 14-days in seedlings subjected to vibration stress.	100
Figure 5.3: Expression of candidate wind stress genes in the rosette leaves of plants subjected to wind stress.	103
Figure 5.4: Expression of candidate wind stress genes in the inflorescence stems of plants subjected to wind stress.	104
Figure 5.5: Hierarchical cluster analysis of gene expression ratios of mechanically stressed seedlings/plants versus unstressed seedlings/plants.	106
Figure 5.6: Distribution of selected binding motifs in the <i>Cis</i> regulatory regions of candidate wind/mechanical stress genes.	113
Figure 6.1: Expression of EXT1 in seedlings subjected to vibration stress.	119
Figure 6.2: Expression of EXT1 in plants subjected to wind stress.	120
Figure 6.3: Distribution of selected binding motifs in the <i>Cis</i> promoter region of EXT1.	124
Figure 6.4: Development of CaMV: atEXT1 seedlings subjected to vibration stress.	126
Figure 6.5: Phenotypic analysis of CaMV: atEXT1 plants subjected to wind stress.	128
Figure 7.1: Linear plasmid map of pRNAi vector showing restriction sites used for directional cloning of sequence specific fragments.	134
Figure 7.2: Number of efficient siRNAs predicted by siRNA Scan for each hpRNA construct.	137
Figure 7.3: General cloning strategy for generation of a RNA interference construct.	139

Figure 7.4: PCR fragments generated for each of the candidate wind stress genes to be cloned.	141
Figure 7.5: Restriction map of pBluescript II SK (PSKII).	142
Figure 7.6a: Diagram showing the gene specific fragment inserted in the sense orientation.	143
Figure 7.6b: Example of gene specific fragment (CCR2) ligated to the RNAi vector in the sense orientation.	144
Figure 7.7: Cloning of sense fragments into the pRNAi vector.	145
Figure 7.8a: Diagram showing the gene specific fragment inserted in the antisense orientation.	146
Figure 7.8b: Example of gene specific fragment (CCR2) ligated to the RNAi vector in the antisense orientation.	147
Figure 7.9: Cloning of antisense fragments into pRNAi vector.	148
Figure 7.10: EcoRI fragments released from RNAi vectors.	149
Figure 7.11: Binary vector pBIN19.	150
Figure 7.12: Cloning of the EcoRI fragment from the RNAi vector into the binary vector pBIN19.	151
Figure 7.13: Transformation of <i>Agrobacterium tumefaciens</i> .	153
Figure 7.14: EcoRI fragment from empty RNAi vector that was used as a radiolabelled probe.	154
Figure 7.15: Transformation of <i>Agrobacterium tumefaciens</i> with the CESA3 RNAi construct.	154
Figure 8.1: Region amplified to check the intactness of the transgene.	159
Figure 8.2: Phenotype of <i>Arabidopsis</i> RNAi: TCH4 T ₁ plants.	162
Figure 8.3: Verification of the presence of the transgene in RNAi: TCH4 transgenic lines.	163
Figure 8.4: Verification of the intactness of the transgene in RNAi: TCH4 Transgenic lines.	163
Figure 8.5: Gene expression in RNAi: TCH4 transgenic seedlings subjected to vibration stress.	165
Figure 8.6: Hypocotyl elongation at 14-days old of RNAi: TCH4 transgenic seedlings subjected to vibration stress.	166
Figure 8.7: Phenotype of RNAi: EXP3 T ₁ plants.	168

Figure 8.8: Verification of the presence of the transgene in RNAi: EXP3 transgenic lines.	169
Figure 8.9: Verification of the intactness of the transgene in RNAi: EXP3 Transgenic lines.	170
Figure 8.10: Gene expression in RNAi: EXP3 transgenic seedlings subjected to vibration stress.	172
Figure 8.11: Hypocotyl elongation at 14-days old of RNAi: EXP3 transgenic seedlings subjected to vibration stress.	173
Figure 8.12: Phenotype of RNAi: CCRF T ₁ plant from 4 to 6 weeks after germination.	174
Figure 8.13: Phenotype of RNAi: CCR2 T ₁ plants.	176
Figure 8.14: Evidence for the presence of the transgene in RNAi: CCR2 transgenic lines.	176
Figure A1: Protein standard curve.	185
Figure B1: TCH3 gene sequence; calmodulin-related protein.	189
Figure B2: CCR2 gene sequence; putative cinnamoyl-CoA reductase.	190
Figure B3: TCH4/XTH22 gene sequence; Xyloglucan endotransglycosylase.	191
Figure B4: CESA3 gene sequence; cellulose synthase catalytic subunit.	193
Figure B5: GRP6 gene sequence; glycine-rich protein.	194
Figure B6: EXP3 gene sequence; putative expansin.	195
Figure B7: AGP3 gene sequence; arabinogalactan protein.	196
Figure B8: PAL1 gene sequence; phenylalanine ammonia lyase.	197
Figure B9: MEK1 gene sequence; protein kinase, homologue of MAP kinase Kinase.	198
Figure B.10: EXT1 gene sequence; extensin.	199
Figure C1: Fragment used for generation of an RNAi construct targeting cinnamoyl CoA reductase 2.	200
Figure C2: Fragment used for generation of an RNAi construct targeting touch gene 4.	201
Figure C3: Fragment used for generation of an RNAi construct targeting expansin 3.	202
Figure C4: Fragment used for generation of an RNAi construct targeting cellulose synthase 3.	203

Figure C5: Fragment used for generation of an RNAi construct targeting the cinnamyl CoA reductase family.	204
Figure D1: Efficient siRNAs predicted by siRNA Scan for the CCR2 construct.	205
Figure D2: Efficient siRNAs predicted by siRNA Scan for the CCRF construct.	206
Figure D3: Efficient siRNAs predicted by siRNA Scan for the TCH4 construct.	207
Figure D4: Efficient siRNAs predicted by siRNA Scan for the CESA3 construct.	208
Figure D5: Efficient siRNAs predicted by siRNA Scan for the EXP3 construct.	209

List of Tables

Table 1.1:	Phenotypic responses to wind and other mechanical stresses.	4
Table 2.1a:	Growth stages for the plate-based phenotypic analysis.	35
Table 2.1b:	Measurements taken during the plate-based phenotypic analysis.	35
Table 2.2a:	Growth stages for the soil-based phenotypic analysis.	36
Table 2.2b:	Measurements taken during the soil-based phenotypic analysis.	36
Table 5.1:	Details of selected candidate wind/mechanical stress genes.	93
Table 5.2:	RT-PCR primers based on candidate wind/ mechanical stress genes.	95
Table 5.3:	Designation of motifs generated by MotifSampler.	109
Table 5.4:	Frequency of binding motifs associated with transcription factors involved in plant defence found in the promoters of candidate wind/mechanical stress genes.	112
Table 6.1:	RT-PCR primers based on EXT1 and RT-PCR controls.	118
Table 6.2:	Frequency of binding motifs associated with transcription factors involved in plant defence found in the EXT1 promoter.	124
Table 7.1:	Details for each sequence specific fragment generated by PCR.	136
Table 7.2:	Predicted off-targets for each construct as determined by the siRNA Scan database.	137
Table 7.3:	Primers used for amplification of PCR fragments with additional restrictions sites to aid cloning.	140
Table 7.4:	Primer pairs used for colony PCR of pRNAi + Sense insert constructs.	144
Table 7.5:	Primer pairs used for colony PCR of pRNAi + Sense insert + Antisense insert constructs	147
Table 8.1:	Definition of the transgenic generations used in this study.	158
Table 8.2:	Primers used to check the intactness of the transgene.	159
Table 8.3:	Primers used to check whether the transgene is expressed in transgenic lines.	160
Table 8.4:	Kanamycin resistance of RNAi: TCH4 T ₂ seedlings.	164
Table 8.5:	Kanamycin resistance of RNAi: EXP3 T ₂ seedlings.	171
Table A1:	Guaiacol assay data for <i>Arabidopsis</i> seedlings subjected to vibration stress.	186

Table A2:	Guaiacol assay data for <i>Arabidopsis</i> plants subjected to wind and mechanical stresses.	186
Table A3:	Syringaldazine assay data for <i>Arabidopsis</i> seedlings subjected to vibration stress.	188
Table A4:	Syringaldazine assay data for <i>Arabidopsis</i> plants subjected to wind and mechanical stresses.	188
Table D1:	List of efficient siRNAs predicted by siRNA Scan for the CCR2 construct.	205
Table D2:	List of efficient siRNAs predicted by siRNA Scan for the CCRF construct.	206
Table D3:	List of efficient siRNAs predicted by siRNA Scan for the TCH4 construct.	207
Table D4:	List of efficient siRNAs predicted by siRNA Scan for the CESA3 construct.	208
Table D5:	List of efficient siRNAs predicted by siRNA Scan for the EXP3 construct.	209

Abbreviations

A₆₀₀: Absorbance at 600nm
AOS: Active oxygen species
cDNA: complementary DNA
Col: *Arabidopsis* ecotype Columbia
dH₂O: distilled water
DAB: diaminobenzadine
DEPC: diethyl pyrocarbonate
DNA: deoxyribonucleic acid
IAA: isoamyl alcohol
IMS: industrial methylated spirit
LB: Luria-Bertani media
MOPS: 3-(N-morpholino) propanesulphonic acid
mRNA: messenger RNA
MS: Murashige & Skoog media
m/s: meters per second
NCBI: National center for Biotechnology Information
NO: Nitric oxide
OD₆₀₀: Optical density
PCR: Polymerase chain reaction
RNA: Ribonucleic acid
RNAi: RNA interference
RT: Reverse transcription
SA: salicylic acid
SD: standard deviation
TBE: Tris-borate (buffer)
TE: TRIS-EDTA (buffer)
UV: Ultra violet light
Ws: *Arabidopsis* ecotype Wassilewskija

IUPAC codes

Where any nucleotide ambiguity is noted in the text, the International Union of Pure and Applied Chemistry (IUPAC) codes are used.

A = Adenine

C = Cytosine

G = Guanine

T = Thymine

U = Uracil

B = C, G or T/U

D = A, G or T/U

H = A, C or T/U

V = A, C or G

R = A or G (purines)

Y = C or T (pyrimidines)

K = A or T/U

M = A or C

S = G or C

W = A or T/U

N = Any nucleotide

Acknowledgements

I would like to gratefully acknowledge the support of the following people throughout my doctoral research.

To Dr Anil Shirsat who has offered me advice when it was most needed, and read this thesis, giving me constructive feedback. Thanks also to Dr Mark Hooks and Prof. Deri Tomos, who have promoted the development of plant physiology and molecular biology in the department where I did my research. Also to other members of staff in the School of Biological Sciences whose help has been invaluable; Andrew Davies, Barry Grail, Wendy Grail, Debbie Henderson, Cath Kay and Gwyn Morris.

My thanks to the Natural Environmental Research Council who funded this project and my studentship.

I would particularly like to acknowledge the support of the 'Woman in Science' group, especially Liz Allen, Alessa Jaendling, Sarah Nicholl and Guo Wei. Thanks for sharing problems in the lab, and going for a coffee (or a glass of wine) whenever it was needed. I wish you all the best of luck for the future. Thank you to Jane Lee for keeping me company on the train to Bangor every day. I would also like to apologize to my friends outside of science for being so elusive over the last few years.

Many, many thanks to my long-suffering family: Mum & Dad, Paul & Sandra, Derek & Cathy and the Sayce clan; who have given me your unfailing support, as always.

Finally, to my husband Neil, who has been my most loyal supporter, and has always encouraged me, even when this has caused us to spend so much time apart.

Should auld acquaintance be forgot, And never brought to mind?

Should auld acquaintance be forgot, And days o' lang syne?

Robert Burns

1. INTRODUCTION

1.1 Introduction

Mechanical stress in plants may be stimulated in the natural environment by wind, rain, hail and through contact with animals. These stresses commonly result in the development of shorter stems, reduced leaf area and changes in leaf angle (Jones, 1997). In many cases stems also become thicker. The combination of these morphological changes results in a reduction of the plant surface area exposed to wind. Although plants subjected to wind stress are typically shorter and stockier, they can also be hardened against other stresses.

The impacts of wind on plant growth and development are likely to be heightened as a result of rising wind speeds, which are predicted as a result of rapid climate change. Furthermore, the increasing duration of chronic winds and frequency of extreme wind events such as hurricanes will present a challenge to those growing plants in the field. Previous studies on the response of trees to extreme winds show that damage increases linearly with wind exposure (Foster & Boose, 1992). During extreme conditions such as a hurricane there is a high frequency of stem breakage; in a study over a quarter of all trees surveyed were severely damaged by a hurricane and 9% died (Zimmerman, 1994).

Relatively few studies have considered the effect of wind stress on plants compared to other environmental stresses. The main reason for this is the apparent difficulty in separating the effects of wind stress from other factors in the field (Ennos, 1997). In addition to the intrinsic value of wind/mechanical stress studies, growers may need to make changes to their existing practices to avoid some impacts of mechanical stress such as lodging. Paradoxically, subjecting plants to wind or mechanical stresses under controlled conditions can be used to promote plant hardening. Optimizing conditions for hardening via exposure to mechanical stress may have wide ranging applications in agriculture, horticulture and forestry. Finally, in the specialized area of space biology; mechanical stress will probably have an influence on the growth of plants on spacecraft. Plants may be more susceptible to mechanical stress in space than on earth as plants developing in space, where there is little force of gravity are likely to be

deficient in cell wall support material such as lignin and cellulose (Mitchell & Myers, 1995). Furthermore, plants would be subjected to intense vibration stress on take-off and more persistent vibration stress or 'g-jitter' onboard a spacecraft (Mitchell & Myers, 1995).

1.2 Defining Wind and Mechanical stresses

Mechanical stress is defined as continuous shaking, rubbing, bending, twisting and vibration of plants (Jones, 1997). Thigmomorphogenesis has been defined as the response to mechanical perturbation (Biro & Jaffe, 1984). More specifically, thigmic stress is simulated by bending, flexing or rubbing tissues, which all involve contact with tissues of the plant. In comparison, seismic stress refers to a shaking stimulus resulting in seismomorphogenesis. Seismic stress may be applied through shaking to and fro in a horizontal plane in a gyratory shaker, or shaking around on the horizontal plane in a rotary shaker. As a rule, seismic stress is applied to the whole plant and thigmic stress is a brief exposure applied to one or more tissues of the plant, but not to the whole plant (Mitchell & Myers, 1995). Vibromorphogenesis is growth induced by vibration stress (Jones, 1997). Vibration stress and seismic stress are similar; apparently they only differ by the frequency of the stimulus.

1.3 Growth and developmental effects of wind stress on plants

The shorter and stockier growth habit of plants grown in windy habitats is demonstrated by the observation that the shortest stalks of maize (*Zea mays*) in a field are usually found on the windward edge (Mitchell & Myers, 1995). A similar growth response may be observed in trees in exposed coastal and mountainous regions, where species are physiologically dwarfed. Such species grow leaning away from the wind and most of their branches develop on their leeward side (Mitchell & Myers, 1995). Thus the phenotypic changes observed in herbaceous plants in response to wind stress are comparable to those observed in woody species. In addition, wind specifically causes lodging, leaf stripping, sandblasting, leaf tearing and abrasion of plants *in situ* (Cleugh *et al*, 1998).

In woody species wind exposure may cause the formation of reaction wood; compression wood in gymnosperms and tension wood in angiosperms (Timell, 1986). Wind stress may cause flexing/bending of stems and branches. Formation of compression wood on the lower side of a branch or stem allows it to recover to its original orientation. Reaction wood is formed in the xylem tissue in response to wind (Plomion *et al*, 2000). Furthermore, due to the effect of wind, almost all conifers have some compression wood (Timell, 1986). There is more lignin and less cellulose in compression wood than in normal wood. Phenylalanine ammonia lyase and other lignin pathway genes are upregulated in compression wood (Plomion *et al*, 2000). Conversely, in tension wood there is more cellulose and less lignin than in normal wood (Timell, 1986). Cellulose synthase A (PtCesA) is a gene from the angiosperm tree *Populus tremuloides*. Stems of transgenic *Populus* plants with a PtCesA-GUS construct were flexed to create tension stress (Wu *et al*, 2000); this induced phloem-specific GUS expression but not xylem-specific expression. After 20 hours of flexing, GUS expression was seen in both xylem and phloem from the stressed section of the stem. On the opposite side to the mechanically stressed section of the stem there was no PtCesA-GUS expression. This indicates PtCesA is associated with cellulose synthesis in xylem cells during normal development, and is induced in phloem (and xylem) in response to repeated mechanical stress, thus providing greater tensile strength.

With the exception of vibration, the physiological responses to other mechanical stresses are similar to wind stress, as outlined in Table 1.1. Thigmic stresses and seismic stresses have been found to lead to the overall dwarfing of plants when compared to unstressed plants. Vibration stress has been shown to promote hypocotyl, shoot and root growth in specific species (Takahashi *et al*, 1991, Johnson *et al*, 1998). Relatively few studies have considered the effects of wind and mechanical stresses on photosynthesis, respiration and transpiration. Existing studies suggest there is variation between species. Kraus *et al* (1994) found that a fast-respiring and low-yielding population (GL66) of perennial ryegrass (*Lolium perenne*) was more susceptible to mechanical stress than a slow-respiring and high-yielding population (GL72) in terms of thigmomorphogenesis. Thigmic stress did not result in a change in photosynthesis. There was a transient increase in respiration in the slow-respiring population but a decrease in the high-respiring population. Transpiration was

increased in response to thigmic stress in the slow-respiring population under light conditions but not under darkness. Conversely, transpiration was decreased in the fast-respiring population under dark but not light conditions. GL66 (fast respiring/low yielding) may have some advantage in dry conditions.

Table 1.1: Phenotypic responses to wind and other mechanical stresses.

Stress	Stimulus	Response <i>compared to unstressed control</i>	Plant species (Latin)	Reference
Wind	Wind	Thicker trunk, shorter/thicker branches	<i>Didymopanax pittieri</i>	Lawton (1982)
		Reduced stem length, leaf area and biomass	<i>Sinapis alba</i>	Retuerto & Woodward (1992)
		Reduced stem length	<i>Arabidopsis thaliana</i>	Johnson <i>et al</i> (1998)
			<i>Cucumis sativus</i>	Moran & Cipollini (1999)
		Greater number of stem branches	<i>Arabidopsis thaliana</i>	Pigliucci (2002)
Seismic	Shaking	Dwarfing	<i>Lycopersicon</i>	Mitchell <i>et al</i> (1975)
		Dwarfing	<i>Chrysanthemum</i>	Beyl & Mitchell (1977)
		Inhibition of shoot growth	<i>Lycopersicon</i>	Heuchert & Mitchell (1983)
		Dwarfing	<i>Helianthus annuus</i>	Beyl & Mitchell (1983)
		Reduced stem height, leaf expansion & biomass	<i>Glycine max</i>	Jones <i>et al</i> (1990)
		Reduced seed dry weight	<i>Glycine max</i>	Jones & Mitchell (1992)
Vibric	Vibration	Promotion of shoot & root growth	<i>Cucumis sativus</i> <i>Oryza</i>	Takahashi <i>et al</i> (1991)
		Promotion of hypocotyls elongation	<i>Arabidopsis thaliana</i>	Johnson <i>et al</i> (1998)

Stress	Stimulus	Response <i>compared to unstressed control</i>	Plant species	Reference
Thigmic	Rubbing internode	Reduced elongation of internodes	<i>Phaseolus vulgaris</i>	Erner <i>et al</i> (1980)
	Rubbing leaves	Leaf senescence	<i>Avena sativa</i>	Giridhar & Jaffe (1988)
	Brushing	Reduced plant height	<i>Lycopersicon esculentum</i> <i>Phaseolus vulgaris</i> <i>Solanum melongena</i> <i>Cucumis sativus</i> <i>Cucurbita pepo</i> <i>Brassica oleracea</i>	Baden & Latimer (1992)
	Brushing	Shorter plants & a reduction in leaf dry weight	<i>Lycopersicon esculentum</i>	Keller & Steffen (1995)
	Brushing	Shorter, thicker stems	<i>Brassica napus</i>	Cipollini (1999)
	Flexing stem	Increased radial growth	<i>Populus sp.</i>	Pruyn <i>et al</i> (2000)
	Flexing	More numerous, thicker roots	<i>Zea mays</i>	Goodman & Ennos (2001)
	Brushing	Dwarfing	<i>Arabidopsis thaliana</i>	Montgomery <i>et al</i> (2004)

1.4 Plant Hardening

Various hardening factors co-exist with wind in the natural environment, for example temperature extremes and drought. The sensitivity of unhardened plants is a problem in horticulture and agriculture. Mechanical stress induces physiological changes which are part of the natural hardening process that plants face when they are transferred to field conditions. Prior exposure to wind or mechanical stresses may confer a level of hardening to plants. Exposure to wind/mechanical stress can harden the stems of plants and improve resistance to lodging; which is characterised by the uprooting of trees and the buckling of stems in cereals (Jones, 1997). Furthermore, adaptation to mechanical stress is important for annual plants growing in habitats where wind intensity fluctuates within a given season (Cipollini, 1999).

In addition, it has been proposed that exposure to mechanical stress can also enhance resistance to other abiotic and biotic stresses. Brushing has been shown to increase cold tolerance in tomato (Keller & Steffen, 1995). Tomato plants are sensitive to chilling; during acclimatization to cold, non-structural carbohydrates increase. Accumulation of soluble sugars was enhanced in brushed plants that were subsequently exposed to cold stress. The authors suggest that this is due to the brushed plants maintaining a higher level of photosynthetic activity compared to plants that were not mechanically stressed. Increased levels of soluble sugars under cold stress may be an adaptation induced by mechanical stress. Brushing has also been shown to increase cold tolerance in other species such as beans and maize (Jaffe & Biro, 1979).

Exposure to wind stress/stimulation may also impact the resistance of plants to pathogens. A number of authors have shown a correlation between accelerated lignification as a result of mechanical stress and disease resistance (De Jaegher *et al*, 1985, Cipollini, 1997). Cipollini (1997) investigated whether exposure to wind increases pest resistance in bean plants. They found that exposure to wind was linked with resistance to an arthropod herbivore and a fungal pathogen. Furthermore, it was found that resistance was associated with enhanced lignification: peroxidase activity and lignin content in the leaves of wind-stressed plants were greater than in unstressed plants subjected to these pathogens. In an independent study, repeated exposure to

wind stress was shown to enhance resistance of cucumber plants to melon aphids and to fungal infection with *Cladosporium cucumerinum* (Moran & Cipollini, 1999).

Potentially growers could manipulate wind and mechanical stresses to improve pathogen resistance in un-hardened plants. Greenhouse-grown tomato plants are more susceptible to mechanical stress during the winter months than in summer months (Mitchell & Myers, 1995). However, if the intensity of mechanical stress is increased during the summer, a dwarfed phenotype can be induced. Obviously during the summer months the days are warmer and there are more hours of sunshine and the days are cooler and there are fewer hours of sunshine in winter. Montgomery *et al* (2004) have investigated the relationship between temperature, levels of irradiance and mechanical stress resulting in the dwarfing of *Arabidopsis* seedlings. Hypocotyl elongation increased with daily temperatures in the range of 22-28°C, but sensitivity to mechanical stress declined. Although the effect of day length was not significant *per se*, increasing daylength and photosynthetic photon flux (PPF) under experimental conditions led to decreased sensitivity to brushing (thigmic stress). The authors suggest that the optimal conditions for dwarfing of *Arabidopsis* are low PPF lighting at 55 to 60 $\mu\text{mol m}^{-2}\text{s}^{-1}$, 22°C to 25°C and a brushing treatment twice daily (Montgomery *et al*, 2004).

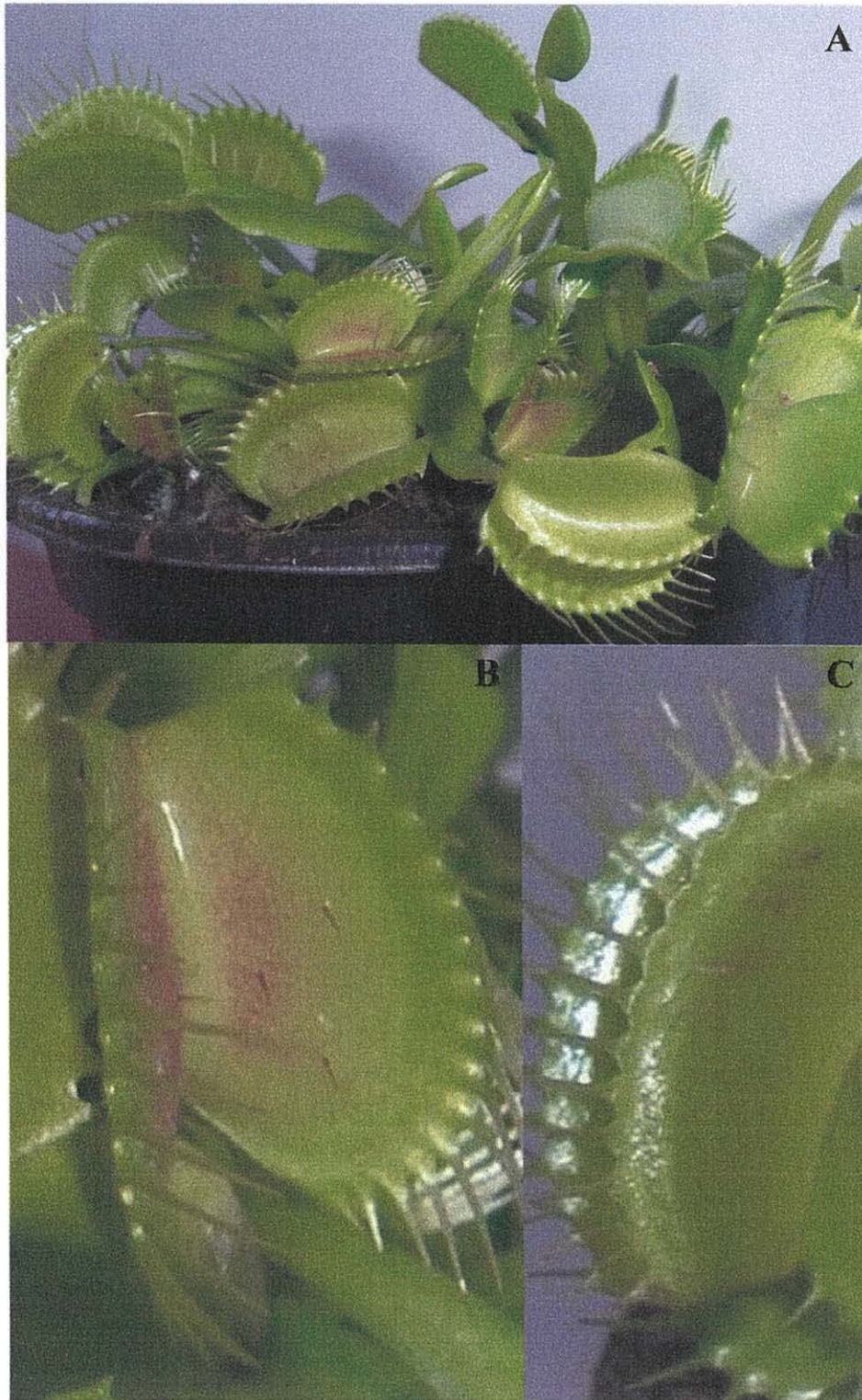


Figure 1.1: Thigmonastic responses of the Venus fly-trap.

A. Venus fly-trap (*Dionaea muscipula*) **B.** Close-up view of the trap showing the leaf hairs. **C.** A closed trap; entrapping a fly.

1.5 Mechanoperception

The extraordinary capacity of plants to perceive and respond to mechanical stress can be seen in species such as *Dionaea muscipula*, *Drosera rotundifolia*, *Mimosa pudica*, and members of the Bladderwort family (*Utricularia*). *Dionaea muscipula*, which is commonly known as the Venus fly-trap (Figure 1.1) shows an impressive thigmonastic response. Insects landing on the leaves of this plant trigger small hairs, generating electrical signals that lead to the closure of the trap. The plant subsequently uses its prey as a source of nitrogen which is advantageous in environments where nitrogen is limited (Braam, 2005). Sundew (*Drosera rotundifolia*) was studied extensively by Charles Darwin (1893) - it is so-called because its leaf hairs exude a dew-like substance which glistens in the sunlight. This dew-like substance is also attractive to insects that fly in to it; the leaf hairs then bend over, trapping the insect. Although Sundew is highly sensitive to the thigmic stimuli induced by insects, it is not triggered by rain showers in the same way (Braam, 2005). This suggests that the plant can distinguish between these mechanical stimuli.

Thigmonastic responses are likely to share common mechanisms with those of other mechanical stimuli, although they are likely to occur more quickly (Mitchell & Myers, 1995). Indeed, the rise time for a bioelectrical potential in response to thigmic stress is ~25 seconds, compared with only ~0.9 seconds in the Venus fly-trap (Jaffe *et al*, 2002). Cells from *Characeae* (a large multi-cellular alga) have been used for electrophysiological studies on mechano-perception because the complexity of plant tissues makes such studies difficult *in planta*. Shepherd *et al* (2002) found that mechanosensitive ion channels are activated by mechanical stress in *Characeae*, which are then transduced into electrical signals.

A number of possible models for mechanosensing in higher plants have been proposed (reviewed by Fasano *et al*, 2002). While a distinction can be made between mechanical stresses which involve a direct membrane deformation, such as touch, and those that do not, such as wind stress, Fasano *et al* (2002) suggest that models for mechanoperception (Figure 1.2 A-C) are equally applicable whether the force is generated internally or externally. In the simplest model (A), plasma membrane deformation may induce activity of mechanosensitive ion channels, as observed in

Characeae. Alternatively, mechanical stimuli may be transmitted through external membranes to the cytoskeleton, and subsequently to internal membranes (B). The Plasmalemmal Control Center Model (Pickard & Ding, 1993) involves an integrin-like transmembrane linkage that is attached to both the plant cell wall and the cytoskeleton (C).

A number of authors have suggested that touch and gravity sensing share common elements (Trewavas & Knight, 1994; Haley *et al*, 1995; Fasano *et al*, 2002), despite the fact that the touch stimulus involves a direct membrane deformation while gravity stimuli generate an internal force. The Starch Statolith Model (Sack, 1997) has been used to describe gravity sensing - graviperception is mediated by the sedimentation of amyloplasts (starch-filled plastids) within statocytes. Statocytes are found in the columella cells of the root cap, and the endodermal and bundle sheath cells of shoots (Blancaflor, 2002). It has been shown that statoliths are not necessarily required for graviperception, as no starch mutants continue to be sensitive to gravity stimulation (Trewavas & Knight, 1994). An alternative model, the gravitational pressure model involves sensing via the entire mass of cytoplasm (Wayne & Staves, 1996).

Nevertheless, the starch statolith model has generally been given more credence due to the fact that it is supported by data from a greater number of laboratories than the pressure model (Blancaflor, 2002). However, neither model can be entirely discounted; it is likely that more than one mechanism for gravity sensing exists in plants.

A further two variants of the starch statolith model may be considered - restrained and unrestrained gravity sensing (Baluška & Hasenstein, 1997). In the restrained gravity sensing model, statoliths are attached to the cytoskeleton, which is linked to the plasma membrane and thus plasma membrane receptors and ion channels. In this model gravity stimulation would induce sedimentation of the statoliths, which would induce changes in cytoskeletal tension, and subsequently stimulate ion channels and signalling cascades, resulting in an effect on growth. By contrast, in the unrestrained model the cytoskeletal system is not sufficient to anchor the statoliths to the plasma membrane, resulting in the free sedimentation of the statoliths in the cell. Unrestrained sedimentation of the statoliths would have knock-on effects on other cell structures such as the endoplasmic reticulum, as well as on signalling cascades. The two models converge at this level, prior to induction of signalling pathways, which result in a

growth response. The relative merits of these two models have also been widely debated though most researchers agree on the central role of the cytoskeleton.

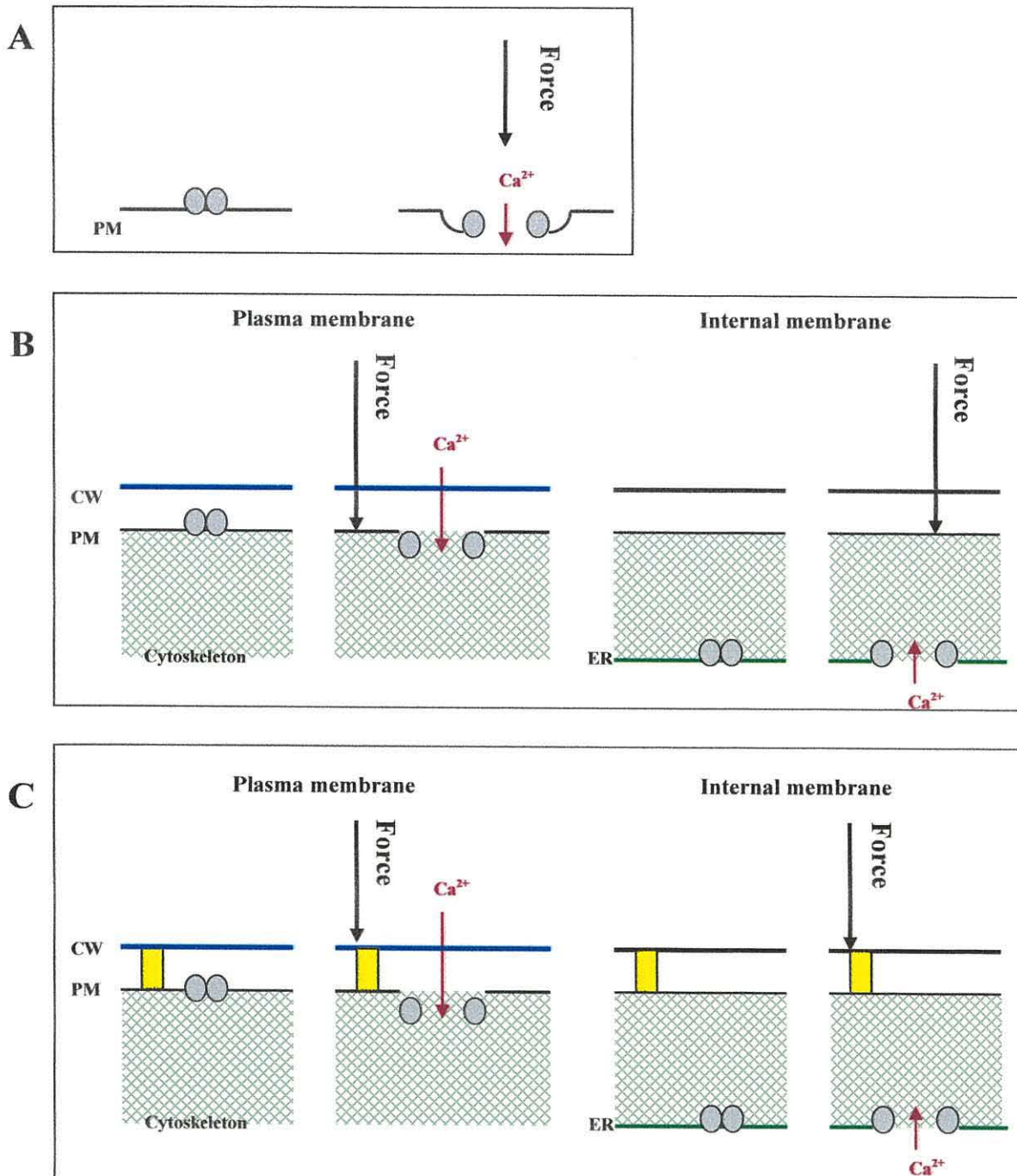


Figure 1.2: Prospective models for perception of mechanical stresses.

A. Simple membrane deformation model: membrane deformation induces mechanosensitive ion channels **B.** Membrane/cytoskeleton model: mechanical stimuli are transmitted through external membranes to the cytoskeleton, and subsequently to internal membranes **C.** Plasmalemmal Control Center Model (Pickard & Ding, 1993). Diagrams are based on those by Fasano *et al* (2002). CW: cell wall, PM: plasma membrane.

1.6 Signal Transduction of plant responses to wind and mechanical stresses

Wind-induced plant motion immediately increases cytosolic calcium (Knight *et al*, 1992). Aequorin is a calcium-sensitive luminescent protein from *Aequorea victoria* that has been used to aid the measurement of cytoplasmic Ca^{2+} concentrations. When Ca^{2+} binds to aequorin, the luminophore is released, emitting blue light. Injected aequorin is routinely used for calcium measurement in animal cells and to some extent in large plant cells (Knight *et al*, 1991). A transgenic construct fusing the apoaequorin coding region from *A. victoria* with the Cauliflower Mosaic virus 35S promoter was used to transform tobacco plants, and designated MAQ 2.4 (Knight *et al*, 1991). The effect of touching cotyledons of the resulting transgenic seedlings with a fine wire was a spike in the cellular Ca^{2+} concentrations with each touch. Furthermore, there was an immediate increase in calcium associated with exposure of these seedlings to wind stress, which declined with repeated exposures to wind after short intervals (Knight *et al*, 1992). Sensitivity to the wind stimulus resumed after a short recovery period.

In a further experiment, MAQ 2.4 and an additional transgenic (MAQ 7.11), in which a fusion protein was made between a nuclear protein and aequorin were used to investigate whether the calcium signal was compartmentalized to either the cytoplasm or nucleus respectively (Van der Luit *et al*, 1999). The response of these transgenic plants to wind stress and cold-shock were significantly different - wind stress induced calcium in MAQ 2.4 after only 0.3 seconds, followed by MAQ 7.11 after 0.6 seconds. Cold-shock did not stimulate a calcium peak until after 4 seconds in the cytoplasm, followed by a peak in the nucleus. In addition, expression of the tobacco calmodulin (calcium sensor) gene NpCaM-1 was primarily regulated by calcium in the nucleus in response to wind stress, and by calcium in the cytoplasm in response to cold-shock (Van der Luit *et al*, 1999). This supports the idea that various stresses/stimuli induce calcium signatures, which have markedly different cellular distributions and durations.

Calmodulin is the foremost sensor for changes in calcium levels in plants. Other calcium sensors include calcium dependent protein kinases and annexins (Snedden & Fromm, 2001). Although calmodulin has no catalytic capability *per se*, after binding calcium it can trigger various target proteins. Three of the four touch genes (TCH1-3)

that are up-regulated in response to wind, rain, and touch encode calmodulin or calmodulin-like proteins (Braam & Davis, 1990). TCH4 encodes xyloglucan endotransglucosylase (XET). TCH genes are also induced by non-mechanical environmental stresses such as darkness and extremes of temperature. Some but not all TCH genes are also upregulated in response to applied auxin (Xu *et al*, 1995) or brassinosteroid (Iliev *et al*, 2002). Braam (1992) has suggested that TCH gene induction is an early response to stimulation and elevated expression of these genes is temporary. For example, TCH mRNAs were found to return to normal levels within 1 to 3 hours after touch stress.

Touch gene 3 (TCH3) is a calmodulin-related protein that binds Ca^{2+} and accumulates at sites of mechanical stress in the plant such as the attachment point of branches (Sistrunk *et al*, 1994). TCH3 is also upregulated in response to gravity stimulation (Antosiewicz *et al*, 1995). It is thought that an increase in cytoplasmic Ca^{2+} may be sufficient to induce TCH3 expression (Braam, 1992). Wright *et al* (2002) proposed that there is staurosporine-sensitive protein kinase activity involved in the induction of TCH3 expression in *Arabidopsis*. Staurosporine inhibits signal transduction in plants. A mitogen-activated protein kinase (MAPK) cascade is activated by mechanical stress, which may be a target for staurosporine. The authors found that protein phosphatase negatively regulates TCH3, which supports the involvement of staurosporine sensitive protein kinase activity in TCH3 regulation in *Arabidopsis*. Furthermore, when protein phosphatase activity is inhibited, TCH3 is highly expressed. TCH3 may be constitutively expressed, and is subject to inhibition unless there is a mechanical or other stress stimulus (Wright *et al*, 2002).

Various environmental stresses such as touch, wounding, cold and drought induce rapid activation of *Arabidopsis* MAPK (Ichimura *et al*, 2000). ATMEKK1 (MAPKKK), ATMPK3 (MAPK) and ATPK19 mRNA levels have been shown to increase simultaneously in response to thigmic stress (Mizoguchi *et al*, 1996). The pattern of expression of these MAPK genes was comparable with the expression of a gene encoding calmodulin. ATMPK1, which is upregulated within 30 minutes of wounding, was not significantly affected by thigmic stress. This result confirms that the rise in expression of ATMEKK1, ATMPK3 and ATPK19 is attributable to thigmic stress and not wounding (Mizoguchi *et al*, 1996).

1.7 Biophysical properties pertaining to the response and adaptation to wind and mechanical stresses

The biophysical properties of plants and plant cells are fundamental to their response and adaptation to wind and other mechanical stresses. The plant cell wall is essential in maintaining the mechanical integrity of plants (Braam, 1999) - it is also central to the control of cell elongation and expansion, is involved in signalling, and is a physical barrier to pathogens. The main primary cell wall constituents are polysaccharides, lignin, suberin, waxes, proteins, calcium, boron and water (Cassab, 1998). From these constituents, the cell wall forms a matrix of non-cellulosic polysaccharides - cellulose microfibrils are embedded in this matrix, and proteins and pectins are linked to it by non-covalent interactions (Darley *et al*, 2001). The primary cell wall is shown diagrammatically in Figure 1.3.

The cellulose/matrix glycan network is a primary determinant of cell wall extension (Darley *et al*, 2001). Cellulose is composed of long chains of β -D-glucans arranged as crystalline microfibrils; the crystalline domains contribute to the structural strength of the cell wall. The non-cellulosic matrix polysaccharides include pectins and cross-linking glycans. The main cross-linking glycan in the primary cell walls of dicots (and some monocots) is xyloglucan, which is entrapped within the cellulose microfibril and may assist in tethering the microfibril to the matrix (Cosgrove, 1997). The cellulose-xyloglucan network is embedded in a layer of pectin.

a) Acid-growth & Turgor

Plant cell growth is governed by turgor pressure but limited by the capacity of the cell wall to extend (Figure 1.3). The concept of “acid-growth” involves the role of the growth hormone auxin, which activates a plasma membrane proton pump that acidifies the cell wall. The decrease in pH activates hydrolases (probably xyloglucan endotransglucosylase/hydrolase or glucanases) in the cell apoplast. These hydrolases cleave bonds between cellulose microfibrils and other polysaccharides resulting in cell wall loosening and an uptake of water. Above the minimum turgor pressure necessary for growth, growth rate is determined by the excess in turgor pressure (Cosgrove, 1997).

The mechanism responsible for growth inhibition by wind/mechanical stresses could be the rapid loss of turgor in growing cells. The effect of mechanical stress on turgor in plants is characterized by the drooping of leaves in stressed plants. Drooping leaves and petioles were observed in response to 5-10 minutes of seismic stress in sunflower and soybean (Jones, 1997). Plasmolysis in the cells of the elongation zone of the hypocotyl may be one of the earliest responses to thigmic stress of dark-grown soybean seedlings (Myers *et al*, 1993). Calcium and potassium are not available at high enough concentrations in the affected cells to account for the rapid loss in turgor. When soybean seedlings were grown in media supplemented with increasing concentrations of calcium the growth rate and turgor pressure continued to be reduced but less severely with increasing concentrations of calcium. Additionally, when the growth media was supplemented with calcium and potassium, the rate of recovery of growth rate after thigmic stress improved. Calcium and potassium therefore appear to facilitate recovery of turgor pressure after mechanical stress.

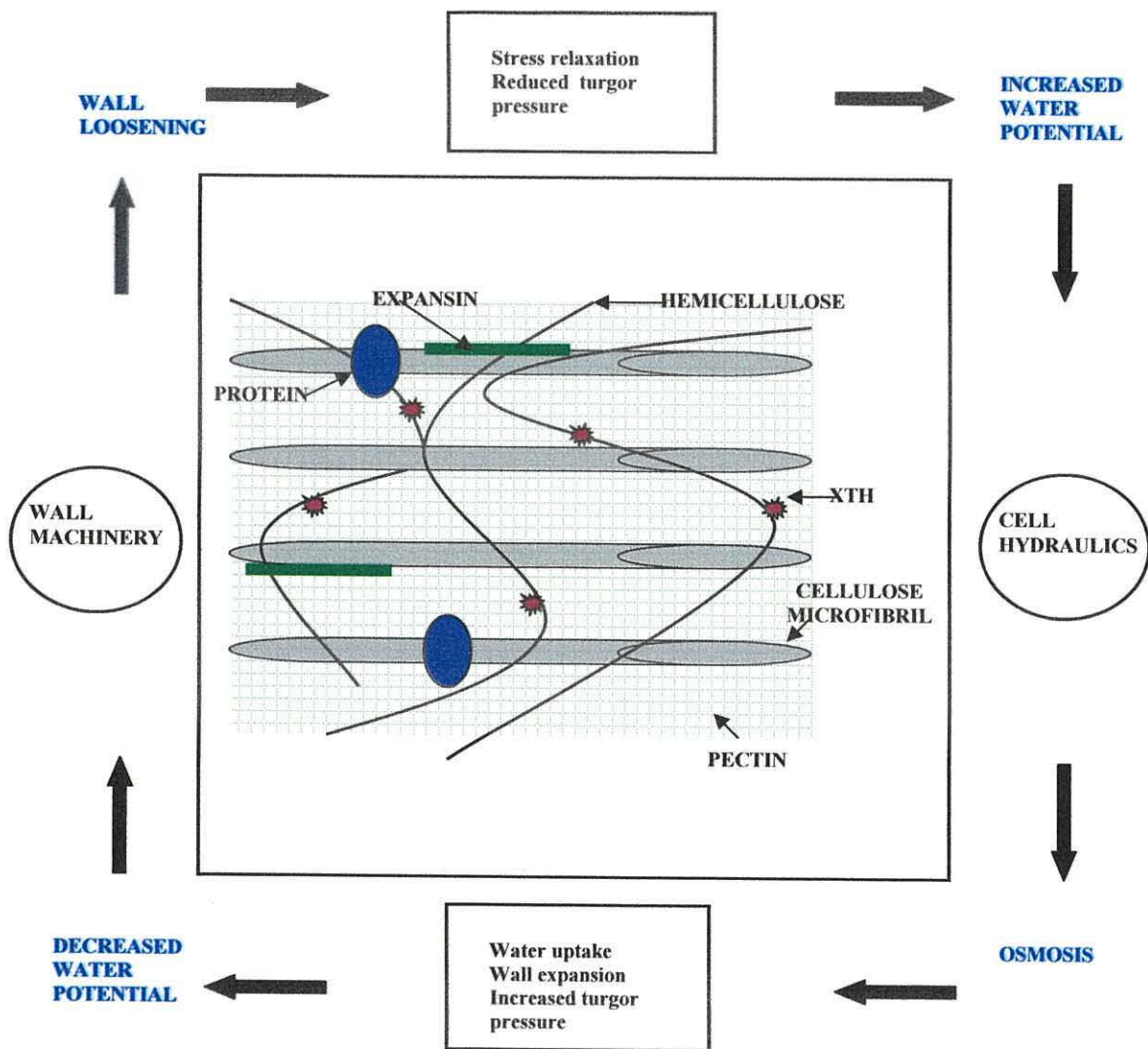


Figure 1.3: The cell wall and processes involved in cell growth.

The central diagram shows the plant cell wall components involved in growth. The exterior schematic, based on Cosgrove (1997) shows the main processes involved in growth.

b) Expansins and Xyloglucan endotransglycosylases

Expansin and xyloglucan endotransglucosylase/hydrolase (XTH) gene families are intimately associated with cell growth. Expansins are invariably described as the mediators of acid growth or cell wall creep; they are thought to mediate cell extension by loosening bonds between the cellulose and the matrix glycan network (Li *et al*, 2003). The activity of expansin has been linked with growing segments of cucumber hypocotyls, oat coleoptile, and the internodes of deepwater rice (Cosgrove, 1997). Furthermore, at the cessation of growth, expansin genes are not expressed. Expansins may also have a role in cell wall degradation as expansin mRNAs have been correlated with ripening in fruit (Hiwasa *et al*, 2003). There is little evidence to support a cooperative interaction between expansins and XTHs (Darley *et al*, 2001), XTHs catalyse the cleavage of xyloglucan chains and transfer the new chain to the end of another xyloglucan chain (Campbell & Braam, 1999). XTH activity is also associated with the growing regions of plants, including dicotyledons, monocotyledons, mosses and liverworts (Fry *et al*, 1992). However, XTH activity is also found at low levels in regions in which growth is completed (Pritchard *et al*, 1993). The apparent paradox between expression and function suggests that XTH has alternative functions. XTHs may be involved in integrating new xyloglucans in the cell wall which would account for the persistent levels of XTH activity even after growth is completed (Campbell & Braam, 1999). Braam *et al* (1996) also suggest that XTHs may show differential expression in particular tissues, and XTH proteins may be targeted to specific sections of the cell wall.

XTH22/Touch gene 4 (TCH4) transcripts rapidly accumulate after thigmic stresses (Iliev *et al*, 2002), wind and wounding (Braam & Davis, 1990), darkness, heat shock, cold shock (Xu *et al*, 1995) and application of brassinosteroids (Iliev *et al*, 2002). A 102 base pair untranscribed region was found to be responsible for TCH4 induction in response to touch, darkness, cold, heat and brassinosteroid application (Iliev *et al*, 2002). This suggests that the signaling pathways of these stresses converge prior to TCH4 expression. The expression of TCH4 seems to emphasize the inconsistencies between the expression of this gene and the responses that the stimulus may produce. Thigmic stress inhibits elongation, while darkness promotes hypocotyl elongation. Xu *et al* (1995) suggest that TCH4-encoded XTH expression is specifically involved in

incorporating xyloglucan into cell walls. Accordingly, increasing incorporation of xyloglucan in the cell walls may be associated with cross-linking and strengthening in response to thigmic stress, and development of mechanical integrity in seedlings grown in darkness.

c) Plant cell wall proteins

Plant cell wall proteins include extensins, arabinoglactan proteins (AGP), glycine-rich proteins (GRP) and proline-rich proteins (PRP). All of these proteins, except glycine-rich proteins are hydroxyproline rich and contain repetitive sequences (Cassab, 1998). These proteins are found in different amounts in the cell walls of different cell types.

Extensin is one of the most widely studied plant cell wall proteins. Extensins are hydroxyproline-rich glycoproteins that are commonly found in the cell walls of dicots but also in monocots. Using the strictest definition, extensins are hydroxyproline-rich glycoproteins with a repeated Ser (Hyp)₄ pentapeptide. Extensins are also rich in the amino acids valine, tyrosine, lysine and histidine (Cassab, 1998). Functions of extensin proteins include increasing the tensile strength of tissues (Shirsat *et al*, 2003, Elliott & Shirsat, 1998), and contributing to plant defenses against pathogen attack (Guo & Shirsat, 2006) and wounding (Merkouropoulos *et al*, 1999).

Arabinoglactan proteins (AGPs) are highly glycosylated hydroxyproline-rich glycoproteins. AGPs are usually but not exclusively characterised by a hydroxyproline-rich core protein with arabinose and galactose-rich polysaccharide additions (Showalter, 2001). Hyp-poor AGPs are included in the non-classical group of AGPs. A role in the inhibition of cell division and expansion has been correlated with AGPs; inhibition of cell division and expansion is induced by Yariv reagent, a dye which specifically reacts with AGPs (Showalter, 2001). Glycine-rich proteins (GRPs) have a glycine content of 60-70%, and they have been shown to contribute to structural strength in the cell wall (Ringli *et al*, 2001). The mechanism by which GRPs are cross-linked into cell walls is not known, however, the most likely mechanism is crosslinking via linkages involving tyrosine (Ringli *et al*, 2001). It may be said that the predicted role of these proteins suggests they may be involved in the inhibition/cessation of growth and thus the response to wind/mechanical stresses.

d) Secondary growth

Secondary growth in trees results in the formation of wood. Wood differentiates from vascular cambium by the addition of secondary xylem. *Arabidopsis* has the capacity for secondary growth as it has been shown to exhibit all of the requirements for the development of secondary xylem (Oh *et al*, 2003). Secondary growth can be induced in *Arabidopsis* by repeated decapitation of developing inflorescence stems (Lev-Yadun, 1994), thus preventing flowering and reduced cambial activity. However, wounding due to the decapitation may itself contribute to secondary xylem development. Lev-Yadun (2002) found that wound effects are significant in the first 5 centimeters below the point of decapitation in juvenile pine plants. On this basis an alternative procedure was devised for induction of secondary growth, without the need for decapitation and thus the complication of wounding effects (Ko *et al*, 2004). As *Arabidopsis* is a facultative long-day plant it was grown under short-day conditions (8 hours light/16 hours darkness), to prevent flowering and induce secondary growth.

It has been suggested that the weight of the developing stem is sufficient to induce differentiation of the vascular cambium as there is a correlation between plant height and development of secondary xylem (Ko *et al*, 2004). Weights (2.5 gram) were added to immature stems of *Arabidopsis thaliana* in an attempt to replicate the transition from primary to secondary growth (Ko *et al*, 2004). Microarray analysis showed that gene expression in the weighted stem was comparable to that in an intermediate stem undergoing the transition from primary to secondary growth. Genes up-regulated in these stems as compared to immature control stems (no weight) included those encoding signal transduction intermediates and transcription factors. Three calmodulin/calmodulin-like proteins including TCH2 and TCH3 were up-regulated at least five-fold, as well as xyloglucan endotransglycosylase 22 (TCH4), cinnamoyl CoA reductase (CCR2), and specific WRKY and MYB transcription factors. It has therefore been shown that mechanical stresses induce secondary growth.

1.8 The role of plant growth regulators in the response to wind/mechanical stresses

Plant growth regulators (plant hormones) are also important components in the global response of plants to mechanical stress. Typically, mechanical stimuli inhibit synthesis of growth promoters such as auxins, cytokinins and gibberellins, and stimulate synthesis of growth inhibitors such as ethylene and abscisic acid. However, as discussed below there are a few specific exceptions to these rules.

Auxin promotes cell wall loosening which causes the cell wall to give way to turgor pressure and promote cell expansion (acid-growth hypothesis). Generally, tissue auxin levels are reduced by mechanical stress (Mitchell, 1977, Boyer, 1967). However, Erner & Jaffe (1982) observed an increase in an auxin-like substance in stems following thigmic stress. These conflicting observations may be explained by inhibition of auxin transport in the first case, and increased auxin metabolism in the latter (Jones, 1997). Inhibition of auxin transport may result from a mechanical stress-induced increase in peroxidases (Boyer *et al*, 1979). Alternatively, auxin may accumulate in regions of the plant where the stress is applied, stimulating ethylene production and subsequently inhibiting growth (Erner & Jaffe, 1982). The response of auxin to mechanical stress may also be species specific. Mitchell & Myers (1995) state that irrespective of whether there is a mechanical stress-induced increase or decrease in auxin, an interaction between auxin and ethylene is important in growth inhibition.

The role of cytokinins and gibberellins/gibberelic acid in mechanical stress responses has not been extensively considered to date. Cytokinins can both stimulate an increase in leaf area and inhibit leaf senescence. Gibberelic acid (GA) stimulates cell division and cell expansion. As mechanical stresses can induce the opposite of these growth responses there are reasonable grounds to assume they may be involved in the response to mechanical stress; an enhanced level of a cytokinin-like substance was associated with exudates obtained from plants subjected to seismic stress. However, a GA-like substance was not found in these plants but was found in the unstressed controls (Beyl & Mitchell, 1983). This suggests inhibition of elongation in

mechanically stressed plants is associated with the promotion of cytokinin activity and an inhibition of GA activity. Inhibition of GA activity may therefore be due to the action of inhibitors.

Absciscic acid (ABA) is a general growth inhibitor. Increased levels of ABA can cause organ abscission, dormancy and reduced turgor of guard cells (Ridge, 2002). A number of abiotic stresses induce absciscic acid accumulation. Thigmic stress induced ABA synthesis in bean plants (Erner & Jaffe, 1982). It has been found that exogenously applied ABA inhibits internode elongation without affecting internode diameter - in sunflower plants subjected to thigmic stress by rubbing and flexing stems, high levels of inhibitor activity attributed to ABA were found in xylem exudates from roots (Beyl & Mitchell, 1983). Inhibitor activity was not found in the roots of unstressed plants, suggesting that there is communication between the roots and the aerial parts of the plant, and that ABA transported from the roots has a role in growth inhibition in the shoots.

Ethylene has received the most attention of all the plant hormones in connection with mechanical stress (Mitchell & Myers, 1995). The increased synthesis of ethylene in response to environmental stress in plants has led it to be known as the “stress hormone” or “stress ethylene”. The classic assay for mechanical stress induced ethylene production is the ‘triple response’ of dark grown peas. Dark grown pea seedlings propagated in a column of glass beads exhibit three main growth characteristics; slower growth, swollen epicotyls and non-vertical growth. These characteristics are symptomatic of ethylene generation. Ethylene is produced via the conversion of methionine and S-adenosylmethionine and 1-aminocyclopropane-1-carboxylic acid (ACC). ACC is the predominant precursor to ethylene, although stress may impact the ethylene synthesis pathway at many points. Furthermore, it has been shown that the rate of ethylene generation is controlled by ACC synthase (Morgan & Drew, 1997) - ACC synthase is encoded by a multigene family, but only some of these genes are expressed in the response to stress.

Thigmic stress of bean internodes causes a burst of ethylene production, which is maintained for up to three hours (Biro & Jaffe, 1984). Elongation is inhibited in the stressed internode and in other internodes; although the surge in ethylene is not

observed in these internodes. Application of exogenous ethylene and ACC result in the expected inhibition of elongation and increase in radial growth (Biro & Jaffe, 1984). Cobalt chloride and EDTA, which inhibit the conversion of ACC to ethylene, prevented the increased radial growth but not the inhibited elongation of stressed plants (Biro & Jaffe, 1984). Thus, other hormones are also likely to be involved in thigmomorphogenesis; as Mitchell & Myers (1995) have pointed out, there may be an interaction between ethylene and auxin involved in thigmomorphogenesis.

Induction of ethylene by mechanical stress and the generation of a mechanically-stressed phenotype after exogenous application of ethylene suggest that it is involved in thigmomorphogenesis. However, this does not directly prove that ethylene is involved in the pathway linking mechanical stress to gene expression. Mutants of *Arabidopsis thaliana* have allowed an increased understanding of the role ethylene plays in stress responses and adaptation. The ethylene-insensitive mutants *ein2* and *etr1* showed wild-type growth responses after exposure to mechanical stress as well as an up-regulation of touch gene 3 (TCH3) (Johnson *et al*, 1998). In a wider study of ethylene mutants (including ethylene-insensitive mutants and mutants overproducing ethylene), Wright *et al* (2002) found that apart from the *ein6* mutant, the mutants tested showed a wild-type TCH3 response to mechanical stress; suggesting that EIN6 is involved in both mechanical stress signalling and ethylene signalling but independently.

1.9 The experimental approach

Traditionally, studies of abiotic stresses have been predominantly physiological, comparing the response of stressed plants to control plants (Bohnert *et al*, 1995). In line with these studies there has been a need for more consistency in the morphological data produced. A growth stage phenotypic analysis has been developed by Boyes *et al* (2001), which has been used in this study to compare the response of wind stressed plants to control plants at different stages of development. Wind and other mechanical stresses have been used to mimic those experienced by plants *in situ* in an attempt to establish growth conditions that give rise to a significant change in phenotype.

Studies were done to identify and characterize the genes affected by wind and other mechanical stresses that could be correlated with the phenotypes observed. Reverse transcriptase-PCR (RT-PCR), Northern analysis and cDNA microarrays are being used for analysis of mRNA levels during development and under stress - microarrays give a global picture of gene expression and can result in the identification of hundreds of genes that are differentially expressed in response to a stress. Lee *et al* (2005) used such an approach to identify genes that were differentially regulated in response to thigmic stress- over 500 genes were found to be up-regulated and 171 genes down-regulated in response to touch. In this study, literature and database searches were used to identify a small set of candidate wind/mechanical stress genes. RT-PCR was used to monitor their expression in plants subjected to wind and other mechanical stresses. Subsequently, gene silencing and overexpression of selected candidate genes was used to characterize their role in the adaptation and response of plants to windy habitats.

The sequencing of plant genomes, especially that of *Arabidopsis thaliana* has greatly advanced the area of functional genomics. *Arabidopsis* was used as the model plant in this study, as it is widely used in molecular/genetic studies. *Arabidopsis*, commonly known as thale cress is universally used because it is a small plant, which requires little space to grow, and it has a short life cycle of only 6 to 8 weeks (seed to seed). Furthermore, *Arabidopsis* has a relatively small nuclear genome (125Mb) that is fully

sequenced, and which contains little repetitive DNA (Arabidopsis Genome Initiative, 2000). Comparative genetic mapping studies have shown conservation of genome organization between *Arabidopsis* and crop plant species, especially the *Brassicaceae* family (Arabidopsis Genome Initiative, 2000). To some extent this supports the application of *Arabidopsis* research to crop plant improvement.

Over-expressing or silencing a gene allows it to be linked to a phenotype. Furthermore, the fitness of transgenic plants under stress conditions can be indicative of an adaptive function. Gene silencing can be induced by mutagenesis (chemical or insertional) or by RNA interference (RNAi). Chemical mutagenesis may be induced using ethylmethane sulphonate, however insertional mutagenesis using T-DNA or transposons is more commonly used (Matthew, 2004). T-DNA from *Agrobacterium tumefaciens* can be inserted into a gene, which both mutates the gene and allows the flanking plant DNA to be isolated (Feldmann, 1991). Additionally, reporter genes can be used to screen for insertions in genes (Alvarado *et al*, 2004). However, T-DNA mutagenesis cannot be targeted to specific genes; 120,000 independent inserts would be needed to give a 95% chance of having one insertion in any gene in the *Arabidopsis* genome (Bouchez & Höfte, 1998). Lethal gene knock-outs and gene redundancy are also problems with insertional mutagenesis, and insertional mutagenesis is not effective in polyploids.

RNA interference (RNAi) is an alternative approach to silencing gene expression - introducing double stranded RNA promotes the degradation of homologous mRNAs, thus inhibiting gene expression. Double stranded RNA can be inserted in plants by transformation with hairpin constructs, in which gene specific fragments are inserted in the sense and antisense orientations either side of an intron sequence. The main advantage of RNAi over insertional mutagenesis is that it can be used to target specific genes and gene families. RNAi transgenics are likely to show varying degrees of gene silencing; if a complete gene knock-out is lethal, a lesser degree of silencing may be selected. Gene redundancy is also not limiting as individual genes can be silenced using a gene-specific fragment and entire gene families can be silenced using a conserved sequence. RNAi can also be used to silence homologous genes in polyploids such as hexaploid bread wheat (Travella *et al*, 2006).

1.10 Aims

1. To establish growth conditions that give rise to a significant change in phenotype when *Arabidopsis* plants are subjected to wind/mechanical stresses.
2. To investigate whether active oxygen species are produced in *Arabidopsis* plants as a response to wind/mechanical stresses.
3. To identify, using database searches, candidate wind/mechanical stress genes that may be involved in the response observed in (1.).
4. To design primers based on the genes identified in (3.).
5. To use primers designed in (3.) in RT-PCR reactions on plant material generated in phenotypic studies (1.).
6. To investigate expression patterns of genes highlighted in (5.) at different stages of development.
7. To examine the phenotype of *Arabidopsis* plants over-expressing extensin under stress conditions (1.)
8. To switch off selected genes using RNA interference in *Arabidopsis* to examine their phenotype under stress conditions (1.)

2. MATERIALS & METHODS

2.1 General Materials & Methods

2.1.1 General chemicals, consumables and equipment

General-purpose chemicals and reagents were commonly obtained from Sigma (Poole, Dorset. UK); BDH (Poole, Dorset. UK); LABM™ (Bury, Lancashire. UK), and Melford Laboratories Ltd (Ipswich. Suffolk. UK). Restriction endonucleases and their buffers were acquired from Promega (Madison. Wisconsin. USA.). The source of all other chemicals and reagents used are noted in the text.

Consumables such as 1.5ml Eppendorf tubes, Gilson pipette tips and Petri dishes were obtained from Greiner Bio-one GmbH (Frickenhausen, Germany). Thin wall PCR tubes were purchased from Axygen Scientific Inc. (Union City. California. USA.), and 1.5ml screw cap tubes were purchased from Starlab (UK) Ltd. (Balklands. Milton Keynes. UK).

Different centrifuges were used, depending on the sample volume. For Eppendorf tubes a Hettich Mikro 20 bench-top centrifuge (Hettich, Germany) was used, and where the temperature of the sample was required to be controlled a Hawk 15/05 refrigerated centrifuge (Sanyo, Uxbridge. UK) was used. For larger sample volumes of 5ml to 50ml a Beckman Mistral 3000i centrifuge was used (Beckman Coulter™, Buckinghamshire. UK). For sample volumes greater than 50ml a Beckman J2-21 centrifuge was used (Beckman Coulter™, Buckinghamshire. UK). Samples could be chilled in either of the latter two centrifuges.

2.1.2 Preparation of solutions

Solutions were made up to their final concentration with autoclaved distilled water (dH₂O), unless otherwise stated in the text. For restriction digests and DNA analysis autoclaved Ultra-pure water for molecular biology (Sigma, Poole. Dorset. UK) was used. For preparation of all RNA solutions diethyl pyrocarbonate - treated water (DEPC- dH₂O) was used. Where solutions were filter-sterilized, a Nalgene® filter (Rochester. New York. USA) was used with a 10ml syringe (Becton Dickson Ltd, Cowley. Oxford. UK).

2.1.3 Commonly used buffers

- **TRIS-EDTA (T.E.) Buffer (pH 7.6):** 10mM Tris.Cl, pH 7.6; 1mM EDTA, pH 8.0.
- **T.E. Buffer (pH 8.0):** 10mM Tris.Cl, pH 8.0; 1mM EDTA, pH 8.0
- **50mM Phosphate buffer (100ml):** 5.77ml 1M Na₂HPO₄ (pH 7.0); 4.23ml NaH₂PO₄ (pH 7.0) 50mM in terms of phosphate at 25°C, made up to 100ml with dH₂O.

2.1.4 Phenol: Chloroform solutions

- **Phenol: chloroform: Isoamyl alcohol (IAA) 25:24:1 (v/v/v):** Equilibrated phenol and chloroform mixed with IAA. Solution saturated with TE buffer (pH 8.0). Stored at 4°C.
- **Chloroform: Isoamyl alcohol (IAA) 24:1 (v/v):** Chloroform and IAA mixed, solution saturated with TE buffer (pH 8.0).

2.1.5 Growth media and antibiotic supplements

- **LB (Luria-Bertani) liquid media (1000ml):** 10g Tryptone (LAB M™, International Diagnostics Group Plc., Lancashire. UK.); 5g Yeast extract (LAB

MTM); 10g NaCl (Sigma Aldrich, Dorset. UK.); pH adjusted to 7.0 with KOH; made up to 1000ml with dH₂O and autoclaved.

- **LB (Luria-Bertani) solid media plate:** 1.5% Agar (LAB MTM) added to LB liquid media prior to autoclaving. Antibiotics were added if necessary after medium was cooled to 50°C, and then poured into sterile petri- dishes.
- **2XL Media (1000ml):** 20g Tryptone (LAB MTM); 10g Yeast Extract (LAB MTM); 1g NaCl; pH adjusted to 7.0; autoclaved. 10ml 20% glucose (w/v) added after autoclaving.
- **Ca/Mn Media:** 100mM CaCl₂; 70mM MnCl₂; 40mM Sodium acetate; pH adjusted to 5.5; Filter sterilize (0.45 µM filter).
- **Ampicillin (Amp):** 50mg.ml⁻¹ Ampicillin sodium salt (Sigma) dissolved in 70% Ethanol; stored at -20°C.
- **Kanamycin (Kan):** 50mg.ml⁻¹ Kanamycin powder (Sigma) dissolved in autoclaved dH₂O; filter-sterilized; stored at -20°C.
- **Rifampicin (Rif):** 25mg.ml⁻¹ Rifampicin powder (Sigma) dissolved in autoclaved dH₂O; filter- sterilized; stored at -20°C.
- **Streptomycin (Str):** 100mg.ml⁻¹ Streptomycin powder (Sigma) dissolved in autoclaved dH₂O; filter sterilized; stored at -20°C.
- **100mM IPTG:** 0.2g isopropylthio-β-D-galactoside (Melford Laboratories Ltd Ipswich. Suffolk. UK) in 10ml dH₂O; filter-sterilized. Solution dispensed into 2ml eppendorfs and stored at -20°C.
- **X-Gal:** 50mg.ml⁻¹ 5-bromo-4-chloro-3-indolyl-β-D-galactoside salt (Melford Laboratories Ltd) dissolved in dimethylformamide; tubes foil wrapped and stored at -20°C.

2.1.6 Oxidative stress assay solutions

- **DAB solution:** 1mg.ml⁻¹ 3, 3-diaminobenzadine (DAB) added to 400µl dimethyl sulfoxide (DMSO), and made up to final concentration with dH₂O (pH 3.8).
- **Guaiacol solution:** 0.25% guaiacol (v/v) in 10mM sodium phosphate buffer (pH 6.0), 0.125% H₂O₂ (v/v).

- **Syringaldazine/methanol:** 0.8mg.ml⁻¹ syringaldazine added to 1ml DMSO, and made up to a final concentration with methanol.
- **Syringaldazine solution (30ml):** 30ml 30mM phosphate buffer (pH 7.0), to which 0.05% H₂O₂ (v/v) and 600µl syringaldazine/methanol (as above) was added.
- **Bradford reagent:** Bio-Rad Bradford dye reagent concentrate (Bio-Rad, Hercules, USA) was diluted by one fifth with distilled water and filtered through Whatman #1 filter paper. The reagent was stored for up to two weeks at room temperature.

2.1.7 RNA extraction buffers

- **Guanidine buffer:** 8MGuanidine HCl; 20mM Mes; 20mM EDTA; 50mM Mercaptoethanol; pH adjusted to 7.0; made up to final volume with DEPC-dH₂O and autoclaved.

2.1.8 Formaldehyde gel solutions

- **10X MOPS, pH 8.0 (100ml):** 4.18g 3-(N-Morpholino) propanesulphonic acid (200mM); 0.68g sodium acetate (50mM); 0.37g EDTA (10mM); pH adjusted to 7.0 with NaOH; made up to 100ml with DEPC-treated water.
- **Sample buffer:** 0.9% Ethidium bromide (v/v); 23% 10X MOPS, pH 8.0 (v/v); 6.2% Formaldehyde (v/v); 69% Deionised formamide (v/v).

2.1.9 Agarose gel electrophoresis

- **5X TBE buffer (1000ml):** 54g Tris base; 27.5g Orthoboric acid; 20ml 0.5M EDTA, pH8.0 (10mM). Diluted with autoclaved dH₂O to a working solution of 1X TBE.
- **Type IV loading buffer:** 0.25% bromophenol blue (w/v); 40% (w/v) sucrose in dH₂O; autoclaved and stored at 4°C.

- **DNA ladders:** 1Kb and 100b.p. DNA ladders were supplied in 10mM Tris-HCl, 1mM EDTA (Promega Corporation, Madison. USA.); 5 μ l of each ladder as supplied in 2 μ l type IV loading buffer (as above) was used for loading onto agarose gels.
- **Preparation of dialysis tubing:** Dialysis tubing (Size 1, diameter 6.3mm) was obtained from Medicell International Ltd. (London. UK) and cut into lengths of 10-20cm. These pieces were boiled for 10 minutes in 2% sodium bicarbonate (w/v), 1mM EDTA (pH 8.0); and then washed with distilled water. The dialysis tubing was then boiled in 1mM EDTA (pH 8.0) for a further 10 minutes. When the tubing had cooled it was stored in 70% ethanol (v/v). Prior to use, dialysis tubing was washed thoroughly with dH₂O.

2.1.10 Minipreparation of plasmid DNA

- **Solution I:** 50mM Glucose; 25mM Tris.Cl; 10mM EDTA.
- **Solution II:** 0.2M NaOH; 1% SDS (w/v); prepared fresh.
- **Solution III** (100ml): 3M Potassium acetate; 11.5ml glacial acetic acid.

2.1.11 Southern blotting and hybridization

- **Protease:** 5mg.ml⁻¹ Pronase (Promega) dissolved in 10mM Tris.Cl (pH 7.6), 10mM NaCl, and incubated at 37°C for 1hour prior to storage at -20°C in sterile Eppendorfs.
- **Denaturing solution:** 1.5M NaCl; 0.5N NaOH; autoclaved.
- **Neutralization solution:** 1M Tris (pH7.4); 1.5M NaCl; autoclaved.
- **20X SSC** (1000ml): 175.3g NaCl; 88.2g Sodium citrate; Adjusted pH to 7.0 with NaOH and autoclaved.
- **Pre-hybridisation solution:** 5X SSC; 5X Denhardt's solution; 0.5% SDS (v/v); 100 μ g/ml salmon sperm DNA; made up with distilled water. Salmon sperm DNA was boiled for 5 minutes and snap-cooled on ice before adding.
- **Hybridization solution:** 5X SSC; 5X Denhardt's solution; 0.1% SDS (v/v); 100 μ g.ml⁻¹ salmon sperm DNA was made up with distilled water. Salmon

sperm DNA was boiled for 5 minutes and snap-cooled on ice before adding. Denatured, radiolabelled DNA probes were labeled as stated in section 2.6.3 and added to the solution prior to hybridization.

- **50X Denhardt's solution** (500ml): 5g Ficoll (Type 400, Pharmacia Biotech Limited); 5g polyvinylpyrrolidone (Sigma-Aldrich); 5g bovine serum albumin (Sigma-Aldrich); filter-sterilized and stored at -20°C. This was used at 1X concentration.
- **Salmon Sperm DNA** (20ml): 200mg DNA from salmon testes (Sigma-Aldrich) was dissolved in 20ml dH₂O, autoclaved, cooled on ice and sonicated in a MSE Soniprep sonicator, and stored at -20°C in sterile Eppendorf tubes at a concentration of 10 mg.ml⁻¹.

2.1.12 Radioactive labeling of DNA probes

- **OLB**: Solutions A, B and C mixed in a ratio of 10:25:15 respectively; stored at -20°C in sterile Eppendorf tubes.
- **Solution A**: 1ml solution O, 18μl 2-mercaptoethanol and 5μl of dATP, dGTP and dTTP (Pharmacia Biotech Limited).
- **Solution B** (100ml): 47.7g HEPES (N-[2-Hydroxyethyl]piperazine-N'-[2-ethanesulphonic acid]) to obtain a final concentration of 2M, pH6.6.
- **Solution C**: 90 OD units/ml hexadeoxyribonucleotides (Pharmacia Biotech Limited) in TE buffer (pH 7.5).
- **Solution O** (100ml): 15.1g Tris-HCl (1.25M), 1.19g MgCl₂ (0.125M); pH adjusted to 8.0.

2.1.13 Extraction of plant genomic DNA

- **CTAB buffer** (200ml): 4g Hexadecyltrimethylammonium bromide, 20ml 1M Tris-Cl (pH 8.0), 56ml 5M NaCl, 8ml 0.5M EDTA (pH 8.0) and 115ml dH₂O; autoclaved and cooled, and 400μl Mercaptoethanol added.
- **Wash buffer** (200ml): 152ml ethanol, 200μl ammonium acetate, made up to 200ml with dH₂O.

- **10M Ammonium acetate (20ml):** 15.4g of ammonium acetate made up to 20ml with dH₂O, and filter sterilized.

2.2 Plant Materials and Growth Conditions

2.2.1 Plant material

Wild-type *Arabidopsis thaliana* (L.) Heyhn ecotypes Wassilewskija-0 (Ws) and Columbia-0 (Col) were obtained from the Nottingham *Arabidopsis* stock centre and were used in this work. The Ws ecotype (NASC, line N1602) is characterized by a large rosette leaves, and grows to approximately 33-38cm in height (NASC, 2006). This ecotype was used predominantly as it was the background ecotype for any transgenic lines generated in this study. The Col ecotype (NASC, line N1093) has smaller rosette leaves, the leaf margins are serrate, and the plants grow to 15-24cm in height (NASC, 2006).

2.2.2 Propagation of plant material

a) Sterilizing *A.thaliana* seed:

Seeds were surface sterilized in a concentrated bleach solution (see below) and repeatedly washed with ethanol prior to drying under sterile conditions. 0.75g of a Covclor chlorine tablet (Coventry chemicals Ltd., Coventry. UK) was dissolved in 8ml distilled water containing 70µl 1% Tween ® 20 (v/v) (BDH). The sterilizing stock solution (1ml) was subsequently diluted in 9ml absolute ethanol, and spun down at 2500rpm for five minutes to pellet the precipitate. The aqueous phase was transferred to a new tube and spun down for a further five minutes. The resulting sterilizing solution was used to surface sterilize seed. The sterilizing solution was added to an Eppendorf of seeds and incubated for 30 minutes. The solution was removed with a pipette and replaced with 95% (v/v) ethanol for 1 minute. The ethanol wash was repeated for a further minute. All ethanol was then removed and seed were

spread around the Eppendorf tube to aid drying. Seed were dried for at least two hours in a laminar flow cabinet prior to plating on agar.

b) Plate-based germination of *A.thaliana* seed:

Sterilized seed was plated on ½ strength MS basal salt media (Murashige & Skoog, 1962) supplemented with sucrose, ± antibiotics. Wild-type *A.thaliana* seed were grown on media with no antibiotic supplement and transgenic *A.thaliana* seed were grown on media containing an appropriate antibiotic for selection of transgenic seedlings. Plates were sealed with Parafilm “M” laboratory film (Pechiney Plastic Packaging, Chicago, USA), and then wrapped in foil and stored at 4°C for three days to stratify germination. Plants were then grown under growth room conditions (20-25°C, 8 hours light/ 16 hours dark cycle) *in vitro* until they were 14 days old, after which they were transferred to soil.

At 14 days, plants were transferred to sterile compost: vermiculite mixture of 5 parts Growman multi-purpose compost (Humax, Carlisle, UK) mixed with 3 parts vermiculite (J. Arthur Bowers, William Sinclair Horticulture Ltd., Lincoln, UK). The compost: vermiculite mixture was wetted with an insecticide solution; “Intercept 70WG” (Scotts Company Ltd, Bromford, Ipswich, UK) at 0.1 g.l⁻¹. Seedlings were potted in separate pots in a seedling tray containing 24 pots. Plants were watered regularly with distilled water, and fed with 0.2 g.l⁻¹ Phostrogen® (Pbi Home & Garden Ltd., Waltham Cross, Hertfordshire, UK.)

c) Soil-based growth of *A.thaliana* seed:

Wild type *Arabidopsis* seed were incubated in dH₂O at 4°C in an Eppendorf for 3 days to stratify germination. Seeds were then sprinkled on to sterile compost: vermiculite mixture wetted with insecticide solution (as previously), and covered with a transparent lid until seedlings had germinated. Plants were grown under growth room conditions (20-25°C, 8 hours light/ 16 hours dark cycle). When they were 14-days old, seedlings were thinned out to one plant per pot in a seedling tray containing 24 pots. Plants were watered regularly from their base with distilled water, and fed with the

plant food Phostrogen® (Pbi Home & Garden Ltd., Waltham Cross, Hertfordshire, UK.) at a concentration of 0.2 g.l⁻¹.

2.2.3 Phenotypic analysis of *Arabidopsis* plants

a) Plate-based phenotypic analysis of *Arabidopsis* plants

Where plate-based phenotypic analysis was used, sterilized *Arabidopsis* seed were plated on half-strength MS media, stratified at 4°C in darkness and then transferred to standard growth room conditions (20-23°C, 8hrs light/16hrs dark cycle). Day 0 was counted as the day on which plates were removed from 4°C to growth room conditions. Plants were monitored using the plate-based phenotypic analysis from imbibition until seedlings reached 14-days old. The *Arabidopsis* growth stages used for the plate-based analysis as defined by Boyes *et al* (2001) are outlined in Table 2.1a. Various measurements were taken during the plate-based phenotypic analyses, as shown in Table 2.1b. Measurements were taken every day from day 1 until day 14.

b) Soil-based phenotypic analysis of *Arabidopsis* plants

Where the soil-based phenotypic analysis was used, wild type *Arabidopsis* seed were stratified at 4°C in dH₂O, and sprinkled on wetted compost: vermiculite mixture (section 2.2.2). Plants were grown under growth room conditions until 14 days. At 14-days seedlings were thinned out to one seedling per pot and grown with regular watering and feeding until maturity. The principle growth stages for soil-based phenotypic analysis are shown in Table 2.2a (Boyes *et al*, 2001). Measurements were taken every 2-3 days as outlined in Table 2.2b, commencing when seedlings were 14-days old and continuing until plant maturation.

Table 2.1a: Growth stages for the plate-based phenotypic analysis

Stage	Description of stage
Principal stage 0	Seed germination
0.10	Seed imbibition
0.50	Radicle emergence
0.7	Hypocotyl and cotyledon emergence
Principal stage 1	Leaf development
1.0	Cotyledons fully open
1.02	2 rosette leaves >1mm
1.04	4 rosette leaves >1mm
R6	More than 50% seedlings have primary root ≥6cm

Table 2.1b: Measurements taken during the plate-based phenotypic analysis

Stage	Measurement	Unit
0.50	Has radicle emergence been reached or passed?	Y/N
0.7	Are the cotyledons visible?	Y/N
1.0	Have the cotyledons fully opened?	Y/N
1.0	Number of rosette leaves	Count
1.0	Length of primary root	mm

Table 2.2a: Growth stages for the soil-based phenotypic analysis

Stage	Description of stage
Principal stage 1	Leaf development
Principal stage 3	Rosette growth
Principal stage 5	Inflorescence emergence
Principal stage 6	Flower production
Principal stage 8	Silique ripening
Principal stage 9	Senescence

Table 2.2b: Measurements taken during the soil-based phenotypic analysis

Stage	Measurement	Unit
3	Rosette radius	mm
5.10	Are flower buds visible?	Y/N
6	Is first flower open?	Y/N
6.50	Length of stem	mm
6.50	Number of stem branches on main bolt	Count

2.2.4 Subjecting plants to wind and mechanical stresses

a) Vibration stress (in seedlings)

Vibration stress was applied via a platform covering a subwoofer speaker cone. The apparatus was custom built but based on a design by Takahashi *et al* (1991). The frequency of vibration (1-250Hz) was controlled through a variac (Zenith Electric Company Ltd, London.UK). *Arabidopsis* seed were sterilized, plated on half-strength MS media, stratified at 4°C in darkness and then transferred to standard growth room conditions (20-23°C, 8hrs light/16hrs dark cycle). Vibration was applied at imbibition, germination or the two-leaf stages of development. Seedlings were monitored using a plate-based phenotypic analysis, and hypocotyls and root lengths were measured when seedlings reached 14-days old.

b) Seismic stress

Arabidopsis seed were sterilised, plated on half-strength MS media, stratified at 4°C in darkness and then transferred to standard growth room conditions (20-23°C, 8hrs light/16hrs dark cycle). Plates were subsequently placed on a gyratory laboratory shaker for 72hrs constantly from imbibition, germination or the two-leaf stages of development. The shaker operated on a horizontal plane, and was used at 600 rpm. A plate-based phenotypic analysis was used (table 2.1).

c) Gravity stimulation

Seed were sterilized, plated on half-strength MS media, stratified at 4°C in darkness and then transferred to standard growth room conditions (20-23°C, 8hrs light/16hrs dark cycle). Plates were clamped at 135°; continuous gravity stimulation at this angle was applied for 72 hours from germination. The lengths of the primary roots and hypocotyls of both stressed and unstressed control seedlings were measured at 14-days.

d) Wind stress

Arabidopsis plants were subjected to wind stress. Two 9" desk fans were used to simulate wind stress (GET Plc, New Southgate. UK), which generated an average wind speed of 2.7 m/s. Wind stress was applied for two hours three times per day; commencing at 08:00, 12:00 and 16:00. The stress was first applied at 17-days and continued daily until maturation. Seedling trays were turned every few days so that each row in the tray received approximately the same dose of wind stress over the duration of the experiment. A soil-based phenotypic analysis (table 2.2) was used to compare wind stressed plants with control plants that were not exposed to wind stress.

e) Thigmic stress

Arabidopsis plants were subjected to thigmic stress. Thigmic stress was applied by touching a single rosette leaf on each plant daily by stroking the leaf back and forth with a gloved hand. Thigmic stress was applied at approximately the same time every day (09:00). The stress was first applied at 17-days and continued daily until maturation. A soil-based phenotypic analysis (table 2.2) was used to compare plants subjected to thigmic stress with control plants that were not exposed to thigmic stress.

f) Vibration stress (in plants)

Soil-based *Arabidopsis* plants were subjected to vibration stress. Vibration stress was applied via a platform covering a subwoofer speaker cone (as section 2.2.4a). Vibration at 40Hz was applied daily from 17-days until maturation, during which a soil-based phenotypic analysis (table 2.2) was used.

2.3 Oxidative stress assays

2.3.1 Detection of hydrogen peroxide by the DAB-uptake method

The protocol for the detection of hydrogen peroxide by uptake of Diaminobenzadine (DAB) solution was based on that described by Thordal-Christensen *et al* (1997). Leaf samples were placed in an Eppendorf containing DAB solution (section 2.1.6), such that only the cut end of the petiole was submerged in the solution. Samples were incubated in the DAB solution overnight under standard growth room conditions. Subsequently leaves were boiled in ethanol for 10 minutes or until the tissues were cleared of chlorophyll. Samples were stored in 100% IMS. The localization of sites of H_2O_2 synthesis was observed as a red/brown pigment.

2.3.2 Monitoring Peroxidase activity by use of Guaiacol

The methodology for determination of peroxidase activity using guaiacol was based on an original protocol devised by Hammerschmidt *et al* (1982), and a subsequent protocol focusing on determination of peroxidase activity in wind stressed bean plants (Cipollini, 1998). Leaf or seedling samples were harvested, frozen in liquid nitrogen and stored at $-80^{\circ}C$ until they were processed. Approximately 100mg of leaves or 10mg of seedlings were ground in 500 μ l of 0.1M sodium phosphate buffer (pH 7.0) in a pre-chilled Eppendorf with a plastic pestle. Samples were centrifuged at 12,000xg for 15mins at $4^{\circ}C$. The resulting supernatant was used as an enzyme extract for further analysis.

Enzyme extract (50 μ l) was added to 950 μ l of Guaiacol solution (section 2.1.12), and mixed thoroughly. Peroxidase activity was monitored spectrophotometrically as the rate of decomposition of hydrogen peroxide, where guaiacol is a hydrogen donor, to tetraguaiacol. Changes in absorbance at 470nm were monitored for 3 minutes. Peroxidase activity was expressed as an increase in absorbance at 470nm $min^{-1} mg^{-1}$ fresh mass. The amount of protein in each leaf extract was determined using the

Bradford reagent, as outlined below. Peroxidase activities were normalized against protein concentration.

2.3.3 Monitoring peroxidase activity involved in the lignification process using Syringaldazine

A scaled-down version of the protocol outlined by De Jaegher *et al* (1985) was used to determine how much peroxidase activity was specifically involved in the lignification process. The enzyme extract outlined in the previous section was also used in a reaction with syringaldazine solution (section 2.1.6). Enzyme extract (50 μ l) was added to 950 μ l syringaldazine solution. Changes in absorbance were monitored for 3 minutes at 530nm, and peroxidase activity was recorded as the change in absorbance at 530nm min⁻¹ mg⁻¹ fresh weight of tissue. Results were normalized against protein concentration.

2.3.4 Bradford Assay for protein determination

The Bradford Assay (Bradford, 1976) was used to determine the total protein concentration of samples. Coomassie brilliant blue G-250, a major constituent of the Bradford dye reagent, binds proteins proportionally, and absorbs at 595nm. Bovine serum albumin (BSA) was used as a protein standard; the standard was serially diluted in the range of 2.5 μ g.ml⁻¹ to 10 μ g.ml⁻¹. The protein concentration of the leaf extracts were calculated from the linear absorbance plot (Appendix A) of these dilutions. The leaf extract assay contained: 10 μ l leaf extract diluted in 790 μ l distilled water, to which 200 μ l of Bradford dye reagent was added. Samples were incubated for 10 minutes and their absorbance was then measured at 595nm.

2.4 Analysis of Gene Expression

2.4.1 RNA Extraction

Total RNA was extracted from *Arabidopsis* tissue using a protocol based on Logemann *et al*'s (1987) improved method for the isolation of RNA from plant tissues. 10mg of *Arabidopsis* tissue was homogenized to a fine powder in liquid nitrogen in an Eppendorf pre-cooled with liquid nitrogen. One volume of guanidine buffer and one volume of phenol: chloroform: IAA was added, and the samples stored on ice. Samples were then centrifuged in a pre-cooled centrifuge (4°C) for 10 minutes at 10,000 rpm. The supernatants were removed to a new tube, and 0.5 volume of phenol: chloroform: IAA was added. The samples were gently mixed on a rotating wheel for 10 minutes at 4°C and then subsequently centrifuged at 10,000 rpm for 45 minutes. RNA in the aqueous phase was collected and mixed with 100µl of ethanol and 250µl of 1M acetic acid, and incubated at -80°C for 1 hour to allow RNA precipitation. Samples were centrifuged at 10,000 rpm for 10 minutes. The resulting pellets were washed with one volume of 3M sodium acetate at room temperature, and recovered by centrifugation at 10,000 rpm for 5 minutes. The pellets were then washed with 70% ethanol (v/v); air dried and re-suspended in 50µl DEPC-treated water.

2.4.2 Estimation of RNA concentration

The concentration of RNA in a sample was estimated by measuring the absorbance at 260nm and 280nm of 1µl of the sample diluted in 69µl of TE buffer (pH 8.0). A Unicam UV 500 spectrophotometer (Thermofisher Scientific, UK) was used. An absorbance of 1.0 at 260nm is approximately equal to 40µg.ml⁻¹ of single stranded RNA. The A₂₆₀/A₂₈₀ ratio is indicative of the purity of the RNA sample; values between 1.9 and 2.1 are adequate. RNA absorbs strongly at 260nm, while proteins absorb strongly at 280nm.

2.4.3 Denaturing formaldehyde agarose gel electrophoresis

Denaturing formaldehyde agarose gel electrophoresis was used for analysis of RNA. The gel (150ml) contained; 1X 3-(N-Morpholino) propanesulphonic acid (MOPS) buffer (pH 8.0), 2.5% formaldehyde (v/v), and 1.3% agarose (w/v) made up with DEPC-treated water. The agarose and MOPS buffer were melted in a microwave oven, and cooled to 60°C. The formaldehyde was then added and mixed by swirling. The gel was poured into a DEPC-treated gel mold and allowed to set for 45 minutes. Samples were prepared by making 1 µg of RNA up to 8 µl with DEPC-treated water, adding 6 µl of sample buffer, heating at 65°C for 2.5 minutes and then snap cooling on ice. The gel was submerged in 1X MOPS in the electrophoresis tank prior to loading. Samples were loaded, and the gel was run at 40V for 3 hours. The gel was visualized under UV light using a TM-20 UV-Transilluminator (UVP products, San Gabrielle, USA) and a photograph was taken of the gel with a KGIB Mitsubishi video copy processor (Mitsubishi, Tokyo, Japan).

2.4.4 RT-PCR analysis of gene expression

First strand cDNA was synthesized from total RNA using the Qiagen Omniscript Reverse Transcription kit (Qiagen). 1 µg total RNA was added to 1x RT Buffer, 0.5mM of each dNTP, 1 µM oligo-dt primer (MWG Biotech, London, UK), 10 units RNasin® ribonuclease inhibitor (Promega), and 4 units of Omniscript reverse transcriptase in a final volume of 20 µl made up with DEPC-treated water. The reaction was incubated at 37°C for 90 minutes. Reverse transcription reaction products were stored at -20°C.

The reverse transcription reaction was diluted by one tenth with DEPC-treated water, and 5 µl was then added to a standard PCR mix. The PCR mix contained 1x GO Taq Flexi buffer (Promega), 2mM MgCl₂, 0.2mM dNTP mix (Qiagen), 0.5mM each gene specific primer (MWG Biotech) and 1 unit of GO Taq polymerase in a final volume of 25 µl. Thermal cycling conditions were: 95°C for 5 mins; 35 cycles of 94°C for 40

seconds, 55°C for 40 seconds and 72°C for 2.5 mins; 72°C for 10 mins; cooling to 4°C, unless otherwise stated.

2.4.5 Polymerase Chain Reaction

The standard PCR mix contained 1x GO Taq Flexi buffer (Promega), 2mM MgCl₂, 0.2mM dNTP mix (Qiagen), 0.5mM of each forward and reverse gene specific primers (MWG Biotech, Germany), and 1 unit of GO Taq polymerase in a final volume of 25µl. A PTC-150 Minicycler (MJ Research Inc, Watertown, USA) was used for thermal cycling. Thermal cycling conditions were as follows 95°C for 5 mins; 35 cycles of 94°C for 40 seconds, 55°C for 40 seconds and 72°C for 2.5 mins; 72°C for 10 mins; cooling to 4°C, unless otherwise stated.

2.4.6 Agarose gel electrophoresis

The percentage of agarose that was used in each gel was dependant on the size of fragments that required to be separated. 0.7% and 2% agarose gels (w/v) were commonly used in this work for the separation of linear DNA fragments in the ranges 1-20Kb and 0.1-2Kb respectively (Sambrook *et al*, 1989). Molecular biology grade agarose (Melford laboratories) was used, diluted in 1x Tris-borate buffer (TBE), and heated in a microwave oven until the agarose had completely dissolved. The solution was allowed to cool to 60°C, when 0.5µg.ml⁻¹ ethidium bromide (Promega) was added and mixed, to aid visualization of the DNA. The gel was poured into a mold containing a sample comb, and set for at least 45 mins at room temperature.

Gels were run in an electrophoresis tank attached to a power source. The gel was covered with running buffer (1x TBE), and the sample comb removed. DNA samples were made up to 28µl with dH₂O and 2µl of type IV loading buffer was added. A DNA ladder (section 2.1.9) was usually run in the first well of each gel, to which 2µl of type IV loading buffer was also added. 50ml minigels (9.5cm x 8.0cm) were run at 5-8 V/cm for approximately 60 mins, while 200ml large gels (20cm x 18cm) were run at 3-5 V/cm for 3 hours.

2.5 Cloning Techniques

2.5.1 Purification of PCR products and DNA

DNA and PCR products used for cloning were purified by extraction with phenol: chloroform: IAA and subsequently precipitated with absolute ethanol. Each DNA sample or PCR reaction was made up to a minimum volume of 100µl with TE buffer. An equal volume of phenol: chloroform: IAA was added to each sample, and mixed by inversion. The sample was centrifuged at 15,000xg for 5 minutes in a pre-cooled (4°C) centrifuge. The top aqueous phase was removed and extracted with an equal volume of chloroform: IAA and centrifuged at 15,000xg for 5 minutes at 4°C. The aqueous phase was then removed and gently mixed with 0.1 volume of sodium acetate (pH 5.6) and 2 volumes of ice-cold absolute ethanol, and stored at -70 °C for 1-2 hours. The sample was then centrifuged at 15,000xg for 30 minutes and the ethanol/aqueous phase removed. The DNA pellet was washed with 70% ethanol and then all ethanol was removed from the tube. The pellet was air dried for 10-15 minutes and then re-suspended in 20µl TE buffer or dH₂O.

2.5.2 Estimation of DNA concentration

The concentration of DNA in a sample was estimated by measuring the absorbance at 260nm and 280nm of 1µl of the sample diluted in 69µl of TE buffer (pH 8.0). A Unicam UV 500 spectrophotometer (Thermofisher Scientific, UK) was used. An absorbance of 1.0 at 260nm is approximately equal to 50µg.ml⁻¹ of double stranded DNA. The ratio of A₂₆₀/A₂₈₀ is indicative of the purity of the DNA sample; values between 1.8 and 2.0 are adequate (Sambrook *et al*, 1989). DNA absorbs strongly at 260nm, while proteins absorb strongly at 280nm.

In certain cases DNA concentration was estimated by comparing the DNA band intensity of the sample with that of a known concentration of DNA. DNA fluorescence under UV light is proportional to its concentration. The commonly used Promega DNA ladders were diluted and used as a marker of DNA intensity.

2.5.3 Extraction of plasmid DNA

a. Minipreparation of plasmid DNA

Minipreparations of plasmid DNA were used to screen transformants and for restriction analysis. A single bacterial colony containing the plasmid of interest was grown up overnight in 5ml of LB media containing the appropriate antibiotic for selection. The culture was pelleted by centrifugation at 2500 rpm for 18 minutes at room temperature. The bacterial pellet was then re-suspended in 200µl of solution I, transferred to a 1.5 ml Eppendorf tube, and placed on ice for 30 minutes. 300µl of solution II was then added and mixed by inversion, before incubating on ice for 5 minutes. 225µl of solution III was added prior to a further 5 minute incubation on ice. The sample was then centrifuged at 15,000 rpm for 15 minutes at room temperature. The supernatant was collected and extracted with an equal volume of phenol: chloroform: IAA, mixed, and centrifuged at 15,000 rpm for 8 minutes. Chloroform (300µl) was then added to the top aqueous phase before centrifuging for an additional 8 minutes at 15,000 rpm. The aqueous phase from this extraction was precipitated with ethanol and the DNA pellet was finally re-suspended in 50µl of TE buffer (pH 7.6)

b. Purification of small amounts of high quality plasmid DNA using a Qiagen Qiaprep Mini kit

The Qiagen Qiaprep miniprep kit (Qiagen) was used to purify up to 20µg of high quality plasmid for use in cloning applications. An overnight culture was processed as outlined in the manufacturer's instructions for the kit.

c. Purification of large amounts of high quality plasmid DNA using a Qiagen Midi kit

The Qiagen Midi kit (Qiagen) was used to purify larger amounts of high quality plasmid. Up to 100µg of high copy number plasmid was purified from 100ml of overnight culture. An optimized protocol was used for low copy number plasmids

such as pBIN19, according to the instructions supplied in the kit a larger culture volume (100ml) was used but yields were still relatively low (~ 20µg)

2.5.4 Restriction enzyme digests

Restriction endonucleases were used for cleaving DNA at specific sites. A common digest of $\leq 1\mu\text{g}$ of DNA was usually carried out in a volume of 30µl and contained 10 units of restriction endonuclease (Promega) and 1x optimal reaction buffer (specific to the enzyme). RNase (10µg/µl) was added to digests of DNA samples contaminated with RNA, such as DNA minipreparations. Typically digests were incubated at 37°C for 3 hours, but this was dependent on the enzyme used for the digest.

Where the digest involved two restriction endonucleases, 10 units of each enzyme were used. A double digest was performed where the buffers for each enzyme were compatible. Alternatively, two single digests were used, the sample was extracted with phenol and then ethanol precipitated after the first digest, and then digested with the second enzyme. When larger amounts of DNA were digested, the amount of restriction endonuclease and buffer used was increased proportionally, and the restriction was incubated overnight.

2.5.5 Electroelution & purification of DNA bands from agarose gels

DNA fragments were recovered from agarose gels by electroelution into dialysis tubing. Sufficient DNA was digested so that ~1µg of the fragment of interest was obtained. Fragments were separated on an agarose gel by electrophoresis. The fragment of interest was identified under UV light and excised from the gel with a sterile scalpel. The piece of gel containing the fragment of interest was placed inside a length of pre-treated dialysis tubing, which was clamped at one end with a Mediclip. T.E. buffer was added to the dialysis tubing so as to just cover the gel slice, and the tubing was sealed with another Mediclip. The dialysis tubing was then placed in an electrophoresis tank and submerged in 1X TBE buffer. A voltage of 150V was passed through the gel for 10-15 minutes, allowing the DNA to be electroeluted from the gel into the dialysis tubing. The buffer from the tubing (containing the DNA) was

carefully removed using a pipette to a sterile eppendorf tube. The DNA sample was subsequently processed as detailed in section 2.5.1.

2.5.6 Ligation of plasmid and insert DNA

T4 DNA ligase (Promega) was used to ligate plasmid vector and insert DNA with cohesive termini. A 1:3 molar ratio of vector to insert was used unless otherwise stated. Typical ligation reactions used 100ng of plasmid vector. The final reaction volume was 20µl; 2µl ligase buffer and 0.6µl T4 DNA ligase (1.8 units) were added. The reaction was incubated at 16°C overnight. 5µl of the ligation reaction was used to transform competent *E.coli* cells.

2.5.7 Transformation of competent *E.coli* cells

a. Preparation of competent *E.coli* cells

Competent *E.coli*, strain DH5α was prepared using the Ca/Mn method. A glycerol stock of *E.coli* DH5α was streaked on LB media and incubated at 37°C overnight. A single colony from the resulting plate was used to inoculate 5ml of 2XL medium, and incubated at 37°C with vigorous shaking (1000 rpm) overnight. 1ml of this starter culture was used to inoculate 100ml of 2XL medium (pre-warmed to 37°C) and incubated at 37°C with gentle shaking until an OD₆₀₀ of ~2.0 was reached. 1M MgCl₂ was then added to a final concentration of 20mM, and the culture was allowed to grow until it reached an OD₆₀₀ of 0.5. Bacterial growth was stopped by chilling in ice-water for 1-2 hours. The culture was then centrifuged at 3,000 rpm for 5 minutes at 4°C, and the supernatant discarded. The bacterial pellet was gently re-suspended in 50ml of freshly prepared and filter sterilized ice-cold Ca/Mn medium, and stored on ice for 1-2 hour. The solution was centrifuged at 2,500 rpm for 5 minutes and the pellet was gently re-suspended in 5ml of ice-cold Ca/Mn medium containing 15% (v/v) sterile glycerol. The prepared cells were dispensed into 200µl aliquots in Eppendorf tubes pre-cooled with liquid nitrogen and snap frozen. Competent *E.coli* cells were stored at -80°C until use.

b. Transformation of competent *E.coli* cells

Competent *E.coli* cells were allowed to partially thaw on ice. 5µl (from 20µl) of a ligation reaction was added to a 200µl aliquot of competent *E.coli* cells and mixed gently, and then kept on ice for 30 minutes. The sample was heated to 42°C for 90 seconds only and then snap cooled on ice for 1-2 minutes. 800µl of LB medium (pre-warmed to 37°C) was added prior to incubation at 37°C for one hour with moderate shaking (200 rpm). The transformation was plated on several selective media plates and left until the culture was absorbed into the media plate. Plates were then inverted and incubated at 37°C overnight. Typical transformation efficiencies were in the order of $> 10^7$ colonies.µg⁻¹ of plasmid DNA.

2.5.8 Colony PCR to screen transformants

A single colony from a selective media plate representing a potentially successful transformant was picked with a sterile toothpick and dipped in 25µl of TE buffer. The sample was boiled for 2 minutes and then spun down at 13,000 xg for 2 minutes. 2µl of this preparation was added to a standard 25µl PCR reaction; 1X Go Taq Flexi buffer, 2mM MgCl₂, 0.2mM dNTP mix, 1 unit of Go Taq Polymerase and 0.5mM of each forward and reverse primer specific to the insert of interest. The thermal cycle was 95°C for 5 mins; 35 cycles of 94°C for 40 seconds, 55°C for 40 seconds and 72°C for 2.5 mins; 72°C for 10 mins; cooling to 4°C, unless otherwise stated. Colony PCRs were checked on agarose gel against a positive control PCR.

2.5.9 Storage of bacteria as Glycerol stocks

A single bacterial colony of interest was used to inoculate 5ml of selective media, which was grown overnight (usually at 37°C) with moderate shaking. Two selective media agar plates were spread with 100µl of this culture and incubated overnight. Bacteria were scraped from these plates and re-suspended in 500µl of sterile LB medium in a screw-cap tube using aseptic technique. The suspension was mixed thoroughly before 500µl of 80% glycerol (v/v) was added and mixed by vortexing.

The glycerol stock was immediately plunged in liquid nitrogen and subsequently stored at -80°C.

2.6 Generation of Transgenic Plants

2.6.1 Tri-parental mating of *Agrobacterium tumefaciens*

Colonies from cultures of the *Agrobacterium tumefaciens* strain LBA4404, *E. coli* HB101 containing the helper plasmid pRK2013, and *E. coli* DH5 α containing the recombinant binary vector (pBIN19R-) were used to inoculate 5ml cultures of selective media. *A. tumefaciens* was grown in LB media containing 500 $\mu\text{g}.\text{ml}^{-1}$ streptomycin and 100 $\mu\text{g}.\text{ml}^{-1}$ rifampicin at 30°C overnight. Overnight cultures of *E. coli* pRK2013 and *E. coli* pBIN19R were grown separately in LB media supplemented with 50 $\mu\text{g}.\text{ml}^{-1}$ kanamycin at 37°C overnight. 400 μl of each culture was subsequently transferred to individual sterile Eppendorf tubes, and washed three times with sterile LB medium. The three cultures were then combined in a single Eppendorf tube, and plated on two LB plates (no antibiotics) and incubated at 30°C overnight. Bacterial cells were then scraped from these plates and re-suspended in 5ml T.E. buffer. Several serial dilutions were made with T.E. buffer, and plated on LB media containing 500 $\mu\text{g}.\text{ml}^{-1}$ streptomycin, 100 $\mu\text{g}.\text{ml}^{-1}$ rifampicin and 50 $\mu\text{g}.\text{ml}^{-1}$ kanamycin. Colonies which appeared on these plates after 2-3 days were then checked for the expected insert by Southern blotting.

2.6.2 DNA extraction from *Agrobacterium tumefaciens*

Glycerol stocks of recombinant *Agrobacterium tumefaciens* were streaked on LB medium supplemented with 500 $\mu\text{g}.\text{ml}^{-1}$ streptomycin, 100 $\mu\text{g}.\text{ml}^{-1}$ rifampicin and 50 $\mu\text{g}.\text{ml}^{-1}$ kanamycin, and incubated at 30°C for 1-2 days. A single colony was taken and used to inoculate 5ml of LB liquid media containing the same antibiotics, and grown overnight at 30°C. Subsequently, 1.5ml of the culture was removed to a sterile Eppendorf tube and centrifuged at 13,000xg for 5 minutes. The bacterial pellet was re-

suspended in 300µl TE buffer (pH 7.6), and 100µl 5% sarkosyl (v/v) (Sigma) was added and gently mixed. 150µl 5µg.ml⁻¹ Protease (Promega) was then added, and incubated at 37°C for 1 hour. Next, 500µl of phenol: chloroform: IAA was added and the sample was passed through a 19 gauge needle (Terumo Neolus, Belgium) several times to shear viscous chromosomal DNA, until it passed through the needle freely. The sample was then centrifuged at 13,000xg for 5 minutes, and the supernatant was extracted with an equal volume of phenol: chloroform: IAA and a further three times with chloroform: IAA to remove proteins. The *Agrobacterium* DNA was then precipitated by the addition of 0.1 volume of 3M sodium acetate (pH 5.6) and 2 volumes of ice-cold ethanol, and kept at -70°C for 1-2 hours. After centrifugation at 13,000xg for 10 minutes, the supernatant was discarded and the pellet washed with 70% (v/v) ethanol, air-dried and re-suspended in 50µl dH₂O.

2.6.3 Southern blotting and hybridization to screen transformants

a. Capillary transfer of DNA to nylon membranes

Capillary transfer was used to transfer DNA fragments from agarose gels to Hybond nylon membranes (Amersham Pharmacia Biotech, Buckinghamshire, UK). DNA fragments were run on an agarose gel using the standard protocol (section 2.4.6). After electrophoresis, the gel was photographed under UV, with a transparent ruler so that the distance each band had migrated on the gel could be measured. The gel was placed in a glass dish and the DNA denatured by soaking in denaturation solution for 45 minutes with gentle agitation. After rinsing with dH₂O, the gel was soaked in neutralization solution for 30 minutes with gentle agitation. Fresh neutralization solution was added and the gel agitated for a further 15 minutes.

A blot based on a solid support (Figure 2.1) was prepared, and placed in a reservoir of 20X SSC until the liquid almost reached the top of the support. Two sheets of Whatmann 3MM paper (Whatmann International Ltd, Maidstone, UK) wetted with 20X SSC were placed on top of the support. The support was surrounded with cling film to prevent flooding the blot with SSC from the reservoir. The pre-treated gel was placed directly on top of the wetted papers. A piece of Hybond nylon membrane,

1mm larger than the gel on each side was immersed in 20X SSC for a few minutes and used to cover the gel, taking care to remove air bubbles. Another two sheets of wetted 3MM paper (the same size as the gel) were added on top of the membrane, followed by three dry sheets of Whatmann 3MM chromatography paper. A stack of paper towels and a 500g weight were placed on top of the blot to promote the uptake of buffer, through the gel and into the paper towels. The capillary transfer was continued for 16-24 hours at 4°C. The paper towels and 3MM papers above the gel were then removed. The nylon membrane was marked to indicate the orientation of the gel, removed from the support and placed on board covered with wetted 3MM paper. The DNA was cross-linked to the nylon membrane through a short exposure to UV in a UV crosslinker (UVP products, San Gabrielle, USA) and then baked in an oven at 80°C for 1 hour. The membrane was stored at room temperature under low humidity until required. The used gel was then soaked in 0.5 $\mu\text{g}.\text{ml}^{-1}$ ethidium bromide to assess the efficiency of DNA transfer from the gel to the membrane.

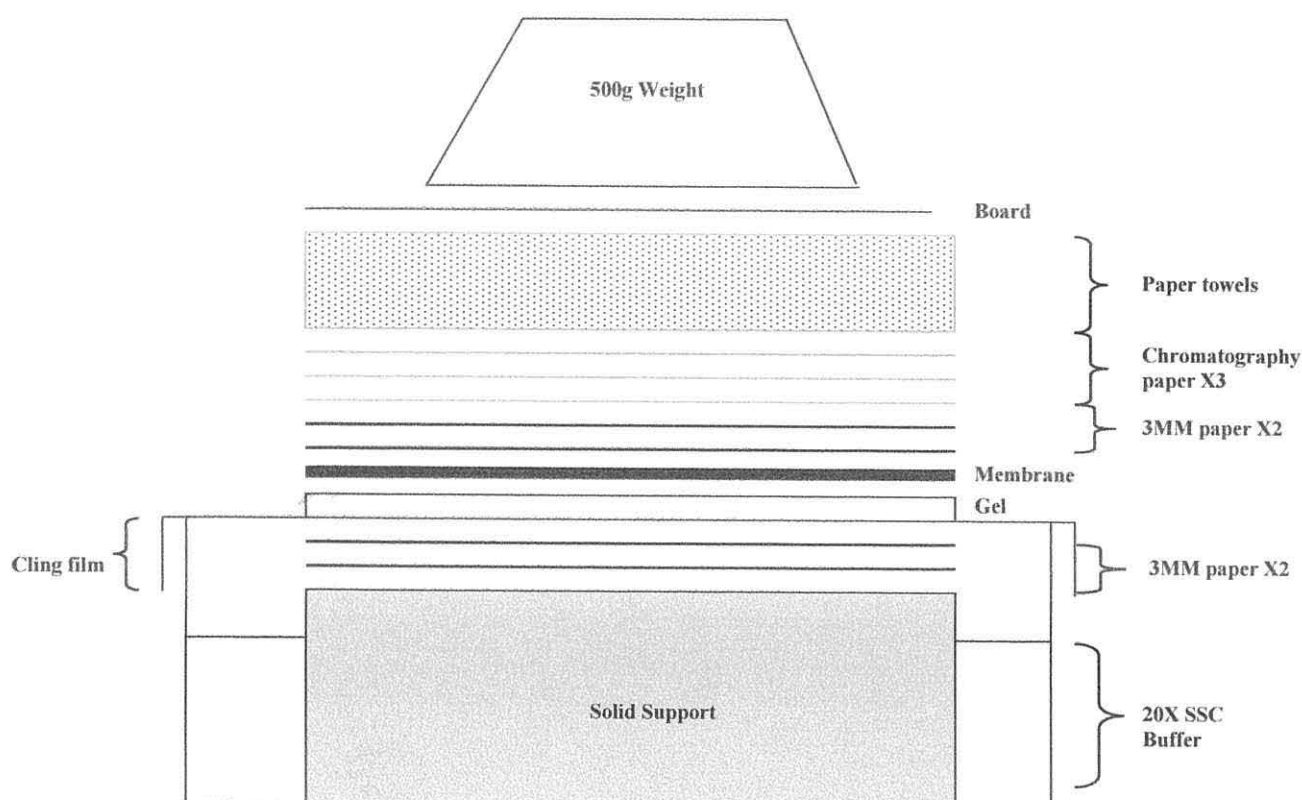


Figure 2.1: Blotting apparatus for capillary transfer of DNA to nylon membranes.

b. DNA hybridization

DNA hybridization was carried out in a Techne FHB11 hybridizer oven (Techne, Cambridge, UK) using Techne hybridization tubes. The nylon membrane was first soaked in 5X SSC for 20 minutes. The SSC was replaced with 30-50ml pre-hybridization solution and incubated at 65°C for 2 hours. The pre-hybridization solution was removed and 25-30ml hybridization solution containing labeled denatured probe was added. Hybridization was continued for 16-24 hours at 65°C. Following hybridization, the membrane was washed for an hour with each of a series of increasingly stringent washes; 3X SSC, 1X SSC, 0.5X SSC, each with 0.1% SDS (v/v). The membrane was then heat sealed in a plastic bag and placed in an intensifying screen.

c. Radioactive labeling of DNA probes

The protocol used was based on the method of Feinberg & Vogelstein (1983) for labeling of DNA restriction endonuclease fragments. 50-100ng of DNA to be labeled was made up to 34µl with dH₂O and denatured by boiling for 7 minutes, and then snap cooled on ice. The DNA mixture was added to 10µl OLB and mixed. This was combined with 3µl 370 MBq.ml⁻¹ deoxycytidine 5'-[α-³²P]triphosphate, triethylammonium salt) and 1µl 5U.ml⁻¹ DNA polymerase I large (Klenow) fragment (Epicentre,UK), and then incubated at 37°C for 3-4 hours. Subsequently unincorporated radioisotope was separated from labeled probe by gel filtration through a 1ml Sephadex G-50 column. The labeled DNA probe was stored at -20°C until required. Prior to use, the probe was denatured by boiling for 7 minutes and then snap cooled on ice.

d. Imaging

Intensifying screens were viewed using a Bio-Rad Molecular Imager (Bio-Rad, Hercules, USA) a phosphor imager with associated software, Quantity One for analysis (Bio-Rad, Hercules, USA). Files were exported as jpeg files.

2.6.4 *Arabidopsis* plant transformation by the floral dip method

Arabidopsis thaliana plants were transformed by the floral dip method, a technique used for *Agrobacterium*-mediated transformation, which was conceived by Bechtold *et al* (1993) and modified by Clough & Bent (1998). The protocol used was based on that of Logemann *et al* (2006), which removes the need for large-scale bacterial cultures.

Arabidopsis thaliana *Ws* plants were grown in individual pots covered with fine netting, one plant per pot until they flowered. The first inflorescence bolts were clipped to encourage proliferation of secondary bolts. Plants were ready for transformation 4-6 days after clipping, when bolts were 2-10cm in height and had only a few open flowers. A single *Agrobacterium tumefaciens* colony was re-suspended in 100µl of dH₂O, and plated on LB medium supplemented with 500µg.ml⁻¹ streptomycin, 100µg.ml⁻¹ rifampicin and 50µg.ml⁻¹ kanamycin. The plate was incubated for 2-3 days at 30°C. Bacteria were scraped from the plate and re-suspended in 30ml of sterile LB media until the OD₆₀₀ reached ~2.0. The bacteria were then added to 120ml of 5% sucrose (w/v) solution supplemented with 0.05% Silwet L-77 (v/v) (Lehle seeds, Round Rock, USA). Five plants per transformation were dipped in the solution containing *Agrobacterium* so that all aerial parts of the plant were evenly covered. The dipped plants were placed on their side and covered for 16-24 hours. After this time, plants were placed upright and kept under standard growth conditions. The treatment was repeated one week later, after which plants were grown under standard growth conditions until maturity. Seeds were harvested and dried.

2.6.5 Selection of transgenic *Arabidopsis thaliana* plants

Seeds from transformed plants were surface sterilized as detailed in section 2.2.2 and sown on half-strength MS media supplemented with kanamycin for selection of transformants. Sterilized seed (section 2.2.2) was plated on half-strength MS basal salt media supplemented with sucrose and 35µg.ml⁻¹ kanamycin, stratified in darkness at 4°C for three days, and then removed to growth room conditions. Wild-type seeds

were grown on media supplemented with kanamycin as a control; after germination, wild-type seedlings bleached and died on this media. After 14 to 21 days under growth room conditions the number of transgenic seedlings surviving on media supplemented with kanamycin was recorded. These seedlings were subsequently transferred to soil as outlined in section 2.2.2.

2.6.6. Extraction of plant genomic DNA

The protocol for extraction of genomic DNA from plant tissues was a scaled-down version of that described by Doyle & Doyle (1987). Leaf tissue (0.25-0.75g) was harvested from the plant and stored in liquid nitrogen. Frozen tissue was ground to a fine powder in a sterile Eppendorf tube with a plastic pestle and homogenized with 1ml CTAB buffer (pre-heated to 60°C). Samples were incubated at 60°C for 30 minutes, with occasional mixing. One volume of chloroform: IAA was added, and samples were mixed on a rotating wheel for 15 minutes. After centrifugation at 7,500xg for 10 mins, the aqueous phase was transferred to a new tube, and 0.7 volumes of ice-cold isopropanol was added. The DNA was pelleted by centrifugation for 1 min at 12,000xg. The pellet was washed with 500µl wash buffer and incubated on ice for 30 minutes. Prior to removing the wash buffer, the sample was pulse spun to recover the DNA pellet. The pellet was air dried and then re-suspended in 100µl of TE buffer (pH 7.6). RNase (10µg.ml⁻¹) was then added to remove RNA contamination, and incubated at 37°C for 2 hours. The DNA was precipitated with 20µl 10M filter-sterilized ammonium acetate and 240µl ice-cold absolute ethanol, and incubated at –70°C for 1-2 hours. A subsequent centrifugation at 12,000xg for 2 minutes isolated the DNA, which was washed with 70% ethanol (v/v). The DNA pellet was air dried and re-suspended in 25µl TE buffer (pH 7.6).

3. PHENOTYPIC ANALYSIS OF *ARABIDOPSIS* PLANTS SUBJECTED TO WIND/MECHANICAL STRESSES

3.1 Introduction

This chapter outlines various methods that were used to simulate wind and mechanical stress. The aim of these studies was to establish growth conditions that gave rise to a significant change in phenotype when *Arabidopsis* plants were subjected to wind and mechanical stresses.

3.1.1 Simulating wind/mechanical stresses

A number of researchers have previously sought to simulate wind and mechanical stress under laboratory conditions. Some of the methods used are summarised below.

a.) **Wind stress:** Fans and wind tunnels have been used to directly simulate the effect of wind on plants. Box fans have been used under various regimes depending on the species being investigated, for example 2hrs/day in cucumber (Moran & Cipollini, 1999) and 6hrs/day and 16hrs/day in *Arabidopsis* (Pigliucci, 2002). Pigliucci (2002) did not observe a significant reduction in height or delay in flowering in 11 natural accessions of *Arabidopsis thaliana* which were exposed to wind. However, wind did influence the degree of branching in these accessions, resulting in a “bushy” or highly branched phenotype. The author concluded that the wind speed generated by the fan (1.8 m/s) might have been insufficient to induce widespread phenotypic changes. This wind speed is comparable to a “natural” British average wind speed of 4.5 m/s (Retuerto & Woodward, 1992). Retuerto & Woodward (1992) suggested that wind operates in a logarithmic manner; with little effect at lower wind speeds and a much greater effect at higher wind speeds.

Wind tunnels have been used to simulate wind conditions on a larger scale. It is possible to approximate wind and other environmental variables in a wind tunnel. White mustard (*Sinapis alba*) was grown in wind tunnels at velocities of 0.3 m/s

(control), 2.2 m/s and 6.0 m/s for 42 days (Retuerto & Woodward, 2001). This study considered the impacts of both wind and plant aging, and found that interactions between wind speed and plant age affected growth and biomass allocation of white mustard. These results highlight the need to consider the long-term responses to wind stress; it cannot be assumed that short-term responses to wind stress reflect the long-term responses and adaptation to wind stress.

b.) **Vibration stress:** There have been relatively few studies using vibration as a mechanical stress stimulus. An advantage of studying the vibratory stimulus is that it can be quantified in terms of both frequency and amplitude (Johnson *et al*, 1998). Takahashi *et al* (1991) applied vibration stress to seedlings via a bass speaker, adapted by the addition of a loading tray for plants. Vibration at 50Hz promoted the growth of rice and cucumber seedlings. Shoot growth was promoted when vibration was applied from imbibition but not when it was applied from two days of age or at the two-leaf stage. Elongation of roots was promoted when vibration was applied at every stage. From this research Takahashi *et al* (1991) proposed that the promotion of shoot growth by vibration might be limited to the early stages of growth. Furthermore, it was suggested that the effects of various frequencies of vibration on growth required to be studied in order to determine whether the effects of vibration differed significantly from those induced by gyratory shaking.

In *Arabidopsis* ecotype Columbia, vibration of seedlings at 50Hz for 72 hours from germination resulted in an enhanced hypocotyl elongation rate (Johnson *et al*, 1998). Further studies in the Columbia ecotype found that vibration at frequencies greater than 70Hz increased the rate of seed germination (Uchida & Yamamoto, 2002). However, no data on the subsequent development of these seedlings was presented. It has been suggested that the amyloplast is likely to play a role in the perception of vibration, as it does in the perception of gravity stimulation (Uchida & Yamamoto 2002). Gravity induces the acceleration of starches and sediments in the amyloplast; in the *Arabidopsis pgm* mutant, which lacks fully developed amyloplasts, the increased rate of germination of vibrated wild type seedlings was eliminated (Uchida & Yamamoto 2002).

c.) **Seismic stress:** Seismic stress (by shaking of the entire shoot on modified laboratory shakers) has also been used to mimic mechanical stress. Beyl & Mitchell (1977, 1983) are exponents of this method. They developed 'Automated Mechanical Oscillatory Shaking' devices (AMOS). These devices are laboratory shakers that are modified by the addition of multiple platforms, and thus have a capacity to shake many plants simultaneously. The AMOS shaking devices were conceived with a potential commercial application, which was the mass mechanical conditioning of plants. Chrysanthemum (1977) and sunflower (1983) plants were initially shaken on these AMOS devices. Studies of Chrysanthemum plants using AMOS showed that the early morning was the most effective time for shaking in terms of inducing a dwarfed phenotype (Mitchell, 1996). Rotary shakers are now commonly used to induce seismic stress. Shaking of tomato plants on a gyratory shaker at 282 rpm daily resulted in dwarfed plants (Mitchell *et al*, 1975). Furthermore, in every crop species that seismic stress has been studied, shaking has resulted in a yield reduction to some degree.

d.) **Thigmic stress:** Brushing, rubbing, flexing and touching plants induce thigmomorphogenesis. Cipollini (1999) brushed *Brassica napus* plants resulting in decreases in height, increases in stem thickness and increases in stem mass. Goodman & Ennos (2001) investigated the effect of thigmic stress on roots of maize. Roots of flexed plants were thicker and more numerous than those of plants that were not flexed. Thigmomorphogenesis is not restricted to the part of the plant to which the stress is applied; in bean (*Phaseolus vulgaris*) plants, rubbing of the first internode inhibits elongation of the other internodes (Erner *et al*, 1980). However, changes in internode length are less conspicuous the further from the internode where stress was applied. One disadvantage of contact methods of applying stress is their potential to cause tissue damage, which may promote susceptibility to pathogen attack.

3.1.2 Phenotypic analysis of *Arabidopsis* plants

Functional analysis of genes has gained momentum since the sequencing of the *Arabidopsis* genome, and has created a need for rapid and accurate phenotypic analysis. Boyes *et al* (2001) devised a model for phenotypic analysis based on the developmental growth stages of *Arabidopsis*. The growth stages used to perform an analysis are based on the BASF, Bayer, Ciba-Geigy, Hoechst (BBCH) scale conceived by Lancashire *et al* (1991), and cover the development of *Arabidopsis* from imbibition of seed to maturation of plants. The model generates two distinct analyses, a plate-based phenotypic analysis monitoring seedling development, and a soil-based phenotypic analysis monitoring plant development to maturation. These analyses can be used to detect phenotypic changes resulting from ecotypic distinctions and from exposure to stresses (Boyes *et al*, 2001). A growth stage based phenotypic analysis, based on Boyes *et al*'s (2001) growth stages and outlined in the Materials & Methods (section 2.2.3), was used to monitor seedlings and plants subjected to wind and mechanical stresses. In the initial studies, the effects of wind and mechanical stresses were monitored in both Ws-0 (Ws) and Col-0 (Col) wild-type *Arabidopsis* accessions so that any differences in response between the different ecotypes could be detected.

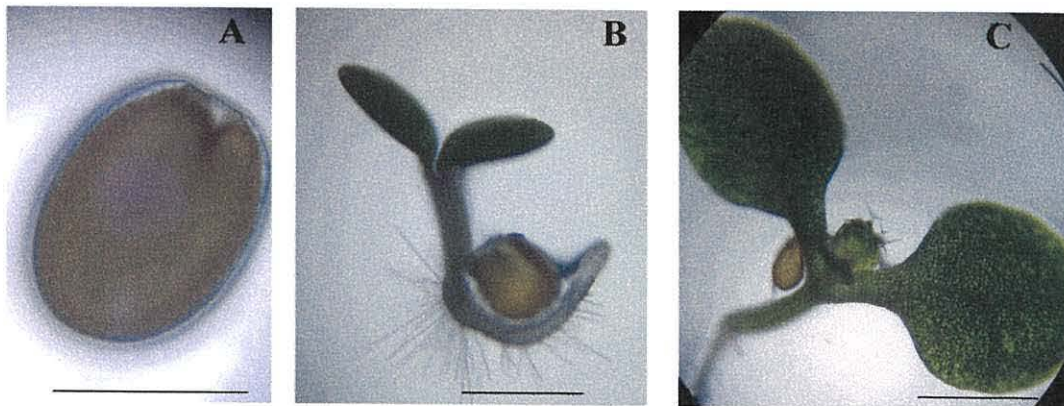


Figure 3.1: Growth stages where mechanical stresses were applied.

A. Imbibition: the seed was stratified under darkness at 4°C and has just been moved to growth room conditions. **B.** Germination: both cotyledons have fully emerged. **C.** Two-leaf stage: the first two true leaves are emerging. Scale bar is equal to 1mm in each picture.

3.2 Phenotypic analysis of *Arabidopsis* seedlings subjected to mechanical stresses

3.2.1 Vibration stress

Vibration at 40Hz (section 2.2.4a) was applied for 72hrs constantly from imbibition, germination or the two-leaf stages of development (shown pictorially in Figure 3.1) in Col and Ws seedlings. In a subsequent experiment, different frequencies of vibration (40Hz – 70Hz) were applied from the germination stage of development. Seedlings vibrated at 40Hz reached each of the principal stages of development as far as the two leaf-stage (stage 1.0) at approximately the same time as the unstressed seedlings (data not shown).

a) Hypocotyl elongation in seedlings subjected to vibration stress

Hypocotyl elongation at 14-days was promoted in Col seedlings when they were subjected to 72 hours of vibration from germination (Figure 3.2), and in Ws seedlings when they were subjected to 72 hours of vibration from germination or the two-leaf stages of development (Figure 3.3). Vibration applied at imbibition in these ecotypes resulted in increased hypocotyl elongation but it was not significantly greater than that in the unstressed control. The greater hypocotyl elongation observed in response to vibration applied from germination was also seen when the vibration frequency was increased in the range of 40Hz to 70Hz (Figure 3.4). However, hypocotyl elongation did not increase sequentially with the increase in vibration frequency.

b) Root elongation in seedlings subjected to vibration stress

Root elongation at 14-days of *Arabidopsis* seedlings subjected to vibration stress was not significantly different from that of unstressed seedlings in Col, or in Ws as shown in Figure 3.5. In the Ws ecotype, the roots of vibrated seedlings were generally shorter than those of the unstressed control.

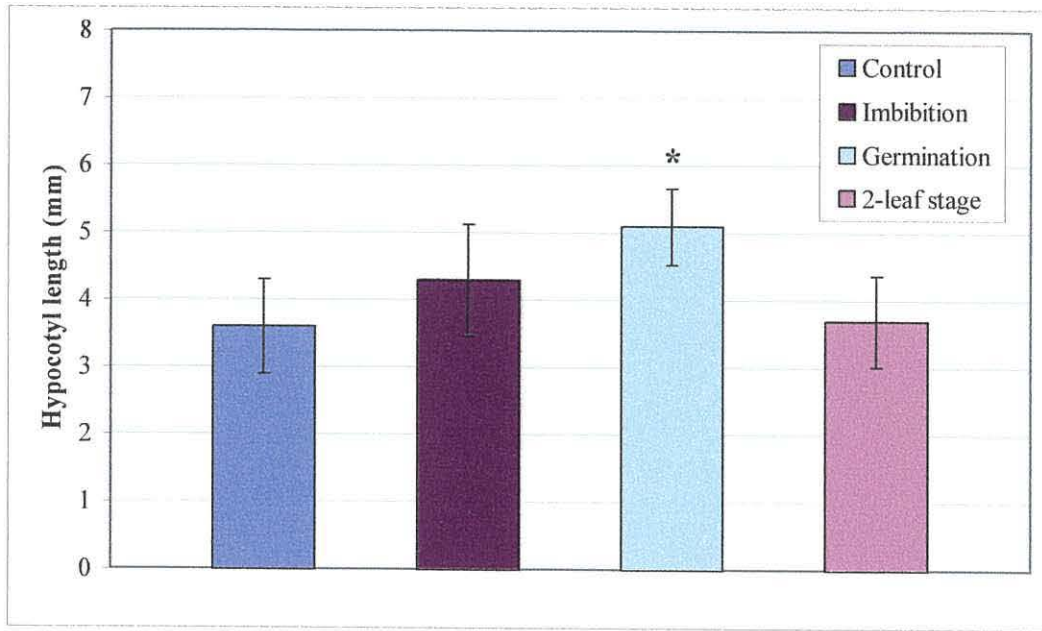


Figure 3.2: Hypocotyl elongation at 14-days old of *Arabidopsis* Col seedlings subjected to vibration stress.

Vibration stress (40Hz) was applied for 72 hours from imbibition, germination or the 2-leaf stages of development. Values are \pm SD of 20 seedlings. * Indicates results with $\geq 95\%$ significance as determined by an ANOVA with a Dunnett test.

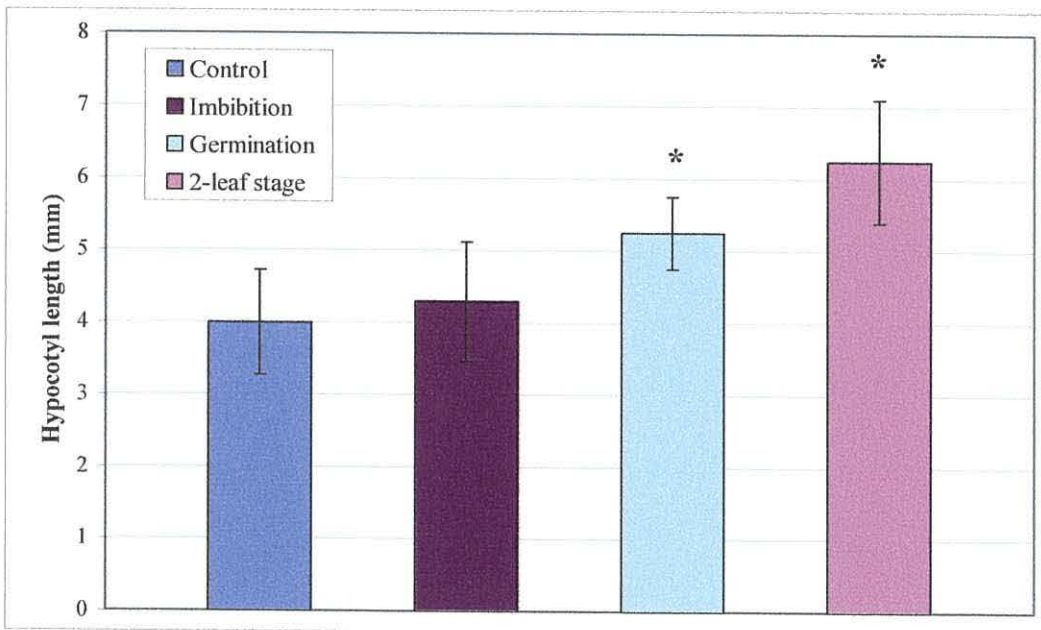


Figure 3.3: Hypocotyl elongation at 14-days old of *Arabidopsis* Ws seedlings subjected to vibration stress.

Vibration stress (40Hz) was applied for 72 hours from imbibition, germination or the 2-leaf stages of development. Values are \pm SD of 20 seedlings. * Indicates results with $\geq 95\%$ significance as determined by an ANOVA with a Dunnett test.

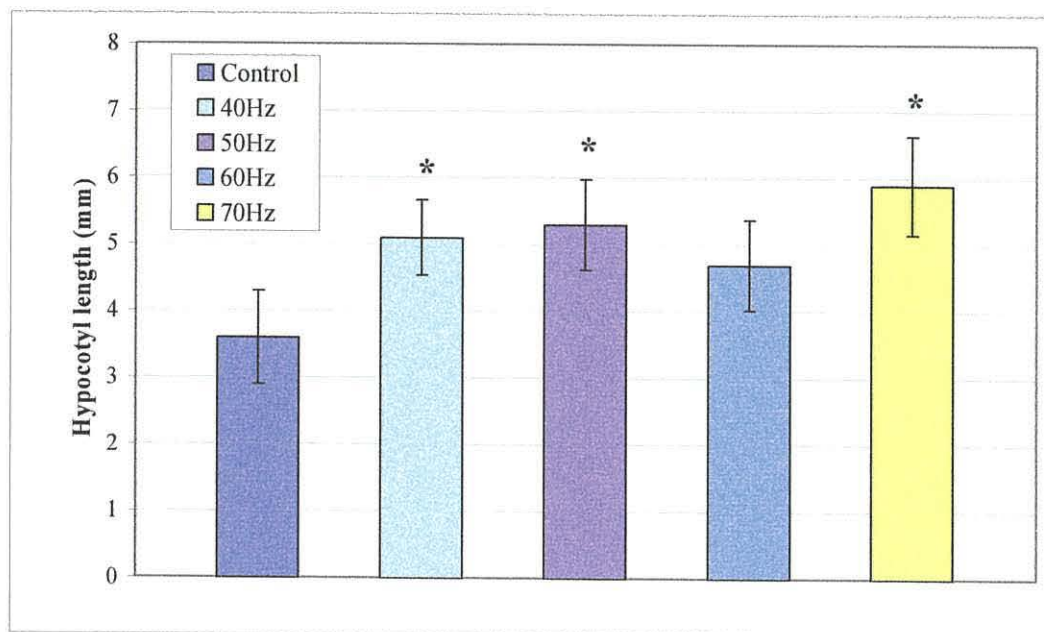


Figure 3.4: Hypocotyl elongation at 14-days old of *Arabidopsis Col* seedlings subjected to increasing intensities of vibration stress.

Vibration stress was applied for 72 hours from germination. Values are \pm SD of 20 seedlings.* Indicates results with $\geq 95\%$ significance as determined by an ANOVA with a Dunnett test.

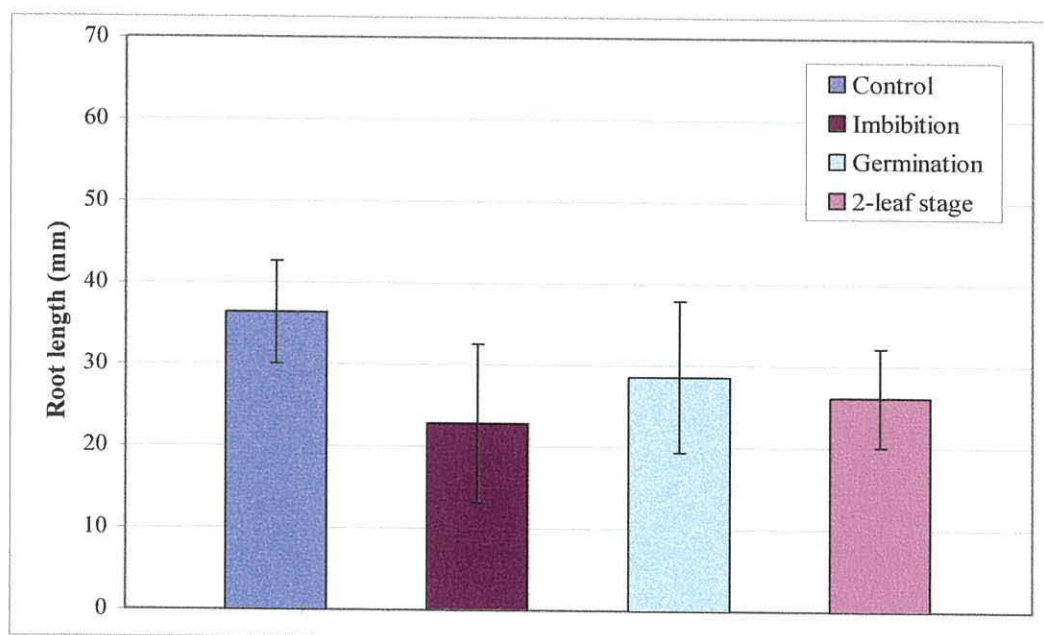


Figure 3.5: Root elongation at 14-days old of *Arabidopsis Ws* seedlings subjected to vibration stress.

Vibration stress (40Hz) was applied for 72 hours from imbibition, germination or the 2-leaf stages of development. Values are \pm SD of 20 seedlings.

* Indicates results with $\geq 95\%$ significance as determined by an ANOVA with a Dunnett test.

3.2.2 Seismic stress

Plates containing *Arabidopsis* Col seedlings were placed on a gyratory laboratory shaker (section 2.2.4b) for 72hrs constantly from imbibition, germination or the two-leaf stages of development (Figure 3.1).

a) Hypocotyl elongation in seedlings subjected to seismic stress

Hypocotyl elongation in seedlings subjected to seismic stress for 72 hours from germination was greater than that seen in unstressed control seedlings (Figure 3.6). Where seismic stress was applied from imbibition or the two-leaf stage hypocotyl elongation was not significantly different from that seen in the control. These results were similar to those seen when vibration was applied to seedlings at each of these stages in the Col ecotype.

b) Root elongation in seedlings subjected to seismic stress

Root elongation of seedlings was also not significantly affected by exposure to seismic stress when it was applied at imbibition or the two-leaf stages of development (Figure 3.7). However, root elongation was inhibited when seedlings were subjected to seismic stress for 72 hours from germination. Although root elongation was not significantly inhibited in vibrated seedlings, as is the case in seedlings subjected to seismic stress, the data suggests these stresses are more likely to inhibit rather than promote root elongation.

3.2.3 Gravity stimulation

It has been suggested that the sensing of vibration stress is similar to that of gravity stimulation, as outlined in the introduction to this chapter. *Arabidopsis* Ws seedlings were subjected to transient gravity stimulation so that the phenotype of these seedlings could be compared to that of vibrated seedlings. Plates of wild-type *Arabidopsis* seedlings were clamped at 135°; continuous gravity stimulation at this angle was applied for 72 hours from germination. The lengths of the primary roots and hypocotyls of both stressed and unstressed control seedlings were measured at 14-days. Seedlings that were subjected to gravity stimulation for 72 hours from germination developed longer hypocotyls and roots by 14-days.

a) Hypocotyl elongation in seedlings subjected to gravity stimulation

Hypocotyls of seedlings subjected to gravity stimulation were significantly longer than those of unstressed control seedlings (Figure 3.8). This result was similar to that found when *Arabidopsis* Ws seedlings were subjected to vibration stress.

b) Root elongation in seedlings subjected to gravity stimulation

Similarly to vibrated seedlings, where root elongation was unaffected by the mechanical stimulus; the root elongation of seedlings subjected to gravity stimulation was not significantly affected (Figure 3.9). However, the average root length of gravistimulated seedlings is greater than in unstressed seedlings; the trend is towards promotion of root elongation by gravity stimulation.

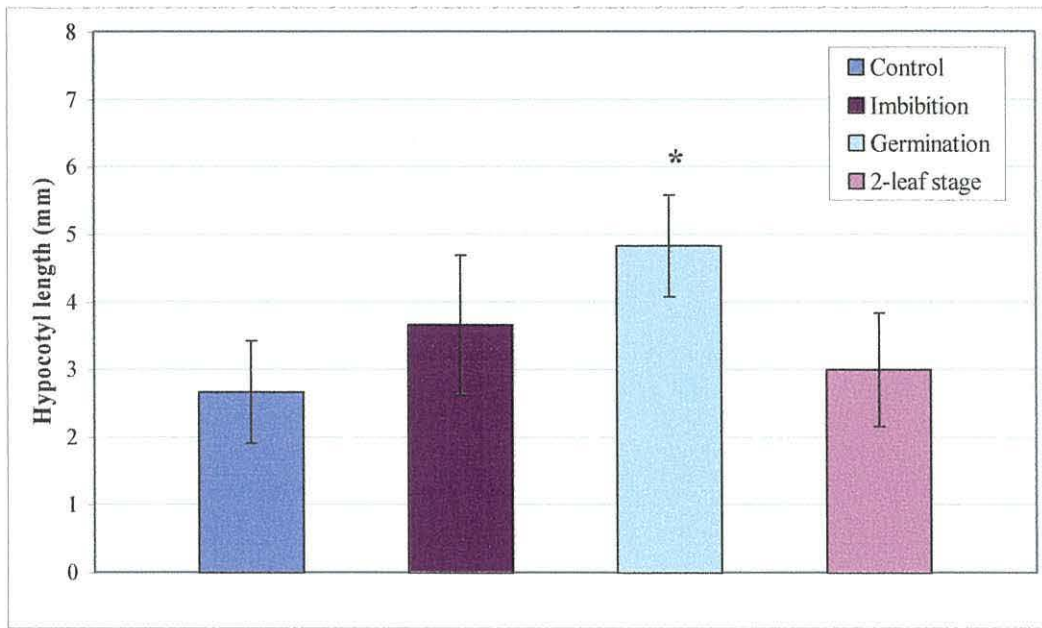


Figure 3.6: Hypocotyl elongation at 14-days old of *Arabidopsis* Col seedlings subjected to seismic stress.

Seismic stress (600 rpm) was applied for 72 hours from imbibition, germination or the 2-leaf stages of development. Values are \pm SD of 20 seedlings. * Indicates results with $\geq 95\%$ significance as determined by an ANOVA with a Dunnett test.

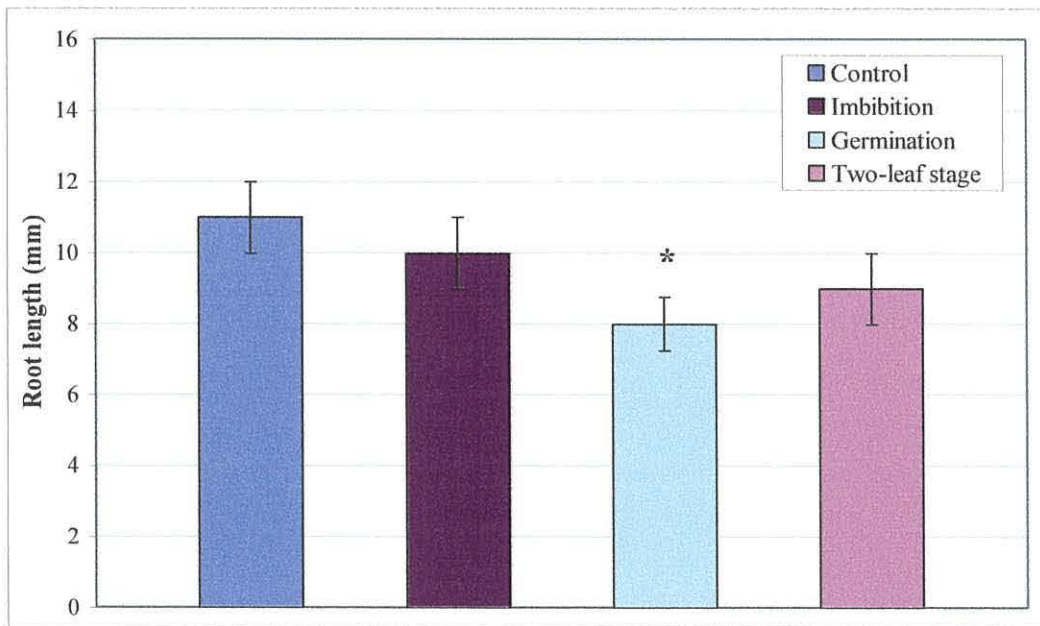


Figure 3.7: Root elongation at 14-days old of *Arabidopsis* Col seedlings subjected to seismic stress.

Seismic stress (600 rpm) was applied for 72 hours from imbibition, germination or the 2-leaf stages of development. Values are \pm SD of 20 seedlings.

* Indicates results with $\geq 95\%$ significance as determined by an ANOVA with a Dunnett test.

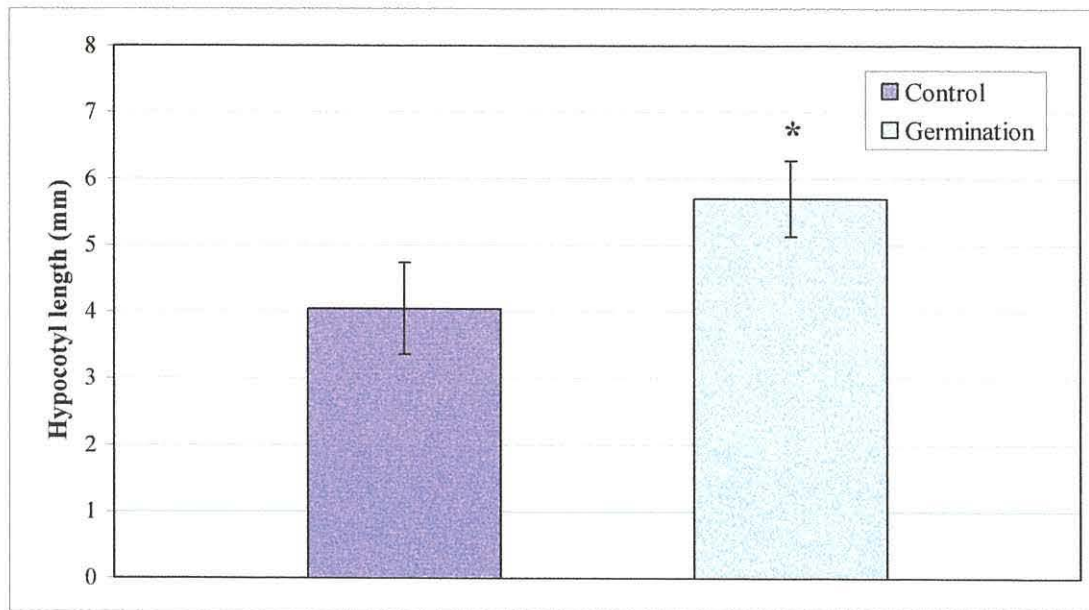


Figure 3.8: Hypocotyl elongation at 14-days old of *Arabidopsis* Ws seedlings subjected to gravity stimulation.

Gravity stimulation (135°) was applied for 72 hours from germination. Values are \pm SD of 20 seedlings. * Indicates results with $\geq 95\%$ significance as determined by a Student t-test.

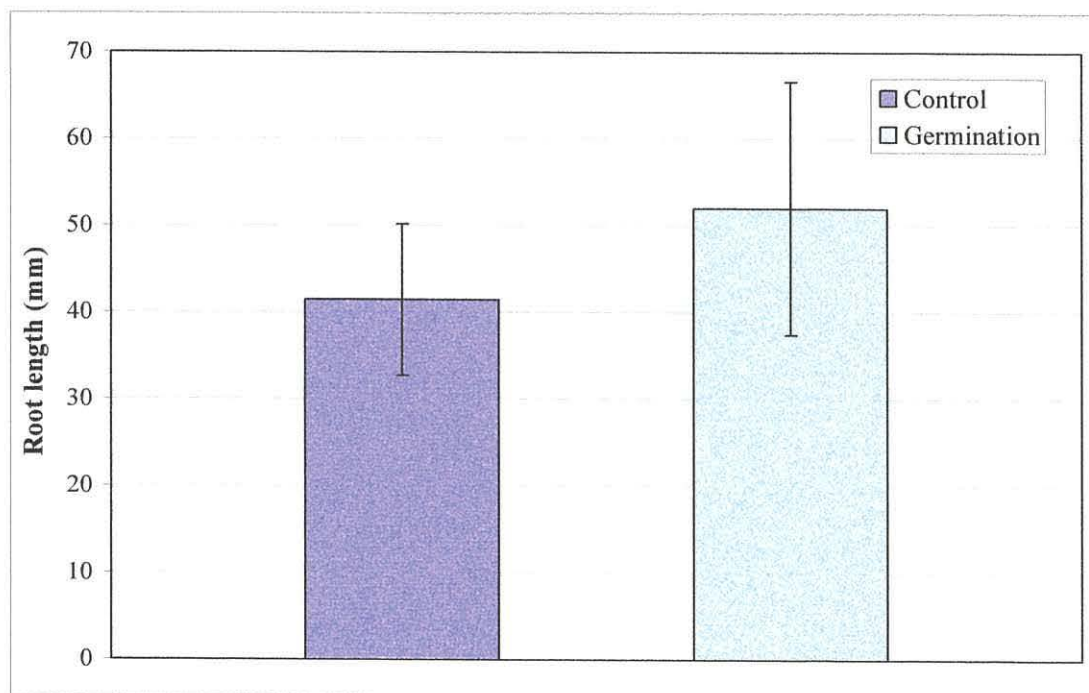


Figure 3.9: Root elongation at 14-days old of *Arabidopsis* Ws seedlings subjected to gravity stimulation.

Gravity stimulation (135°) was applied for 72 hours from germination. Values are \pm SD of 20 seedlings. * Indicates results with $\geq 95\%$ significance as determined by a Student t-test.

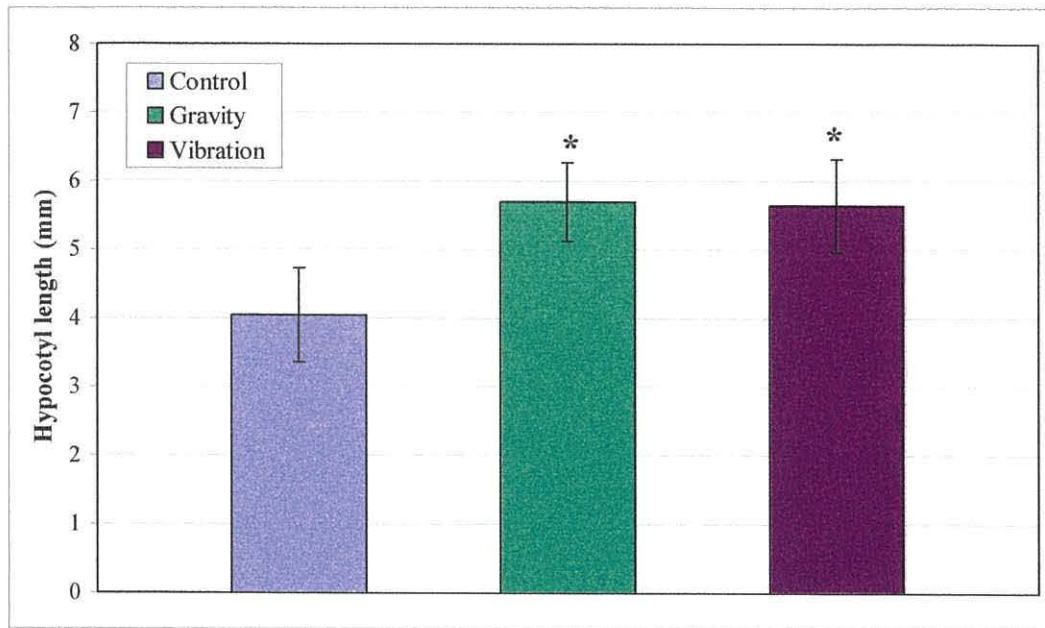


Figure 3.10: Comparison of hypocotyl elongation at 14-days old in *Arabidopsis* seedlings subjected to mechanical stresses.

Stresses were applied for 72 hours from germination. Values are \pm SD of 20 seedlings. * Indicates results with $\geq 95\%$ significance as determined by an ANOVA with a Dunnett test.

3.2.4 Discussion

Subjecting *Arabidopsis* wild type Ws and Col seedlings to vibration stress, seismic stress or a gravity stimulus at specific stages of development resulted in the promotion of hypocotyl elongation. These findings are atypical because it is generally accepted that mechanical stresses inhibit growth. The promotion of hypocotyl elongation by vibration is however consistent with the results of Johnson *et al* (1998) in *Arabidopsis* seedlings, and Takahashi *et al* (1991) in cucumber and rice seedlings. Neither of these two previous studies considered root elongation of the seedlings. In this study none of the stresses applied induced a significant change in root elongation, although overall seedlings subjected to vibration stress or seismic stress had shorter roots, and seedlings subjected to gravity stimulation had longer roots than the unstressed control. Vibration stress and seismic stress appear to induce mechanical stress primarily in the aerial parts of the seedling; this may account for the lack of effect on root elongation.

All vibration frequencies in the range of 40Hz to 70Hz promoted hypocotyl elongation when vibration was applied from germination, and where seismic stress was applied, hypocotyl elongation was stimulated. The vibration and gyratory shaking used seem to differ only by frequency and amplitude. Furthermore, the two stresses induce a similar phenotype in *Arabidopsis* seedlings, which is more marked when vibration stress is applied. This seems to suggest that vibration and gyratory shaking affect plant development in similar ways and are the same type of mechanical stress.

Few explanations for the promotion of hypocotyl elongation by vibration have been put forward; one reason for this is that the mechanisms of sensing and signal transduction of vibration stress are not well understood. It seems likely that Uchida & Yamamoto's (2002) suggestion that the perception and signal transduction of vibration is similar to that of gravity stimulation may be true as these stresses induce similar phenotypes in *Arabidopsis* seedlings (Figure 3.10). Gravity and light are the primary signals in seedling development, and it is light that controls the rate of growth (Ridge, 2002). The stressed and control seedlings were grown under the same light regime but the seedlings subjected to vibration stress were phenotypically distinct; the phenotype they display is comparable to that of shade-avoiding seedlings, which also show increased hypocotyl elongation and reduced cotyledon expansion (McNellis & Deng, 1995). It is possible that vibration stress impacts the seedlings ability to perceive light quality causing it to respond as shaded seedlings do, that is to grow up into direct sunlight.

3.3 Phenotypic analysis of *Arabidopsis* plants subjected to wind stress

In the Col ecotype long-term exposure to wind stress at a velocity of 2.7 m/s (section 2.2.4d) did not induce any significant phenotypic changes (Figure 3.11). In contrast, in the Ws ecotype wind induced notable changes in phenotype. Wind stress caused plants to have smaller rosette leaves as determined by measurement of their radius (Figure 3.12 B). In addition the inflorescence stem of wind stressed plants was shorter than unstressed plants, and they had fewer stem branches (Figure 3.12 C & D). Wind

stressed plants did not have a significantly different number of rosette leaves compared to unstressed plants however (Figure 3.12A).

3.4 Phenotypic analysis of *Arabidopsis* plants subjected to thigmic stress

Arabidopsis Col-0 plants subjected to thigmic stress (section 2.2.4e) did not have a significantly different phenotype to unstressed plants based on the parameters measured (Figure 3.13); it is possible that the intensity of thigmic stress may not have been sufficient to induce widespread phenotypic changes in this ecotype.

3.5 Phenotypic analysis of *Arabidopsis* plants subjected to vibration stress

Subjecting *Arabidopsis* Ws plants to vibration stress throughout the life of the plant (see section 2.2.4f) did not result in a significant change in phenotype in the stressed plants when compared to unstressed plants of the same ecotype (Figure 3.14).

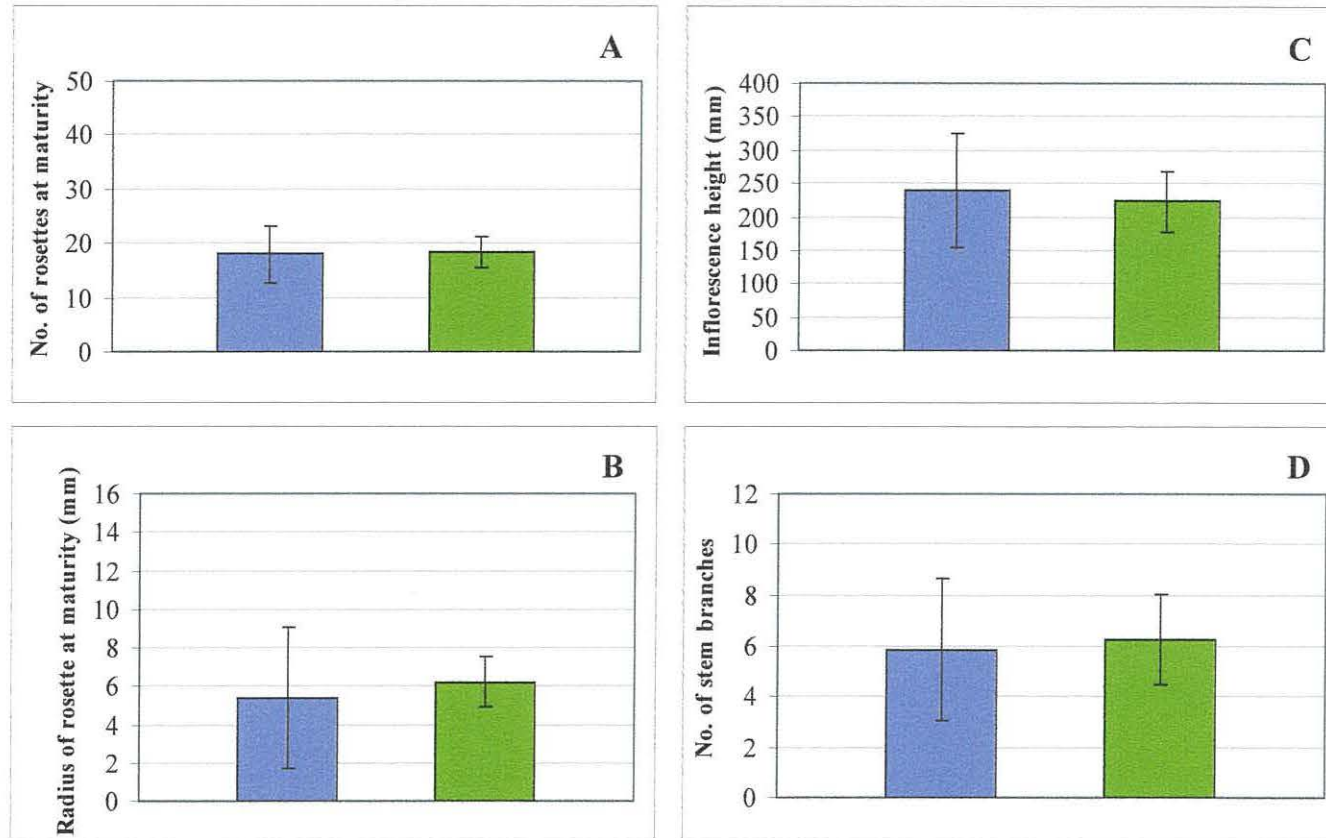


Figure 3.11: Phenotypic analysis of *Arabidopsis Col* plants subjected to wind stress. Control ■ Wind stress ■
A. Number of rosettes **B.** Radius of rosettes **C.** Length of inflorescence stem **D.** number of stem branches at maturity.
 Values are \pm SD of 24 plants. * Indicates results with $\geq 95\%$ significance as determined by a Student t-test.

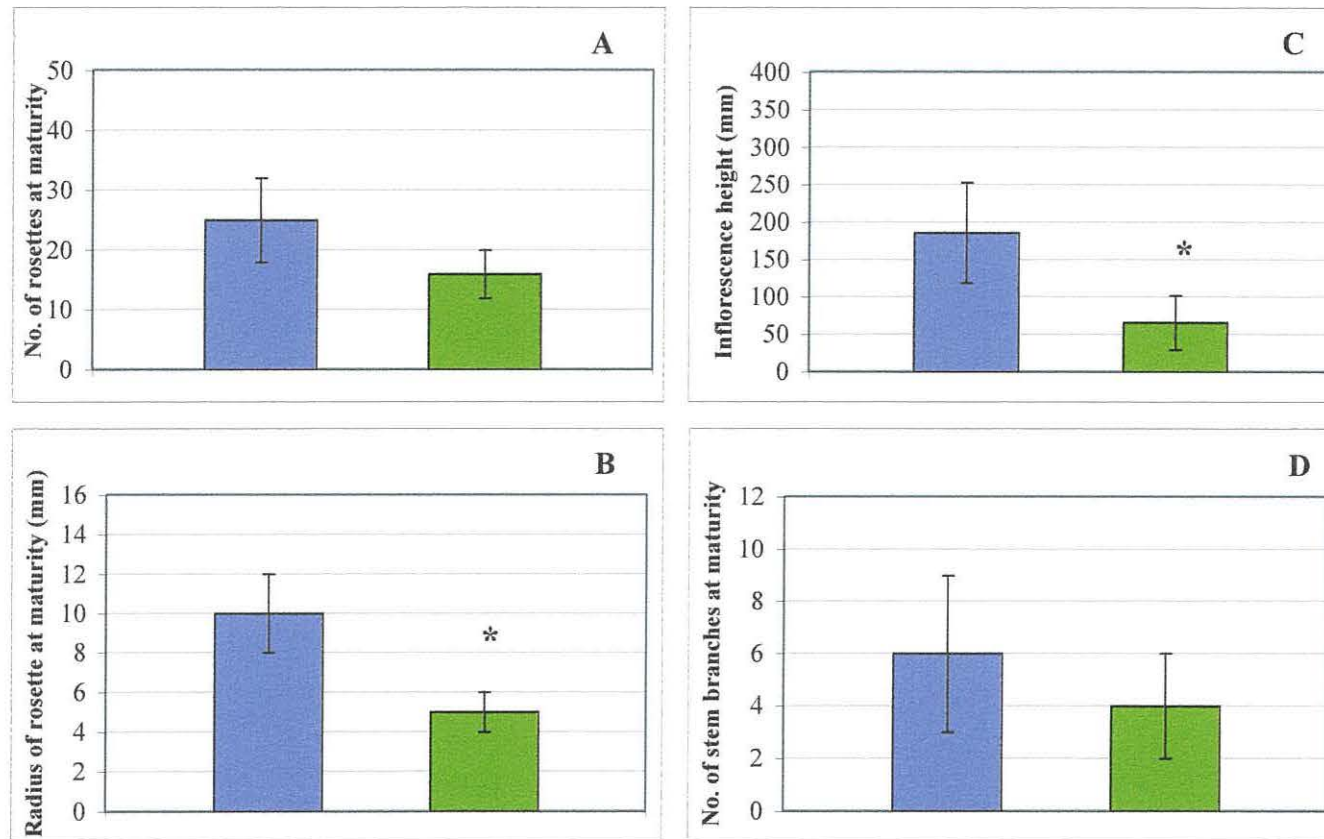


Figure 3.12: Phenotypic analysis of *Arabidopsis* *Ws* plants subjected to wind stress. Control ■ Wind stress ■
A. Number of rosettes B. Radius of rosettes C. Length of inflorescence stem D. number of stem branches at maturity.
Values are \pm SD of 24 plants. * Indicates results with $\geq 95\%$ significance as determined by a Student t-test.

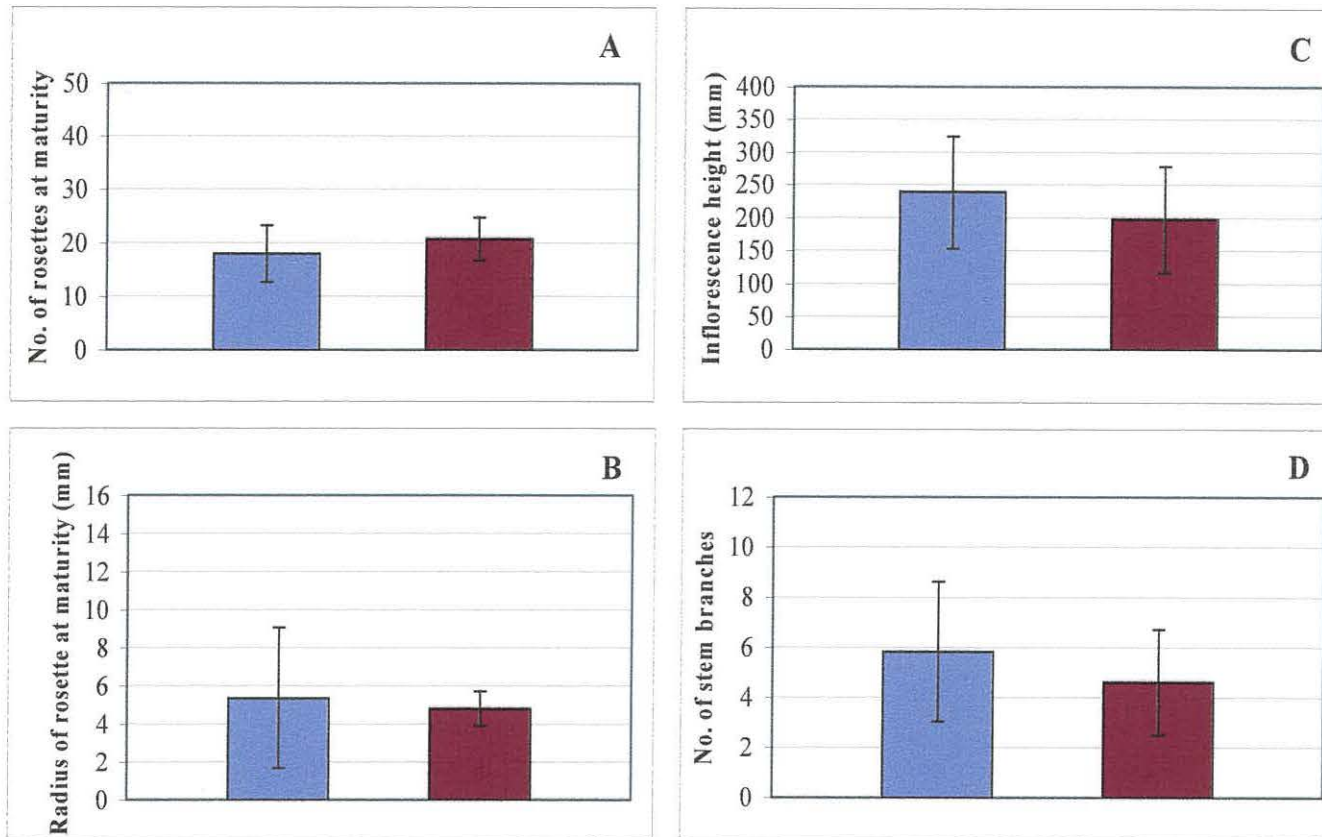


Figure 3.13: Phenotypic analysis of *Arabidopsis Col* plants subjected to thigmic stress. Control ■ Thigmic stress ■
A. Number of rosettes **B.** Radius of rosettes **C.** Length of inflorescence stem **D.** number of stem branches at maturity.
 Values are \pm SD of 24 plants. * Indicates results with $\geq 95\%$ significance as determined by a Student t-test.

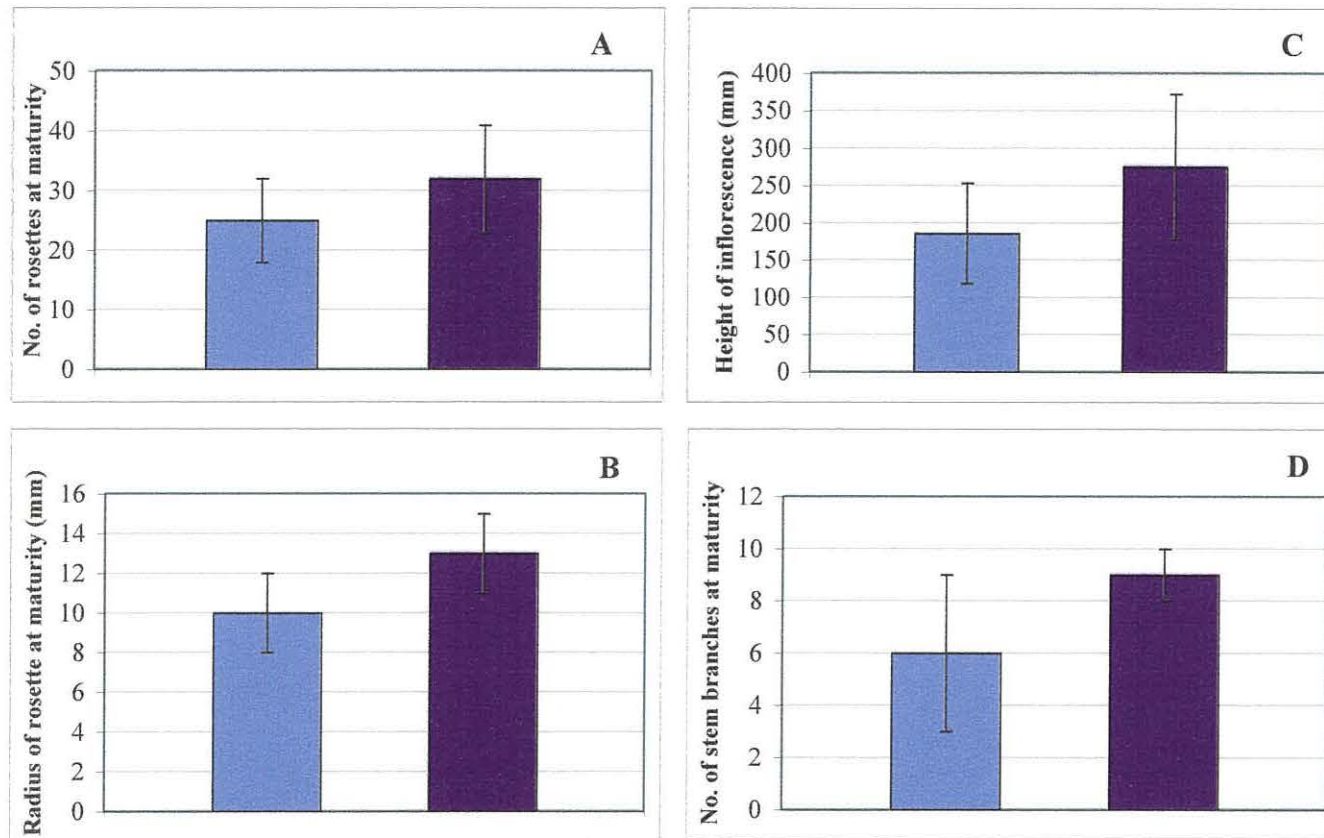


Figure 3.14: Phenotypic analysis of *Arabidopsis Ws* plants subjected to vibration stress. Control ■ Vibration stress ■
A. Number of rosettes **B.** Radius of rosettes **C.** Length of inflorescence stem **D.** number of stem branches at maturity.
 Values are \pm SD of 24 plants. * Indicates results with $\geq 95\%$ significance as determined by a Student t-test.

3.6 Discussion

Subjecting *Arabidopsis* *Ws* plants to wind stress resulted in the expected dwarfing of plants. In contrast, neither thigmic stress nor vibration stress induced a significant change in phenotype. The dwarfing of *Arabidopsis* *Ws* plants by exposure to a wind speed of 2.7 m/s was not reflected in the Col-0 ecotype, this difference in phenotype may be attributed to ecotypic differences. Furthermore, in the unstressed wild type plants of these ecotypes, a greater degree of variance was measured in the Col plants than the *Ws* plants. Although the wind speed was not detailed in the previous study by Johnson *et al* (1998), a similar phenotype to that outlined in this study (using a velocity of 2.7 m/s) was found when *Arabidopsis* plants were subjected to wind stress. In Pigliucci's (2002) study of 11 natural accessions of *Arabidopsis* a wind speed of 1.8 m/s was used daily, which did not affect the height of the inflorescence stem or radius of rosettes but did influence the degree of branching of the main bolt. It may also be possible that ecotypic differences exist between these natural accessions, and that a greater degree of adaptation is established in this population. Comparing the results from this study with previous studies in *Arabidopsis* seems to support the assertion that wind has little effect at low wind speeds and greater effect as wind speeds increase.

Thigmic stress applied once per day throughout the life of the plant was insufficient to induce a novel phenotype in stressed *Arabidopsis* Col plants. Previous studies in *Arabidopsis* used different ecotypes of the plant, and a higher intensity and/or duration of stress, which did induce a different phenotype. In one previous study, touching the leaves of Col-0 plants twice daily led to a delay in flowering and an inhibition of inflorescence elongation (Braam, 2005). Vibration of *Arabidopsis* *Ws* plants promoted growth to some extent (not significant) as compared to unstressed plants in this study. This result is not completely unexpected in the light of our previous findings in vibrated seedlings; however no previous published studies have considered the long-term impact of vibration stress on growth of *Arabidopsis*. Nevertheless Japanese horticulturists have used vibrating growth benches to stimulate growth of crops, as well as generating vibration frequencies by playing music through loud speakers (Mitchell, 1996).

3.7 Summary

This series of experiments established conditions that gave rise to a significant change in phenotype when *Arabidopsis* seedlings and plants are subjected to wind and mechanical stresses. When *Arabidopsis* Ws seedlings are subjected to vibration stress for 72 hours from germination, hypocotyls were longer than those of unstressed seedlings. When *Arabidopsis* Ws plants were subjected to wind stress (2.7 m/s) for 2 hours, three times per day throughout the life of the plant, inflorescence stems were shorter and rosettes had a smaller radius at maturity than in unstressed plants. In the following chapters the response and adaptation of seedlings and plants subjected to these stresses will be described.

4. OXIDATIVE STRESS IN PLANTS SUBJECTED TO WIND AND MECHANICAL STRESSES

4.1 Introduction

Active oxygen species (AOS) are produced by plants in response to stresses but also at low levels during normal development. Abiotic and biotic stresses have been shown to enhance the production of AOS, including cold, UV light, drought, wounding and pathogen attack (Rentel & Knight, 2004). AOS are reduced forms of oxygen, and include superoxide radicals, hydrogen peroxide and hydroxyl radicals. The rapid induction of hydrogen peroxide (known as the oxidative burst) is a characteristic feature of the plant defense response to pathogen attack. Scavengers of hydrogen peroxide and other AOS include peroxidase, catalase and superoxide dismutase (Mittler, 2002).

To date, the role of active oxygen species in the response to wind/mechanical stresses has not been studied in *Arabidopsis*. This chapter details the detection of hydrogen peroxide and peroxidase activity in plants in response to wind and other mechanical stresses.

4.1.1. The role of active oxygen species in plant development and defense pathways

Active oxygen species play a fundamental role within the plant, during development and in the response to pathogen attack. Hydrogen peroxide has been shown to have multiple roles, causing ion fluxes, acting as a substrate for cross linking of cell wall proteins, inducing the phenylpropanoid pathway and regulating defense-related gene expression. However, the signaling pathways linking hydrogen peroxide synthesis and gene expression are not well understood (Rentel & Knight, 2004).

Pedreira *et al* (2004) have stated that the cessation of growth is related to cross linking between the pectic components of the cell wall due to the action of peroxidases

(stimulated by hydrogen peroxide). The addition of hydrogen peroxide to the incubation medium of pine hypocotyls led to a reduction in auxin-induced growth (Pedreira *et al* 2004). In an independent study, an inverse relationship was found between peroxidase levels and growth, and plant age (Sanchez *et al*, 1997). A number of previous studies have also determined that hydrogen peroxide and lignin are commonly at the same location and histochemical staining shows they have a similar distribution (Olson & Varner, 1993).

Hydrogen peroxide is produced at an elevated level in response to a number of abiotic and biotic stresses. Abiotic stresses activate AOS-scavenging mechanisms, involving peroxidase, catalase and superoxide dismutase. Mechanisms for avoiding AOS complement these scavenging mechanisms, including anatomical, physiological and molecular mechanisms (Mittler, 2002). It is important to note, however, that H₂O₂ is a major player in inducing the systemic acquired resistance response; the activity of peroxidase and catalase was found to be suppressed during pathogen attack due to activity of salicylic acid (SA) and nitric oxide (NO). This resulted in the induction of plant defenses including the activation of programmed cell death (PCD). The inhibition of AOS-scavenging mechanisms is critical to the activation of PCD in response to pathogen attack, the differing roles of AOS in response to abiotic and biotic stresses may be explained by the action of SA and NO, signaling cross-talk and/or a difference in the steady state level of AOS in response to specific stresses (Mittler, 2002).

4.1.2. Evidence for an oxidative burst in response to mechanical stress

Mechanical stress has been shown to induce an oxidative burst in soybean cell cultures (Yahraus *et al*, 1995). Hydrogen peroxide was rapidly generated in response to a mechanical stimulus; furthermore, peroxidase activity was stimulated by mechanical stress in cucumber (Moran & Cipollini, 1999), bean (Cipollini, 1998) and *Bryonia dioica* (DeJaegher *et al*, 1985). Apart from these studies, studies on the induction of AOS by mechanical stresses have been limited.

The induction of peroxidase activity in response to mechanical stresses occurs at different times in different species. Elevated levels of peroxidase were observed in cucumber after 9 days (Moran & Cipollini, 1999) and in bean after 7 days (Cipollini, 1997) when the plants were exposed to wind stresses, but after only one day in *Bryonia dioica* plants subjected to stem rubbing (De Jaegher *et al*, 1985). As well as increasing peroxidase activity, rubbing of the stems of *Bryonia dioica* plants caused an increase in the transcription of phenylalanine ammonia lyase (PAL), which is a key enzyme of the lignin biosynthetic pathway (De Jaegher *et al*, 1985). These authors suggest that the increase in peroxidase activity and lignin leads to cell wall rigidification via cross-linking in cell walls and lignification.

4.2 The induction of active oxygen species & peroxidase activity in *Arabidopsis* seedlings subjected to vibration stress

Seedlings were subjected to 72 hours of vibration stress commencing at germination, as outlined in Chapter 3. Seedlings were sampled immediately after the cessation of vibration and at 14-days old, and assayed for sites of hydrogen peroxide synthesis using the diaminobenzadine-uptake (DAB-uptake) method (section 2.3.1). Peroxidase activity was determined by using a guaiacol-based assay (section 2.3.2) and a syringaldazine-based assay (section 2.3.3), for peroxidase activity specifically involved in the lignification pathway. Five individual seedlings from each treatment and time point were assayed for hydrogen peroxide using the DAB-uptake method; seedlings were placed in DAB solution overnight under standard growth room conditions. Seedlings were boiled in ethanol until the tissues cleared and the degree of red/brown staining then seen was indicative of the extent and localization of hydrogen peroxide accumulation. Samples were stored in pure ethanol at 4°C. In addition, approximately 10mg of seedlings from each treatment and time point were frozen in liquid nitrogen and stored until assayed for soluble peroxidase activity using guaiacol solution and syringaldazine solution.

a) Localization of H₂O₂ synthesis in seedlings subjected to vibration stress

A high level of staining was observed in both vibrated and control seedlings assayed by the DAB-uptake method at each time point, such that the aerial parts of the seedling were saturated with stain.

b) Soluble peroxidase activity in seedlings subjected to vibration stress

Immediately after the cessation of vibration stress, peroxidase activity was significantly greater in the unstressed control seedlings as determined by the guaiacol method (Figure 4.1A). However, after 14-days peroxidase activity did not differ significantly between the control and vibrated seedlings. The decreased peroxidase activity seen in vibrated seedlings immediately after the cessation of vibration stress could be explained by variation in the seedlings. However, because the activity is significantly lower, it is more likely that peroxidase activity is repressed in these seedlings.

c) Lignin pathway specific soluble peroxidase activity in seedlings subjected to vibration stress

The level of peroxidase activity involved in the lignin pathway, as determined by the syringaldazine assay does not differ significantly between the stressed and unstressed samples immediately after the cessation of stress (Figure 4.1B), even though overall levels of peroxidase (measured by the guaiacol assay) are suppressed in the vibrated seedlings (Figure 4.1A). However, at 14-days the activity is significantly higher in vibrated seedlings (Figure 4.1B).

d) Discussion

In the previous chapter it was shown that vibration of seedlings under the conditions outlined resulted in the promotion of hypocotyl elongation. The decreased level of peroxidase activity in stressed seedlings seen immediately after the cessation of vibration stress seems to suggest that there is a negative correlation between

peroxidase activity and growth, which is consistent with the findings of Sanchez *et al* (1997) who showed such a correlation in seedlings under normal development. After 14-days, when the phenotypic difference was observed, the levels of peroxidase were higher in stressed seedlings but not significantly so. In view of this finding, it is surprising that the level of peroxidase associated with lignification is higher in the vibrated seedlings after 14-days than in the control seedlings. Sanchez *et al* (1997) showed that peroxidase activity increased with hypocotyl age in pine seedlings, although this was not found to be the case in unstressed *Arabidopsis* seedlings; higher levels of peroxidase in vibrated seedlings especially that associated with lignification could be indicative of an accelerated ageing process.

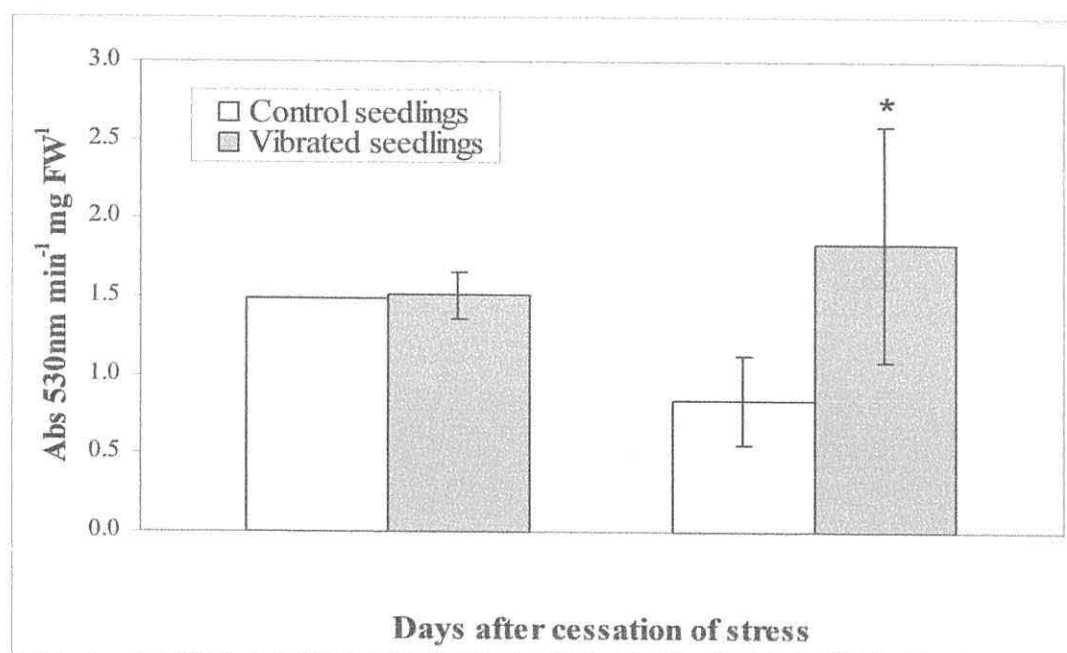
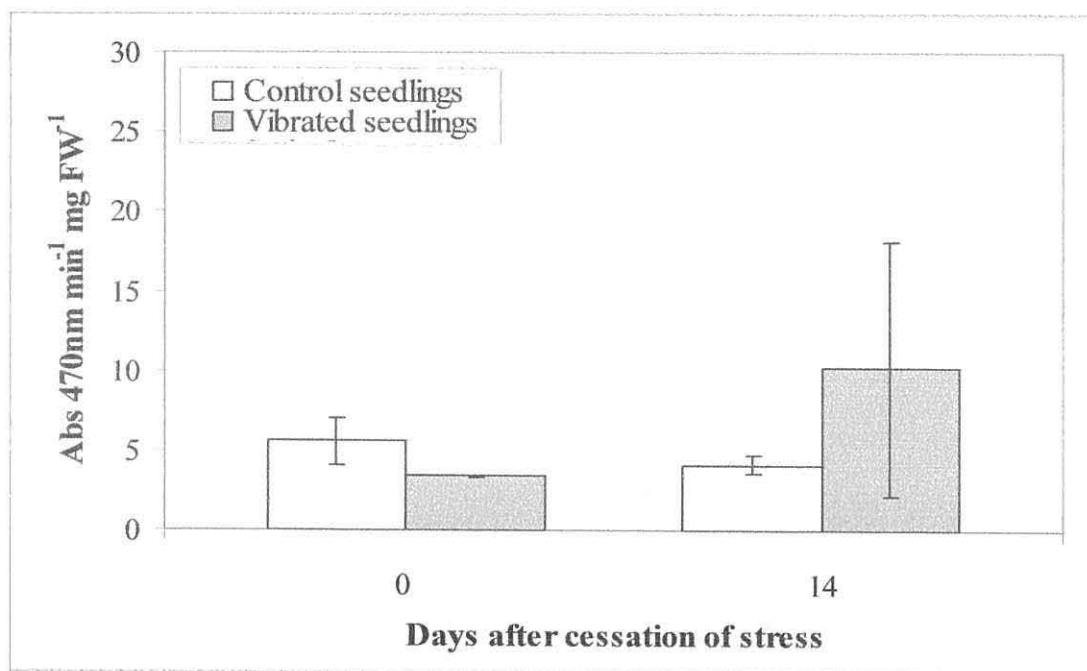


Figure 4.1: Soluble peroxidase activity in seedlings subjected to vibration stress. Vibration at 40Hz was applied for 72 hours commencing at germination. **A.** Soluble peroxidase activity determined by the guaiacol assay. **B.** Soluble peroxidase activity determined by the syringaldazine assay for peroxidases involved in the lignification process. Samples were taken immediately after the cessation of stress (time point 0) and 14 days later. Values are \pm SD of 2 samples from each time point shown. * indicates statistically significant results at $\geq 95\%$ level, calculated by a Student t-test.

4.3 The induction of active oxygen species & peroxidase activity in *Arabidopsis* plants subjected to wind stress

Wild type Ws soil-based *Arabidopsis* plants were subjected to wind stress (as outlined in Chapter 3). In one set of plants, wind stress was applied for two hours three times per day; commencing at 08:00, 12:00 and 16:00. The stress was first applied when the plants were 17-days and continued daily until rosette maturation, this is referred to as long-term wind stress. In another set of plants wind stress was applied for a single two hour period (08:00-10:00) at rosette maturation, this is referred to as short-term wind stress. Leaf samples were harvested from each of the sets of plants and from a set of unstressed control plants at various time points after the cessation of the stress stimulus. The first sample was taken immediately after the cessation of the wind stress (0 hours), and further samples were taken 24 and 48 hours later.

Leaves were assayed for hydrogen peroxide synthesis using the diaminobenzadine-uptake (DAB-uptake) method (section 2.3.1), and for peroxidase activity using the guaiacol (section 2.3.2) and syringaldazine assays (section 2.3.3) outlined previously. Five leaves from five different plants from each treatment and time point were assayed for hydrogen peroxide synthesis using the DAB method outlined in the previous section. In addition, approximately 100mg of leaves from each sample were frozen in liquid nitrogen and stored until they were assayed for soluble peroxidase activity using guaiacol and syringaldazine solutions. The total protein concentrations of each sample as determined by the Bradford method did not differ significantly between these samples; however peroxidase activity was again normalized against protein concentration across the entire data set (Appendix A).

a) Localization of H₂O₂ synthesis in plants subjected to wind stress

Immediately after the cessation of stress, levels of hydrogen peroxide were seen to be greater in the wind stressed samples than in the unstressed control as shown by the extent of red/brown staining in the leaf tissue (Figure 4.2). In the unstressed control, staining is restricted to the point of excision and to the vascular tissues. Up to 48 hours following the cessation of wind stress the extent of staining remained greater in the wind stressed samples than in the control.

b) Soluble peroxidase activity in plants subjected to wind stress

The level of soluble peroxidase activity, as determined by the guaiacol assay did not change significantly in control and wind stressed plants immediately after cessation of the stress stimulus (Figure 4.3A). Peroxidase activity was induced sometime after the termination of the wind stresses in these experiments, after 24 hours, peroxidase levels were increased to a small degree in the plants which were exposed to the single 2 hour period of wind stress at rosette maturation (short-term), and to a greater extent in the plants that were exposed to wind stress daily (long-term). Peroxidase levels in the plants exposed to the single short exposure of wind had returned to control levels 48 hours after the cessation of the stress. By contrast, peroxidase activity remained elevated in the plants subjected to the long-term wind stimulus.

c) Lignin pathway specific soluble peroxidase activity in plants subjected to wind stress

The syringaldazine assay for peroxidases involved in the lignification process showed a relatively high level of peroxidase in leaves (24 hours after cessation of stress), indicating that some of the peroxidases are involved in lignification (Figure 4.3B). Comparatively low peroxidase levels were found in unstressed plants and those exposed to a short-term exposure to wind stress using this assay.

d) Discussion

These results show that long-term or transient exposure to wind stress results in an oxidative burst in *Arabidopsis* plants. This is followed by an increase in peroxidase activity, occurring before 24 hours after the cessation of the wind stress. Enhanced peroxidase activity is sustained in stressed plants for at least 48 hours (or more where long-term stress is applied). This pattern is similar to that seen in other plant species subjected to mechanical stresses (De Jaegher *et al*, 1985, Cipollini, 1999) although there is temporal variation between *Arabidopsis* and the other species reported.

Peroxidase activity is greatest in plants subjected to long-term exposure to wind stress; furthermore it is sustained for a longer period when compared with plants subjected to a short-term exposure to wind stress. These results do not identify whether peroxidase levels return to normal/control levels over a longer time period. There is scope to investigate the profile of peroxidase activity after each repeated exposure to wind stress over the long term period.

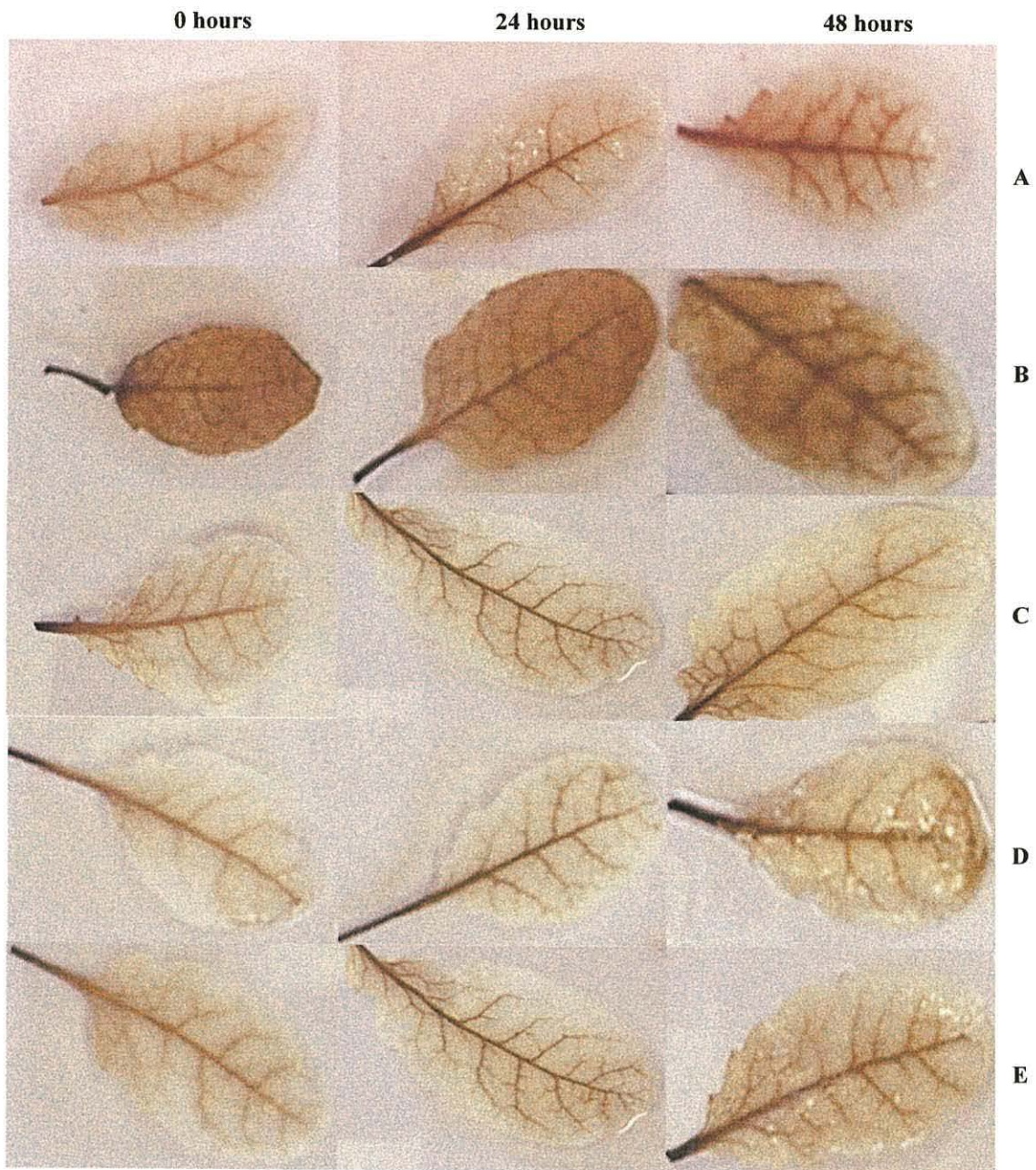


Figure 4.2: Detection of Hydrogen peroxide in wind and mechanically stressed plants as determined by the DAB-uptake method.

A. Control. B. Long-term wind stress. C. Short-term wind stress. D. Long-term vibration stress. E. Short-term vibration stress.

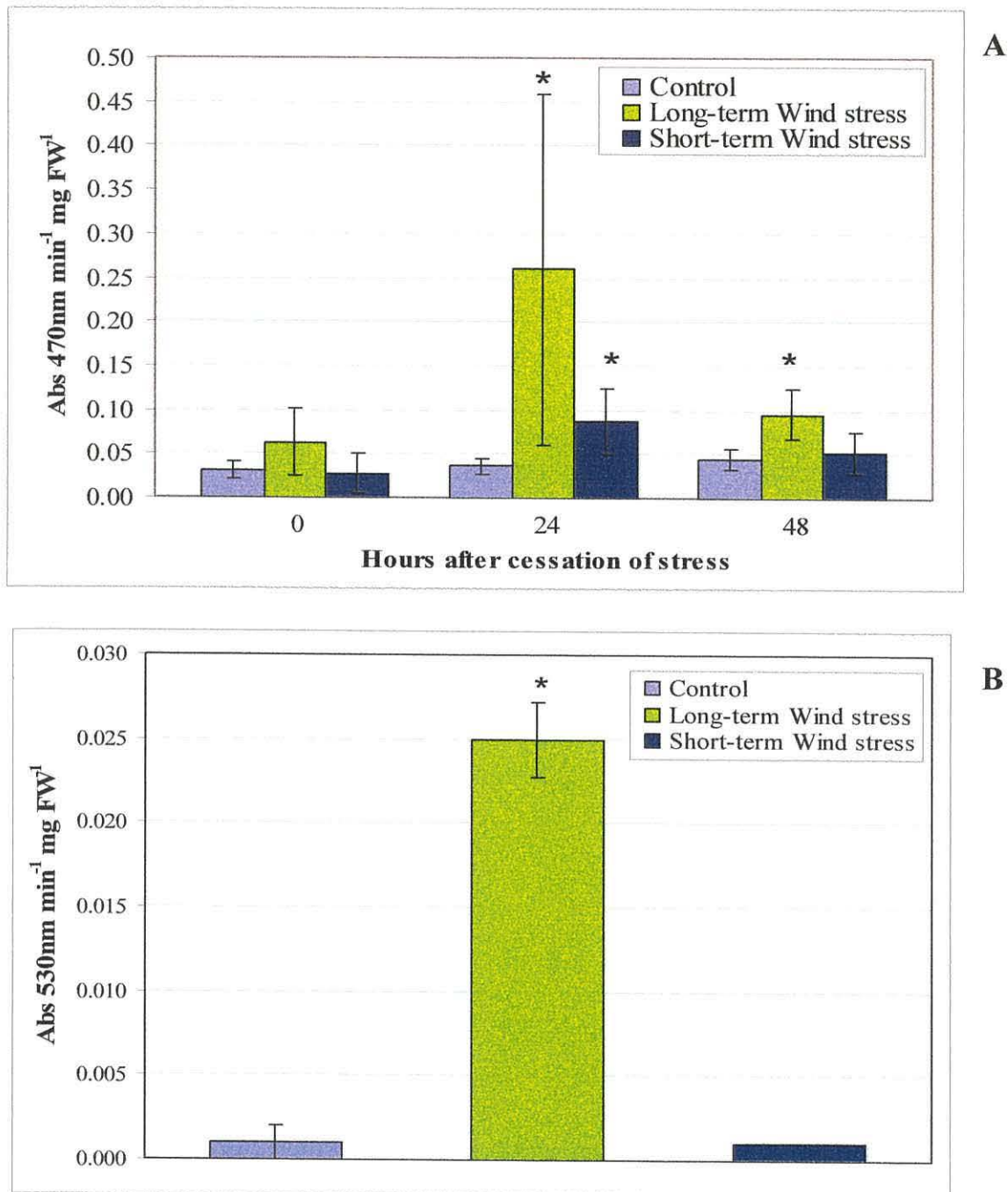


Figure 4.3: Soluble peroxidase activity in the rosette leaves of wind stressed plants. *Arabidopsis* plants were subjected to long-term wind stress for 6 hours per day from 17-days until rosette maturation or for a single short-term exposure at rosette maturation. Samples were taken immediately after the cessation of stress (time point 0) and 24 and 48 hours later. **A.** Guaiacol assay on leaf extracts from each time point. **B.** Syringaldazine assay on leaf extracts taken 24 hours after cessation of vibration stress. Results are \pm SD of 3 samples from each time point shown. * indicates statistically significant results at $\geq 95\%$ level, as calculated by an ANOVA with a Dunnett test.

4.4 Monitoring of active oxygen species in *Arabidopsis* plants subjected to vibration stress

Wild type Ws soil-based *Arabidopsis* plants were subjected to 40Hz vibration stress (as outlined previously). In one set of plants, vibration stress was first applied at 17-days and continued constantly until rosette leaf maturation, and is referred to as long-term vibration stress. In another set of plants vibration stress was applied for a single two hour period (08:00-10:00) at maturation, which is referred to as short-term vibration stress. Rosette leaf samples were harvested from each set of plants and from a set of unstressed control plants at various time points after the cessation of the stress stimulus. The first sample was taken immediately after the cessation of the vibration stress (0 hours), and then 24 and 48 hours later. Leaves were assayed for hydrogen peroxide using the DAB-uptake method (section 2.3.1), and for peroxidase activity using a guaiacol based assay (section 2.3.2) and a syringaldazine assay (section 2.3.3), as outlined earlier. This experiment was run in parallel with the wind stress experiment in the previous section (section 4.3).

a) Localization of H₂O₂ synthesis in plants subjected to vibration stress

The levels of hydrogen peroxide detected by the DAB-uptake method are approximately the same in vibrated plants as they are in the unstressed control plants (Figure 4.2). There is no observable difference between the localization of staining between the samples. These results suggest that vibration stress does not induce an oxidative burst in *Arabidopsis* plants.

b) Soluble peroxidase activity in plants subjected to vibration stress

The soluble peroxidase activity recorded for vibrated plants immediately after the cessation of stress did not show a significant increase over control levels (Figure 4.4A). Furthermore, levels were not significantly different between unstressed control and vibrated plants when they were sampled 24 and 48 hours later.

c) Lignin pathway specific soluble peroxidase activity in plants subjected to vibration stress

24 hours after the cessation of vibration stress, the level of peroxidase activity involved in the lignin pathway was significantly higher in plants subjected to long-term vibration but not short-term vibration when compared to the unstressed control (Figure 4.4B).

d) Discussion

Overall there was no significant difference between the levels of hydrogen peroxide or peroxidases in vibrated plants and unstressed control plants. This reflects the fact that there was not a significant difference in phenotype between these plants (outlined in Chapter 3). In plants subjected to a long-term exposure to vibration stress, however, there was an increased level of lignification-specific peroxidase activity 24 hours after the cessation of the stress stimulus despite the fact that overall levels of peroxidase were not increased. It is unclear why this is the case; however it may be indicative of accelerated ageing in these plants. Further studies, over a longer time frame would be needed to investigate this theory.

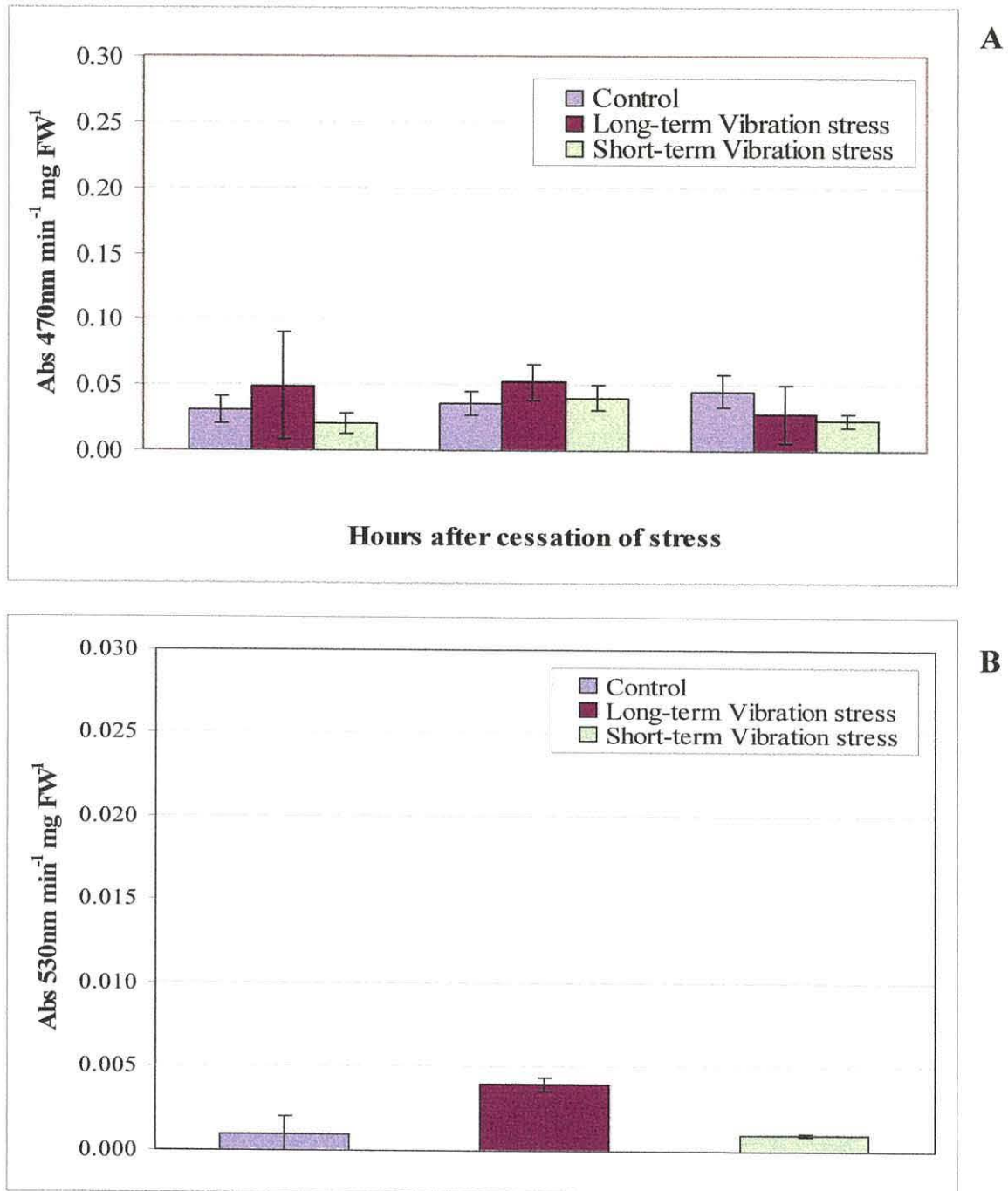


Figure 4.4: Soluble peroxidase activity in the rosette leaves of vibrated plants *Arabidopsis* plants were subjected to long-term vibration stress from 17-days until rosette maturation or for a single short-term exposure at rosette maturation. Samples were taken immediately after the cessation of stress (time point 0) and 24 and 48 hours later. **A.** Guaiacol assay on leaf extracts from each time point. **B.** Syringaldazine assay on leaf extracts taken 24 hours after cessation of vibration stress. Average results for three samples from each time point are shown.* indicates statistically significant results at $\geq 95\%$ level, as calculated by an ANOVA with a Dunnett test.

4.5 Summary

In this chapter the levels of active oxygen species and peroxidases in response to wind and mechanical stresses were investigated. Hydrogen peroxide and peroxidases are present at relatively high levels in seedlings even during normal development. Where seedlings were subjected to vibration stress, there was an apparent decrease in peroxidase activity compared with normal levels immediately after cessation of the stress, which is consistent with the phenotype observed. Evidence for an oxidative burst in *Arabidopsis* plants subjected to wind stress has been shown. Furthermore, it has been shown that peroxidase activity is induced by short-term or long-term exposure to wind stress. In plants subjected to a long-term exposure to wind stress a considerable amount of peroxidase activity is involved in the lignin pathway. There is comparatively little evidence to support the role of an oxidative burst and/or enhanced peroxidase activity in the response to vibration stress in plants.

5. EXPRESSION OF CANDIDATE WIND/MECHANICAL STRESS GENES IN PLANTS SUBJECTED TO WIND AND MECHANICAL STRESSES

5.1 Introduction

Previous studies have shown that specific genes are expressed in response to wind and other mechanical stresses. These studies have been used in this work to identify a number of candidate wind/mechanical stress genes. This is an alternative approach to global gene expression studies such as microarrays, which result in the identification of hundreds of candidate genes. By using a more focused approach this study aimed to gain a greater insight into the role of these candidate genes in the response and adaptation of plants to windy habitats.

5.2 Candidate wind/mechanical stress genes

Candidate wind/mechanical stress genes that were identified from literature searches included the *Arabidopsis* genes TCH4 and EXT1 encoding plant cell wall proteins, and TCH3 and MEK1 encoding cell signalling pathway intermediates. Previous studies involving these genes and their regulation by wind/mechanical stresses are outlined in the introduction to this work. Other candidate genes were chosen on the basis of their involvement in the response of *Arabidopsis* plants to other abiotic and biotic stresses, and/or their involvement in phenotypes comparable to those induced by wind and other mechanical stresses. These genes include those involved in cell expansion (expansin 3), lignin biosynthesis (phenylalanine ammonia lyase 1 and cinnamoyl CoA reductase 2), cellulose biosynthesis (cellulose synthase 3), and plant cell wall proteins (arabinogalactan protein 3 and glycine rich protein 6). A full list of the candidate genes selected for this study and their functions is given in Table 5.1.

5.2.1 Expansin (EXP3)

Expansins are encoded by a large multigene family in *Arabidopsis* and in other species such as rice. In *Arabidopsis* three families of expansins have been defined based on sequence homology (α , β and γ). The α expansins form the largest group of 26 proteins. Expansin 3 (EXP 3) of *Arabidopsis* is closely related to two other *Arabidopsis* expansin genes, 1 and 2, and two expansin genes from rice, 20 and 21 (Li *et al*, 2003). EXP3 is up-regulated in the hypocotyls and cotyledons of dark-grown (etiolated) seedlings when compared to light-grown seedlings (Ma *et al*, 2005).

5.2.2 Phenylalanine ammonia lyase (PAL1) and Cinnamoyl coenzyme A reductase (CCR2)

The oxidative burst associated with the plant response to abiotic and biotic stresses is known to induce the phenylpropanoid pathway, which is responsible for the production of phytoalexins and lignins. Lignification has been identified as a defense response to stresses such as wounding and pathogen attack (Lauvergeat *et al*, 2001). Lignin biosynthesis begins in the phenylpropanoid pathway; the first enzyme of this pathway is phenylalanine ammonia lyase (PAL), which deaminates phenylalanine. There are three PAL genes in the *Arabidopsis* genome (PAL 1-3) of which PAL1 is the most extensively expressed in tissues of the plant (Goujon *et al*, 2003). Cinnamoyl coenzyme A reductase (CCR) is considered to be the first enzyme of the monolignol specific pathway, which is the pathway dedicated to lignin synthesis. Two CCR cDNAs were identified in *Arabidopsis* by Lauvergeat *et al* (2001), AtCCR1 is expressed during normal development, while AtCCR2 is induced by pathogen infection and is expressed in stems near maturation.

5.2.3 Cellulose synthase (CESA 3)

Rates of cell wall expansion and cell wall synthesis fluctuate simultaneously; cellulose is a requirement for cell wall synthesis. The conversion of the substrate UDP-glucose to cellulose is catalysed by the enzyme cellulose synthase (CesA). Complementation studies have produced genetic proof for the role of CesA genes in the synthesis of

cellulose in *Arabidopsis* (Wu *et al*, 2000). Ten full-length CesaA genes have now been sequenced from *Arabidopsis*. CESA3 is associated with primary cell wall development but is also found in developing vascular tissues, and is induced by ethylene (Doblin *et al*, 2002).

5.2.4 Arabinogalactan protein (AGP 3)

There are 15 classical Arabinogalactan protein (AGP) genes expressed in *Arabidopsis* (Schultz *et al*, 2000). Some AGPs have GPI anchors; it has been proposed that GPI anchors have a role in signal transduction between cells via interactions with other membrane-bound proteins. Most of the classical AGPs are expressed in more than one tissue type in plants during normal development (Schultz *et al*, 2000), AGP3 is predominantly expressed in roots during normal development but its induction under stress conditions has not been reported.

5.2.5 Glycine rich protein 6 (GRP6)

GRP6 has been included in the list of candidate genes as a negative control. Previous studies found that GRP6 was flower-specific during normal development and that it was not induced in other tissues by inoculation with pathogens, salicylic acid, abscisic acid or ethylene (Oliveira *et al*, 1993). It was therefore not expected to be expressed in any of the tissues sampled from either stressed or unstressed plants, and was thus chosen as an ideal control gene.

Table 5.1: Details of selected candidate wind/mechanical stress genes.

Abbreviations given are used throughout the following text. Identifiers are those assigned to the ORF of each gene sequence in the NCBI GenBank. Genes have either been shown to be regulated by wind/mechanical stress Y (yes), or this has not been shown to date (NS). * The expression of the candidate gene EXT1 will be considered in Chapter 6.

Gene Abv.	Protein	Identifier	Function	Regulated by wind/MS
TCH3	Calmodulin-like protein	At2g41100	Calcium signalling; binds Ca ²⁺ .	Y
TCH4	xyloglucan endotransglycosylase	At5g57560	Structural role in the primary cell wall.	Y
CESA3	Cellulase synthase catalytic subunit	At5g05170	Cellulose synthesis.	NS
MEK1	Mitogen-activated protein kinase	AL049483	Signalling protein; involved in signalling cascades triggered by abiotic and biotic stresses.	Y
EXP3	Expansin	At2g37640	Role in loosening and extension of cell walls.	NS
AGP3	Arabinogalactan protein	At4g40090	Correlated with inhibition of cell division and expansion.	NS
PAL1	Phenylalanine ammonia lyase	At2g37040	Lignin biosynthesis; first enzyme of the phenylpropanoid pathway.	NS
CCR2	cinnamoyl CoA reductase	At1g80820	Lignin biosynthesis; first enzyme of monolignol specific pathway.	NS
EXT1*	Extensin	ATU43627	Crosslinking of cell walls. Tensile strength.	Y
GRP6	Glycine-rich protein	Z11858	Cell wall structure and function. Flower-specific expression.	NS

5.3 RT-PCR primers for candidate wind/ mechanical stress genes

Genomic DNA and mRNA sequences for each candidate wind/mechanical stress gene were obtained from the National Center for Biotechnology Information (NCBI) database (2005). The DNA and mRNA sequences were aligned using the BLAST function on the NCBI website (NCBI, 2005) in order to identify introns within the genes (Appendix B). Primers were predominantly based on gene sequences spanning an intron so that the PCR products generated from cDNA could be distinguished from those generated by amplification of contaminating DNA; the Arabinogalactan 3 primers were the only exception, as the AGP3 gene has no introns. Primers were designed to amplify at least 100bp of sequence from each gene. Primer3 software (Rozen & Skalestky, 2000) was used to optimize primer design by checking for primer dimers and hairpins, and identifying stretches of sequence with a GC content $\geq 50\%$ and an annealing temperature $\geq 55^{\circ}\text{C}$ but $\leq 70^{\circ}\text{C}$. Each selected primer was subsequently subject to a Nucleotide BLAST (NCBI) check to confirm that it was complementary to its target but not to any other gene in the *Arabidopsis* genome. The primers designed for each candidate wind/mechanical stress gene are outlined in Table 5.2. Additionally, primers were designed to amplify 18S rRNA, as a control. Primers were ordered from MWG Biotech; lyophilized stocks were reconstituted to $100\mu\text{M}/\mu\text{l}$ with distilled water and then diluted by one tenth for use in PCR reactions.

Table 5.2: RT-PCR primers based on candidate wind/ mechanical stress genes.

Gene	Primers	Size of genomic DNA fragment b.p.	Size of cDNA fragment b.p.
TCH3	F: CCATCGATTTCCTGAGTTCT R: TGGAGCTCAAGCTTTTGTGTTG	333	235
TCH4	F: GGTCGTGGACAGATCAAGAAC R: CTTTGTCTCCTTTGCCTTCTG	361	277
CESA3	F: AGAACCCTTGAAAGCTGGAAG R: CGATTTGGACAGTCTGCTGTT	357	263
MEK1	F: TCATCGGGACTTAAAGCCTTC R: CTCGTACACGCTACTCCATCC	385	277
EXP3	F: CCTCACCCAATCTGTCTTTGA R: TCCGGGAAATCCATCTATTCT	1106	322
AGP3	F: TCAGGTTTCTATCTCTCTCGT R: TACAATCAGAACTTCTTCCCT	679	679
GRP	F: CCACGGCATTAAACCATAACAA R: CCCTGGTTTATTTCCGAATGT	611	277
PAL1	F: CTAGAGCCGGTGTGAATGCTA R: GATACCGGAAAATCCTTGGAG	724	268
CCR2	F: CAAGCGCGTGGTTTTTCAC R: CTGACTGGAGCGGTGGTC	373	241
EXT1*	F: CCACACCAACCCTACCTTTAC R: CACCAAACGATTCTTTGT	206	111
18S rRNA	F: TCCTAGTAAGCGCGAGTCATC R: CGAACAACCTCACC GGATCAT	100	100

5.4 Gene expression analysis of candidate wind/mechanical stress genes in *Arabidopsis* seedlings & plants

5.4.1 Analysis of gene expression of candidate wind/mechanical stress genes in seedlings subjected to vibration stress

It was established in Chapter 3 that vibration stress results in a novel phenotype when it is applied to seedlings at specific stages of development. An analysis of gene expression of candidate wind/mechanical stress genes in seedlings subjected to vibration stress was carried out; *Arabidopsis* wild-type Ws seeds were sterilized, plated on half-strength MS media, stratified at 4°C in darkness and then transferred to standard growth room conditions (20-23°C, 8hrs light/16hrs dark cycle). Vibration at 40Hz was applied for 72 hours constantly from germination. Immediately after the cessation of vibration, seedlings were harvested, frozen in liquid nitrogen and stored at -80°C until RNA was extracted. When the vibrated seedlings reached 14-days old, additional seedlings were harvested and stored in liquid nitrogen. Unstressed control seedlings were also harvested and stored at these time points.

RNA was extracted from each sample as outlined in the Materials and Methods chapter (section 2.4.1). First strand cDNA was synthesized from total RNA using the Qiagen Omniscript Reverse Transcription kit (Qiagen). 1µg of total RNA was added to a Reverse Transcription reaction (section 2.4.4). The reverse transcription reaction was diluted by one tenth with DEPC-treated water, and 5µl was then added to a standard PCR mix. The PCR mix contained 1x GO Taq Flexi buffer (Promega), 2mM MgCl₂, 0.2mM dNTP mix (Qiagen), 0.5mM each gene specific primer (MWG Biotech) and 1 unit of GO Taq polymerase in a final volume of 25µl. Thermal cycling conditions were: 95°C for 5 mins; 35 cycles of 94°C for 40 seconds, 55°C for 40 seconds and 72°C for 2.5 mins; 72°C for 10 mins; cooling to 4°C.

RT-PCR products were examined on a 2% agarose gel; the expected size of each cDNA fragment is given in Table 5.2. All RT-PCR products (stress and control) were run on the same gel, and a digital image of the gel was taken using the UVP-Biodoc-

IT-system. BioRad “Quantity One” quantification software (BioRad) was used to measure the density of each cDNA band produced. The densities of the 18S rRNA bands generated from the stress and control samples were compared, and all densities of bands resulting from expressed genes were corrected accordingly. Subsequently, the percentage of up- or down-regulation of each candidate gene in the stress sample was calculated with respect to the unstressed control sample. This analysis was repeated three times on three sets of plants and the average results are summarized in the following figures.

Immediately after the cessation of the vibration stimulus, all candidate wind/mechanical stress genes were up-regulated in the stressed seedlings as compared to the unstressed control seedlings with the exception of the negative control GRP6 (Figure 5.1). Thus, the candidate genes are differentially expressed in response to vibration stress. By 14-days, expression of TCH3, EXP3 and CCR2 was down-regulated in vibrated seedlings compared with unstressed seedlings (Figure 5.2).

The genes involved in signaling pathways, MEK1 and TCH3 both showed an up-regulation of expression immediately after stress. TCH3, expressing a calmodulin-like protein was highly expressed, which suggests a role in cell signaling in response to vibration stress. MEK1 was expressed to a lower level; however it is differentially expressed in stressed seedlings (Figure 5.1), and therefore is likely to play a role in signaling in response to vibration stress. MEK1 is expressed to a lower level by 14-days in vibrated seedlings, while TCH3 is not expressed.

Immediately after the cessation of vibration stress the touch genes TCH3 and TCH4 are both up-regulated to a similarly high level. At 14-days the expression levels of the genes varied; TCH3 was not expressed in vibrated seedlings (but was expressed in the control), whereas TCH4 levels were high. This may reflect the different functions of these two touch genes. TCH3 may only be transiently up-regulated in response to vibration. The apparent enhanced expression of TCH3 in the control seedlings at 14-days could be explained by the accidental induction of the touch gene through sample handling. However, global gene expression was not affected, as determined by a lack of expression of the GRP6 gene.

CESA3 and PAL1 show relatively high levels of expression in both vibrated and control samples. The enhanced regulation of CESA3 is consistent with the expression of CESA3 in young expanding tissues (Doblin *et al*, 2002). Although PAL1 is ubiquitously expressed in the developing seedling, PAL1 expression appears to be enhanced in seedlings subjected to vibration stress. This is in keeping with the findings in Chapter 4 that a greater proportion of peroxidase activity in vibrated seedlings was destined for the lignin pathway than in unstressed seedlings. Active oxygen species (and thus scavengers of these species such as peroxidase) are found concomitantly with lignin (Olson & Varner, 1993). Both of the candidate genes involved in lignin biosynthesis were up-regulated in response to vibration; however PAL1 was expressed to a higher level than CCR2 after stress and at 14-days. CCR2 was expressed in vibrated seedlings and to a lower level in control seedlings immediately after cessation of stress (Figure 5.1). This is the first time CCR2 has been shown to be induced by mechanical stress in seedlings. With this in mind, it is surprising that CCR2 is expressed at a lower level in vibrated seedlings at 14-days than in the unstressed seedlings.

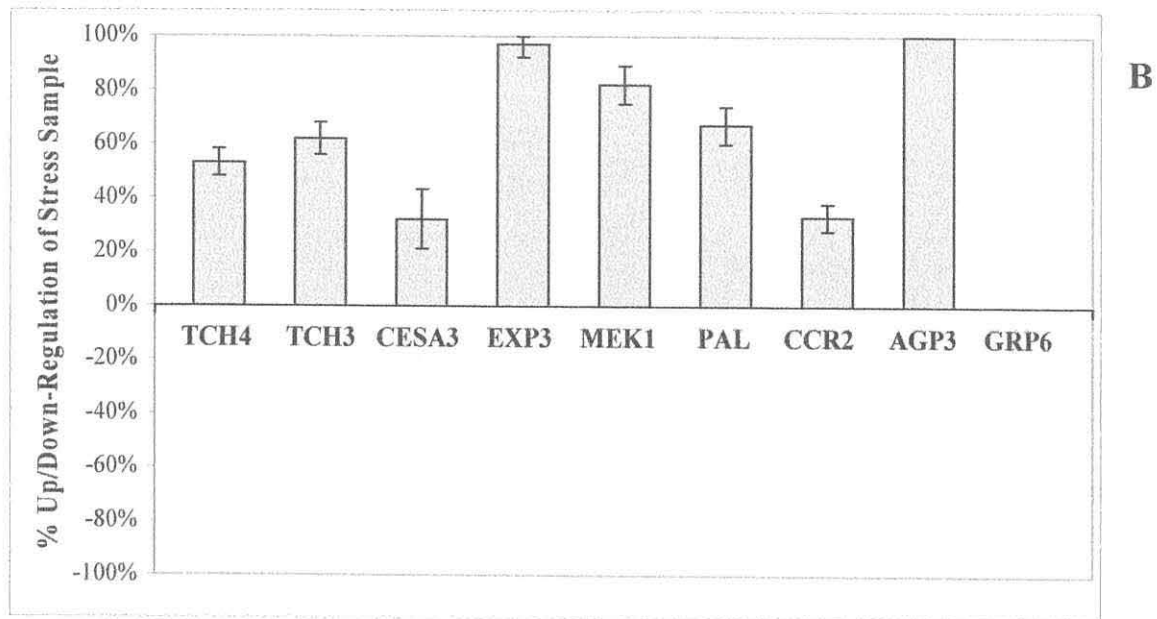
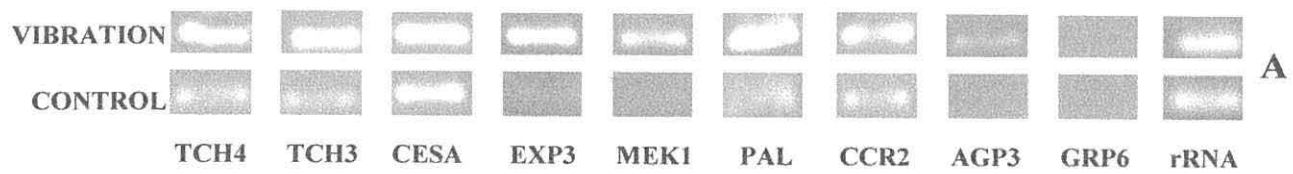


Figure 5.1: Expression of candidate wind stress genes immediately after cessation of stress in seedlings subjected to vibration stress. Vibration stress was applied for 72 hours continuously from germination. **A.** 2% agarose gel showing RT-PCR products from vibrated seedling RNA and control (unstressed) seedling RNA. **B.** Up/Down-regulation of candidate wind/mechanical stress genes in seedlings subjected to vibration stress with respect to unstressed control seedlings. Values are \pm SD of 3 samples.

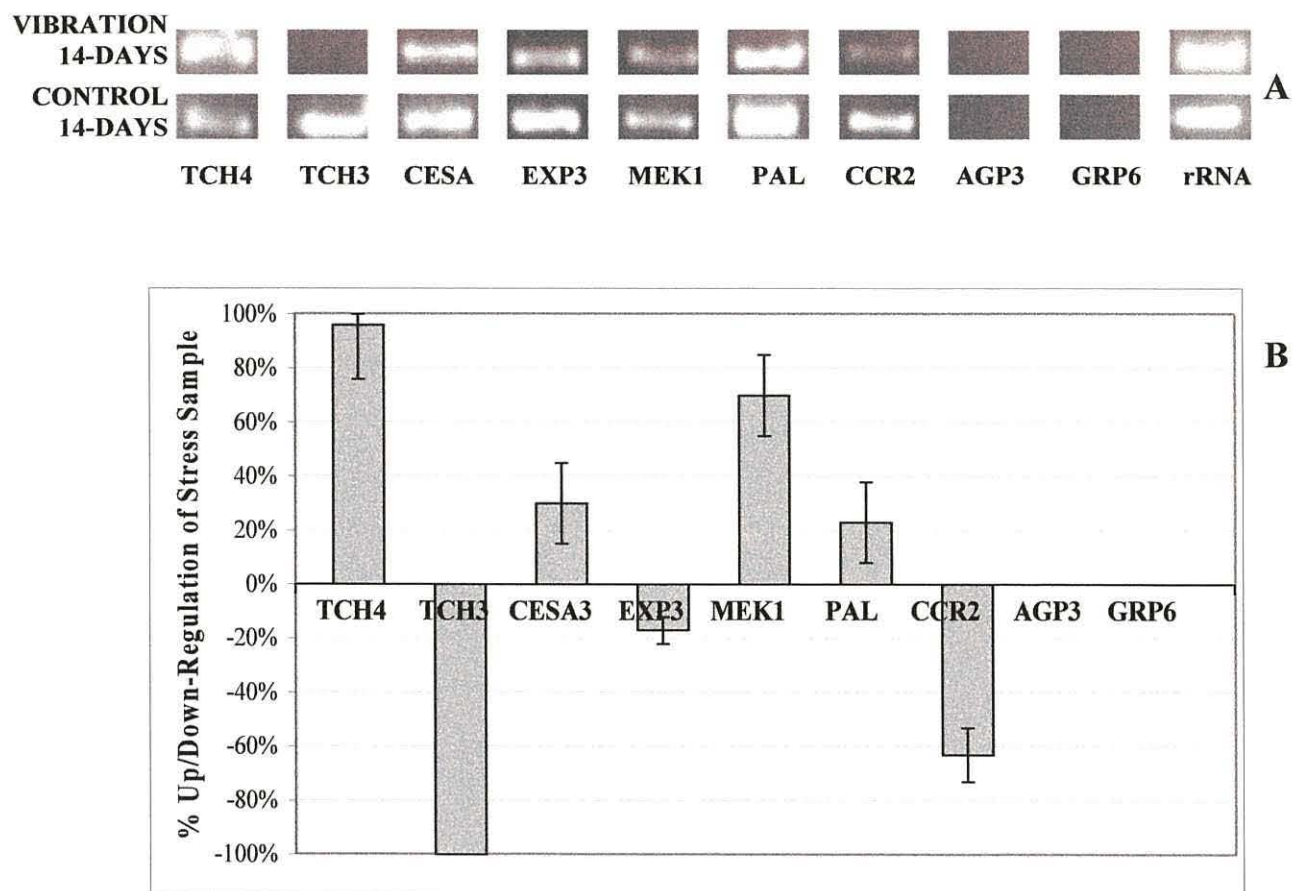


Figure 5.2: Expression of candidate wind stress genes at 14-days in seedlings subjected to vibration stress. Vibration stress was applied for 72 hours continuously from germination. **A.** 2% agarose gel showing RT-PCR products from vibrated seedling RNA and control (unstressed) seedling RNA. **B.** Up/Down-regulation of candidate wind/mechanical stress genes in seedlings subjected to vibration stress with respect to unstressed control seedlings. Values are \pm SD of 3 samples.

5.4.2 Analysis of gene expression of candidate wind/mechanical stress genes in plants subjected to wind stress

In chapter 3, conditions that induced a novel phenotype when plants were subjected to wind stress were established. These conditions were reproduced in the current set of experiments so that the expression of candidate wind/mechanical stress genes could be analyzed in the tissues of the stressed plants. *Arabidopsis* Ws seed were stratified at 4°C in dH₂O, and sprinkled on wetted compost: vermiculite mixture. Plants were grown under growth room conditions until 14 days. At 14-days seedlings were thinned out to one seedling per pot and grown with regular watering and feeding. At 17-days some plants were subjected to wind stress (2.7 m/s) for 2 hours three times per day (as described previously). Other plants were not subjected to wind stress, and acted as controls. All plants were grown until maturity.

Rosette leaf tissue was sampled from both sets of plants when rosette growth was complete, that is when control plants reached growth stage 3.9. Rosette leaves were frozen in liquid nitrogen and stored at -80°C. The inflorescence stem was sampled from control and stressed plants when the control plants reached maturation; samples were taken from the first centimeter of the basal stem. Samples were also stored at -80°C until RNA was extracted. RNA was extracted (section 2.4.1) and cDNA synthesized from it by reverse transcription (section 2.4.4). The reverse transcription reaction was diluted (1:10), 5µl was then added to a standard PCR mix, and amplified with specific candidate wind/mechanical stress gene primers as outlined in the previous section. PCR products were examined on a 2% agarose gel, and subject to the same analyses as were used in the previous section.

In plants subjected to long-term wind stress, GRP6 was not expressed in rosette or inflorescence stem tissues as expected (Figures 5.3 and 5.4 respectively). In rosette tissues sampled at rosette maturity from wind-stressed plants, TCH4 was up-regulated but all other candidate genes were down-regulated with respect to the expression in unstressed plants (Figure 5.3). By contrast, with the exception of AGP3, each of the candidate genes was up-regulated in wind-stressed inflorescence stems (Figure 5.4).

The most highly induced genes in wind-stressed stems were CESA3, EXP3, PAL1 and CCR2 (which were amongst the most repressed genes in wind-stressed rosettes).

It is perhaps not surprising that Touch gene 4 is up-regulated in rosettes subjected to wind stress as it has previously been shown that this gene is expressed in response to wind/mechanical stresses (Braam & Davis, 1990). In addition, this result shows that TCH4 continues to be expressed in response to wind stress even after repeated exposure to the stimulus. The other touch gene (TCH3) in this group of candidate wind/mechanical stress genes was expressed to a high level in both unstressed and wind stressed rosette leaves. Overall the expression of the candidate genes does not vary widely between the control and wind stressed rosettes, although the majority are repressed to a low level in wind stressed rosette leaves.

Signalling and lignification may be expected to increase while cell wall synthesis and expansion should slow down in tissues affected by wind/mechanical stresses. Each of the candidate genes was up-regulated in wind stressed inflorescence stems, which are shorter than unstressed stems. TCH3 and MEK1 are both up-regulated in the stress sample but these genes are also expressed, although to a lower level in control stems. Thus, these genes are likely to have a role during development of the inflorescence stem. Both PAL1 and CCR2 genes from the lignin pathway were found to be highly up-regulated in the wind stressed stem indicating enhanced lignification in response to wind stress. Additionally, TCH4 was upregulated in the stress stem sample. Both TCH4 and CCR2 have been shown to be involved in secondary growth in *Arabidopsis* (Ko *et al*, 2004). Wind stress may promote secondary growth over and above that induced by the weight of the developing stem.

Both CESA 3 and EXP 3 genes were also up-regulated in wind stressed stem. This may indicate that both cellulose synthase 3 and expansin 3 have alternative roles under normal development and under stress as TCH4 does, although further investigation is needed to substantiate this claim. CESA3 expression is normally associated with primary growth, although CESA3 and other genes encoding cellulose synthases may be induced under stress conditions.

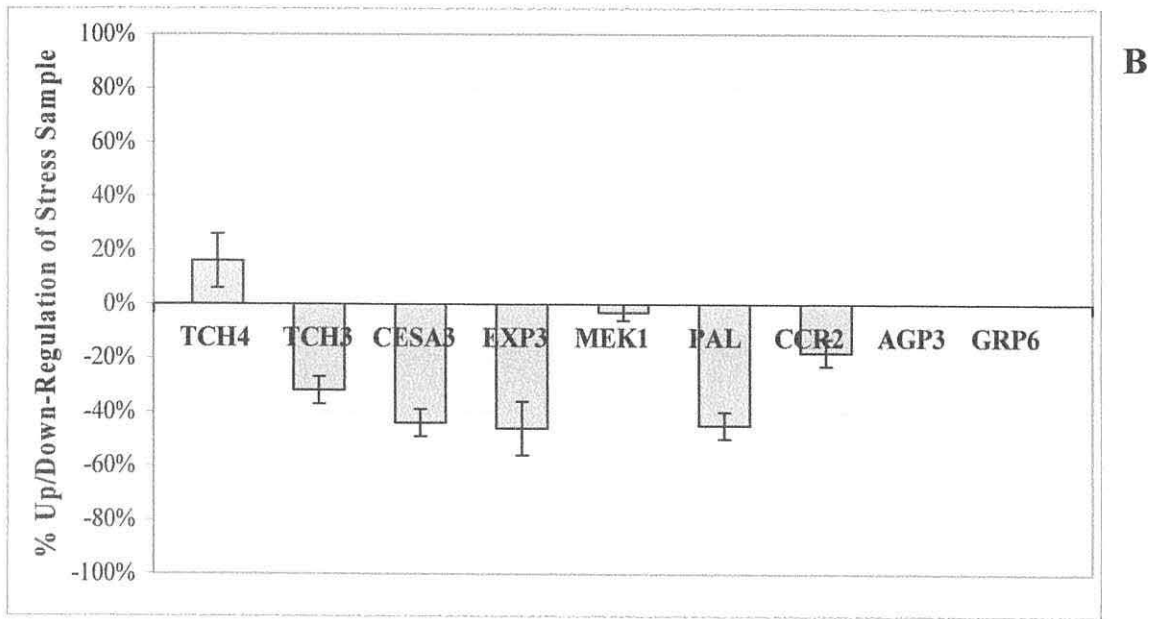


Figure 5.3: Expression of candidate wind stress genes in the rosette leaves of plants subjected to wind stress. Wind stress was applied from 17-days onwards. Samples were harvested when rosette development was complete in control plants (stage 3.9) **A.** 2% agarose gel showing RT-PCR products from wind stressed and control rosette leaf RNA **B.** Up/Down-regulation of candidate wind/mechanical stress genes in the rosette leaves of plants subjected to wind stress with respect to unstressed control plants. Values are \pm SD of 3 samples.

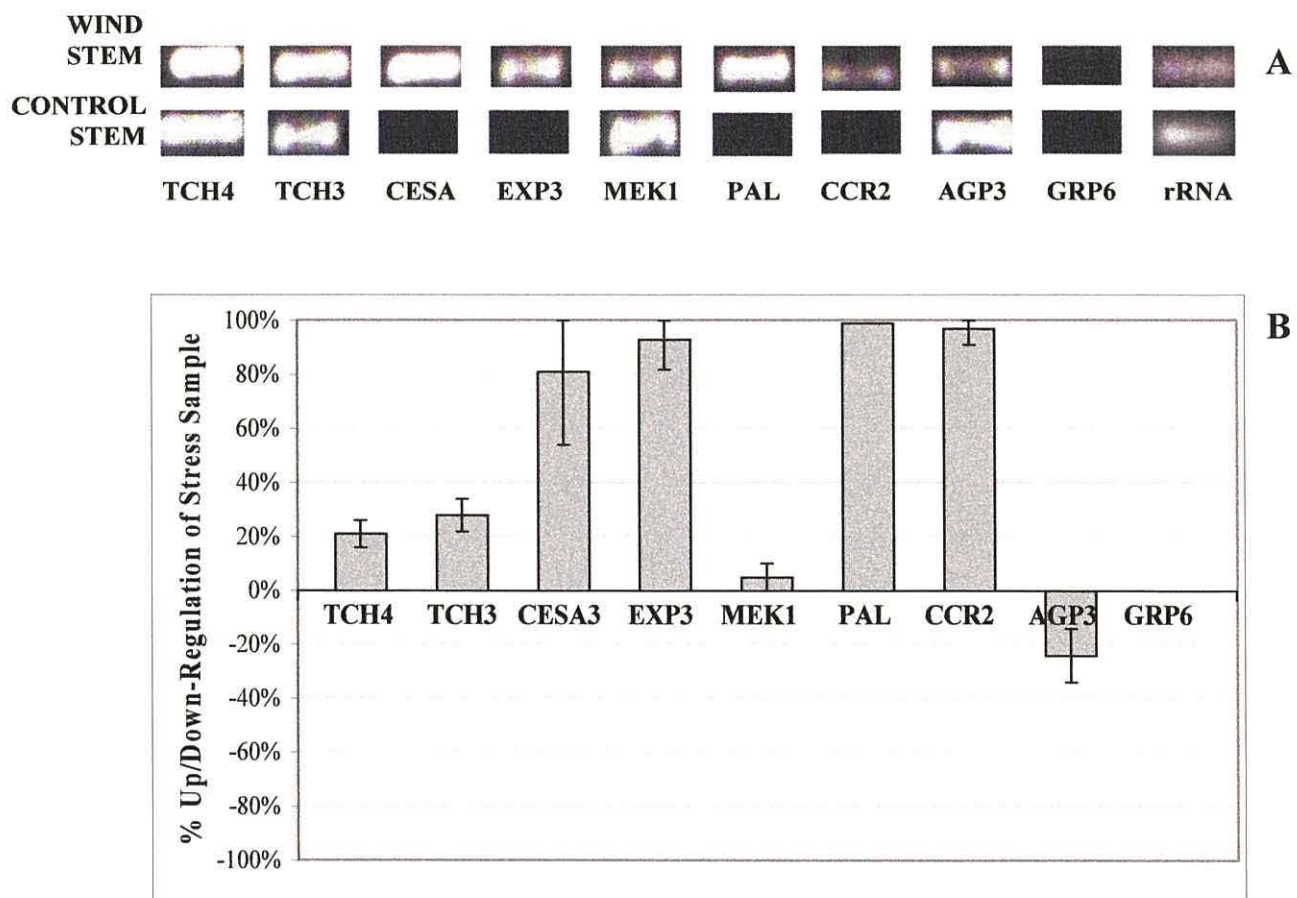


Figure 5.4: Expression of candidate wind stress genes in the inflorescence stems of plants subjected to wind stress. Wind stress was applied from 17-days to maturation, and stem samples were harvested at maturation (stage 9.0). **A.** 2% agarose gel showing RT-PCR products from wind stressed and control inflorescence stem RNA **B.** Up/Down-regulation of candidate wind/mechanical stress genes in the inflorescence stem of plants subjected to wind stress with respect to unstressed control plants. Values are \pm SD of 3 samples.

5.4.3 Summary of gene expression

A hierarchical cluster analysis, using Genesight software (Biodiscovery Inc., UK) was used to delimit the expression of candidate wind/mechanical stress genes in stressed seedlings and plants compared to control (unstressed) seedlings and plants, and to identify groups of co-expressed genes. These analyses were based on an agglomerative approach; clusters of genes were sorted on the basis of the gene expression ratios using a distance coefficient (Euclidean distance). Finally a dendrogram was generated summarizing the differential expression of candidate wind/mechanical stress genes under wind and mechanical stress conditions (Figure 5.5). From the analysis, two main clusters of genes were identified. The first cluster, (designated cluster 1) includes CCR2, AGP3, MEK1, TCH4 and TCH3. Cluster 2 comprises CESA3, PAL1 and EXP3.

Overall, expression ratios of candidate wind/mechanical stress genes are more similar in wind stressed stem and in seedlings immediately after the cessation of vibration than in any of the other samples taken. There is an apparent paradox in these results in that the same genes appear to be up-regulated in wind stressed stems that are dwarfed, and in vibrated seedlings, in which a promotion of hypocotyl elongation is observed. However, as was implied in the previous discussions, a number of the candidate genes seem to have alternative roles in the different phenotypes observed in response to mechanical stresses and at different stages of development. Touch gene 4, cellulose synthase 3, Expansin 3 and cinnamoyl CoA reductase 2 are all differentially expressed in both vibrated seedlings and wind stressed stems, in which growth is respectively promoted and inhibited. Further work is needed to elucidate the roles of specific candidate genes.

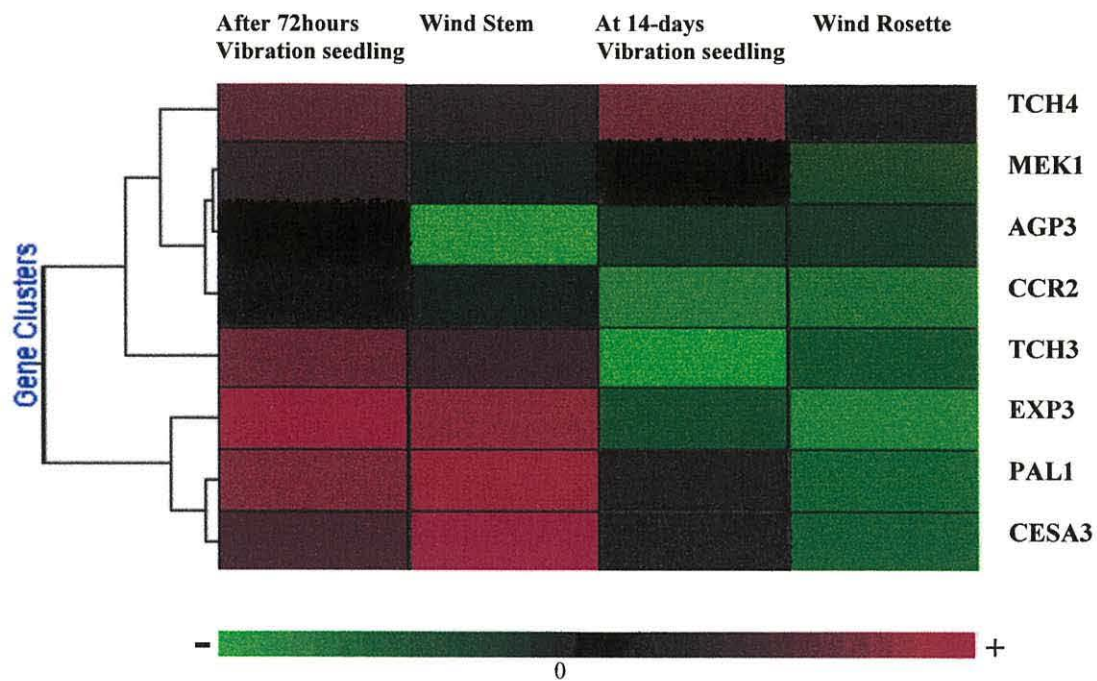


Figure 5.5: Hierarchical cluster analysis of gene expression ratios of mechanically stressed seedlings/plants versus unstressed seedlings/plants.

The colour scale shown below the dendrogram shows the scale of up-/down-regulation of gene expression in the stressed sample with respect to an equivalent unstressed sample.

5.5 Identification of common regulatory elements in the promoters of co expressed genes

Hierarchical cluster analyses similar to those used in the previous section of this chapter are used to group together genes with similar patterns of expression. This approach is now commonly used in transcriptome analysis; co-expressed genes may have shared transcriptional control elements (Maleck *et al*, 2000). Thus, the promoters of co-expressed genes may contain consensus motifs that are overrepresented when compared to a set of genes that are not co-expressed. These motifs may represent important points of regulation. Accordingly, the upstream regions of co-expressed candidate wind/mechanical stress genes were analysed to identify over-represented consensus motifs.

5.5.1 Detection of common motifs in the promoters of co expressed genes

Methods for determining consensus motifs fall into two classes; those based on the frequency of nucleotides, and those based on probability matrices (Thijs *et al*, 2002). MotifSampler (Thijs *et al*, 2001) is a computer-based algorithm that can be used to find over-represented motifs in the promoter regions of co-expressed genes. MotifSampler is based on a position probability matrix that takes into account the effect of background noise on the designation of a motif (Thijs *et al*, 2001). The noisy background effect is caused by a combination of the small size of the motif compared to the sequences being analysed and the fact that many upstream sequences do not contain the motif. Furthermore, the influence of background noise is greater in higher eukaryotes such as *Arabidopsis* (Thijs *et al*, 2001). The algorithm is defined by a modified form of Gibbs sampling for maximum likelihood estimation. One such modification is the use of a higher order background model. This model takes into account the complexity of the genome and thus shows better discrimination between motifs occurring by chance and those that are biologically relevant (Thijs *et al*, 2002).

Most *Arabidopsis* promoters have control elements located within the first 1000 base pairs of the translation start site (Maleck *et al*, 2000). For analysis of upstream regions

of candidate wind/mechanical stress genes, 1.5 Kb of the upstream sequence from the translation start site was used as it should have covered the majority of control elements. Sequences were obtained from NCBI as outlined previously. The sequence for each gene in the identified clusters (Figure 5.5) was saved together in FASTA format as a text file (.txt). These input files were run through the MotifSampler program (Linux version) using the third-order background model from *Arabidopsis thaliana* (Thijs *et al*, 2002). The program parameters were set to identify a single motif per program cycle, and 30 cycles were run as a batch for each cluster of genes. Motifs in the output file were first organized based on whether they were present in each promoter in the cluster. Motifs that were not present in every candidate gene were deleted. Subsequently, the motif consensus sequences were aligned using the MuSiC-ME (Memory-Efficient tool for Multiple Sequence Alignment with Constraints) tool (Lu & Huang, 2005) to group similar motifs together. Finally, the consensus scores and log likelihood scores for the motifs were used to determine the key motifs to use to search databases of plant *cis* regulatory elements.

5.5.2 Characterization of promoter motifs found in co expressed genes

PlantCARE (Lescot *et al*, 2002) and PLACE (Higo *et al*, 1999) are databases of plant *cis*-acting regulatory DNA elements (CAREs) that are accessible via the World Wide Web. These databases can potentially assign biological functions to promoter motifs. Motifs can be searched using the motif nucleotide sequence, and where the motif matches an accession, an accession identifier and description will be returned. Table 5.3 lists the motifs identified by MotifSampler in the clusters of candidate wind/mechanical stress genes and the corresponding accessions returned by either PlantCARE or PLACE. The motifs returned by the databases do not all occur in *Arabidopsis* genes as indicated in the table. Where the motif searched and the accession differed by a single nucleotide, the IUPAC nucleotide codes have been used.

Table 5.3: Designation of motifs generated by MotifSampler (Thijs *et al*, 2001)

The sequences and descriptions returned are those generated by databases of plant *cis*-acting regulatory DNA elements ^a PLACE (Higo *et al*, 1999) or ^b PlantCARE (Lescot *et al*, 2002). Sequences in **plain bold** text are the complement to the motif searched and those in ***bold italics*** are the reverse complement.

Cluster	Motif searched	Sequence returned	Description	Host
1 (CCR2, AGP3, MEK1, TCH4, TCH3)	ATTATTTA	TATTTAA ^a	Binding site for a transcription binding protein found in the promoter of a phenylalanine ammonia-lyase in rice.	<i>Oryza sativa</i>
		TTATTT ^a	TATA box	<i>Arabidopsis thaliana</i>
	AAACCA	WAACCA ^a	A MYB recognition site found in the promoters of genes, including dehydration responsive gene rd22	<i>Arabidopsis thaliana</i>
		<i>GGTTAA</i> ^b	Light responsive element	<i>Arabidopsis thaliana</i>
	TTGACT	TTGAC ^a	Salicylic acid induced WRKY binding protein	<i>Arabidopsis thaliana</i>
		TGAC ^a	W-box core. Transcriptional control of the gibberellin signalling pathway.	<i>Nicotiana tabacum</i>
2 (CESA3, PAL1, EXP3)	TGACTAA	TGAC<u>Y</u> ^a	May be involved in activation of ERF3 gene by wounding. WRKY binding site.	<i>Nicotiana tabacum</i>
		TGAC<u>B</u> ^b	Correlated with auxin, salicylic acid and methyl jasmonate production in response to stress	<i>Nicotiana tabacum</i>
	TTCGGTTT	<i>CCGAAA</i> ^a	Low-temperature responsive element	<i>Hordeum vulgare</i>

The over-represented motifs identified are predominantly elements that have established links with the regulation of other abiotic and biotic stresses; such as binding sites for the WRKY (Eulgem *et al*, 2000) and MYB (Abe *et al*, 1997) transcription factors. The binding site for WRKY-type transcription factors appears in both clusters. This is noteworthy as WRKY binding sites have also been found in the promoters of several other genes involved in the response to infection and other stresses (Eulgem *et al*, 2000). The WRKY proteins are a large family of transcriptional regulators, which regulate the expression of specific target genes. WRKY proteins bind to a TGAC core nucleotide motif, which is usually preceded by an additional T nucleotide (TTGAC). This binding site is also known as the W box (Eulgem *et al*, 2000). Previous reports suggest that the W box core is usually followed by a C or T (Maleck *et al*, 2000). A distinct group of transcription factors, the TGA-bzip transcription factors (Schindler *et al*, 1992) recognise a TGACG motif which may overlap with the W-box TGAC core motif (Maleck *et al*, 2000). However, in the case of the TGA-bzip transcription factors the TGAC core binding site is not followed by a C or T as it is for the W-box transcription factors.

Table 5.4 summarises the frequency of the WRKY/W-box and associated binding sites in all of the promoters of the candidate wind/mechanical stress genes. The TTGAC motif is found an average of 3.6 times in each promoter, which is comparable to an expected 2.9 times for a 5 base pair motif in a 1.5Kb promoter. The strictest definition of the W-box binding site is TTGACC/T; there is an average of 2.9 copies of this motif per promoter. The TGA-bzip binding motif occurs fewer times than the expected occurrence of 2.9 copies per promoter. Thus, the TGA-bzip transcription factors are not likely to be a common point of regulation for these candidate wind/mechanical stress genes. On the other hand, the W-box transcription factors are overrepresented in the identified cluster of genes, and in this set of candidate wind/mechanical stress genes as a whole. Thus, they are likely to play a role in the regulation of gene expression in response to wind and mechanical stresses, as they do in other plant defence responses.

The distribution of binding motifs is pertinent to the regulation of expression through combinatorial control. Maleck *et al* (2001) have previously stated that W-boxes are commonly clustered together in the promoters of WRKY-regulated genes;

furthermore these motifs occur as palindromes or as uninterrupted repeats. The analysis of the distribution of the W-box/WRKY binding motifs in the *cis* regions of the candidate wind/mechanical stress genes (Figure 5.6) shows that these motifs do occur closely together, in a number of cases within 20-100bp of each other. Furthermore, the W-box binding sites were commonly found to be near to or overlapping with the MYB/MYC motifs.

The MYB and MYC transcription factors have been found to interact with MYB and MYC binding sites in the promoter of the dehydration-responsive gene *rd22* (Abe *et al*, 1997). Induction of the *rd22* gene is mediated by abscisic acid (ABA), as are the majority of other drought-induced genes (Abe *et al*, 2003). However, the *Arabidopsis rd22* gene does not contain the ABA-responsive element (ABRE) that is found in many abscisic acid-responsive genes (Yamaguchi-Shinozaki & Shinozaki, 1993). A 67-bp region of the promoter of the *rd22* gene contains AtMYB2 and AtMYC2 binding sites and can regulate gene expression under drought conditions. Furthermore, AtMYB2 and AtMYC2 bind cooperatively, and induce *rd22* in response to abscisic acid (Abe *et al*, 2003).

The AtMYB2 motif was found to be over-represented in cluster 1 of the candidate wind/mechanical stress genes (Table 5.3). Additionally, the motif was found in all of the candidate genes that were not present in cluster 1. Multiple AtMYC2 binding sites were also found in all candidate genes but not at a greater than expected frequency. AtMYB2 and AtMYC2 binding sites were commonly found in close proximity to each other (Figure 5.6). Thus there is some evidence to suggest that AtMYB2 and AtMYC2 may activate transcription of candidate wind/mechanical stress genes via a pathway mediated by abscisic acid. Alternatively, as each of the candidate genes contained the ABRE motif; gene expression could be regulated through a pathway mediated by abscisic acid and result in the selective binding of ABRE binding proteins.

A microarray study by Lee *et al* (2005) found that a number of WRKY and MYB transcription factor genes are amongst the most highly induced in *Arabidopsis* plants in response to touch. Of the 589 genes up-regulated by at least twofold within 30 minutes of touch stress, 9 were WRKY transcription factors and 5 were MYB

transcription factors. Further studies are needed to investigate the role of these transcription factors in the expression of candidate wind/mechanical stress genes.

Table 5.4: Frequency of binding motifs associated with transcription factors involved in plant defence found in the promoters of candidate wind/mechanical stress genes.

Motif type	Binding site^a	Average frequency in promoters of candidate wind/mechanical stress genes^b	Frequency in GRP6 (negative control)	Statistically expected frequency per 1.5Kb promoter
WRKY/W-box	TTGAC	3.6	2	2.9
WRKY/W-box	TTGACC/T	2.9	1	1.5
TGA-bZIP	TGACG	1.4	2	2.9
MYB	A/TAACCA	4.8	2	1.5
MYC	CANNTG	10.3	10	11.7
ABRE	ACGTGGC	1.5	3	0.18

^a The binding sites used in this analysis are those returned by PlantCare or PLACE databases. ^b 1.5Kb of promoter upstream of the translation start site was analysed for each promoter.

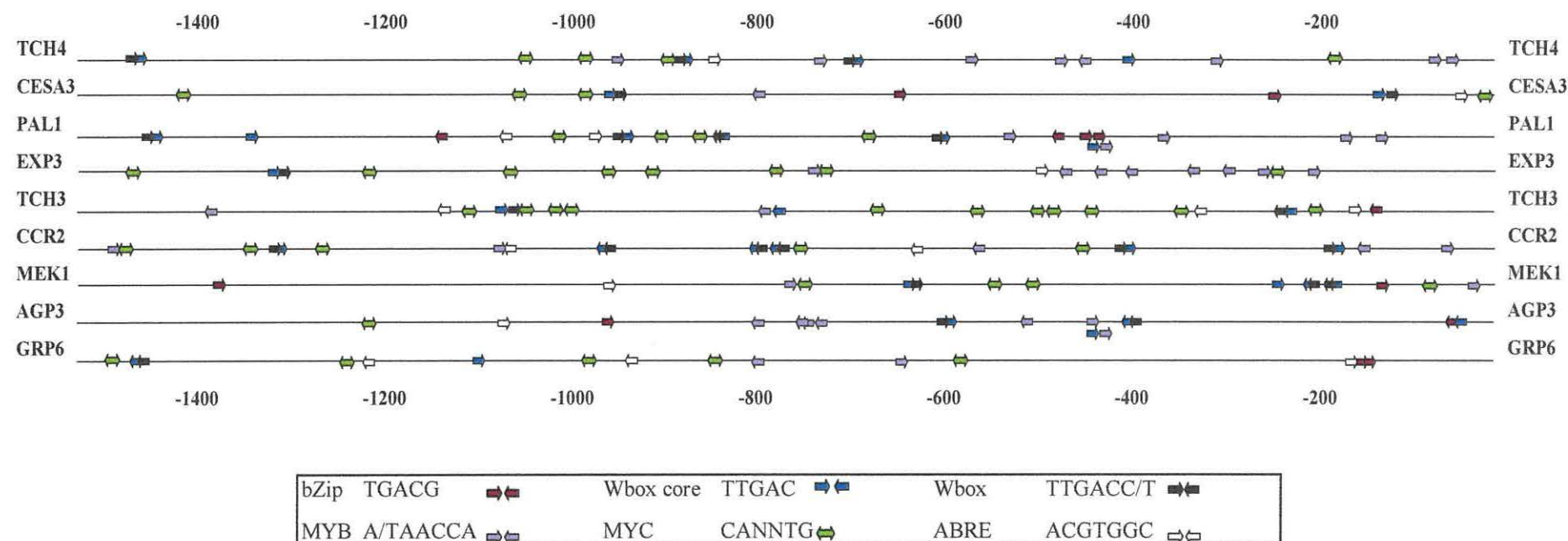


Figure 5.6: Distribution of selected binding motifs in the *cis* regulatory regions of candidate wind/mechanical stress genes.

1500 bp of promoter sequence, upstream from the translation start codon is shown; numbers indicate the relative position of the motifs. Forward arrows (pointing towards the translation start site) shows that the motif was found on the forward strand and correspondingly, reverse arrows show that the motif was found on the reverse strand. In some cases the W box defined as TTGACC/T overlaps with the W box core, as indicated by overlapping arrows. The MYC binding motif is a palindrome, and thus occurs at the same sites on the forward and reverse strands, as indicated by the left-right arrow.

5.6 Summary

In this chapter the expression of specific candidate wind/mechanical genes was shown to be differentially regulated in response to wind and mechanical stresses. Gene expression profiles can be related to biophysical processes occurring during development and under exposure to wind/mechanical stresses. Touch gene 4, cellulose synthase 3, Expansin 3 and cinnamoyl CoA reductase 2 are interesting candidates for further study with transgenes. Selected candidate genes were co-regulated; furthermore they share common regulatory motifs in their promoters. Over-represented motifs include WRKY and MYB motifs, which have previously been associated with plant defense in response to stress.

6. EXPRESSION OF THE *ARABIDOPSIS* EXTENSIN GENE EXT1 IN PLANTS SUBJECTED TO WIND AND MECHANICAL STRESSES

6.1 Introduction

The extensin gene EXT1 from *A. thaliana* was isolated and characterized by Merkouropoulos *et al* (1999) by using the coding sequence of the extensin gene *extA* from *Brassica napus* (Evans *et al*, 1990) as a probe for an *Arabidopsis* genomic library. The gene encodes a protein encompassing 374 amino acids and is rich in Val-Tyr-Lys motifs, suggesting that it may be highly cross-linked in the cell wall. It has been shown that the gene is developmentally regulated, induced by wounding and with treatment by methyl jasmonate, abscisic acid and salicylic acid (Merkouropoulos *et al*, 1999)

In this chapter, the role of EXT1 as a candidate wind/mechanical stress gene is considered. The rationale for its selection will be outlined in the introduction to this chapter. Expression of EXT1 in the samples used in the previous gene expression study (Chapter 5) from mechanically stressed seedlings and plants was monitored using RT-PCR. The *cis* promoter regulatory region of EXT1 was analyzed and compared to that of the other candidate wind/mechanical stress genes. The phenotype of a transgenic line over-expressing EXT1 was observed when it was subjected to wind and other mechanical stresses, and the extent to which the phenotype can be attributed to cross-linking of extensin was considered.

6.1.1 Synthesis of extensins

Extensins are encoded by multigene families that are developmentally regulated and may also be induced by specific abiotic and biotic stresses. Extensin mRNA is translated on the rough ER and subsequently directed into the lumen of the rough ER where most of its proline residues are converted to hydroxyproline (Chrispeels, 1969, Wienecke *et al*, 1982). The hydroxylated protein is then transported to the Golgi

apparatus where specific serine and hydroxyproline residues are glycosylated. Extensins are secreted into the plant cell wall where they become insolubilized through covalent cross-linking; it has long been proposed that extensin is cross-linked in the cell wall by isodityrosine bridges; there is a comparable amount of isodityrosine and hydroxyproline in the cell walls of a number of angiosperms (Fry, 1986). Covalently bound extensin is considered to be that which cannot be extracted by SDS, salt or acidified phenol; covalent binding and isodityrosine bridge formation are both inhibited by peroxidase inhibitors such as ascorbate and cyanide, which suggests that peroxidase can cross-link extensin via the formation of isodityrosine bridges (Fry, 1986). Crosslinking of extensin is likely to be relevant to its proposed function of increasing tensile strength, and limiting the impact of pathogen attack and wounding.

6.1.2 The *Arabidopsis* EXT1 gene: developmental regulation and induction by mechanical stresses

a) Expression of EXT1 during development

The original work by Merkouropoulos *et al* (1999) showed that EXT1 is expressed in roots and to a lesser extent in developing rosettes, being expressed in 2-week and 4-week old rosette leaves. However, EXT1 was not expressed in 6-week old rosette leaves or inflorescence stems. In a subsequent study using an *atEXT1*: GUS gene fusion, these expression patterns were confirmed (Merkouropoulos & Shirsat, 2003). In a more recent study, EXT1 was found to be expressed in seedlings; expression was restricted to the hypocotyls, leaf petioles and roots of 14-day old seedlings (Brown, 2004).

b) Expression of EXT1 in response to mechanical stress

Brown (2004) subjected plants carrying an *atEXT1*: GUS fusion to mechanical stresses by weight-loading and mechanical constraint. Weight loading was achieved by adding a 1.0g weight to the apex of the inflorescence stem, causing the stem to bend over. Mechanical constraint was achieved by covering the growing plants, thereby forcing the inflorescence stems to grow in other directions. It was found that

the EXT1 gene promoter was induced by both weight loading and mechanical stresses: atEXT1: GUS expression was restricted to the upperside of the inflorescence stem, which is the side under tensile stress in both cases. These results are consistent with previous studies in which the extA gene from *Brassica napus* has been shown to be expressed in plants subjected to tensile stress (Shirsat *et al*, 1996, Elliott & Shirsat, 1998).

6.1.3 Phenotypic changes in a transgenic *Arabidopsis* line over-expressing the EXT1 gene

An *Arabidopsis thaliana* line CaMV 35S:: atEXT1 5.13 over-expressing 1.122Kb of EXT1 coding sequence was generated by Brown (2004). The transgenic line was found to have hydroxyproline levels in leaves that were 2-3 times greater than that of wild-type levels (Brown, 2004).

Phenotypic analysis of this transgenic line showed that there was no significant effect on the time taken to reach Boyes *et al*'s (2001) principal stages of development as compared to wild-type. In the 5.13 line that had one of the highest hydroxyproline contents, inflorescence height was reduced (by 5%) in comparison to wild-type (Brown, 2004). However, despite the enhanced levels of hydroxyproline in the leaves of this line, there was no significant difference in the size of rosettes. The reduction in stem height is caused by the cessation of elongation, which may arise from the cross-linking of extensins; this result supports previous work correlating extensin levels with the cessation of cell elongation (Cleland & Karlnes, 1967, Wilson & Fry, 1986). The relatively small inhibition of stem elongation and the lack of an observable change in the rosette leaves suggest that in order to be associated with a major change in phenotype, an increase in extensin must be associated with the induction of cross-linking. Cross-linking may be induced experimentally by treatment with H₂O₂ (which generates peroxidase), or potentially by stresses that induce H₂O₂.

6.2 Expression of EXT1 in wild-type seedlings and plants subjected to wind and other mechanical stresses

EXT1 expression was analyzed in the samples taken to analyze the expression of candidate wind/mechanical stress genes: samples were taken from vibrated seedlings immediately after the cessation of vibration, vibrated seedlings when they reached 14-days old, and wind stressed rosette and inflorescence stem samples. Expression of EXT1 in these samples was compared to that in unstressed control samples.

EXT1 primers were designed to span the 95 bp intron sequence of the gene so that the PCR products generated from cDNA could be distinguished from those generated by genomic DNA contamination. The primer pairs and the sizes of fragment that are expected to be generated are shown in Table 6.1.

Table 6.1: RT-PCR primers based on EXT1 and RT-PCR controls.

Gene	Primers	Size of genomic DNA fragment b.p.	Size of cDNA fragment b.p.
EXT1	F: CCACACCAACCCTACCTTTAC R: CACCAAACGATTCTTTGT	206	111
GRP6	F: CCACGGCATTAAACCATAACAA R: CCCTGGTTTATTTCCGAATGT	611	277
18S rRNA	F: TCCTAGTAAGCGCGAGTCATC R: CGAACACTTCACCGGATCAT	100	100

6.2.1 Analysis of EXT1 expression in seedlings subjected to vibration stress

As detailed in Chapter 5, vibration at 40Hz was applied for 72 hours constantly from germination. Immediately after the cessation of vibration seedlings were harvested, frozen in liquid nitrogen and stored at -80°C until RNA was extracted. When the vibrated seedlings reached 14-days old, additional seedlings were harvested and stored in liquid nitrogen. Unstressed control seedlings were also harvested and stored at these time points. RNA was extracted and added to a reverse transcription reaction, and the reverse transcription product added to a standard PCR mix containing EXT1 primers (Table 6.1)

EXT1 mRNA was seen to be up-regulated in seedlings subjected to vibration stress immediately after the cessation of stress (Figure 6.1), while it was expressed to a low level in control samples taken at the same time point. When seedlings reached 14-days old, EXT1 mRNA expression was approximately the same in vibrated and control seedlings. Loading was not significantly different across the samples as indicated by RT-PCR with 18s rRNA controls. The negative control GRP6 was not expressed in any of the samples.

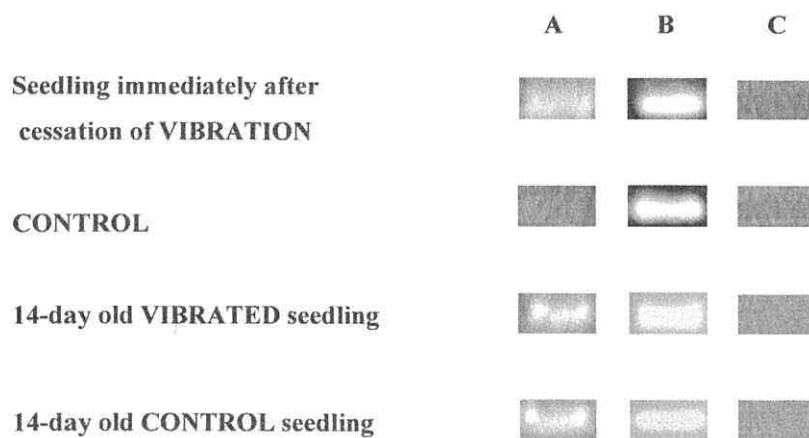


Figure 6.1: Expression of EXT1 in seedlings subjected to vibration stress. Vibration stress was applied for 72 hours continuously from germination. 2% agarose gels showing RT-PCR products from vibrated seedling RNA and control (unstressed) seedling RNA; immediately after the cessation of vibration and when seedlings reached 14-days old. A. EXT1, B. 18s rRNA loading control C. GRP6 negative control.

6.2.2 Analysis of EXT1 expression in plants subjected to wind stress

Soil-grown *Arabidopsis* Ws plants were grown under standard growth conditions until they were 17-days old. From 17-days onwards some plants were subjected to wind stress at 2.7 m/s for 2 hours three times per day. Control plants were not subjected to wind. All plants were grown until maturity, and rosette leaf tissue was sampled from both sets of plants when rosette growth was complete. Samples were taken from the inflorescence stem from control and stressed plants when the control plants reached maturity. Samples were taken from the first centimeter of the basal stem. RNA was extracted (section 2.4.1) and cDNA synthesized from it by reverse transcription (section 2.4.4). The reverse transcription reaction was diluted (1:10), 5 μ l was then added to a standard PCR mix, and amplified with EXT1 primers (Table 6.1).

EXT1 was not expressed in either the wind stressed or control rosettes, while it was expressed to a low level in both wind stressed and control inflorescence stems (Figure 6.2).

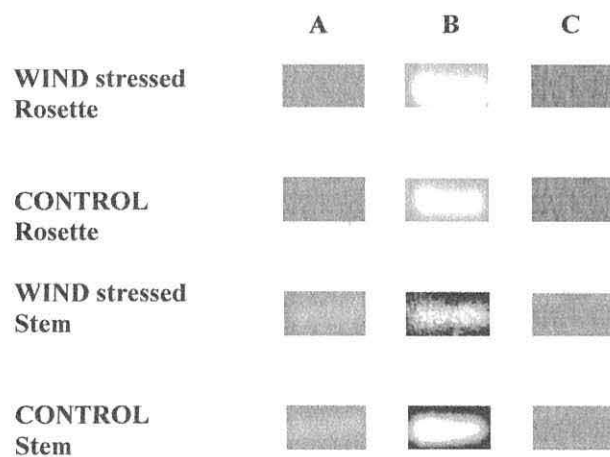


Figure 6.2: Expression of EXT1 in plants subjected to wind stress. Wind stress was applied from 17-days to maturation; rosette samples were harvested at rosette maturation (stage 3.9) and stem samples were harvested at maturation (stage 9.0). 2% agarose gels showing RT-PCR products from wind stressed and control rosette and inflorescence stem RNA **A**. EXT1, **B**. 18S rRNA loading control **C**. GRP6 negative control.

6.2.3 Discussion

a) Up-regulation of expression in seedlings subjected to vibration stress immediately after the cessation of stress

Immediately after the cessation of vibration stress (applied for 72 hours from germination), EXT1 expression is induced, although at 14-days when enhanced elongation of the hypocotyls is observed, EXT1 is expressed at normal levels compared to the control. The induction of EXT1 occurs prior to the development of a novel phenotype in vibrated seedlings, evidently, EXT1 is transiently up-regulated in response to vibration stress and returns to normal levels sometime after the cessation of vibration stress.

Induction of EXT1 expression in vibrated seedlings is surprising in view of the fact that vibrated seedlings subsequently develop a phenotype in which growth is promoted; this is the exact opposite of what might have been expected to occur. As outlined in the introduction to this chapter, EXT1 expression has been associated with the cessation of growth. However, EXT1 expression has also previously been shown to be induced in *Arabidopsis* plants subjected to mechanical stresses (Brown, 2004). Other candidate wind/mechanical stress genes were shown to be induced in seedlings immediately after the cessation of vibration. As GRP6, which is normally only expressed in floral tissues, is not expressed in the vibrated seedlings it is unlikely that vibration causes a global increase in gene transcription. Extensin genes have been shown to be expressed in proliferating cells induced by hormone treatment, which may be indicative of a greater need for extensin in cell wall assembly (Jamet *et al*, 2000). The induction of EXT1 expression in vibrated seedlings could be due to a higher requirement for extensin in cell wall assembly in the hypocotyl.

b) EXT1 expression is not induced in the rosette leaves or inflorescence stems of *Arabidopsis* plants subjected to wind stress

EXT1 expression was not induced by wind stress in either the rosette leaves or in the basal sections of the inflorescence stem, the basal section of the stem was sampled as wind stimulation causes bending at the root/stem junction. However, there was no

induction of EXT1 expression associated with the stem at maturation. In a previous study, atEXT1: GUS expression was seen in the stems of mechanically constrained *Arabidopsis* plants, although expression was restricted to the upper side of the inflorescence stem (Brown, 2004). It is conceivable that EXT1 expression was induced in wind stressed inflorescence stems at a stage of development prior to that sampled. Alternatively, it is possible that bending at the root/stem junction in wind stressed plants is insufficient to induce EXT1 expression. Further studies investigating EXT1 expression in the basal section of the inflorescence stem at different stages of development and under wind stress are needed.

6.3 Analysis of the *cis* promoter region of the EXT1 gene

It has been suggested that it is difficult to determine functional *cis* acting elements in extensin promoters by comparison with other previously characterized extensin promoters or known promoter motifs (Jamet *et al*, 2000). To some extent this is true as the only way to prove the involvement of a particular regulatory motif is by fusion of the promoter region to a reporter gene such as uidA (β -glucuronidase, GUS). However, the analysis of extensin promoters and comparison of their promoters with those of the other candidate wind/mechanical stress genes used in this study could potentially identify common regulatory motifs.

Merkouropoulos (2000) and Brown (2004) previously analyzed 3.2Kb of the EXT1 *cis* regulatory region. In the latter study the promoter sequence was compared to two databases of plant *cis* acting regulatory elements PlantCARE (Lescot *et al*, 2002) and PLACE (Higo *et al*, 1999). As outlined in Chapter 5, these databases were used to search 1.5Kb of the *cis* region of each candidate wind/mechanical stress gene.

Analysis of the first 1.5Kb of the EXT1 sequence upstream of the predicted translation start codon resulted in a similar analysis to that which Brown (2004) produced for that region. As was pointed out, WRKY/W-box binding sites (Eulgem *et al*, 2000) are found repeatedly in the *cis* regulatory region of the EXT1 gene. Figure 6.3 shows the distribution of WRKY/W-box motifs in the EXT1 sequence. The WRKY/W-box is over-represented in the EXT1 promoter and on average is found more frequently than in the other wind/mechanical genes (Table 6.2). The TGA-bZip motif (Schindler *et al*,

1992), which shares a common TGAC core with the WRKY/W-box motif, is unlikely to be involved in the regulation of EXT1 as it occurs less frequently than is statistically expected. This is also the case for the promoters of the other candidate genes. The MYB (Abe *et al*, 1997), MYC (Abe *et al*, 1997) and ABRE (Yamaguchi-Shinozaki & Shinozaki, 1993) motifs are also over-represented in the *cis* regulatory region of the EXT1 gene. The MYC motif occurs particularly frequently, especially in the region 450bp to 650bp upstream of the translation start site (Figure 6.3), where five motifs are clustered together. The MYC motif is also prevalent in the *cis* regulatory regions of the other candidate wind/mechanical stress genes. The highlighted motifs are over-represented in the EXT1 promoter as they are in the other candidate wind/mechanical stress genes, indicating possible common control sites.

From an earlier study using plants containing EXT1 promoter truncations fused to the GUS reporter gene; atEXT1::GUS expression only occurred in plants subjected to mechanical constraint that contained a region between -1963bp and -2209bp upstream of the translation start site (Brown, 2004). This indicates that motifs upstream of the initial 1.5Kb of sequence are involved in the regulation of the EXT1 gene, specifically in response to mechanical stress. Expression of atEXT1::GUS in the roots of plants containing the -1963bp to -2209bp region was greater than in any other regions of the 3.2Kb promoter, especially around the emergence points of lateral roots (Brown, 2004). However, high expression of EXT1 in roots is not necessarily due to the mechanical stress the root faces as it grows through the soil; seedlings grown on 0.8% agar plates, still showed atEXT1::GUS expression in the roots despite limited mechanical constraint (Brown, 2004). atEXT1:: GUS expression in seedlings subjected to mechanical stress was not considered. The -1963bp to -2209bp region of the EXT1 promoter includes WRKY/W-box, MYB, MYC and ABRE transcription factor binding sites. These motifs are over-represented in the first 1.5Kb of sequence upstream of the translation start codon, suggesting there is binding of transcription factors at sites specific to developmental cues and to stress responses.

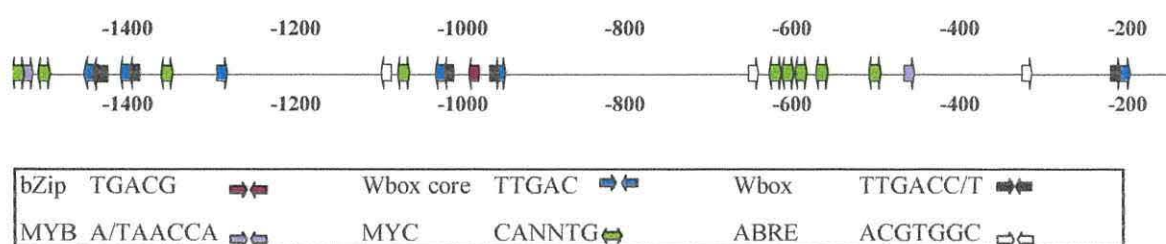


Figure 6.3: Distribution of selected binding motifs in the *cis* promoter region of EXT1.

1500 bp of promoter sequence, upstream from the translation start codon is shown; numbers indicate the relative position of the motifs. Forward arrows (pointing towards the translation start site) shows that the motif is found on the forward strand and correspondingly, reverse arrows show that the motif is found on the reverse strand. In some cases the W box defined as TTGACC/T overlaps with the W box core, as indicated by overlapping arrows. The MYC binding motif is a palindrome, and thus occurs at the same sites on the forward and reverse strands, as indicated by the left-right arrow.

Table 6.2: Frequency of binding motifs associated with transcription factors involved in plant defence found in the EXT1 gene promoter.

Motif type	Binding site ^a	Frequency in EXT1 promoter	Average frequency in promoters of candidate wind/mechanical stress genes ^b	Statistically expected frequency per 1.5Kb promoter
WRKY/W-box	TTGAC	6	3.6	2.9
WRKY/W-box	TTGACC/T	6	2.9	1.5
TGA-bZIP	TGACG	1	1.4	2.9
MYB	A/TAACCA	2	4.8	1.5
MYC	CANNTG	18	10.3	11.7
ABRE	ACGTGGC	3	1.5	0.18

^a The binding sites used in this analysis are those returned by PlantCare or PLACE databases. ^b 1.5Kb of promoter upstream of the translation start site was analysed for each promoter.

6.4 Analysis of CaMV: atEXT1, over-expressing extensin subjected to wind and mechanical stresses

6.4.1 Phenotypic analysis of CaMV: atEXT1 seedlings subjected to vibration stress

Arabidopsis wild-type Ws seeds and transgenic line CaMV: atEXT1 5.13 (over-expressing EXT1) seed were surface sterilized (section 2.2.2) and plated on half-strength MS media; CaMV: atEXT1 seed were plated on media supplemented with $35\mu\text{g.ml}^{-1}$ kanamycin. Seed were stratified at 4°C and then transferred to standard growth conditions as described in the materials and methods section. Vibration was applied for 72 hours from germination and at the two-leaf stage of seedling development (section 2.2.4). Hypocotyl and root elongation were measured in 14-day old vibrated seedlings and unstressed control seedlings for both wild-type and transgenic lines.

a.) Root elongation in extensin over-expressing seedlings subjected to vibration stress

The roots of seedlings from the extensin over-expressing transgenic line 5.13 were significantly shorter than those of the wild-type when compared at 14-days (Figure 6.4A) even in the absence of vibration. Vibration stress did not have a significant impact on root elongation in the transgenic line, whereas vibration stress inhibited root elongation in the wild-type. The over-expression of extensin in roots is the likely cause of the inhibition in root elongation. Furthermore, over-expression of extensin seems to limit the impact of vibration stress.

b.) Hypocotyl elongation in extensin over-expressing seedlings subjected to vibration stress

The hypocotyl length of unstressed transgenic seedlings was not significantly different from the wild-type (Figure 6.4B). However, vibration promoted hypocotyl elongation

in the wild-type but not in the transgenic line. Again, the over-expression of EXT1 seems to have cancelled out the effect of vibration stress on hypocotyl elongation.

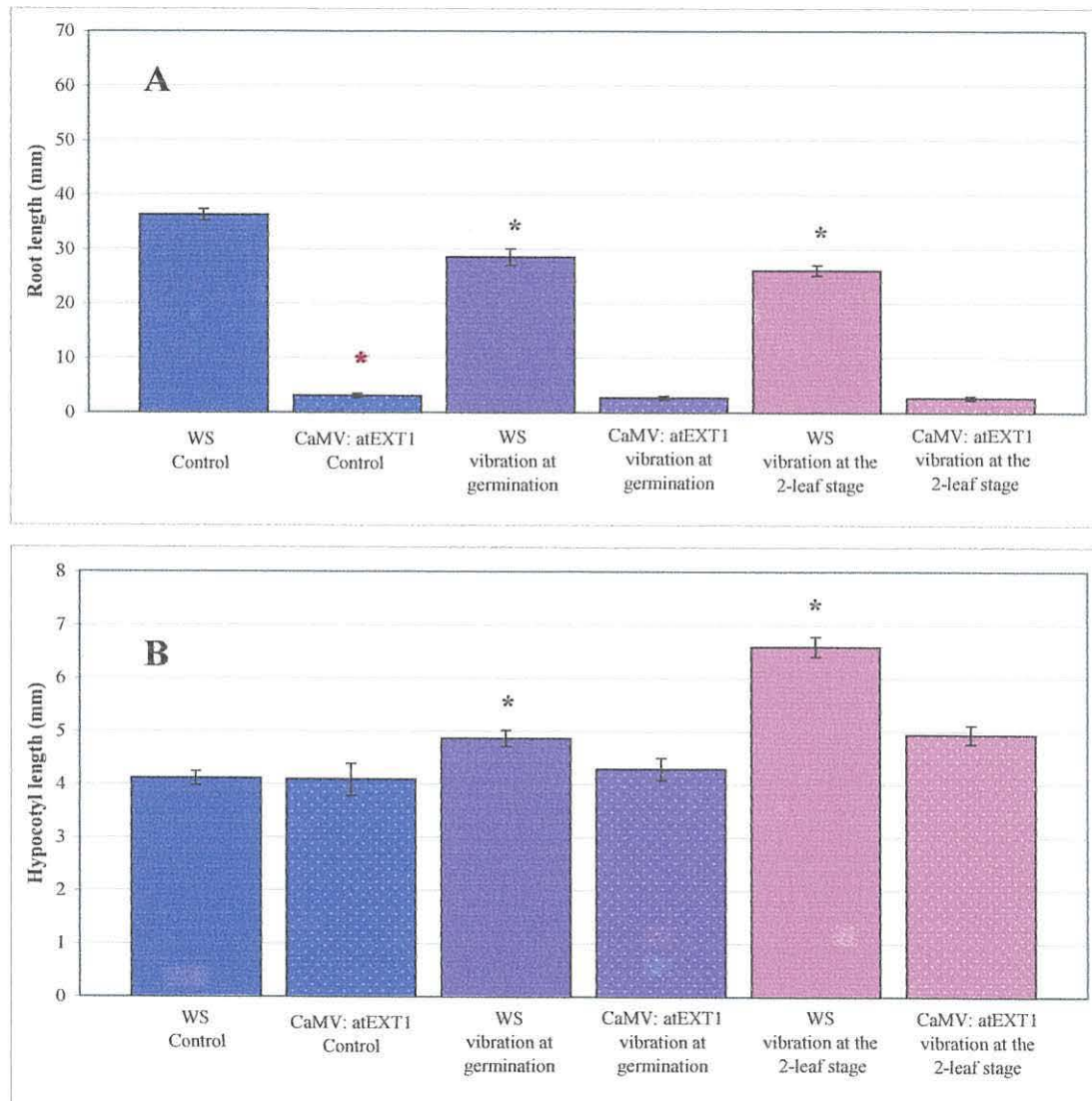


Figure 6.4: Development of CaMV: atEXT1 transgenic seedlings over-expressing extensin subjected to vibration stress

Vibration stress (40Hz) was applied for 72 hours either from germination or at the 2-leaf stages of development. Measurements of hypocotyl and root length were taken at 14-days. **A**. Root length at 14-days old, **B**. Hypocotyl length at 14-days old. Values are \pm SD of 20 seedlings. * Indicate results with $\geq 95\%$ significance as determined by a Two-way ANOVA. * (red) indicates transgenic and wild-type controls are significantly different. * (black) indicates stressed sample is significantly different from its appropriate control, for example CaMV: atEXT1 germination is compared with CaMV: atEXT1 control.

6.4.2 Phenotypic analysis of CaMV: atEXT1 transgenic plants over-expressing extensin subjected to wind stress

Arabidopsis wild-type and transgenic CaMV: atEXT1 (over-expressing EXT1) seedlings were grown *in vitro* until 14-days old when they were transferred to soil (section 2.2.2). As outlined in section 2.2.4, wind stress was applied for two hours three times per day; commencing at 08:00, 12:00 and 16:00. Wind stress was applied when seedlings reached 17-days old and continued daily until maturation. A soil-based phenotypic analysis (section 2.2.3) was used to compare wild-type and transgenic wind stressed plants with control plants that were not exposed to wind stress.

In the phenotypic analysis outlined in Chapter 3 it was shown that subjecting *Arabidopsis* wild-type plants to wind stress inhibited elongation of the inflorescence stem and resulted in a reduced rosette radius. Unstressed (control) transgenic plants had a smaller rosette radius compared to unstressed wild-type plants; however the height of the inflorescence stem was not significantly different between this line and the wild-type (Figure 6.5). Subjecting the plants to wind stress resulted in shorter inflorescence stems in wild-type and CaMV: atEXT1 plants in comparison to their respective non wind stressed controls (Figure 6.5A). In the transgenic line, the reduction in height of the inflorescence between the unstressed and wind stressed plants was not as marked as in the wild-type plants. Furthermore, wind stress does not cause a reduction in rosette radius in the CaMV: atEXT1 plants as it does in wild-type plants (Figure 6.5B).

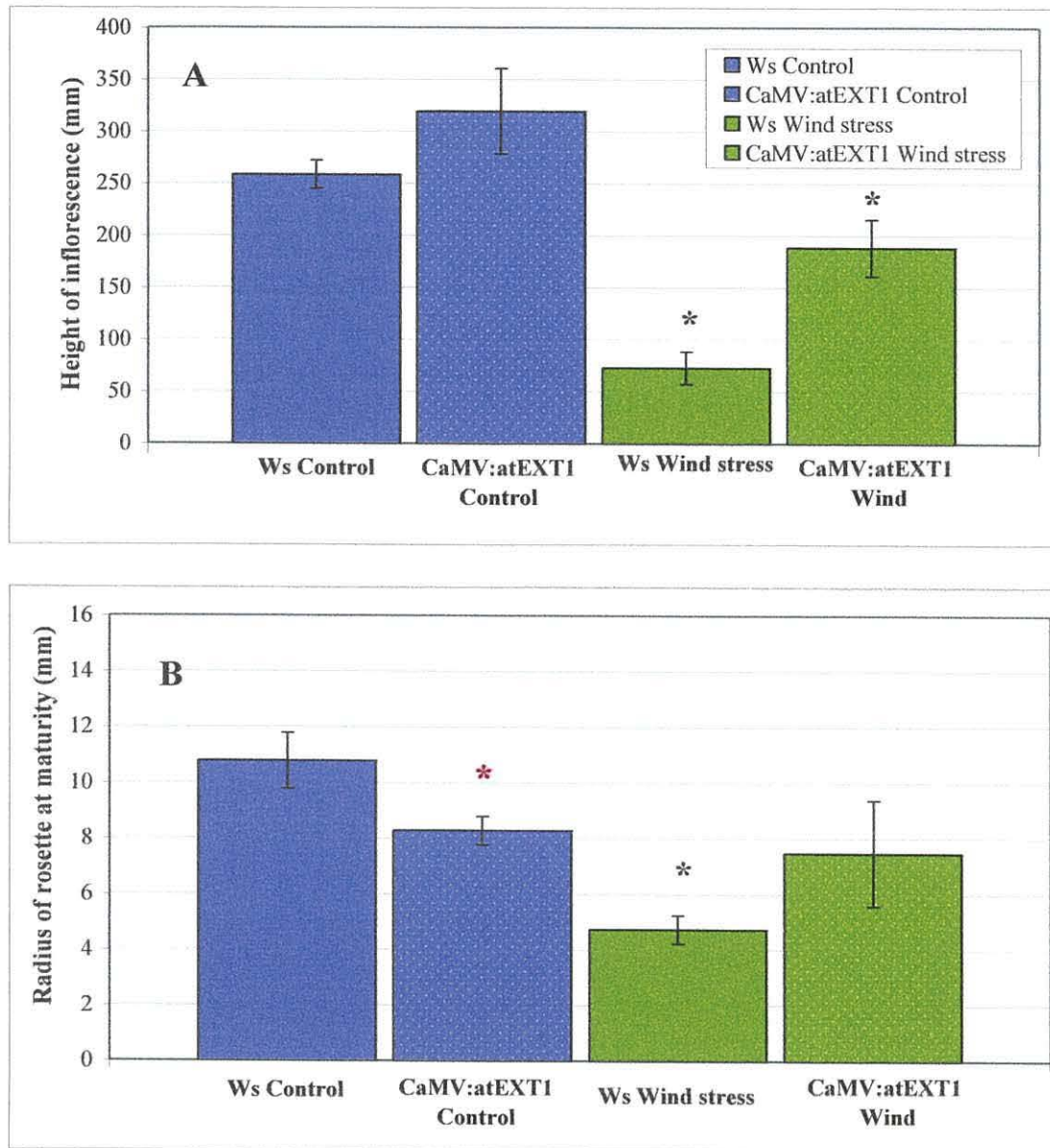


Figure 6.5: Phenotypic analysis of extensin over-expressing CaMV: atEXT1 plants subjected to wind stress.

Wind stress was applied for two hours three times per day when plants were 17-days old until maturation. **A.** Height of inflorescence stem **B.** Radius of rosettes, both measured at maturation. Values are \pm SD of 6 plants. * Indicate results with $\geq 95\%$ significance as determined by a Two-way ANOVA. * (red) indicates that transgenic and wild-type controls are significantly different. * (black) indicates that the stressed sample is significantly different from its appropriate control, for example CaMV: atEXT1 Wind stress is compared with CaMV: atEXT1 control.

6.4.3 Discussion

a) **Root elongation of CaMV: atEXT1 seedlings is inhibited even under limited mechanical stress**

In the root system, the EXT1 gene is developmentally regulated and induced by mechanical stress (Brown, 2004). EXT1 expression is persistently seen in the root particularly in the root hairs, behind the root cap, and in the cells at the emerging sites of lateral roots (Merkouropoulos & Shirsat, 2003, Brown, 2004). Over-expression of EXT1 in CaMV: atEXT1 seedlings resulted in a significantly shorter primary root, even in the absence of vibration stress. Merkouropoulos & Shirsat (2003) found that EXT1 was expressed in the elongating zone of the primary root. Over-expression of EXT1 contributes to the inhibition of root elongation when there is no significant mechanical stress. However, despite the shortness of the roots in the CaMV: atEXT1 seedlings vibration stress does not inhibit root elongation any further. These results seem to support the role of extensin in the cessation of elongation (Wilson & Fry, 1986).

b) **Over-expression of EXT1 limits the promotion of hypocotyl elongation that is induced by vibration stress**

In light of the inhibition of root elongation observed in unstressed CaMV: atEXT1 seedlings, it is surprising that there was no significant inhibition of hypocotyl elongation in those seedlings. However, when the CaMV: atEXT1 seedlings were subjected to vibration stress, over-expression of EXT1 apparently restrained the hypocotyl elongation seen in wild-type seedlings. Cleland & Karlsnes (1967) proposed that extensins were cross-linked in the cell wall, contributing to rigidity and tensile strength. They found that high levels of extensin proteins were associated with non-growing and slow-growing tissues, and furthermore there was an inverse relationship between the level of extensin proteins and cell elongation. Vibration stress is likely to have induced cross-linking of the extensin in the seedlings over-expressing EXT1, leading to an inhibition of hypocotyl elongation.

c) Phenotype of plants over-expressing EXT1 subjected to wind stress.

The original study (Brown, 2004) looking at the phenotype of CaMV: atEXT1 5.13 plants found that the inflorescence stem was 5% shorter than that of the wild-type, and that the rosette length was not significantly different to that of the wild-type. In this study, in which fewer plants were studied, differences were not found between the inflorescence stem heights of CaMV: atEXT1 and wild-type plants but the rosette radius was found to be smaller in plants over-expressing extensin. Other studies in transgenic tobacco lines in which the levels of extensin were altered also did not show a different phenotype to wild-type plants (Jamet *et al*, 2000, Memelink *et al*, 1993), suggesting that specific extensins are not essential under normal development but may be required under stress conditions.

CaMV: atEXT1 plants over-expressing extensin do not have a significantly shorter inflorescence stem than the wild-type; this may be because the available extensin is soluble and not cross-linked in the cell wall. However, although inflorescence stem elongation was inhibited by wind stress in plants over-expressing extensin, it was not as severe as in the wild-type plants, which does not suggest that cross-linking of extensin leads to a reduction in the height of the inflorescence stem. Furthermore, in the plants over-expressing extensin wind stress does not cause a reduction in rosette area, as it does in wild-type plants. In another study on the CaMV: atEXT1 plants, exposing plants to UV light resulted in shorter inflorescence stems in the transgenic line than in the wild-type (Norrgren, 2006). It is therefore possible that exposure to UV light induces cross-linking of EXT1 in the inflorescence stem but wind stress does not and furthermore, that extensin is only cross-linked in response to specific stress conditions.

6.5 Summary

Expression of the EXT1 gene of *Arabidopsis* is induced in seedlings immediately after the cessation of mechanical stress but is not expressed in tissues sampled from wind stressed plants at maturation - EXT1 may be expressed in wind stressed plants at an earlier stage of development. From an analysis of the *cis* promoter region of EXT1, WRKY, MYB, MYC and ABRE transcription factor binding sites were found to be over-represented in the first 1.5Kb of sequence upstream of the translation start codon, as they are in the other candidate wind/mechanical stress genes studied.

Over-expression of extensin in the transgenic line CaMV: atEXT1 limited the impact of vibration stress on seedling development. The phenotype of plants from the transgenic line subjected to wind stress does not suggest wind stress induces cross-linking of extensin.

7. RNA INTERFERENCE STRATEGY

7.1 Introduction

Analysis of gene expression of candidate wind stress genes in *Arabidopsis* plants subjected to wind/mechanical stresses found that the candidate genes were differentially expressed. TCH4, CCR2, EXP3 and CESA were differentially regulated in response to wind stress and other mechanical stresses. Silencing these genes by use of RNA interference (RNAi) could be used to look at the role of the genes in the response and adaptation of the plant to wind stress. Five RNAi constructs were proposed; four constructs using gene specific sequences from each of the four genes, and an additional construct using a sequence homologous to each gene in the cinnamoyl CoA reductase family (CCRF).

7.1.1 Considerations for successful gene silencing by RNAi in plants

Gene silencing can be attained by transformation of plants with a transgenic construct that expresses hairpin RNA (hpRNA) that is complementary to the target gene or genes (Helliwell & Waterhouse, 2003). The hairpin construct can be made by cloning gene specific fragments in the sense and antisense orientations either side of an intron/hinge sequence, all under the control of a constitutive promoter. Gene fragments of 50bp-1Kb have been used to successfully silence genes, however Helliwell & Waterhouse (2003) recommend that fragments of 300-600bp should be used. Short fragments result in a lower frequency of silencing, whereas very long fragments (>1Kb) can induce recombination in the bacterial host. The fragment used may be taken from the 5' or 3' untranslated regions of the gene or from the coding sequence (Helliwell & Waterhouse, 2003). Gene specific fragments can be used to target single genes, or conserved sequences may be used to silence multiple genes in a gene family. RNAi does not require complete sequence homology between the dsRNA and the target RNA. Silencing can be achieved where there is as much as a 10% mismatch between the dsRNA and target RNA (Baulcombe, 2002). For this

reason consideration should be given to the potential silencing of off-target genes. As the final construct is genetically dominant, phenotypes can be observed in the T0 or T1 generations of plants without having to generate homozygous lines (Helliwell & Waterhouse, 2003).

7.1.2 Generic vectors for gene silencing by RNAi in plants

A number of generic vectors exist, which can be used to generate a hairpin construct, pHANNIBAL and pHELLSGATE are the most widely used generic vectors (Wesley *et al*, 2001). These vectors allow gene fragments to be directly cloned in the sense and antisense orientations either side of an intron sequence, all under the control of the CaMV 35S promoter. Hairpin constructs containing a functional intron sequence between the gene fragments have been found to be more efficient at silencing genes. pHANNIBAL and pHELLSGATE contain a Pdk intron. Intron-less constructs resulted in silencing in 58% of transformants, while those containing an intron resulted in silencing in 90% of transformants (Wesley *et al*, 2001). It has been suggested that the intron aligns the arms of the hpRNA, promoting duplex formation. However, it has also been proposed that the efficacy of gene silencing is gene dependent. Up to 100% gene silencing can be achieved, although transgenics are likely to show a series of increasing degrees of gene silencing.

Other generic vectors for gene silencing by RNAi include the one used in this study: A plasmid pRNAi vector derived from pDH51 (Pietrzak *et al*, 1986), which was kindly provided by Professor Keith Lindsey (Durham University, UK). The 4.4kb vector has been manipulated for insertion of fragments in the sense and antisense orientations on either side of a 600bp intron/hinge, all under the control of the CaMV 35S promoter (Figure 7.1). This region can be freed from the plasmid by digestion with EcoRI. The intron/hinge region from pBR322 confers ampicillin resistance.

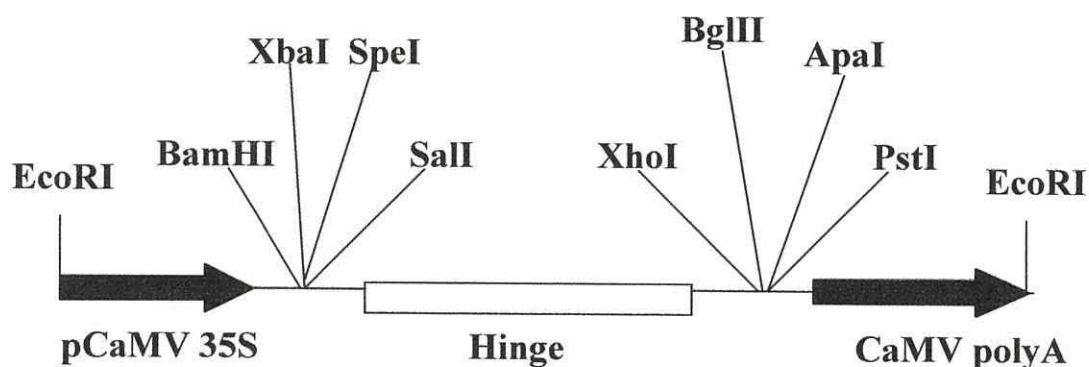


Figure 7.1: Linear plasmid map of pRNAi vector showing restriction sites used for directional cloning of sequence specific fragments.

7.1.3 Estimation of off-target silencing during RNAi

RNAi Scan, available online at <http://bioinfo2.noble.org/RNAiScan.htm> has been developed to optimize RNAi construct design by identifying potential off-targets during post-transcriptional gene silencing, and predicting which siRNAs will be effective (Xu *et al*, 2006). The RNAi Scan tool searches for identical or reverse complementary regions of ≥ 21 nucleotides between the queried sequence and the *Arabidopsis* genome mRNA. Foremost the target gene should be returned, as well as any potential off-targets identified. RNAi Scan users can specify the number of continuous bases of identity (up to 29 nucleotides), and also search for up to three mismatches between the siRNA and the genome. Experimental verification of the off-targets predicted by the database for the *BTII* gene of *Arabidopsis* showed that regions of 22-nucleotide identity were sufficient for off-target silencing (Xu *et al*, 2006). However, genes with 21 or 22-nucleotide identity but with one or more mismatches were not silenced.

The RNAi Scan tool also uses the rules outlined by Ui-Tei *et al* (2004), to predict which siRNAs in the sequence analyzed will be effective. These rules state that siRNAs should have a G or C at the 5' end of the sense strand, have an A or U at the 5' end of the antisense strand, have at least five A/U residues in the 5' termini of the

antisense strand, and not contain stretches of GC over 9 nucleotides long. There are limitations to using these rules alone as they do not take into consideration factors such as the accessibility of the target sequence to siRNAs. Although these rules have not been tested extensively in plants, Sætrom & Snøve (2004) found that they compare favorably with other methods of determining siRNA efficiency.

7.2 Strategy for the silencing of candidate wind stress genes using RNAi

7.2.1 Construct design

Sequence data for each target gene and other genes in their gene families were obtained from the NCBI database. The UTR database on the LION website (LION Bioscience AG, 2003) was used to distinguish the untranslated regions of each gene. Gene specific sequences were identified by BLAST: the target gene sequence was compared against the gene sequences for all other genes in its gene family using the BLAST (to align two sequences) function on the NCBI website (NCBI). Where unique sequences of over 100bp could not be identified in the coding sequence of the target gene, the 3' untranslated region of the gene was used (shown in Table 7.1). In the case of the CCR family construct, the two genes constituting this family, CCR1 and CCR2 were compared against each other to identify regions of high sequence homology. A 372bp sequence from the CCR1 gene with 82% homology to CCR2 was used in an attempt to silence both of the genes.

Table 7.1: Details for each sequence specific fragment generated by PCR.

* Size of fragment including restriction sites.

Gene/Gene family	Target sequence	Homology to target sequence	Size of fragment generated by PCR*
TCH4	3' Untranslated region	100% to XTH22	176 bp
CCR Family	Coding sequence	100% to CCR1 82% to CCR2	372 bp
CCR2	3' Untranslated region	100% to CCR2	117 bp
CESA3	Coding sequence	100% to CESA3	214 bp
EXP3	3' Untranslated region	100% to EXP3	345 bp

The number of efficient siRNAs in hpRNA constructs and the number of off-target sequences that may be silenced by each construct can be forecast using the siRNA Scan tool on the RNAiScan website (Xu *et al*, 2006), as outlined in the introduction to this chapter. This facility was used to optimize construct design and to minimize silencing of off-target genes. Figure 7.2 shows the number of predicted efficient siRNAs for each final construct, which are the stretches of 21 base pairs that best fulfill Ui-Tei *et al*'s (2004) rules for effective siRNAs. As far as these constructs are concerned there are a greater number of predicted efficient siRNAs where the gene specific fragment is larger; accordingly the largest fragment for CCR Family of 372bp is expected to yield the most effective siRNAs. There were few potential off-targets predicted for these final constructs (Table 7.2). Where no mismatches were allowed between the siRNAs and target sequence, no off-target silencing was expected. However, when one mismatch was allowed, the CCR Family and EXP3 constructs are predicted to silence one off-target each; an Acetyl-CoA C-acyltransferase (At1g04710.1) and an S-adenosyl-L-methionine: carboxyl methyltransferase family protein (At3g44840.1) respectively. The expression of these genes could be monitored in any of the transgenic plants generated. Despite this prediction, it has previously been found experimentally that off-target genes with 21 or 22 nucleotide identities to the target gene but with one mismatch are not silenced (Xu *et al*, 2006).

Table 7.2: Predicted off-targets for each construct as determined by the siRNA Scan database.

Gene	No. of nucleotide/siRNA allowed	No. of mismatches allowed	Predicted off-targets	Function of off-target
TCH4	21	0	None	
CCR2	21	0	None	
CCRF	21	0	None	
CESA3	21	0	None	
EXP3	21	0	None	
TCH4	21	1	None	
CCR2	21	1	None	
CCRF	21	1	Atlg04710.1	Acetyl-CoA C-acyltransferase
CESA3	21	1	None	
EXP3	21	1	At3g44840.1	S-adenosyl-L-methionine:carboxyl methyltransferase family protein similar to defense-related protein cjs1

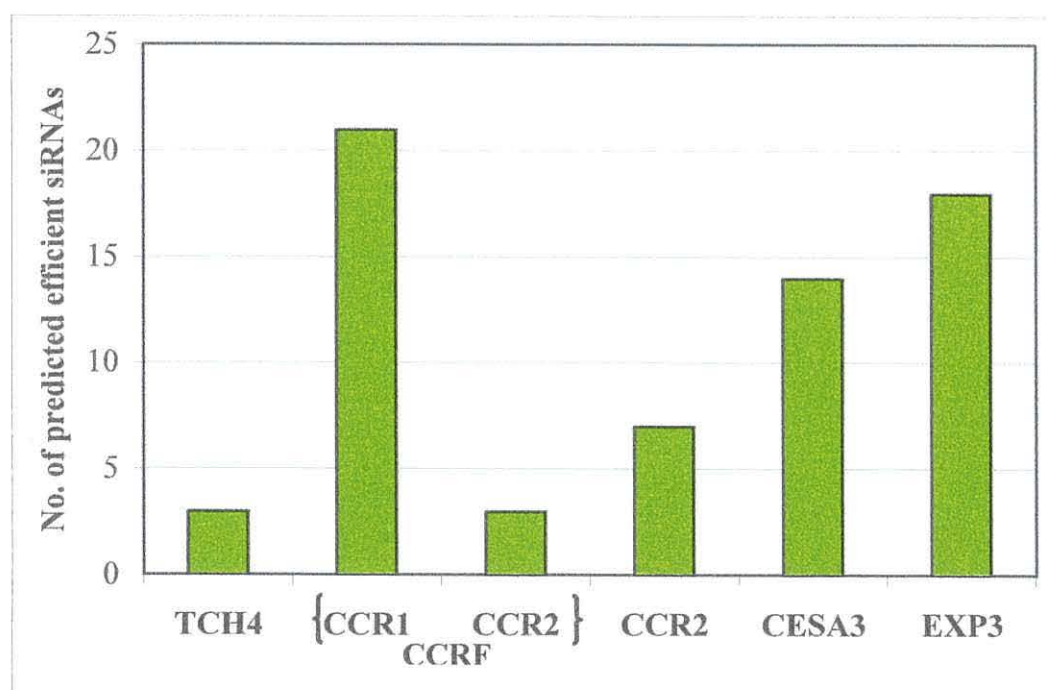


Figure 7.2: Number of efficient siRNAs predicted by siRNA Scan for each hpRNA construct. Gene-specific fragments were analyzed using the siRNA Scan programme (Xu *et al*, 2006) Analysis is based on the prediction of efficient siRNAs of 21 base pairs long. The CCRF construct is predicted to have efficient siRNAs for silencing both members of the CCR family (CCR1 and CCR2). The sequences of the efficient siRNAs are shown in Appendix D.

7.2.2 General cloning strategy

PCR fragments for each of the sequences of interest were generated with additional restriction sites to assist in cloning the fragments in the sense and antisense orientations. Figure 7.3 shows the cloning strategy used. PCR fragments were subcloned into pBluescriptIIISK (pSKII) to conserve each fragment. Fragments with BamHI/SalI cohesive ends were then cloned into the RNAi vector in the sense orientation, and subsequently, fragments with PstI/XhoI cohesive ends were cloned in the antisense orientation. The EcoRI fragment from the RNAi vector was cleaved out and inserted into the binary vector pBIN19 at the EcoRI site. The recombinant pBIN19 was transformed into *Agrobacterium* (LBA4404) by triparental mating with the helper plasmid pRK2013. *Arabidopsis* plants were transformed by the floral dip method.

7.2.3 Generating PCR fragments with cohesive ends for candidate wind stress genes

PCR primers were designed with additional restriction sites for directional cloning of each fragment produced. Primers (Table 7.3) were designed as previously outlined and optimized by selection with Primer3 software. Two primer sets were designed for each sequence, one set with BamHI and SalI restriction sites, and the other set with Pst and XhoI restriction sites. An additional six nucleotides were added to the 5' end of each primer to promote cleavage efficiency, as some restriction endonucleases cleave poorly near the end of fragments (MBI Fermentas, 2003).

The sequence of each fragment generated is shown in Appendix C. PCR fragments were amplified from wind stressed stem cDNA. 1 µg of wind stressed stem RNA was reverse transcribed using a Qiagen Omniscript Reverse Transcription Kit. 5 µl of a 1:10 dilution of the reverse transcription product was used in a standard PCR reaction (section 2.4.5) with the primer pairs outlined in Table 7.3. A fifth of the PCR reaction was run on a 2% agarose gel to check the fragment was the expected size (Figure 7.4) and the remainder of the sample was purified (section 2.5.2).

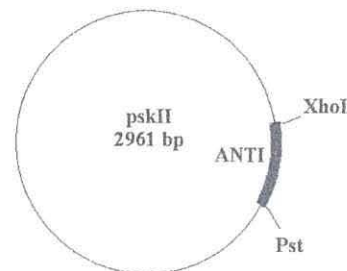
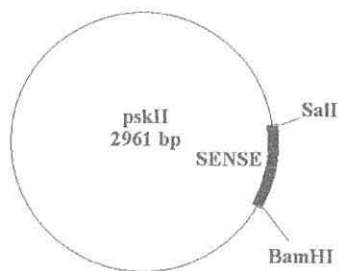
1. Amplify PCR fragments from cDNA with **additional restriction sites**

GTCAGT **GGATCC** [cDNA] **GTCGAC** GTCCGT
 GTCAGT **CTGCAG** [cDNA] **CTCGAG** GTCCGA

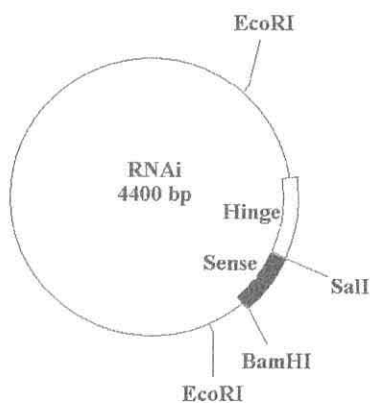
2. PCR fragments digested with restriction enzymes

GATCC [cDNA] **G**
G [cDNA] **C**

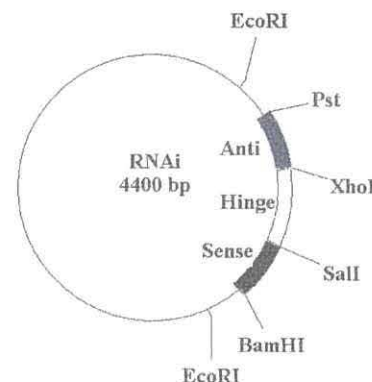
3. Each fragment subcloned into pBluescriptIISK (PSKII)



4. Sense fragment cloned into pRNAi vector (RNAi)



5. Antisense fragment cloned into p RNAi [vector + sense fragment]



6. EcoRI fragment from pRNAi [+ SENSE + ANTISENSE] cloned into pBIN19

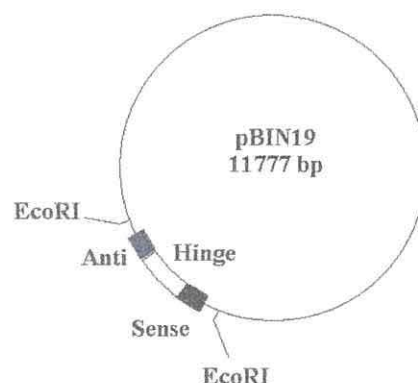


Figure 7.3: General cloning strategy for generation of a RNA interference construct.

Table 7.3: Primers used for amplification of PCR fragments with additional restriction sites to aid cloning. * indicates the orientation of the resulting fragment when cloned into the RNAi vector. Restriction sites are underlined and highlighted in red; BamHI: **GGATCC**, SalI: **GTCGAC**, PstI: **CTGCAG**, XhoI: **CTCGAG**. The six nucleotide base pairs preceding the restriction site are random but were included to enhance cleavage efficiency.

Gene & Orientation*	Primer sequences 5' to 3'
TCH4 Sense	F-GTCAGT GGATCC AAAGAGTTGAGAGAGGAACAA R-ACGGAC GTCGAC AAGCACATTGTAACAAAGAGAA
TCH4 Antisense	F-GTCAGT CTGCAG AAAGAGTTGAGAGAGGAACAA R-ACGGAC CTCGAG AAGCACATTGTAACAAAGAGAA
CCRF Sense	F- GTCAGT GGATCC TATTGTTACGGCAAGATGGT R-ACGGAC GTCGAC ACTTGGTCGGAAGAGGATAC
CCRF Antisense	F- GTCAGT CTGCAG TATTGTTACGGCAAGATGGT R-ACGGAC CTCGAG ACTTGGTCGGAAGAGGATAC
CCR2 Sense	F- GTCAGT GGATCC ACACGATCCACGACCCTAGA R-ACGGAC GTCGAC AACAATACTTTAGTCAAAATCAAAACG
CCR2 Antisense	F- GTCAGT CTGCAG ACACGATCCACGACCCTAGA R-ACGGAC CTCGAG AACAATACTTTAGTCAAAATCAAAACG
CESA Sense	F-GTCAGT GGATCC AGTCCTGCTATTCCTGGTGA R-ACGGAC GTCGAC TGAGACGAGGAAGATGATTG
CESA Antisense	F- GTCAGT CTGCAG AGTCCTGCTATTCCTGGTGA R-ACGGAC CTCGAG TGAGACGAGGAAGATGATTG
EXP3 Sense	F-GTCAGT GGATCC GAAAAACCACCCAAAAGATG R- ACGGAC GTCGAC CCCATTACACGGTCCATT
EXP3 Antisense	F-GTCAGT CTGCAG GAAAAACCACCCAAAAGATG R-ACGGAC CTCGAG CCCATTACACGGTCCATT

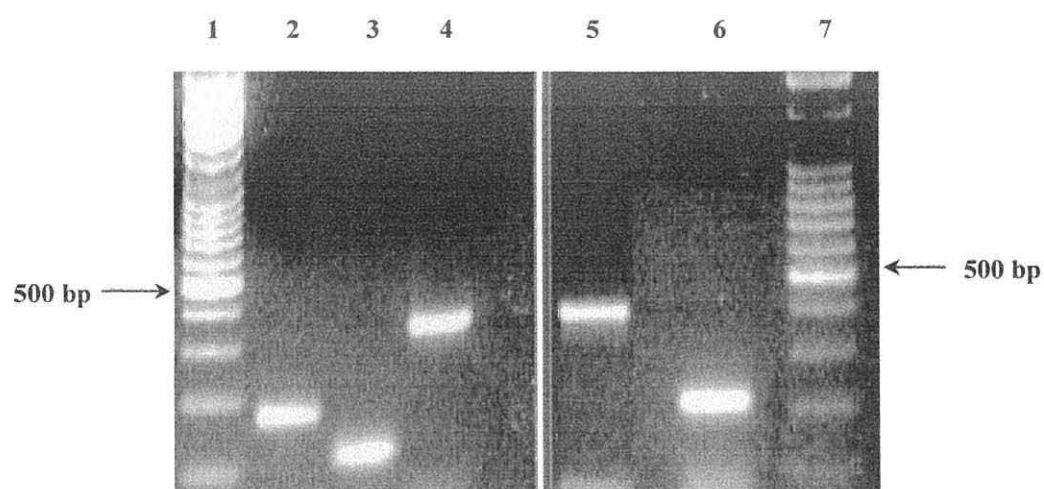


Figure 7.4: PCR fragments generated for each of the candidate wind stress genes to be cloned.

2% agarose gels showing PCR products: TCH4 176 bp (lane 2), CCR2 117 bp (lane 3), EXP3 345 bp (lane 4), CCRF 372 bp (lane 5), CESA3 214 bp (lane 6). A 100 base pair size ladder is shown in lanes 1 and 7.

7.2.4 Sub-cloning PCR fragments from candidate wind stress genes into pBluescriptII SK (pSKII)

Each individual PCR fragment was first subcloned into the vector pSKII (2961bp) to conserve the fragment. pSKII has each of the desired restriction sites as shown in Figure 7.5. pSKII was purified from *E.coli*, extracted and purified using a QIAspin Miniprep kit (Qiagen). The pSKII plasmid vector and each of the purified BamHI/SalI PCR fragments were restricted with BamHI and SalI. Similarly pSKII and each of the purified PstI/XhoI PCR fragments were restricted with Pst and XhoI. pSKII digested with BamHI and SalI yielded 2916bp and 45bp fragments, and pSKII digested with Pst and XhoI yielded 2926bp and 35bp fragments. The two larger fragments were electroeluted from the gel and phenol purified. Restricted PCR fragments were phenol purified and precipitated with ethanol. Each restriction enzyme digested PCR fragment was then ligated to digested pSKII at 16°C overnight. *E.coli* DH5 α competent cells were transformed with 5 μ l of the ligation mixture, and transformants selected on LB plates supplemented with ampicillin, IPTG, and X-GAL. Miniprepations (section 2.5.3a) of each of the white colonies were restricted with BamHI/SalI or Pst/XhoI to confirm the presence of sense and antisense positive inserts respectively.

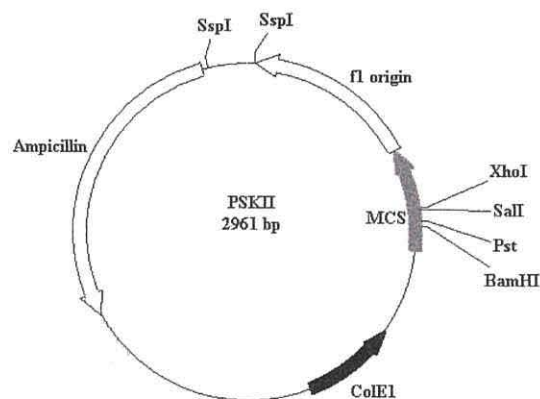


Figure 7.5: Restriction map of pBluescript II SK (pSKII).

The restriction sites used to subclone the sense and antisense PCR fragments into this vector are shown.

7.2.5 Cloning of fragments into the RNAi vector in the sense and antisense orientations.

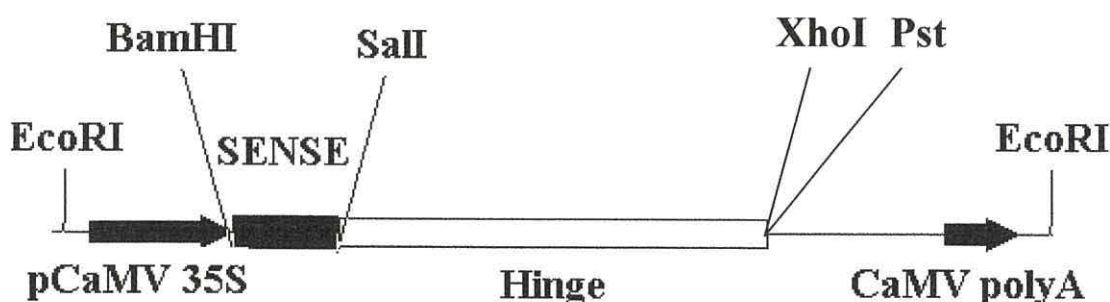


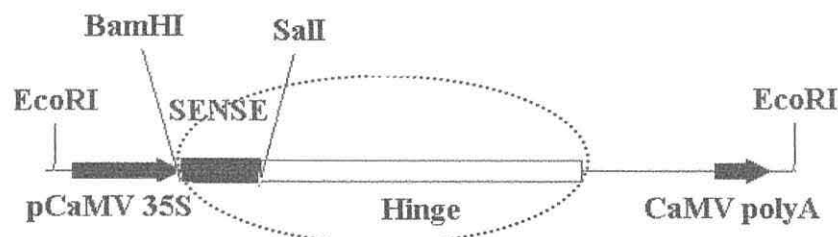
Figure 7.6a: Diagram showing the gene specific fragment inserted in the sense orientation.

Sense orientation fragments were first cloned into the BamHI/SalI sites of the pRNAi vector (Figure 7.6a). The pRNAi vector was digested with BamHI and SalI, the restriction run on a 0.7% agarose gel, and the larger 4376bp band excised, electroeluted and phenol purified. Concurrently, the cloned gene specific fragments were cleaved out of pSKII by restriction with BamHI & SalI, run on 1% gels, and electroeluted and phenol purified. The gene specific fragments were then ligated to the cleaved RNAi vector in the sense orientation at 16°C overnight in a standard 20µl ligation reaction. Competent *E.coli* cells were transformed with 5µl of each of the ligations and plated on LB media supplemented with ampicillin.

Colony PCR (section 2.5.8) of colonies growing on selective media was used to identify transformants. The sense forward primer for each gene sequence was paired to a reverse primer based on the hinge sequence of the RNAi vector (Table 7.4). The reverse primer was designed as outlined previously. The diagram in Figure 7.6b shows the intercept between the sense fragment and the hinge, and highlights the amplified region. Colonies that had positive PCRs for the sense insert (Figure 7.7A) were subsequently checked by miniprep and restriction with BamHI and SalI (Figure 7.7B).

Table 7.4: Primer pairs used for colony PCR of pRNAi + Sense insert constructs.

Gene	Primer sequences
	5'→3'
TCH4	F-GTCAGTGGATCCAAAGAGTTGAGAGAGGAACAA
Sense	R-AGTGCTCATCATTGGAAAAC
CCRF	F- GTCAGTGGATCCTATTGTTACGGCAAGATGGT
Sense	R-AGTGCTCATCATTGGAAAAC
CCR2	F- GTCAGTGGATCCACACGATCCACGACCCTAGA
Sense	R-AGTGCTCATCATTGGAAAAC
CESA	F-GTCAGTGGATCCAGTCCTGCTATTCCTGGTGA
Sense	R-AGTGCTCATCATTGGAAAAC
EXP3	F-GTCAGTGGATCCGAAAAACCACCCAAAAGATG
Sense	R-AGTGCTCATCATTGGAAAAC



GGATCCACACGATCCACGACCCTAGAATCTGATCATACCTACATGAAAAGCTTTATTCTTAAGTAATACATACGT
TTTGATTTTGACTAAAAGTATTGTT**GTCGAC**TCGACCGTGAAGCTGGATCTCAACAGCGGTAAGATCCTTGAGAGTTT
TCGCCCCGAAGAAGCTTTTCCAATGATCAGCACTTTTAAAGTTCTGCTATGTGGCGCGGTATTATCCCGTATTGAC
GCCGGGCAAGAGCAACTCGGTGCGGCATACACTATTCTCAGAATGACTTGGTTGAGTACTCACCAGTCACAGAAA
AGCATCTTACGGATGGCATGACAGTAAGAGAATTATGCAGTGCTGCCATAACCATGAGTGATAACACTGCGGCCA
ACTTACTTCTGACAACGATCGGAGGACCGAAGGAGCTAACCGCTTTTTCACAACATGGGGGATCATGTAACTCG
CCTTGATCGTTGGGAACCGGAGCTGAATGAAGCCATACCAACGACGAGCGTGACACCACGATGCCTGTAGCAAT
GGCAACAACGTTGCGCAAACTATTAACCTGGCGAACTACTTACTCTAGCTTCCCGGCAACAAATTAATAGACTGGATG
GAGGCGGATAAAGTTGCAGGAGCACTTCTGTAC**CTCGAG**

Figure 7.6b: Example of gene specific fragment (CCR2) ligated to the RNAi vector in the sense orientation. The insert/hinge region is highlighted; restriction sites (red), fragment (plain text), primers (bold/underline), hinge (grey highlight).

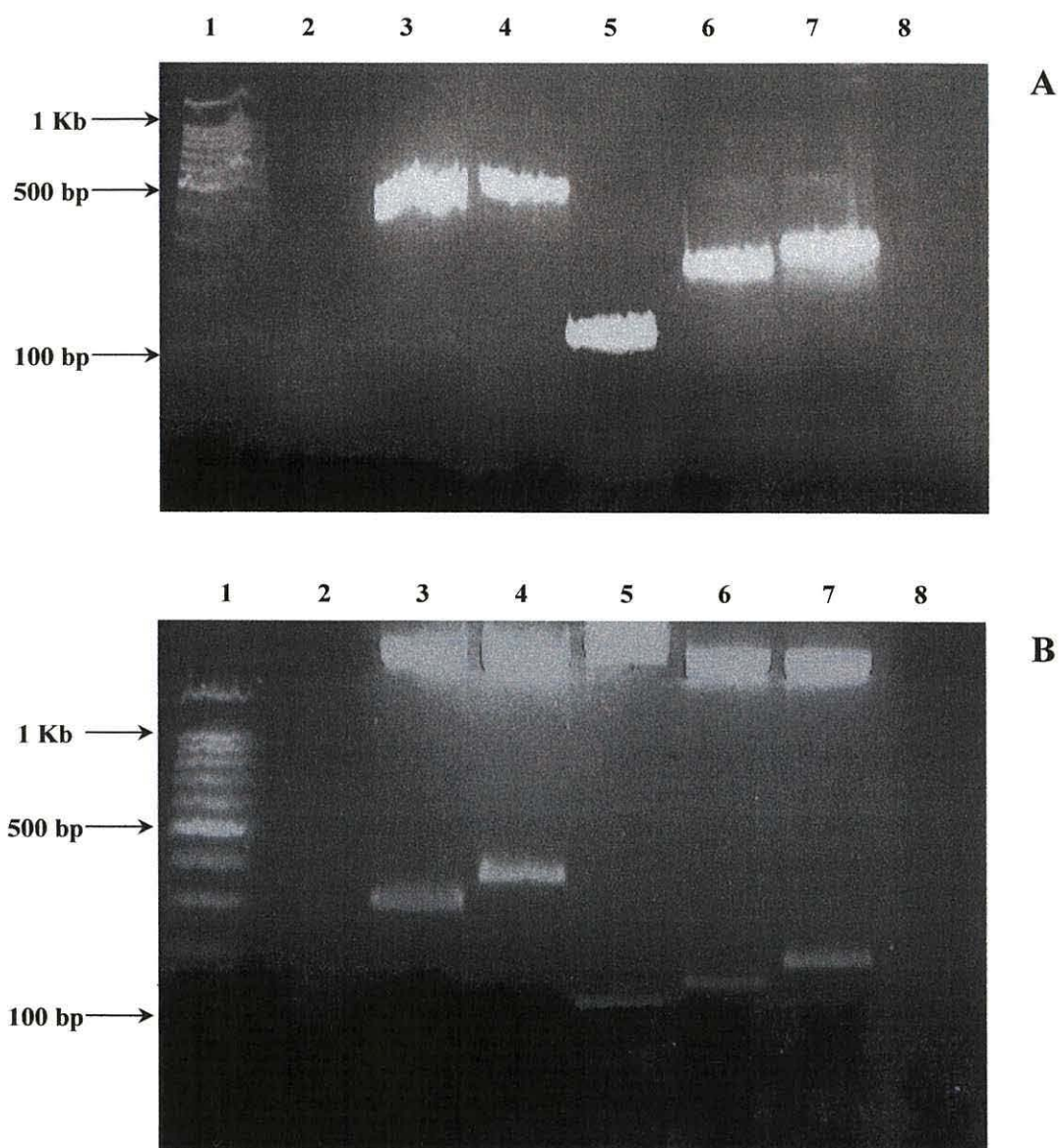


Figure 7.7: Cloning of sense fragments into the pRNAi vector.

A: 2% agarose gel showing colony PCRs with forward primer based on the target sequence and reverse primer based on the hinge sequence of the pRNAi vector. Expected sizes; EXP3 425 bp, CCRF 452 bp, CCR2 197 bp, TCH4 256 bp, CESA3 294 bp (lanes 3-7 respectively)

B: 0.7% agarose gel showing pRNAi [vector + sense] restricted with BamHI & Sall to check the size of the sense insert.

Expected insert sizes; EXP3 345 bp, CCRF 372 bp, CCR2 117 bp, TCH4 176 bp, CESA3 214 bp (lanes 3-7 respectively)

A 100 base pair size ladder is shown in lane 1 of each gel.

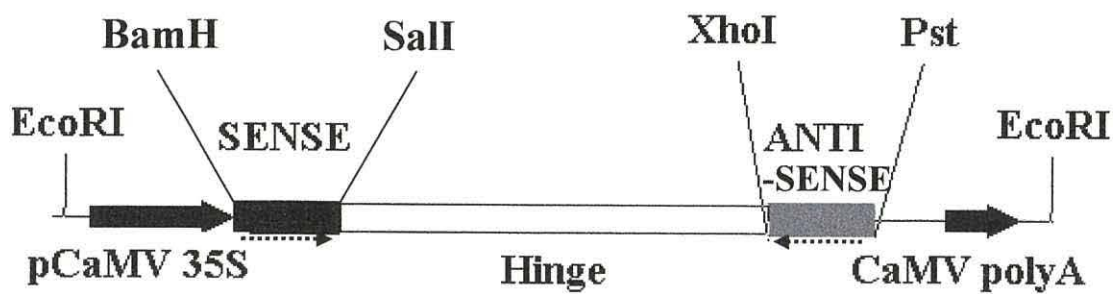


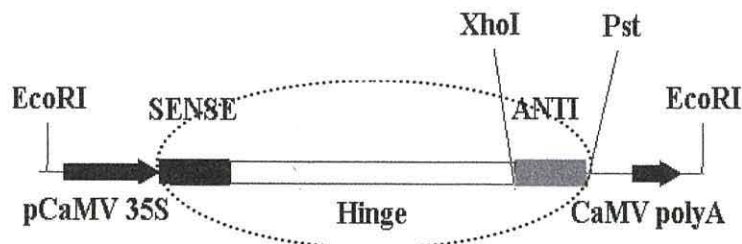
Figure 7.8a: Diagram showing the gene specific fragment inserted in the antisense orientation.

The sequence specific fragments were next excised from pSKII with Pst and XhoI and cloned into the appropriate RNAi vector which already contained the sense fragment (as shown in Figure 7.8a). RNAi + sense insert was then restricted with Pst and XhoI and the antisense sequence specific fragment was cleaved from pSKII with Pst and XhoI and ligated to the Pst/XhoI sites of the RNAi vector (in the antisense orientation). *E.coli* was transformed with 5µl of the RNAi + sense + antisense ligation reaction and transformants were selected on LB media containing ampicillin.

Positive transformants were identified by colony PCR with a forward primer based on the RNAi vector hinge sequence and a reverse primer based on the target gene sequence (Table 7.5). The amplified region is shown in Figure 7.8b. Figure 7.9 shows positive colony PCRs for each construct, and the subsequent restriction of minipreparations of these clones with Pst and XhoI to verify the insert size.

Table 7.5: Primer pairs used for colony PCR of pRNAi + Sense insert + Antisense inserts.

Gene	Primer sequences 5' to 3'
TCH4	F- ATAAAGTTGCAGGAGCACTTC
Antisense	R- GTCAGTCTGCAGAAAGAGTTGAGAGAGGAACAA
CCRF	F- ATAAAGTTGCAGGAGCACTTC
Antisense	R- GTCAGTCTGCAGTATTGTTACGGCAAGATGGT
CCR2	F- ATAAAGTTGCAGGAGCACTTC
Antisense	R- GTCAGTCTGCAGACACGATCCACGACCCTAGA
CESA	F- ATAAAGTTGCAGGAGCACTTC
Antisense	R- GTCAGTCTGCAGAGTCCTGCTATTCCTGGTGA
EXP3	F- ATAAAGTTGCAGGAGCACTTC
Antisense	R- GTCAGTCTGCAGGAAAAACCACCCAAAAGATG



GGATCCACACGATCCACGACCCTAGAATCTGATCATACCTACATGAAAAAGCTTTATTCTTAAGTAATACATACGTTT
TGATTTTGACTAAAGTATTGTT**GTCGAC**TCGACCGTCGAACTGGATCTCAACAGCGGTAAGATCCTTGAGAGTTTC
GCCCCGAAGAACGTTTTCCAAATGATGAGCACTTTAAAGTTCTGCTATGTGGCGCGGTATTATCCCGTATTGACGCC
GGGCAAGAGCAACTCGGTGCGCCGATACACTATTCTCAGAATGACTTGGTTGAGTACTCACCAGTCACAGAAAAGC
ATCTTACGGATGGCATGACAGTAAGAGAATTATGCAGTGTGCCATAACCATGAGTGATAACACTGCGGCCAACTT
ACTTCTGACAACGATCGGAGGACCGAAGGAGCTAACCCTTTTTCGACAAACATGGGGGATCATGTAACCTCGCCTT
GATCGTTGGGAACCGGAGCTGAATGAAGCCATACCAAACGACGAGCGTGACACCAGATGCCTGTAGCAATGGCA
ACAACGTTGCGCAAACTATTAAGTGGCGAACTACTTACTCTAGCTTCCCGGCAACAATTAATAGACTGGATGGAGG
CGGATAAAAGTTGCAGGAGCACTTCTGTAC**CTCGAG**ACAATACTTATGTCAAAATCAAAACGTATGTATTACTTA
AGAATAAAGCTTTTCATGTAGGTATGATCAGAT**TCTAGGGTCGTGGATCGTGTCTGCGAG**

Figure 7.8b: Example of gene specific fragment (CCR2) ligated to the RNAi vector in the Antisense orientation. The gene specific fragment has already been inserted in the sense orientation. The insert/hinge region is highlighted; restriction sites (red), fragment (plain text), primers (bold/underlined) and hinge sequence (grey highlight).

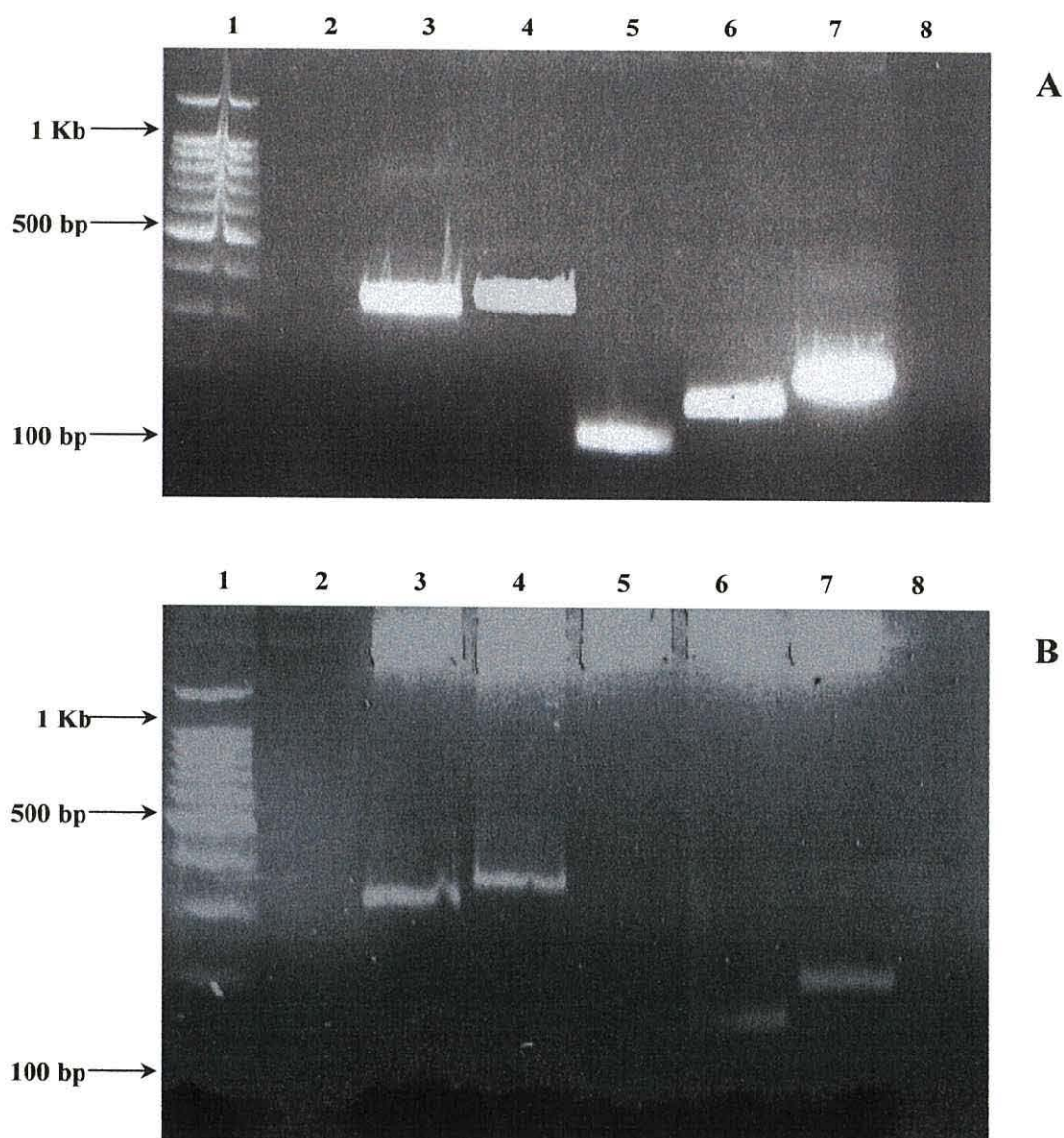


Figure 7.9: Cloning of Antisense fragments into pRNAi vector.

A: 2% agarose gel showing colony PCRs with forward primer based on the hinge sequence of the pRNAi vector and reverse primer based on the target sequence. Expected PCR fragment sizes; EXP3 371 bp, CCRF 398 bp, CCR2 143 bp, TCH4 202 bp, CESA3 240 bp (lanes 3-7 respectively)

B: 0.7% agarose gel showing pRNAi [vector + sense +Antisense] restricted with Pst & XhoI to check the antisense insert.

Expected insert sizes; EXP3 345 bp, CCRF 372 bp, CCR2 117 bp, TCH4 176 bp, CESA3 214 bp (lanes 3-7 respectively)

A 100 base pair size ladder is shown in lane 1 of each gel.

7.2.6 Cloning the EcoRI fragment from RNAi + Sense + Antisense vector into the binary vector pBIN19

The RNAi vector was subsequently cleaved with EcoRI to release a fragment containing the gene specific sequence in the sense and antisense orientations either side of a 600bp hinge, all under the control of the CaMV 35S promoter. An agarose gel showing the fragments generated from each of the constructs is shown in Figure 7.10, each of the smaller fragments (as indicated) were cleaved from the gel, electroeluted and phenol purified. Each fragment was then cloned into the binary vector pBIN19 (Figure 7.11).

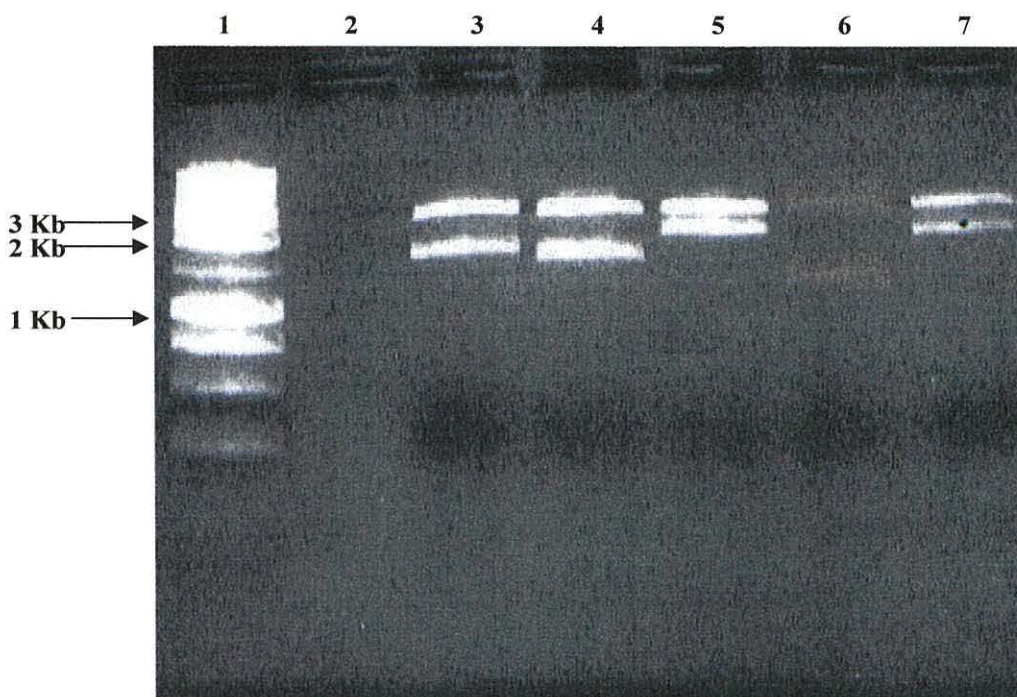


Figure 7.10: EcoRI fragments released from RNAi vectors.

Restriction with EcoRI released a sequence specific fragment from the RNAi vector; CESA3 (1828 bp), TCH4 (1752 bp), CCRF (2144 bp), CCR2 (1634 bp), EXP3 (2090 bp) in lanes 3-7 respectively, leaving a 3Kb RNAi vector fragment to be discarded from each restriction. Lane 1 shows a 1Kb size ladder.

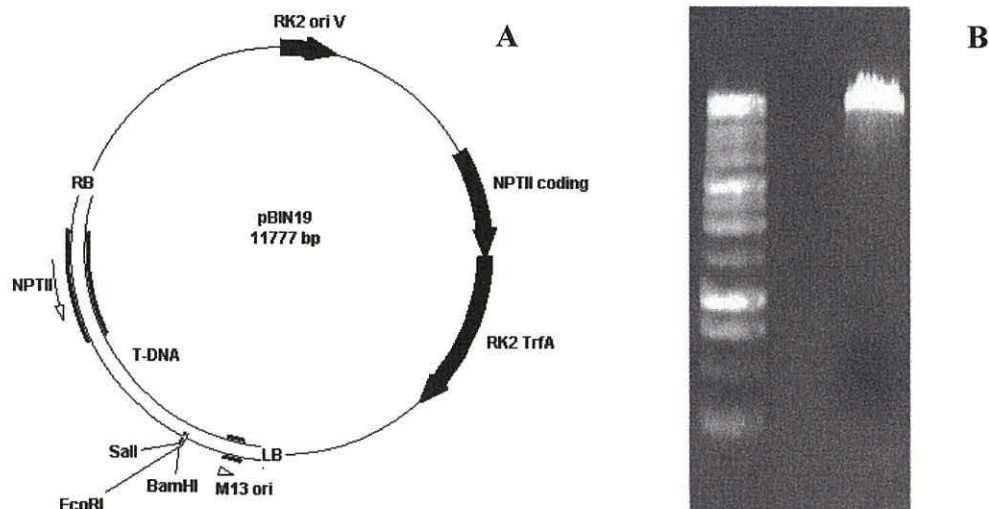


Figure 7.11: Binary vector pBIN19.

A. Plasmid restriction map of the binary vector pBIN19, **B.** 0.7% agarose gel showing the restriction of pBIN19 with EcoRI, which linearizes the plasmid (11777 bp). A 1Kb size ladder is also shown.

pBIN19 was purified from *E.coli* and digested with EcoRI and the restriction run on a 0.7% agarose gel (Figure 7.11B). Linearized plasmid was electroeluted from the gel and purified. The EcoRI fragments released from the RNAi vector were ligated to the pBIN19 vector at 16°C overnight. Competent *E.coli* cells were transformed with each ligation and grown at 37°C overnight on LB media supplemented with kanamycin, IPTG and X-Gal. Colony PCR of white colonies was used to identify transformants. The primers used previously to identify the sense insert in the RNAi vector (Table 7.4) were used again here to identify positive transformants. Minipreparations of positive transformants were restricted with EcoRI to check the size of the insert (Figure 7.12).

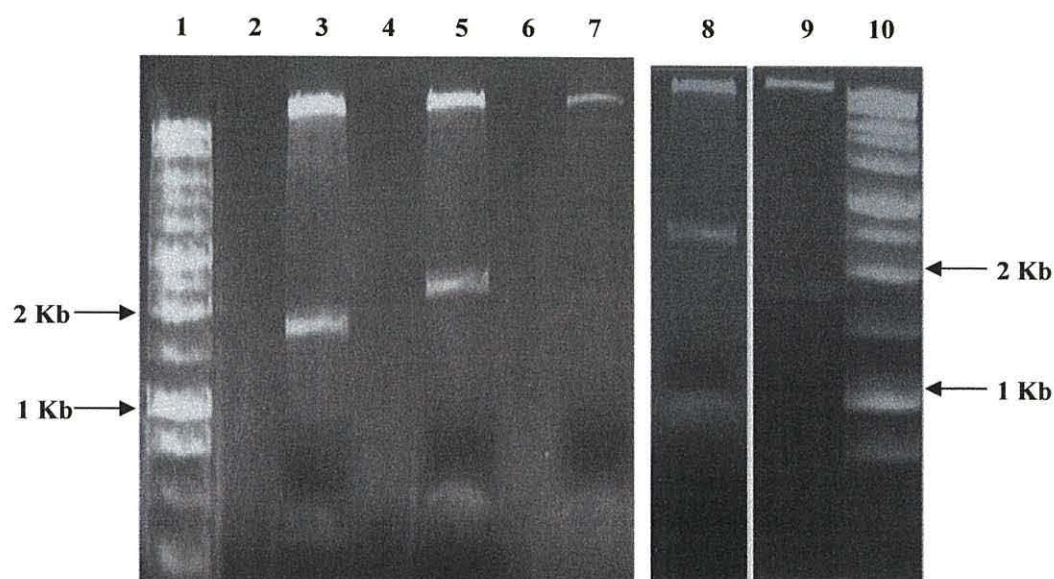


Figure 7.12: Cloning of the EcoRI fragment from the RNAi vector into the binary vector pBIN19.

0.7% agarose gels showing the restriction of pBIN19 [+ fragment from RNAi] restricted with EcoRI to check the size of the insert.

Expected insert sizes; TCH4 1752 bp (lane 3), EXP3 2090 bp (lane 5), CESA3 1828 bp (lane 7), CCRF 2144 bp (lane 8) and CCR2 1634 bp (lane 9). A 1Kb size ladder is shown in lanes 1 and 10.

7.2.7 Transformation of *Agrobacterium tumefaciens* with the binary vector constructs

The *Agrobacterium tumefaciens* strain LBA4404 was transformed with recombinant pBIN19 for each construct by tri-parental mating with the helper plasmid pRK2013 in *E.coli*. *Agrobacterium* DNA was extracted from 5 colonies generated by the mating for each of the constructs. The DNA was restricted with EcoRI to isolate the target fragment. The restrictions were run on a 0.7% agarose gel (Figure 7.13A), Southern blotted to a nylon membrane, and hybridized with a 1.4Kb radiolabelled EcoRI fragment (Figure 7.14) from the pRNAi vector. The same probe was used for each construct, as the 1.4Kb fragment is common to each. Figure 7.13B shows an autoradiograph of positive transformants from each construct. The positive transformants are indicated in the figure and were used to transform *Arabidopsis* plants, as outlined in the following section. There were no positive transformants identified for the CESA3 construct from the first five colonies. A further four colonies were prepared as above, from which two positive transformants were subsequently found (Figure 7.15).

7.2.8 Transformation of *Arabidopsis* plants

Arabidopsis thaliana Wassilewskija (Ws) plants were transformed with each RNAi construct by the floral dip method (section 2.6.4). A single *Agrobacterium* colony for each construct was used to inoculate individual cultures. Five plants were dipped for each construct. Seed designated T₁ (transformant generation 1) were harvested at maturation.

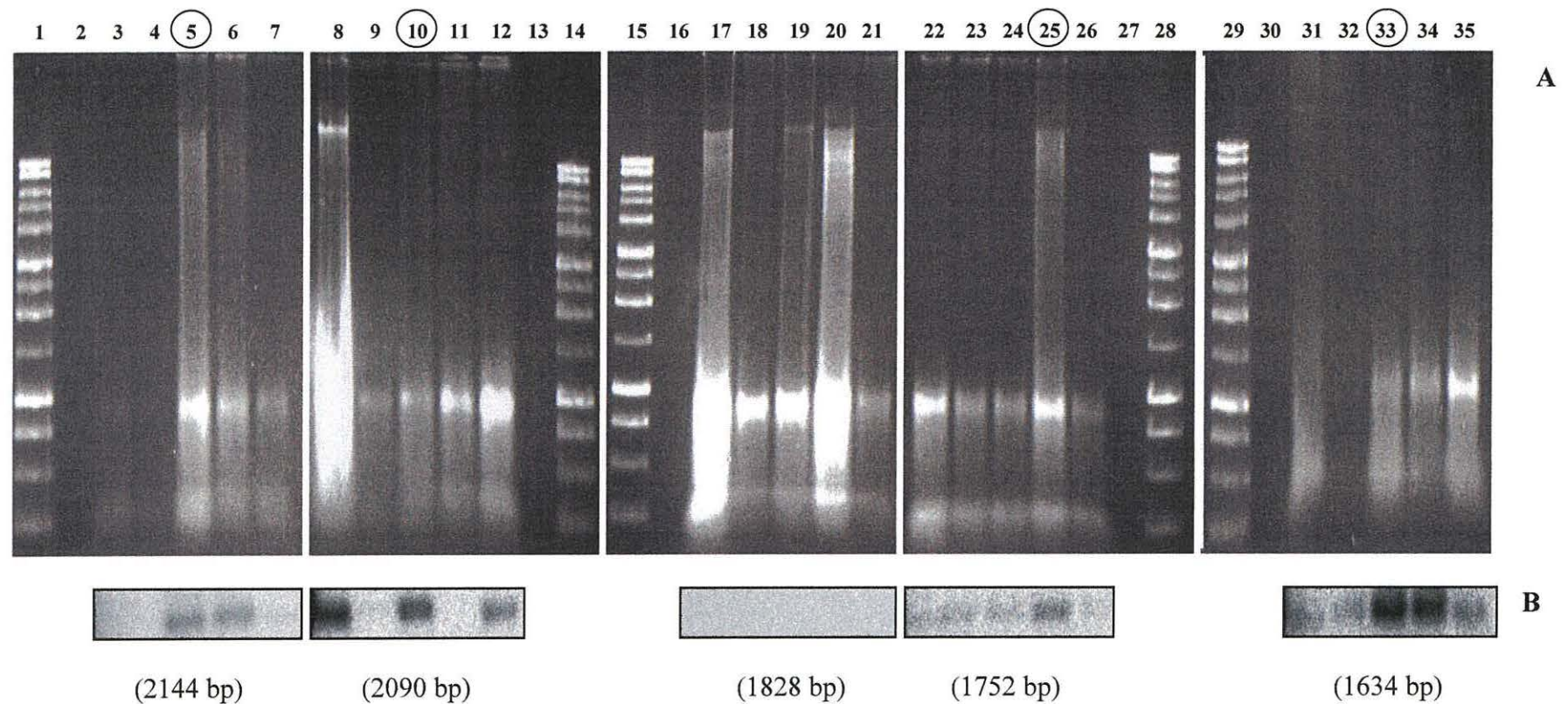


Figure 7.13: Transformation of *Agrobacterium tumefaciens*.

A. 0.7% agarose gels showing genomic DNA extracted from different *Agrobacterium tumefaciens* colonies and restricted with EcoRI. Five colonies extracted for each construct are shown; CCRF (lanes 3-7), EXP3 (lanes 8-12), CESA3 (lanes 17-21), TCH4 (lanes 22-26), and CCR2 (lanes 31-35). **B.** Autoradiographs of the gels shown in A., showing single hybridized bands. The size of each hybridizing band is shown in parentheses. The lane numbers of the colonies used for the subsequent transformation of *Arabidopsis* are circled.

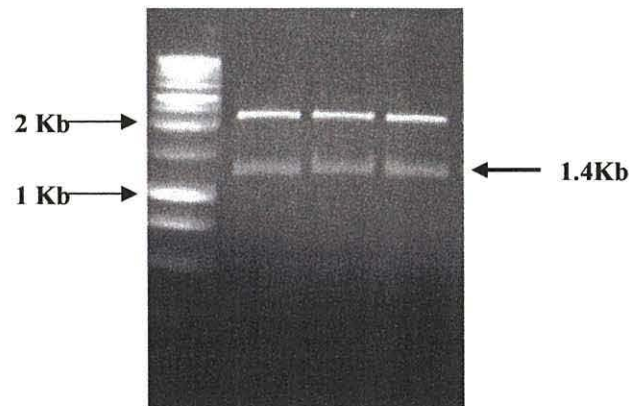


Figure 7.14: EcoRI fragment from the RNAi vector that was used as a radiolabelled probe.

An RNAi vector with no inserts was restricted with EcoRI to release a 1.4Kb fragment, which was electroeluted from the gel, purified and subsequently radiolabelled and used as a probe for DNA hybridization. Restrictions are shown with a 1Kb size ladder.

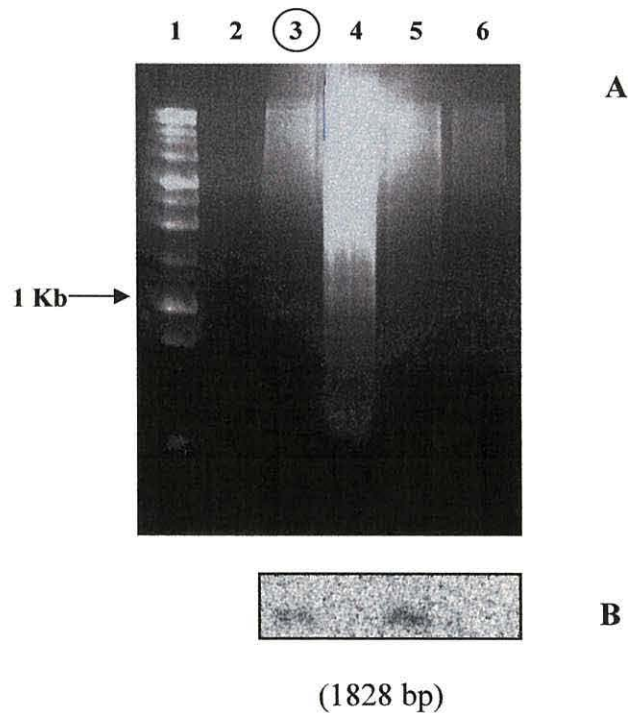


Figure 7.15: Transformation of *Agrobacterium tumefaciens* with the CESA3 RNAi construct.

A. 0.7% agarose gel showing genomic DNA extracted from a further four *Agrobacterium tumefaciens* colonies and restricted with EcoRI. A 1Kb size ladder is shown in lane 1. **B.** Autoradiographs of the gels shown in A., showing single hybridized bands. The size of the hybridizing bands is shown in parentheses. The lane number of the colony used for the subsequent transformation of *Arabidopsis* is circled.

7.3 Summary

Hairpin RNA constructs were generated by cloning gene specific fragments in the sense and antisense orientations either side of an intron/hinge sequence, all under the control of the CaMV 35S constitutive promoter. These constructs were used to transform *Arabidopsis thaliana* plants. The phenotype of the resulting transgenic plants and the expression of specific candidate wind/mechanical stress genes in them will be considered in the following chapter.

8. PHENOTYPIC AND GENE EXPRESSION ANALYSES OF RNAi TRANSGENIC LINES SUBJECTED TO MECHANICAL STRESS

8.1 Introduction

Seed was collected from the five floral-dipped plants for each RNAi construct, as outlined in Chapter 7. This chapter outlines the selection of kanamycin resistant T₁ seedlings, the development of T₁ plants and the extraction of their DNA to check for the presence of an intact transgene. Subsequently, the distribution of kanamycin resistance within the population of transgenic plants was determined in the T₂ generation of these transgenic lines. Finally, T₂ seedlings were subjected to vibration stress to induce expression of candidate wind/mechanical stress genes; RT-PCR was used to assess the effectiveness of gene silencing by RNA interference, and a plate-based phenotypic analysis was used to identify phenotypic change in the RNAi transgenic lines.

8.2 Strategy for the identification of transgenic lines

Seed from the floral-dipped plants were designated generation T₁. Table 8.1 outlines the definition of each of the transgenic generations involved in this study. Approximately 2000 T₁ seed (400 from each dipped plant) were surface sterilized, and grown on a number of plates containing half-strength MS media supplemented with 35µg/ml kanamycin. Healthy transformant seedlings (T₁ seedlings) were transferred to soil at 14-days old (section 2.2.2). T₁ plants were grown to maturity, when their seed was collected. The development of T₁ plants was monitored using a soil-based phenotypic analysis (section 2.2.3). DNA was extracted (section 2.6.7) from the rosette leaves of mature T₁ plants to check the transgene was present and intact; the DNA was amplified by PCR using both sequence specific primers and primers based on the CaMV 35S promoter/pBin19 vector. For each transgene a sense insert/hinge fragment and antisense insert/hinge fragment was amplified to check the transgene was present, described in Chapter 7. Additionally, primers (Table 8.2) based on the

CaMV 35S promoter and T-DNA border sequences of pBIN19, spanning the entire transgene were used to check that the transgene was intact (as shown in Figure 8.1) Seed from T₁ plants containing the appropriate transgene were carried forward for analysis in the next generation.

T₂ seed were germinated on half-strength MS media containing 35µg/ml kanamycin and the proportion of seedlings surviving at 14-days old was calculated. Seedlings could be either homozygous or heterozygous for the inserted DNA as indicated by complete (100% survived) or partial (< 100% survived) kanamycin resistance of the T₂ seeds respectively. Some T₂ seedlings were subsequently exposed to vibration stress to induce expression of the candidate wind/mechanical stress genes (as was shown in section 5.4.1). In parallel studies RT-PCR was used to assess whether the transgene was expressed and monitor the effectiveness of gene silencing by RNA interference, and a plate-based phenotypic analysis was used to identify any phenotypic change in the transgenic lines. As outlined previously, seed were plated on selective media and grown to germination after which vibration at 40Hz was applied for 72 hours. Immediately after the cessation of vibration, seedlings were harvested for RNA extractions and RT-PCR analysis; wild-type Ws seedlings were similarly treated and sampled concurrently with the transgenic lines. Primers based on the hinge sequence of the transgene (Table 8.3) were used to check whether the transgene was expressed in each line, and the PCR primers used for the gene expression analysis in Chapter 5 were used to monitor expression of the target gene in each line. For the phenotypic analysis, after the cessation of vibration seedlings were grown until they reached 14-days old, when their hypocotyls were measured, and compared with those of wild-type Ws. Vibration stress was previously shown to induce elongation of the hypocotyls in wild-type seedlings (section 3.2.1).

Table 8.1: Definition of the transgenic generations used in this study.

* TCH4 is used as an example; the equivalent nomenclature applies to all lines.

Generation	Description	Nomenclature*
T ₀	Wild-type plant that was floral-dipped	None
T ₁	Kanamycin resistant seedlings germinated from the seed of dipped plants.	TCH4 1.1
T ₂	Kanamycin resistant seedlings germinated from the seed of T1 plants. May be homozygous or heterozygous.	TCH4 1.1.1
T ₃	Kanamycin resistant seedlings germinated from the seed of T2 plants. All homozygous	TCH4 1.1.1 progeny

Table 8.2: Primers used to check the intactness of the transgene.

Primer	Primer sequence 5' to 3'
CaMV 35S Forward	GATTCCATTGCCAGCTATC
pBIN19 (LB) Reverse	GCCTGTATCGAGTGGTGATT
pBIN19 (RB) Reverse	AGGGGGCTATGACCGAAAAT

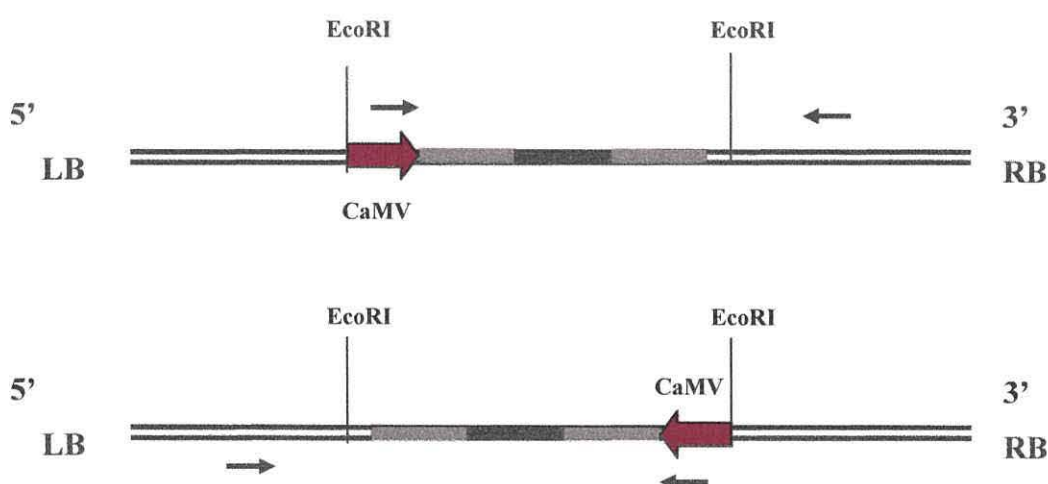


Figure 8.1: Region amplified to check the intactness of the transgene.

The RNAi EcoRI fragments were inserted into the EcoRI sites of the pBIN19 vector in either orientation. The primers shown in Table 8.2 were used to amplify the intact transgene; a primer based on the CaMV 35S promoter was paired with one of the primers based on the border sequence of the T-DNA region of the pBIN19 vector. The sequence on which the primers were based is indicated by a black arrow. LB and RB are the left and right borders of the T-DNA region of pBIN19 respectively.

Table 8.3: Primers used to check whether the transgene is expressed in transgenic lines.

Primers based on the hinge sequence of the transgene were used to determine whether the transgene was expressed in each of the transgenic lines; these primers should amplify a fragment of 467 bp in lines where the transgene is expressed.

Primer	Primer sequence 5' to 3'
Hinge Forward	GTTTCCAATGATGAGCACT
Hinge Reverse	GAAGTGCTCCTGCAACTTTAT

8.3 TCH4 RNAi transgenic lines

8.3.1 T₁ generation TCH4 RNAi transgenic lines

a) Selection of T₁ transgenic seedlings on media supplemented with kanamycin

Eight first generation TCH4 RNAi transgenic seedlings were plated on media supplemented with kanamycin. Two of these seedlings died immediately after they were transferred to soil. As a precaution, the remaining seedlings were maintained *in vitro* for up to 28 days so that they could develop further prior to transfer to soil. Nevertheless, a further three seedlings died soon after their transfer to soil. The remaining seedlings, RNAi: TCH4 1.1, TCH4 3.1 and TCH4 4.1 were grown to maturity.

b) Phenotypic analysis of T₁ generation

With the exception of RNAi: TCH4 4.1, development of the T₁ generation was not significantly different from wild-type Ws; maturity was reached within one week of the wild-type. Figure 8.2 shows that the development of RNAi: TCH4 4.1 plants was much slower than the wild-type; RNAi: TCH4 4.1 eventually reached maturation four weeks later than the wild-type and produced seed. The phenotype of the RNAi: TCH4 4.1 plant at maturation was similar to wild-type Ws but distinct from that of RNAi: TCH4 1.1 or RNAi: TCH4 3.1, which both had more leaves with a smaller radius. The height of the inflorescence stem in all of the analyzed lines was comparable to that of the wild-type.

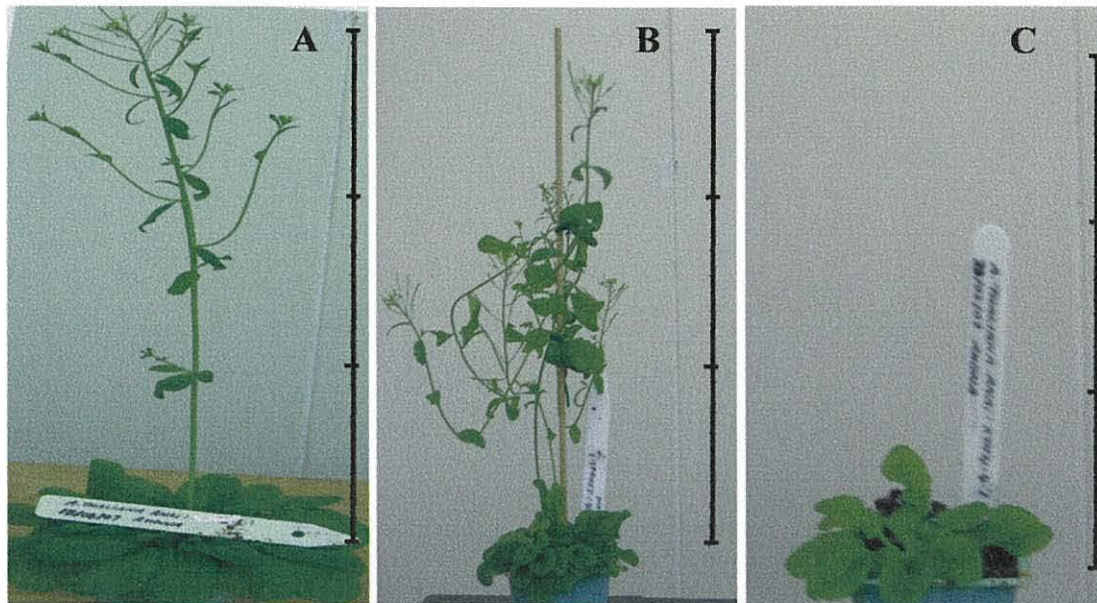


Figure 8.2: Phenotype of *Arabidopsis* RNAi: TCH4 T₁ plants.

Photographs were taken when wild-type Ws plants reached maturity; showing the relative development of the transgenic plants compared to wild-type at maturity.

A. Wild-type Ws B. RNAi: TCH4 1.1, C. TCH4 4.1. Each bar on the ruler is equivalent to 100mm, as a relative measure of the height of each plant.

c) Assaying genomic DNA from T₁ transgenic plants for the presence of an intact transgene

Rosette leaves were harvested from mature T₁ plants and DNA was extracted from these samples, DNA was amplified by PCR using sequence specific primers and a primer based on the hinge section of the construct (section 7.2.5), and on primers spanning the transgene (Table 8.2). The PCR products are shown in Figures 8.3 and 8.4; these confirm that the RNAi: TCH4 1.1, TCH4 3.1, and RNAi: TCH4 4.1 lines all contain the transgene as both the sense and antisense fragments are present either side of the hinge (Figure 8.3). As expected, no product was amplified from Ws genomic DNA as it does not contain the transgene. The DNA was also amplified with primers spanning the entire transgene to check the integrity of the whole construct; Figure 8.4 shows that a single band of the expected size was amplified for each transgenic line.

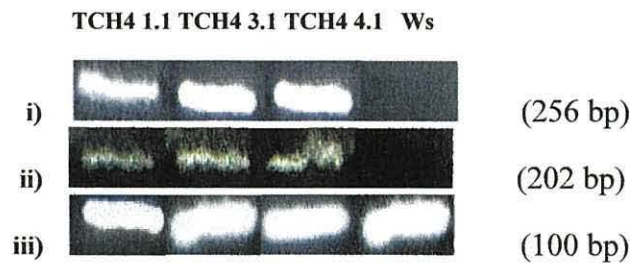


Figure 8.3: Verification of the presence of the transgene in RNAi: TCH4 transgenic lines.

PCR products from the amplification of genomic DNA from RNAi lines: RNAi: TCH4 1.1, 3.1, 4.1 and wild-type Ws. Primers spanning the TCH4 coding sequence and the hinge sequence (section 7.2.5) in the transgene were used to amplify DNA; **i)** Primers spanning the sense sequence and hinge sequence, **ii)** Primers spanning the antisense sequence and the hinge sequence. **iii)** 18S rRNA primers were used to show there was DNA in each sample and that approximately the same amount of product was loaded on the gel. Numbers in parentheses are the size of the band amplified by PCR.

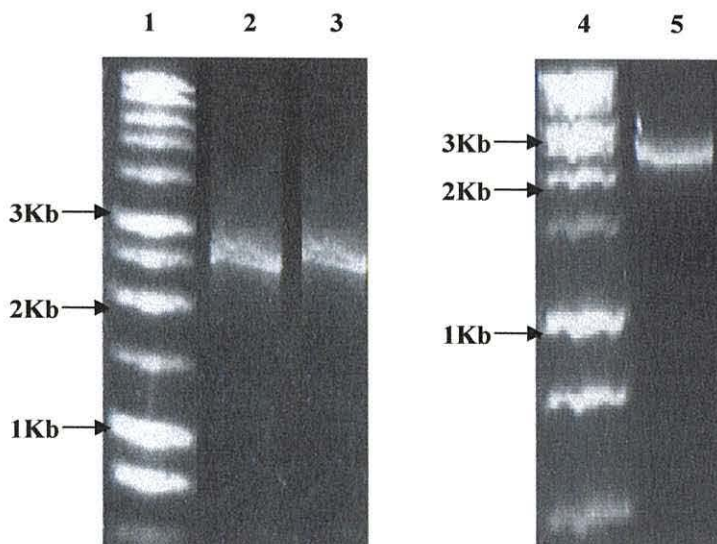


Figure 8.4: Verification of the intactness of the transgene in RNAi: TCH4 transgenic lines.

Primers spanning the transgene were used to verify the intactness of the transgene (Table 8.2), where the TCH4 transgene is intact the expected band size is 2614 bp. 1.2% agarose gels showing PCR products from the amplification of genomic DNA from transgenic lines: RNAi: TCH4 1.1 (lane 2), RNAi: TCH4 3.1 (lane 3), RNAi: TCH4 4.1 (lane 5). A 1Kb size ladder is shown in lanes 1 and 4.

8.3.2 T₂ generation TCH4 RNAi transgenic lines

a) Selection of T₂ transgenic seedlings on media supplemented with kanamycin

T₂ seed were plated on half-strength MS media supplemented with kanamycin, at 14-days old the number of seedlings surviving and the number of seedlings bleached on this media was counted. In the RNAi: TCH4 4.1 line all of the seedlings survived, while the majority (~85%) of seedlings survived from the other two lines (Table 8.4). This shows that RNAi: TCH4 4.1 is homozygous and RNAi: TCH4 1.1 and RNAi: TCH4 3.1 are heterozygous with respect to the inserted DNA.

Table 8.4: Kanamycin resistance of RNAi: TCH4 T₂ seedlings.

T₂ seed were plated on half-strength MS media supplemented with kanamycin. The number of seedlings surviving on this medium was counted when the seedlings reached 14-days old. The percentage of resistant seedlings is expressed as a percentage of the total number of seedlings tested; the remaining seedlings were bleached and non resistant.

Transgenic line	Number of kanamycin resistant seedlings	Total number of seedlings tested	Percentage of kanamycin resistant seedlings
RNAi: TCH4 1.1.1	186	225	83%
RNAi: TCH4 3.1.1	61	72	85%
RNAi: TCH4 4.1.1	116	116	100%

b) Gene expression analysis of transgenic lines by RT-PCR

RT-PCR was used to determine whether the transgene was expressed in the transgenic lines and to assess whether expression of the transgene leads to silencing of the target gene TCH4. Figure 8.5i shows that the transgene is expressed in each of the transgenic lines but not in the wild-type, as would be expected since the wild-type does not contain the transgene. The transgene is expressed to similar levels in both the vibrated and control samples from each line.

From the previous phenotypic analysis and gene expression analysis of wild-type Ws seedlings subjected to vibration stress (Chapters 3 and 5 respectively), it was concluded that TCH4 expression was induced immediately after the cessation of vibration and a novel phenotype was observed in the seedlings when they reached 14-days old. TCH4 expression was induced in response to vibration stress in this analysis (Figure 8.5ii). TCH4 expression was not silenced in any of the transgenic lines subjected to vibration stress (Figure 8.5ii). In transgenic line RNAi: TCH4 1.1 expression of TCH4 was similar to wild-type in vibrated seedlings. However, in RNAi: TCH4 3.1 and RNAi: TCH4 4.1 lines, expression of TCH4 was greater than in the wild-type. Thus, the RNAi transgene has not led to silencing of TCH4 in any of the T2 lines generated. Expression of TCH4 in unstressed seedlings from the transgenic lines was up-regulated with respect to the unstressed wild-type control, indicating that TCH4 is up-regulated in the transgenic lines.

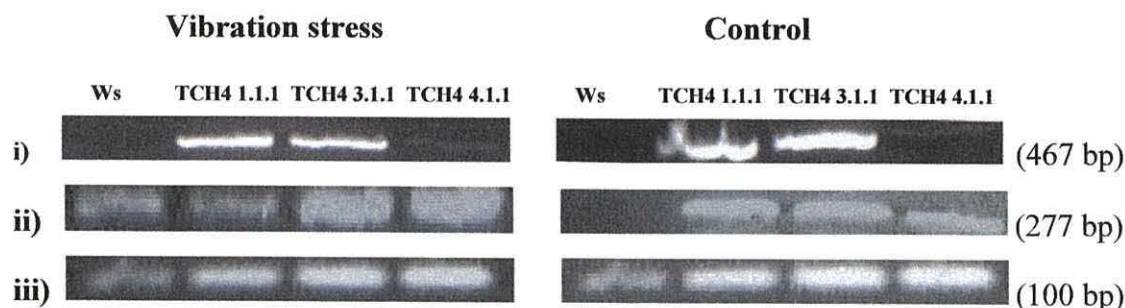


Figure 8.5: Gene expression in RNAi: TCH4 transgenic seedlings subjected to vibration stress.

RT-PCR of RNA extracted from seedlings subjected to vibration stress; vibration stress (40Hz) was applied for 72 hours from seedling germination. Seedlings were harvested immediately after the cessation of vibration, unstressed control seedlings were harvested at the same time point

i) PCR primers based on the hinge in the transgene, to check expression of the transgene. ii) TCH4 PCR primers, to analyze whether the target gene is silenced. iii) 18S rRNA primers, to show an equivalent amount of cDNA was loaded for each sample. Numbers in parentheses are the size of the cDNA band amplified by PCR.

c) Phenotypic analysis of T₂ seedlings subjected to vibration stress

The phenotype of T₂ seedlings was monitored concurrently with sampling for gene expression analysis. Unstressed seedlings from the RNAi: TCH4 1.1.1 and RNAi: TCH4 3.1.1 lines had significantly longer hypocotyls at 14-days old than wild-type Ws (Figure 8.6). However, the hypocotyl length of TCH4 4.1.1 seedlings was not different to that of wild-type seedlings. Vibration stress led to the promotion of hypocotyl elongation in the wild-type and also in the RNAi: TCH4 1.1.1 and RNAi: TCH4 4.1.1 lines. The hypocotyls of vibrated seedlings from the RNAi: TCH4 3.1.1 line were not significantly longer than their control. The transgenic seedlings showed a similar phenotype to wild-type seedlings, although the promotion of hypocotyl elongation by exposure to vibration stress was not as severe as in the wild-type.

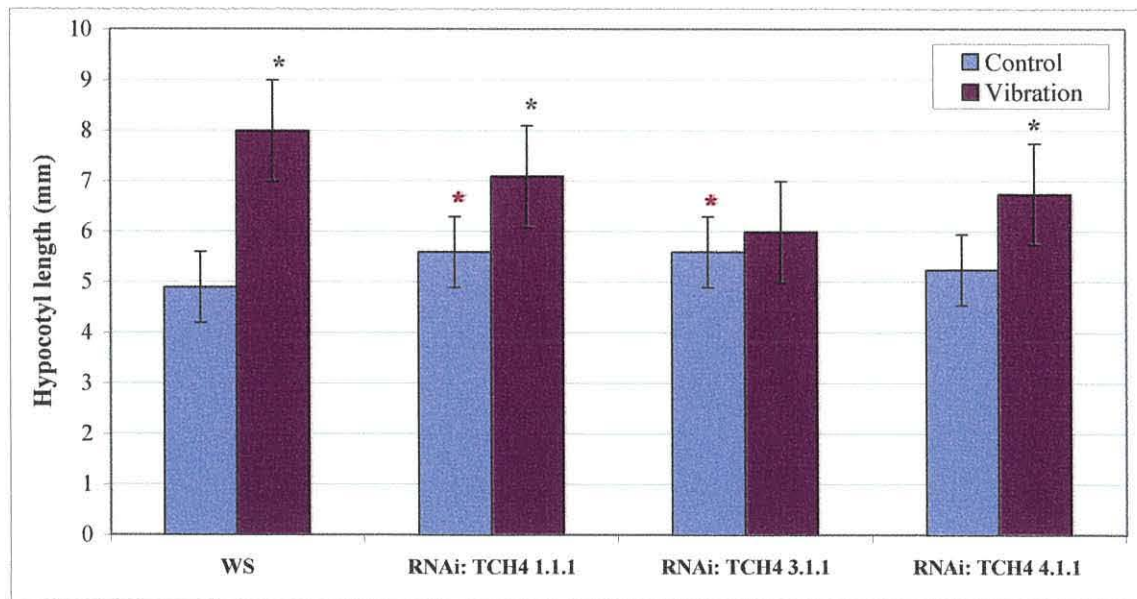


Figure 8.6: Hypocotyl elongation at 14-days old of RNAi: TCH4 transgenic seedlings subjected to vibration stress.

Vibration stress (40Hz) was applied for 72 hours from germination. Values are \pm SD of 20 seedlings. * Indicates transgenic control plants that are significantly different from the wild-type control with $\geq 95\%$ significance and. * indicates vibrated transgenic plants that are significantly different from the transgenic control with $\geq 95\%$ as determined by a Two-way ANOVA.

8.4 Expansin 3 RNAi transgenics

8.4.1 T₁ generation of EXP3 RNAi transgenic lines

a) Selection of T₁ transgenic seedlings on media supplemented with Kanamycin

Twelve T₁ RNAi: EXP3 seedlings were selected on kanamycin media; five of these seedlings died within the first two weeks of germination despite showing no bleaching of the seedlings. A further two seedlings died after they were transferred to soil conditions; although they survived for two weeks in soil, they did not develop any further. The remaining five seedlings survived and developed to maturation.

b) Phenotypic analysis of T₁ generation

Variation was seen in the phenotypes of the T₁ generation of the transgenic lines, when compared to wild-type Ws and with each other. RNAi: EXP3 2.1 and EXP3 2.2 both had smaller rosette leaves than wild-type plants, and a profusion of secondary inflorescences (Figure 8.7). Similarly, RNAi: EXP3 4.1 had smaller rosette leaves than the wild-type but did not have many secondary bolts. RNAi: EXP3 4.3, which was derived from the same parent plant as RNAi: EXP3 4.1 had larger rosette leaves (similar to wild-type) but few branches on the primary inflorescence (Figure 8.7). Rosette development in the RNAi: EXP3 3.2 line was comparable to that of the wild-type but the inflorescence of this plant was thicker than normal. The height of the primary inflorescence stem of the transgenic lines did not differ significantly to wild-type Ws.

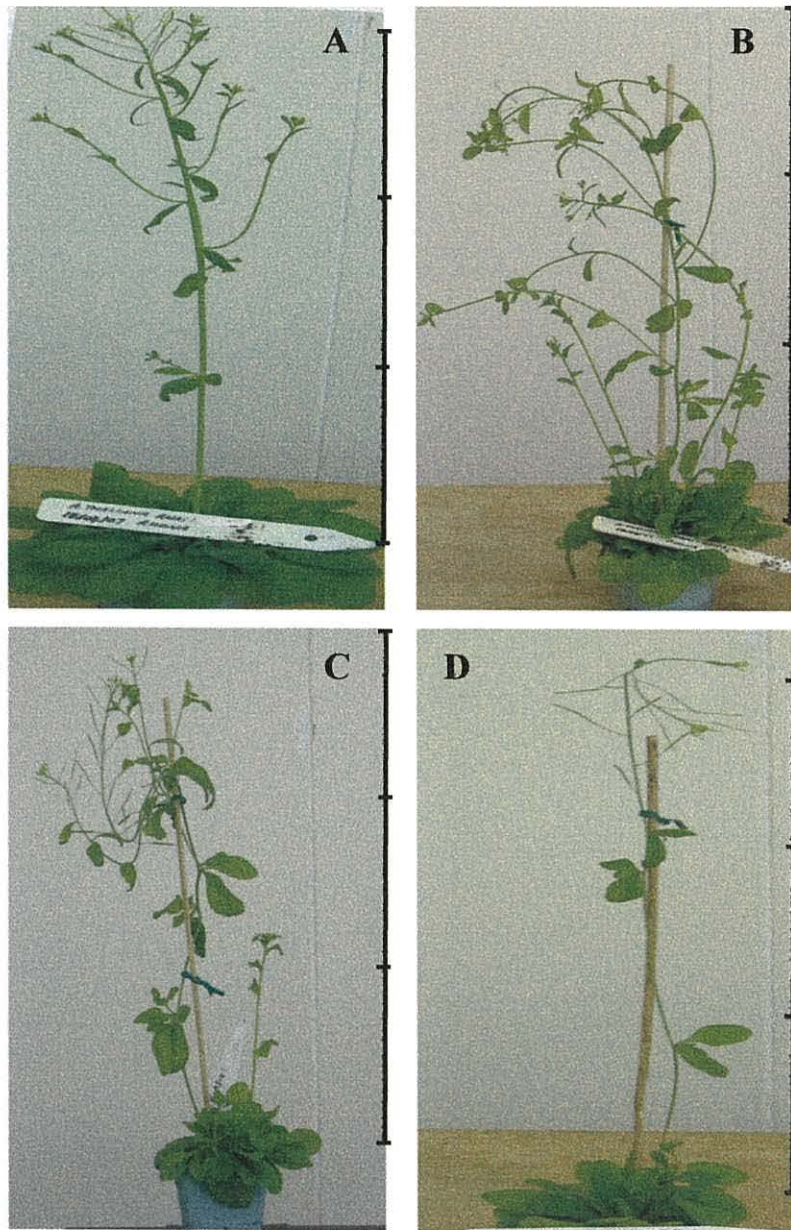


Figure 8.7: Phenotype of RNAi: EXP3 T₁ plants.

Photographs were taken when wild-type Ws plants reached maturity; showing the relative development of the transgenic plants compared to wild-type. **A.** Wild-type Ws, **B.** RNAi: EXP3 2.2, **C.** RNAi: EXP3 4.1, **D.** RNAi: EXP3 4.3. Each bar on the ruler is equivalent to 100mm, as a measure of the height of each plant.

c) Assaying genomic DNA from T₁ plants for the presence of an intact transgene

Rosette leaves were harvested from the mature T₁ plants and DNA was extracted from these samples. DNA was amplified by PCR using sequence specific primers based on the sense or antisense conformation of the sequence and the hinge sequence of the transgene (see section 7.2.5). Primers spanning the entire transgene (Table 8.2) were also used to check the transgene was intact. The PCR amplification products are shown in Figures 8.8 and 8.9. The sense and antisense inserts (Figure 8.8) were confirmed for each transgenic line with exception to RNAi: EXP3 4.3., in which only the antisense section of the transgene was found. This may have occurred due to a rearrangement of the transgene and, therefore this particular line was not used in any of the subsequent analyses.

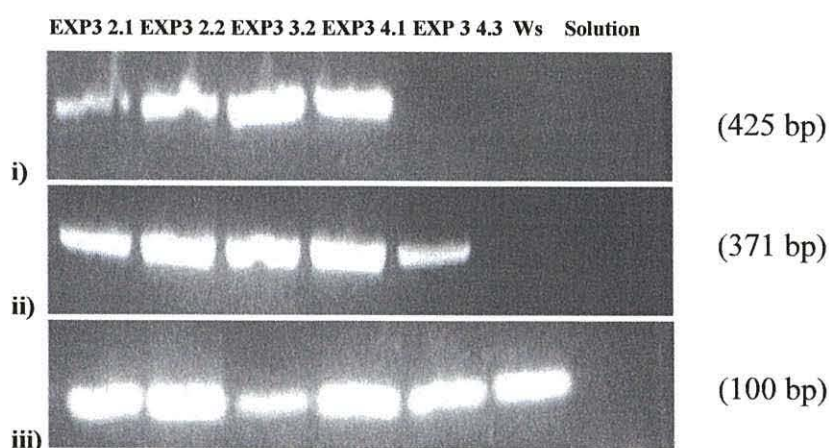


Figure 8.8: Verification of the presence of the transgene in RNAi: EXP3 transgenic lines.

PCR products from the amplification of genomic DNA from RNAi lines: RNAi: EXP3 2.1, 2.2, 3.2, 4.1, 4.3, and wild-type Ws. Primers based on the EXP3 coding sequence and the hinge sequence (section 7.2.5) in the transgene were used to amplify DNA; **i)** Primers spanning the sense sequence and hinge sequence. **ii)** Primers spanning the antisense sequence and hinge sequence. **iii)** 18s rRNA primers were used to show that approximately the same amount of product was loaded on the gel. Numbers in parentheses are the size of the band amplified by PCR.

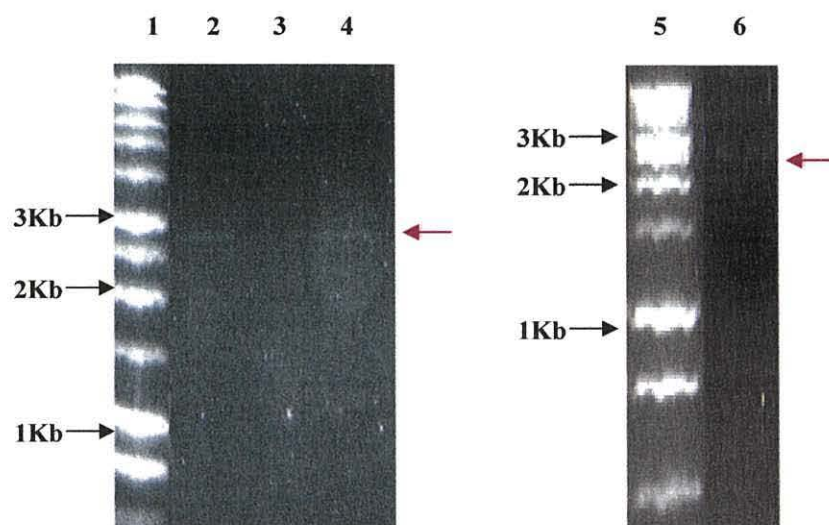


Figure 8.9: Verification of the intactness of the transgene in RNAi: EXP3 transgenic lines.

Primers spanning the transgene were used to verify the intactness of the transgene (Table 8.2), where the EXP3 transgene is intact the expected band size is 2952 bp. 1.2% agarose gels showing PCR products from the amplification of genomic DNA from transgenic lines: RNAi: EXP3 2.1 (lane 2), RNAi: EXP3 2.2 (lane 3), RNAi: EXP3 3.2 (lane 4) and RNAi: EXP3 4.1 (lane 6). A 1Kb size ladder is shown in lanes 1 and 5.

8.4.2 T₂ generation of EXP3 RNAi transgenic lines

a) Selection of T₂ transgenic seedlings on media supplemented with Kanamycin

T₂ seed from the remaining four transgenic lines were selected on half-strength MS media supplemented with kanamycin (35 µg.ml⁻¹). One homozygous line RNAi: EXP3 2.2 was identified, as indicated by 100% kanamycin resistance in the T₂ seedlings (Table 8.5). The other lines exhibited 79% to 89% kanamycin resistance.

Table 8.5: Kanamycin resistance of RNAi: EXP3 T₂ seedlings.

T₂ seed were plated on half-strength MS media supplemented with 35 µg.ml⁻¹ kanamycin. The number of seedlings surviving on this medium was counted when the seedlings reached 14-days old. The percentage of resistant seedlings is expressed as a percentage of the total number of seedlings tested; the remaining seedlings were bleached and non resistant. * Few seedlings were tested as little seed was collected from the parent plant.

Transgenic line	Number of resistant seedlings	Total number of seedlings tested	Percentage of resistant seedlings
RNAi: EXP3 2.1.1	107	121	88%
RNAi: EXP3 2.2.1	50	50*	100%
RNAi: EXP3 3.2.1	42	47*	89%
RNAi: EXP3 4.1.1	157	200	79%

b) Gene expression analysis of transgenic lines by RT-PCR

Gene expression was analyzed by PCR in the transgenic lines; expression of the transgene was checked using primers based on the hinge sequence of the transgene, and expression of EXP3 was monitored using sequence specific primers. The transgene was expressed in each of the transgenic lines (Figure 8.10i). The transgene was expressed at a low level in RNAi: EXP3 4.1.1 compared with the other lines. The transgene was expressed to similar levels in the vibrated and control samples for each line (Figure 8.10i).

Earlier in this study it was established that EXP3 is induced in seedlings immediately after the cessation of vibration stress (Chapter 5). Expansin 3 was not expressed in wild-type seedlings immediately after the cessation of vibration stress, when they were sampled along with the transgenic seedlings (Figure 8.10ii). EXP3 is expressed to a low level in the transgenic line RNAi: EXP3 2.1.1 immediately after the cessation of vibration stress. The lack of expression in the transgenic line may be due to expression of the transgene or because the gene was not induced in this line under the stress conditions. In the other three transgenic lines RNAi: EXP3 2.2.1, RNAi: EXP3 3.2.1 and RNAi: EXP3 4.1.1, expression of EXP3 appears to be up-regulated with respect to wild-type expression. With a view to identify whether EXP3 is over-expressed in these three lines and silenced in RNAi: EXP3 2.1.1, expression was analyzed in the unstressed control seedlings from these transgenic lines (Figure 8.10ii). EXP3 was expressed in all of the transgenic lines but not in wild-type Ws, this suggests that expression of EXP3 is overexpressed in the transgenic lines not silenced.

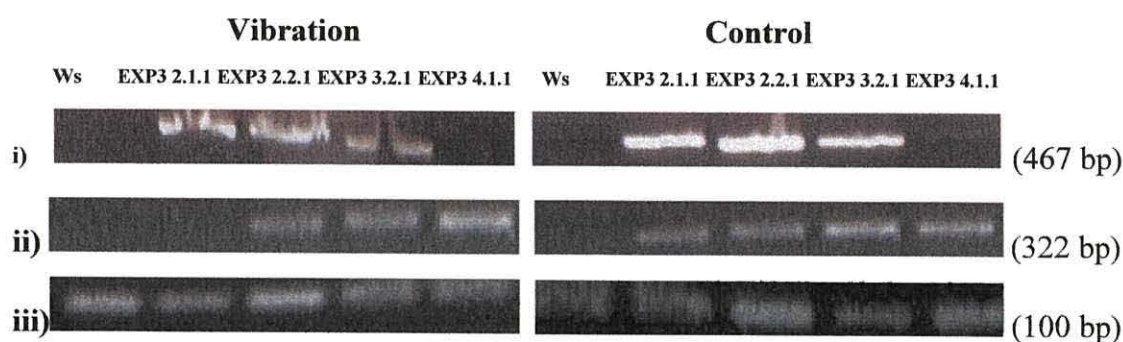


Figure 8.10: Gene expression in RNAi: EXP3 transgenic seedlings subjected to vibration stress.

RT-PCR of RNA extracted from seedlings subjected to vibration stress; vibration stress (40Hz) was applied for 72 hours from seedling germination.

i) PCR primers based on the hinge in the transgene, to check if the transgene is expressed. ii) EXP 3 RT-PCR primers, to determine whether the target gene is silenced. iii) 18s rRNA primers, to show equal loading of the samples. Numbers in parentheses are the size of the cDNA band amplified by PCR.

c) Phenotypic analysis of T₂ seedlings subjected to vibration stress

As Figure 8.11 shows, the unstressed RNAi: EXP3 3.2.1 transgenic line had a shorter hypocotyl than the wild type (control) at 14-days old. Hypocotyl elongation in the other lines was similar to that in the wild-type when they were not subjected to stress. Subjecting the transgenic seedlings to vibration stress resulted in significant hypocotyl elongation in RNAi: EXP3 4.1.1, but not in the other three lines (Figure 8.11).

Although EXP3 was not down-regulated in either RNAi: EXP3 2.1.1 or RNAi: EXP3 2.2.1, vibration stress did not promote hypocotyl elongation in these lines as it does in wild-type Ws.

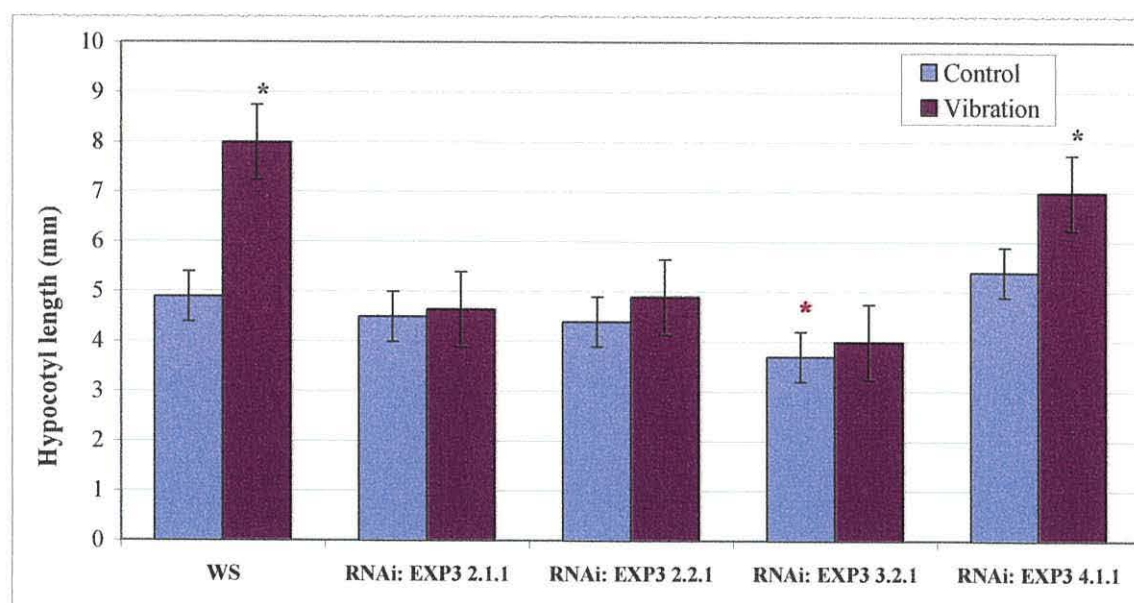


Figure 8.11: Hypocotyl elongation at 14-days old of RNAi: EXP3 transgenic seedlings subjected to vibration stress.

Vibration stress (40Hz) was applied for 72 hours from germination. Values are \pm SD of 20 seedlings. * Indicates transgenic control plants that are significantly different from the wild-type control with $\geq 95\%$ significance and. * Indicates vibrated transgenic plants that are significantly different from the transgenic control with $\geq 95\%$ significance as determined by a Two-way ANOVA.

8.5 CCR2 and CCR family RNAi transgenics

8.5.1 T₁ generation of CCR family (CCRF) RNAi transgenic lines

Only two seedlings survived from the 2000 seed plated for this construct on media supplemented with kanamycin, showing that transformation efficiency was particularly low for this construct. One of the seedlings was transferred to soil conditions after 21 days, while the other was maintained on the original selective media. The seedling survived *in vitro* for a further two weeks, and the seedling transferred to soil survived for a further three weeks. Neither seedling progressed beyond growth stage 1.05, which is the development of five rosette leaves; as shown for the soil-based seedling in Figure 8.12. The presence of the transgene in these two lines was not checked due to their early demise.

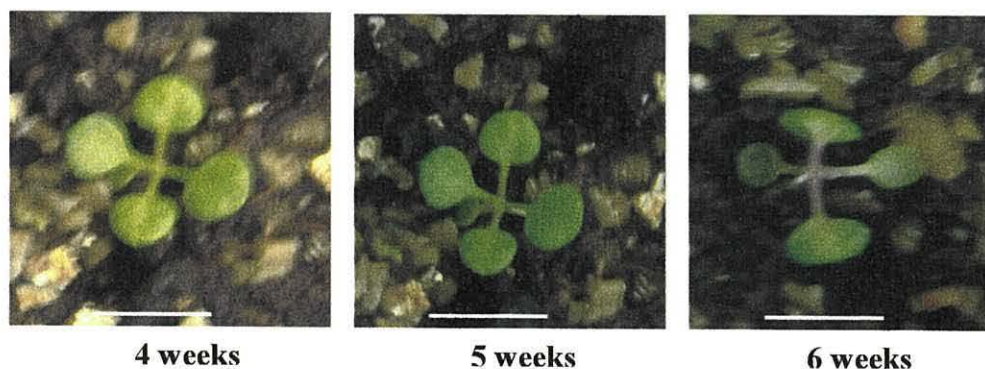


Figure 8.12: Phenotype of RNAi: CCRF T₁ plant from 4 to 6 weeks after germination.

This RNAi: CCRF seedling survived until 6 weeks after germination without developing beyond growth stage 1.05 (5 rosette leaves greater than 1mm in length). By 6 weeks after germination one rosette leaf had withered and the remaining rosettes were glassy. Wild-type Ws plants reached growth stage 5 (inflorescence emergence) in the same time period. Size bar is equal to 10mm.

8.5.2 T₁ generation of CCR2 RNAi transgenic lines

a) Selection of T₁ transgenic seedlings on media supplemented with kanamycin

Eight seedlings survived on selective media from the T₁ seed plated for the cinnamoyl CoA reductase 2 construct. Only two of these seedlings survived the subsequent transfer to soil conditions, and grew to maturity; RNAi: CCR2 1.1 and RNAi: CCR2 2.1.

b) Phenotypic analysis of T₁ generation

The two CCR2 transgenic plants grew slower than wild-type Ws; they reached each of the key stages of development 1-2 weeks after the wild-type. The two transgenic plants had a similar phenotype that was distinct from that of the wild-type (Figure 8.13). The inflorescence stems of RNAi: CCR2 1.1 and RNAi: CCR2 2.1 were thicker than the wild-type but not significantly shorter. The rosette leaves of the two plants had a larger radius than the wild-type plant; Figure 8.13 shows the relative size of the wild-type and RNAi: CCR2 1.1 plants.

c) Assaying genomic DNA from T₁ plants for the presence of an intact transgene

As Figure 8.14 shows, both RNAi: CCR2 1.1 and RNAi: CCR2 2.1 lines contained only the antisense insert but not the sense insert in the transgenes. This is apparently due to the aberrant excision of the sense fragment from the transgene during recombination. As none of the CCR2 lines contained the intact transgene, these lines were not used for further analysis.

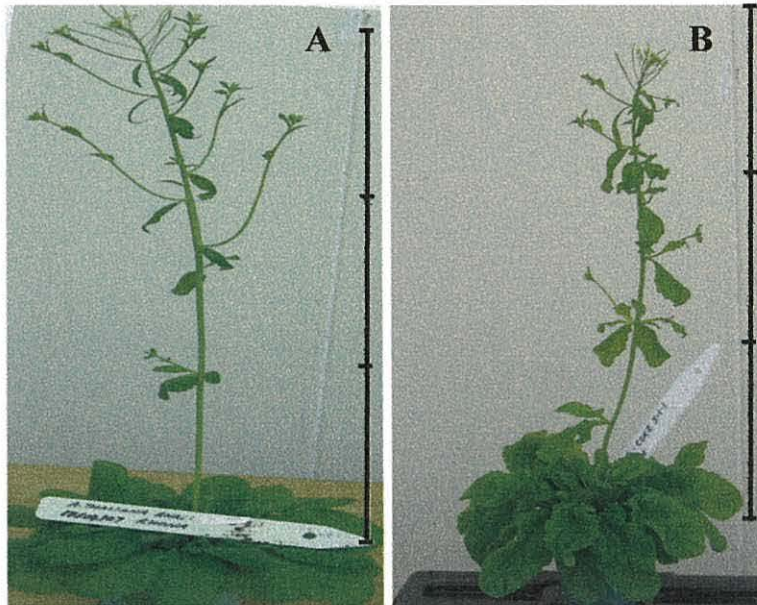


Figure 8.13: Phenotype of RNAi: CCR2 T₁ plants.

Photographs were taken when wild-type Ws plants reached maturity; showing the relative development of the transgenic plant compared to wild-type. A. Wild-type Ws, B. RNAi: CCR2 1.1. Each bar on the ruler is equivalent to 100mm, as a measure of the height of each plant.

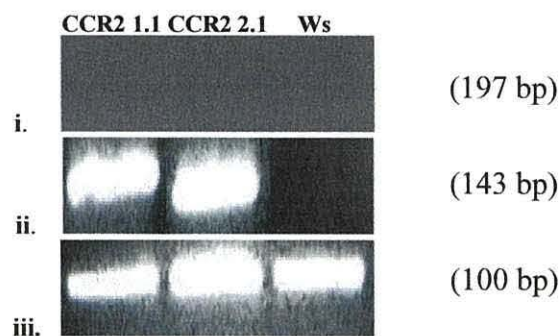


Figure 8.14: Evidence for the presence of the transgene in RNAi: CCR2 transgenic lines.

PCR products from the amplification of genomic DNA from RNAi lines: RNAi: CCR2 1.1, 2.1, and wild-type Ws. Primers based on the CCR2 coding sequence and the hinge sequence (section 7.2.5) in the transgene were used to amplify DNA; i. Primers spanning the sense sequence and hinge sequence, ii. Primers spanning the antisense sequence and hinge sequence, iii. 18s rRNA primers were used to show there was DNA in each sample and that approximately the same amount of product was loaded on the gel.

8.6 CESA 3 RNAi transgenics

Few T₁ seedlings from the CESA RNAi lines survived on selective media. Only two seedlings from the seed germinated survived until they reached 14-days old. Although one seedling was successfully transferred to soil, neither seedling survived. The transgene was not checked in these seedlings.

8.7 Discussion

a) Transformation efficiency using the simplified floral-dip method

The floral-dip method can be used effectively for transformation of *Arabidopsis* plants; commonly up to 1% of all seed produced by dipped plants is transformed (Bent, 2000). Transformation efficiency is dependent on the growth stage at which floral-dipping is applied, the use and concentration of sucrose used, and the use of a surfactant at levels that do not induce necrosis of leaf tissue (Clough & Bent, 1998). In this study, transformation efficiency varied across the five constructs, between 0.1% and 0.6% (number of T₁ kanamycin resistant seedlings/2000 seed plated).

Transformation efficiency was low (0.1%) in the CCRF and CESA lines, despite the fact that sucrose and the surfactant Silwet L-77 were used at optimal concentrations, as determined by Clough & Bent (1998). Low efficiency in the CCRF and CESA lines may be due to variations in the plant growth stage when floral-dipping was applied. The floral-dip was applied at the recommended stage; after the primary inflorescences were clipped, the secondary bolts had reached at least 2cm and there were few flowers open. However, variation in plant development could contribute to the different transformation efficiencies found between lines (Clough & Bent, 1998). The ovules are the site of transformation in the floral-dip method; few unopened flowers on the dipped plants are desirable because *Agrobacterium*, especially in the presence of the surfactant, can infiltrate the flower and gain access to the ovule (Desfeux *et al*, 2000).

b) Plants from the first transgenic generation showed altered phenotypes

The phenotypes of T₁ plants can be screened without having to produce homozygous lines as the hairpin construct is dominant in transgenic plants (Helliwell & Waterhouse, 2003). With few exceptions, plants from the first transgenic generation (T₁) of the TCH4 and EXP3 lines were shown to contain the appropriate intact transgene. The CCR2 transgene was not intact but it was associated with a novel phenotype. In the TCH4 lines the phenotype was distinguishable from that of wild-type Ws, with exception to RNAi: TCH 4.1, although developmental progression was slower in each of the transgenic lines including RNAi: TCH 4.1. Greatest variation was seen amongst the EXP3 transgenic lines; although progeny from the same dipped plant had similar phenotypes. Some delay in development was common to all of the transgenic lines. Overall, the phenotypic changes observed in transgenic lines were restricted to changes in leaf number and radius, and the degree of branching or development of secondary inflorescences but not to the height of the primary inflorescence stem.

As there were relatively few T₁ plants generated in this study, gene expression was not monitored in this generation. Plants from this generation were used to produce the next generation of seed, and as a source of tissue to check the presence and intactness of the transgene.

c) Gene expression of T₂ transgenic lines subjected to vibration stress

Expression of the targeted candidate wind/mechanical stress genes were not silenced in the T₂ generation of the TCH4 and EXP3 transgenic lines. The extent to which the lack of gene silencing can be attributed to heterogeneity of the T₂ populations is debatable, silencing of the target gene was not found in either homozygous or heterozygous T₂ lines. In a previous study using the same RNAi vector as was used in this study, expression of the KNAT6 gene was down-regulated but not knocked out in the roots of a series of homozygous T₃ plants (Dean *et al*, 2004), suggesting that RNAi-induced silencing is heritable. Based on this result some degree of gene silencing would be expected in the T₂ generation and subsequent generations, even though gene silencing may decline significantly between generations (Wang *et al*, 2005).

The apparent overexpression of the target genes in the TCH4 and EXP3 constructs, rather than silencing is surprising. The overexpression of the target gene is associated with lines from two independent constructs, which suggests the aberrant results are associated with the construct. Due consideration was given to the design of the RNAi construct as outlined in Chapter 7; some efficient siRNAs were predicted for both of these constructs (section 7.2.1). In the study by Dean *et al* (2004), where the target gene was down-regulated using the pRNAi vector, the antisense fragment was inserted immediately after the promoter, followed by the hinge and the sense fragment. In spite of this, numerous other studies, although not in the pRNAi vector, have cloned the gene specific fragment in the sense orientation immediately after the promoter, and followed by the intron/hinge and the antisense fragment as was used in this study (Wang *et al*, 2005, Li & Wang, 2004, Fukusaki *et al*, 2004, Wesley *et al*, 2001). As outlined in this chapter, the transgene is present, intact and expressed in each transgenic line.

It seems unlikely that the intact transgene would not result in hairpin formation. However, if a hairpin was not formed it is conceivable that this construct could induce over-expression, because the sense fragment is immediately in front of the CaMV 35S promoter. If this were the case in the lines generated in this study, only the gene specific fragment would be over-expressed, not the entire gene. The expression of the candidate wind/mechanical stress genes were analyzed in the transgenic lines using the primers from the original gene expression analysis in Chapter 5, and not those used to generate the transgenic construct. As the original primers amplify a different region of the candidate gene to the primers used for the RNAi construct, they should only detect an overexpression of the entire gene. Further investigation is needed to verify and establish the cause of the over-expression of the target gene in these transgenic lines.

8.8 Summary

Transgenic seedlings were selected for each construct on media supplemented with kanamycin. Transformation efficiency was low in two of the lines, CCRF and CESA, and normal in the TCH4, EXP3 and CCR2 lines. No T₁ seedlings from the CCRF and CESA lines survived the subsequent transfer to soil conditions; seedlings from the remaining lines were grown to maturity. The presence of the transgenes was checked in the DNA of T₁ plants; CCR2 lines did not contain an intact transgene, however TCH4 and EXP3 did. Homozygous and heterozygous lines were generated in the T₂ generation of TCH4 and EXP3 lines. T₂ seedlings were subjected to vibration stress to induce expression of wind/mechanical stress genes. Gene expression of candidate wind/mechanical stress genes was not knocked-out in the T₂ transgenic lines.

9. Concluding remarks and Future work

9.1 Phenotypic analysis of *Arabidopsis* plants subjected to wind/mechanical stresses

In this work, growth conditions that give rise to a significant change in phenotype when *Arabidopsis* plants are subjected to wind/mechanical stresses were established (Chapter 3). The growth-stage based phenotypic analysis of Boyes *et al* (2001) was used to identify phenotypic differences between stressed and control plants, and between ecotypes of *Arabidopsis*. Under specific conditions wind stress induced the expected dwarfing of plants. Conversely, vibration stress resulted in a promotion of growth in seedlings. However, long-term exposure to vibration stress did not induce a novel phenotype in *Arabidopsis* plants. The differences in response to wind and mechanical stresses seen between Columbia and Wassilewskija ecotypes in this study suggests that certain *Arabidopsis* ecotypes respond differently when subjected to these stresses. Furthermore, Pigliucci (2002) did not observe a significant reduction in height in 11 natural accessions of *Arabidopsis thaliana* which were exposed to wind stress. There is scope to investigate the adaptation and response of different *Arabidopsis* ecotypes to wind and mechanical stresses, especially in natural accessions that are known to grow in windy habitats.

9.2 Generation of active oxygen species in *Arabidopsis* plants subjected to wind stress

Subjecting *Arabidopsis* plants to wind stress was found to induce enhanced levels of active oxygen species and soluble peroxidases in rosette leaves (Chapter 4). The initial study could be developed by considering the impact of wind stress on the levels of both soluble and cell wall-associated peroxidases in the rosette leaves, and in the inflorescence stem of affected plants. The levels of cell wall-associated peroxidases (ionically- and covalently-bound) were increased in line with levels of soluble peroxidases in *Bryonia dioica* plants subjected to thigmic stress (De Jaegher *et al*, 1985). Thus, an increase in cell wall-associated peroxidases would be expected in extracts from wind stressed rosette leaves. Tissue samples could be harvested from

stressed plants over a longer time period than was used in this study, to determine how long peroxidase levels are elevated after exposure to wind stress.

Relatively high levels of peroxidase activity associated with lignification were found in the rosette leaves of plants subjected to long-term wind stress. Thus a tentative relationship can be made between accelerated lignification and reduced rosette leaf area in wind stressed plants. The reduction in height of wind stressed inflorescence stems could also be associated with accelerated lignification. As lignification is also involved in secondary growth, further studies are needed to investigate the possible connection between wind stress and the early onset of secondary growth. In this study, candidate wind/mechanical stress genes, including those from the lignin biosynthesis pathway were up-regulated in wind stressed stems grown under short-day conditions. Furthermore, up-regulation of TCH4 and CCR2, which has previously been associated with the development of secondary wood (Ko *et al*, 2004), was seen in wind stressed stems.

9.3 Expression of candidate wind/mechanical stress genes in plants subjected to wind and mechanical stresses

RT-PCR was used to look at gene expression in tissues sampled from plants subjected to wind and other mechanical stresses (Chapters 5 and 6). The semi-quantitative approach used achieved the overall aim of determining whether candidate wind/mechanical stress genes were differentially expressed in seedlings and plants subjected to wind and mechanical stresses. As the selected genes were differentially expressed in plants subjected to wind and mechanical stresses, they were suitable candidate genes. The expression patterns of TCH4, CCR2, EXP3 and CESA3 particularly singled them out for further analysis. The study of these genes could be widened to include other members of their gene families, a microarray analysis found that genes up-regulated in response to touch included other members of the touch gene, cinnamoyl CoA reductase, expansin and cellulose synthase families, as well as other members of the extensin, mitogen-activated protein kinase and arabinogalactan protein gene families (Lee *et al*, 2005). A number of other genes could also be

designated as candidate wind/mechanical stress genes from microarrays and may be investigated in future studies.

Tissue sampling for RT-PCR was restricted to time points immediately after the cessation of the wind or mechanical stress and/or when a phenotypic change was observed in stressed plants, expression of the candidate genes was commonly found to differ between these time points. Sampling at regular intervals in between these time points could be used to generate further expression patterns and direct future molecular studies on the response and adaptation to wind and mechanical stresses. Furthermore, other tissues could be harvested from the stressed plants. Expression in cotyledons, hypocotyls and roots could be separated from the overall expression in seedlings, as was analyzed in this study. Certainly, the most relevant tissues were sampled from mature plants subjected to wind stress, the rosette leaves and inflorescence stem, as these were where a phenotypic change was observed.

A number of promoter motifs that are associated with transcription factors involved in plant defense were found in the promoters of the candidate genes (Chapters 5 and 6); WRKY, MYB, MYC and ABRE transcription factor binding sites were over-represented in the first 1.5Kb of sequence upstream of the translation start codon. As well as gene expression analysis of transcription factors, promoter deletions fused to a reporter gene could be used to characterize the control of candidate wind/mechanical stress gene expression. Further investigation into the relationship between the responses to wind and mechanical stresses and other plant defense pathways is needed.

9.4 Silencing of candidate wind/mechanical stress gene expression.

The pRNAi vector was used to generate hairpin constructs with a view to silencing selected candidate wind/mechanical stress genes, constructs targeting TCH4, EXP3, CESA3, CCR2 and the CCR gene family were generated (Chapter 7). *Arabidopsis* plants were transformed with these constructs by the floral-dip method. Transgenic lines containing an intact transgene were propagated for two of the genes, TCH4 and EXP3 but the target gene was not silenced in any of these lines (Chapter 8).

Conversely, the target gene was apparently overexpressed in the TCH4 and EXP3 lines. While this apparent overexpression could be investigated further in the next generation, with a view to determining how the RNAi construct promoted overexpression of the target gene, the primary concern remains the generation of lines in which the target gene is silenced. Further primary transformants may be generated from the existing constructs or an alternative strategy may be used. In the study by Dean *et al* (2004) in which the pRNAi vector was used to down-regulate the target gene, the gene specific fragments were cloned in a different order than was used in this study, in their study the antisense fragment, hinge, and sense fragment followed the promoter successively. However, as numerous other studies have cloned the fragments in the same order as was used to generate the constructs in this study (sense fragment, hinge and antisense fragment successively), this would not necessarily be any more successful. An alternative generic RNAi vector could also be used to generate the constructs.

Plants were not generated for the other constructs due in part to either low transformation efficiency (CESA3 and CCRF) or recombination of the transgene (CCR2). In the case of the CESA3 and CCRF lines, it cannot be discounted that few lines were generated because silencing of the target gene generated seedling lethals. As all of the T₁ seed from these two lines has already been plated on media containing the antibiotic selection, more plants would have to be transformed. A greater number of plants may be floral-dipped to generate more seed for the subsequent selections.

Appendix A

Data from assays for the detection of soluble peroxidase activity

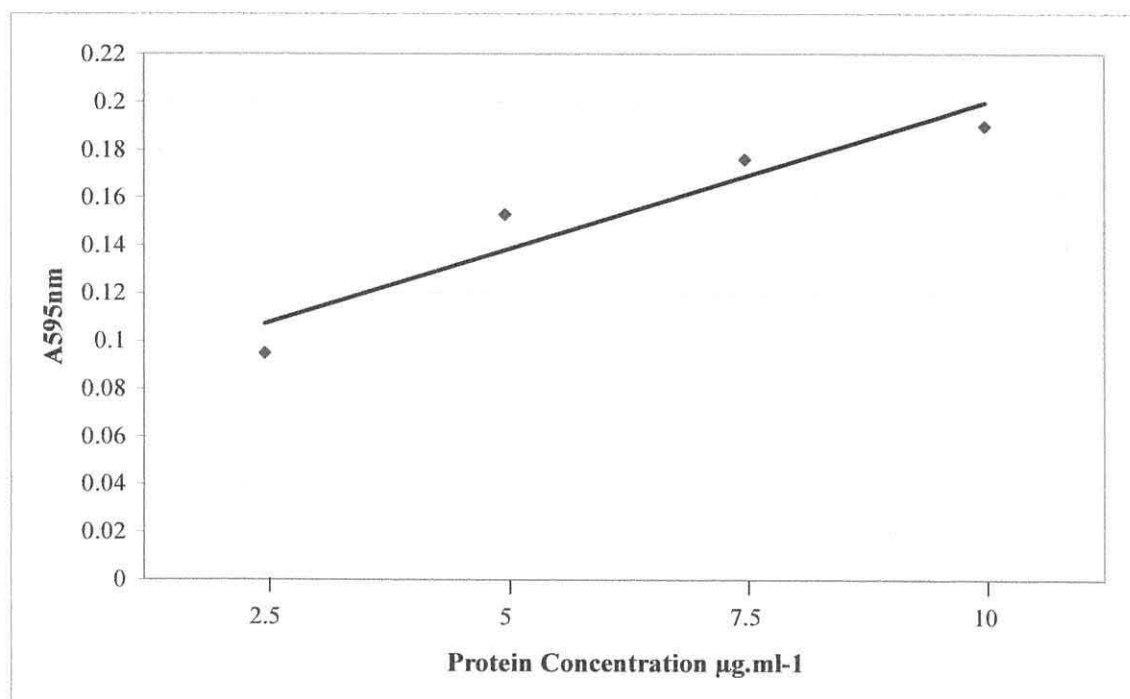


Figure A1: Protein standard curve

A1. Data from the Guaiacol assay for the detection of soluble peroxidase activity

Table A1: Guaiacol assay data for *Arabidopsis* seedlings subjected to vibration stress.

Sample	Bradford 595nm	Protein Concentration µg	Guaiacol 1min	Guaiacol 2min	Guaiacol (A470nm) 3min	Guaiacol 1min Corrected	Guaiacol 2min Corrected	Guaiacol 3min Corrected	Treatment Average	Per mg	SD/mg
Control 0hrs A	0.058	2.50	0.220	0.310	0.380	0.660	0.930	1.140			
Control 0hrs B	0.118	3.75	0.490	0.680	0.810	0.980	1.360	1.620	1.115	5.575	1.450
Vibration 0hrs A	0.105	2.50	0.160	0.230	0.280	0.480	0.690	0.840			
Vibration 0hrs B	0.120	3.75	0.280	0.350	0.410	0.560	0.700	0.820	0.682	3.408	0.082
Control 14-day A	0.156	6.25	0.570	0.770	0.930	0.684	0.924	1.116			
Control 14-day B	0.129	3.75	0.280	0.380	0.460	0.560	0.760	0.920	0.827	4.137	0.570
Vibration 14-day A	0.143	5.00	0.450	0.570	0.660	0.675	0.855	0.990			
Vibration 14-day B	0.107	2.50	0.920	1.100	1.210	2.760	3.300	3.630	2.035	10.175	8.450

Table A2: Guaiacol assay data for *Arabidopsis* plants subjected to wind and mechanical stresses

Sample	Bradford 595nm	Protein Concentration µg	Guaiacol 1min	Guaiacol 2min	Guaiacol (A470nm) 3min	Guaiacol 1min Corrected	Guaiacol 2min Corrected	Guaiacol 3min Corrected	Treatment Average	Per mg	SD/mg
Control 0hrs A	0.119	3.75	0.049	0.115	0.177	0.098	0.230	0.354			
Control 0hrs B	0.125	3.75	0.132	0.212	0.286	0.264	0.424	0.572			
Control 0hrs C	0.133	3.75	0.074	0.139	0.213	0.148	0.278	0.426	0.310	0.031	0.010
Short-term Wind stress 0hrs A	0.160	6.25	0.099	0.182	0.264	0.119	0.218	0.317			
Short-term Wind stress 0hrs B	0.123	3.75	0.024	0.055	0.069	0.048	0.110	0.138			
Short-term Wind stress 0hrs C	0.175	7.50	0.342	0.505	0.720	0.342	0.505	0.720	0.280	0.028	0.022
Long-term Wind stress 0hrs A	0.100	2.50	0.100	0.175	0.245	0.300	0.525	0.735			
Long-term Wind stress 0hrs B	0.151	5.00	0.111	0.205	0.298	0.167	0.308	0.447			
Long-term Wind stress 0hrs C	0.081	1.50	0.124	0.208	0.298	0.620	1.040	1.490	0.626	0.063	0.038
Short-term Vibration stress 0hrs A	0.137	3.75	0.086	0.142	0.213	0.172	0.284	0.426			
Short-term Vibration stress 0hrs B	0.178	7.50	0.110	0.181	0.262	0.110	0.181	0.262			
Short-term Vibration stress 0hrs C	0.160	6.25	0.067	0.119	0.182	0.080	0.143	0.218	0.209	0.021	0.008
Long-term Vibration stress 0hrs A	0.114	2.50	0.046	0.079	0.114	0.138	0.237	0.342			
Long-term Vibration stress 0hrs B	0.083	1.50	0.037	0.054	0.077	0.185	0.270	0.385			
Long-term Vibration stress 0hrs C	0.134	3.75	0.295	0.491	0.663	0.590	0.982	1.326	0.495	0.050	0.041

Sample	Bradford A595nm	Protein Concentration µg	Guaiacol 1min	(A470nm) 2min	3min	Guaiacol 1min Corrected	Guaiacol 2min Corrected	Guaiacol 3min Corrected	Treatment Average	Per mg	SD/mg
Control 24hrs A	0.120	3.75	0.094	0.165	0.223	0.188	0.330	0.446			
Control 24hrs B	0.134	3.75	0.149	0.230	0.309	0.298	0.460	0.618			
Control 24hrs C	0.137	3.75	0.086	0.144	0.198	0.172	0.288	0.396	0.355	0.036	0.009
Short-term Wind stress 24hrs A	0.158	5.00	0.259	0.409	0.564	0.389	0.614	0.846			
Short-term Wind stress 24hrs B	0.174	7.50	0.428	0.688	0.951	0.428	0.688	0.951			
Short-term Wind stress 24hrs C	0.161	6.25	0.707	1.080	1.450	0.848	1.296	1.740	0.867	0.087	0.037
Long-term Wind stress 24hrs A	0.117	2.50	0.455	0.698	0.879	1.365	2.094	2.637			
Long-term Wind stress 24hrs B	0.108	2.50	1.300	1.770	2.000	3.900	5.310	6.000			
Long-term Wind stress 24hrs C	0.127	3.75	0.242	0.360	0.447	0.484	0.720	0.894	2.600	0.260	0.224
Short-term Vibration stress 24hrs A	0.140	5.00	0.160	0.247	0.342	0.240	0.371	0.513			
Short-term Vibration stress 24hrs B	0.116	2.50	0.094	0.172	0.249	0.282	0.516	0.747			
Short-term Vibration stress 24hrs C	0.171	7.50	0.200	0.325	0.455	0.200	0.325	0.455	0.405	0.041	0.010
Long-term Vibration stress 24hrs A	0.142	5.00	0.241	0.388	0.545	0.362	0.582	0.818			
Long-term Vibration stress 24hrs B	0.066	1.00	0.025	0.045	0.074	0.188	0.338	0.555			
Long-term Vibration stress 24hrs C	0.120	3.75	0.192	0.289	0.448	0.384	0.578	0.896	0.522	0.052	0.014
Control 48hrs A	0.127	3.75	0.179	0.294	0.408	0.358	0.588	0.816			
Control 48hrs B	0.156	5.00	0.152	0.251	0.352	0.228	0.377	0.528			
Control 48hrs C	0.141	5.00	0.156	0.273	0.364	0.234	0.410	0.546	0.454	0.045	0.012
Short-term Wind stress 48hrs A	0.145	5.00	0.220	0.362	0.499	0.330	0.543	0.749			
Short-term Wind stress 48hrs B	0.156	5.00	0.329	0.488	0.669	0.494	0.732	1.004			
Short-term Wind stress 48hrs C	0.174	7.50	0.179	0.282	0.389	0.179	0.282	0.389	0.522	0.052	0.023
Long-term Wind stress 48hrs A	0.089	1.50	0.082	0.128	0.170	0.410	0.640	0.850			
Long-term Wind stress 48hrs B	0.142	5.00	0.563	0.748	0.945	0.845	1.122	1.418			
Long-term Wind stress 48hrs C	0.091	2.50	0.278	0.365	0.482	0.834	1.095	1.446	0.962	0.096	0.028
Short-term Vibration stress 48hrs A	0.126	3.75	0.093	0.148	0.205	0.186	0.296	0.410			
Short-term Vibration stress 48hrs B	0.130	3.75	0.088	0.147	0.213	0.176	0.294	0.426			
Short-term Vibration stress 48hrs C	0.166	6.25	0.218	0.342	0.422	0.262	0.410	0.506	0.330	0.033	0.005
Long-term Vibration stress 48hrs A	0.104	2.50	0.048	0.075	0.101	0.144	0.225	0.303			
Long-term Vibration stress 48hrs B	0.110	2.50	0.125	0.207	0.286	0.375	0.621	0.858			
Long-term Vibration stress 48hrs C	0.124	3.75	0.080	0.127	0.171	0.160	0.254	0.342	0.365	0.036	0.022

A2. Data from the syringaldazine assay for the detection of soluble peroxidase activity

Table A3: Syringaldazine assay data for *Arabidopsis* seedlings subjected to vibration stress.

Sample	Bradford 595nm	Protein Concentration µg	Syringaldazine (A530nm)			SYR 1min Corrected	SYR 2min Corrected	SYR 3min Corrected	Treatment Average	Per mg	SD/mg
			1min	2min	3min						
Control 0hrs A	0.058	2.50	0.070	0.105	0.124	0.210	0.315	0.372			
Control 0hrs B	0.118	3.75	0.125	0.158	0.165	0.250	0.316	0.330	0.299	1.494	0.000
Vibration 0hrs A	0.105	2.50	0.079	0.115	0.129	0.237	0.345	0.387			
Vibration 0hrs B	0.120	3.75	0.119	0.147	0.154	0.238	0.294	0.308	0.302	1.508	0.030
Control 14-day A	0.156	6.25	0.171	0.177	0.177	0.205	0.212	0.212			
Control 14-day B	0.129	3.75	0.035	0.074	0.081	0.070	0.148	0.162	0.168	0.842	0.059
Vibration 14-day A	0.143	5.00	0.170	0.176	0.176	0.255	0.264	0.264			
Vibration 14-day B	0.107	2.50	0.154	0.159	0.159	0.462	0.477	0.477	0.367	1.833	0.149

Table A4: Syringaldazine assay data for *Arabidopsis* plants subjected to wind and mechanical stresses

Sample	Bradford 595nm	Protein Concentration µg	Syringaldazine (A530nm)			SYR 1min Corrected	SYR 2 min Corrected	SYR 3 min Corrected	Treatment Average	Per mg	SD/mg
			1min	2min	3min						
Control 24hrs A	0.120	3.75	0.006	0.006	0.006	0.012	0.012	0.012			
Control 24hrs B	0.134	3.75	0.008	0.008	0.008	0.016	0.016	0.016			
Control 24hrs C	0.137	3.75	0.003	0.003	0.003	0.006	0.006	0.006	0.011	0.001	0.001
Short-term Wind stress 24hrs A	0.158	5.00	0.006	0.007	0.010	0.009	0.011	0.015			
Short-term Wind stress 24hrs B	0.174	7.50	0.003	0.003	0.003	0.003	0.003	0.003			
Short-term Wind stress 24hrs C	0.161	6.25	0.003	0.003	0.003	0.004	0.004	0.004	0.006	0.001	0.000
Long-term Wind stress 24hrs A	0.117	2.50	0.054	0.074	0.090	0.162	0.222	0.270			
Long-term Wind stress 24hrs B	0.108	2.50	0.135	0.170	0.179	0.405	0.510	0.537			
Long-term Wind stress 24hrs C	0.127	3.75	0.019	0.019	0.019	0.038	0.038	0.038	0.247	0.025	0.022
Short-term Vibration stress 24hrs A	0.140	5.00	0.005	0.005	0.005	0.008	0.008	0.008			
Short-term Vibration stress 24hrs B	0.116	2.50	0.008	0.008	0.008	0.024	0.024	0.024			
Short-term Vibration stress 24hrs C	0.171	7.50	0.001	0.001	0.001	0.001	0.001	0.001	0.011	0.001	0.001
Long-term Vibration stress 24hrs A	0.142	5.00	0.009	0.010	0.010	0.014	0.015	0.015			
Long-term Vibration stress 24hrs B	0.066	1.00	0.012	0.013	0.013	0.090	0.098	0.098			
Long-term Vibration stress 24hrs C	0.120	3.75	0.012	0.012	0.014	0.024	0.024	0.028	0.045	0.004	0.004

Appendix B

Characterization of the gene sequences for each candidate wind/mechanical stress gene

In the following figures, the gene sequences of each of the candidate wind/mechanical stress genes are detailed. The genomic DNA sequence is shown rather than the cDNA sequence to highlight the fact that most of the PCR primer sets were designed spanning an intron (with exception to AGP3). The primers highlighted were used for the initial gene expression analysis (Chapters 5 and 6) by RT-PCR.

5'-

ATGGCGGATAAGCTCACTGACGATCAGATTACAGAATACAGGGAATCTTTTCAGGTTATTTCGACAAGAA
TGGTGATGGT**ATGGTTCATCAACTCTTTCCATTTAATCGTAATGTTGGATCATGATCATCTTCAAAGCA**
ATGAAATGACTAACACAAGTCCTTGATTACTTTTTGTAGGGTTCATTACGAAAAAGGAGCTCGGTACCA
TGATGCGTTCAATCGGTGAAAAACCGACAAAAGCTGATCTTCAGGACTTGATGAACGAAGCGGATTAG
ATGGTGATGGAACCATCGATTTCCCTGAGTTCTTGTGCGTAATGGCTAAGAATCAAGGTCATGATCAAG
CGCCGCGTCACACTAAAAAAACAATGGCGGATAAGCTCACTGACGATCAGATTACAGAGTACAGGGAAT
CTTTTCAGGTTATTTCGACAAGAATGGTGATGGT**ATGGTTCATCAACTCTTTCCATTTAATCGTAATGTTG**
GATCATGATCATCTTCAAAGCAATGAAATGACTAACACTAGTCCTTGATTACTTTTTGTAGGGTTCATT
ACGAAAAAGGAGCTCCGTACCGTGATGTTTTCCCTCGGTAAAAACCGGACAAAAGCTGATCTTCAGGAC
ATGATGAACGAAGTGGATTTAGATGGTGATGGAA**CCATCGATTTCCTGAGTTCTTGTACCTAATGGCT**
AAGAATCAAGGTCATGATCAAGCGCCGCGTCACACTAAAAAAACAATGGTGGATTATCAGCTCACTGAC
GATCAGATCTTAGAATTCAGGGAAGCCTTCCGCGTATTTCGACAAGAATGGTGATGGTATGGTTCATCGT
CCCTTTCTCGCTAATCGTACATATTGGATCCTGATCATCTTCAAAGCACTGAAATGACTAACATAAGTC
ATTGCTTACTTTTTGTAGGGTTACATTACCGTGAATGAGCTCCGTACTACTATGCGCTCCCTTGGTGAAA
CCAAACAAAAGCTTGAGCTCCAGGACATGATCAACGAAGCGGATGCAGATGGTGACGGAACCATCAGTT
TCTCTGAGTTTGTGTGTGTAATGACTGGTAAATGATTGACACTCAGTCTAAGAAAGAAACGTACAGAG
TTGTGAATCAAGGTCAGGGTCAAGTGCAGCGTCACACTAGAAATGACAGAGCTGGTGGCACCAATTGGG
AGAGGGACATAGCGGTGCGGGTTGCCAGCAATATCATCGCTTCGCCAATTTCCGACTTCATGAAAGATA
GGTTTAAAGATTTGTTTGAAGCGCTGTTATCTTGAAATGACACGTCAGTAACTTTATGCCAATAGGGTC
TGACAATTATGTTAGATCTCTCTCAAAGCGCTTTCATCTAATGACAATAATTTCTATGTAATAAATTT
ATTGCATGTGTTAGTGTGTACCATCTTCAGTTGTGTGCAATTTATTAAAA**TGA**

-3'

Figure B1: TCH3; calmodulin-related protein At2g41100

The coding sequence is shown in black font, the intron sequences in blue font, and the predicted translation start and stop codons are boxed. The region amplified by RT-PCR is highlighted in grey, and the PCR primers used to amplify it are shown in bold font which is double-underlined.

5'-

ATGCTTGTCGACGGGAAACTCGTCTGCGTCACCGGAGCCGGCGGCTACATTGCTTCTTGGATCGTTA
 AGTTACTCTTAGAGAGAGGCTACACCGTTAGAGGAACCGTAAGGAACCCAACTGATCCCAAGAACAACC
 ATCTCAGAGAGCTTCAAGGAGCCAAGGAAAGACTCACTCTTCACAGTGCAGATCTTCTCGACTACGAAG
 CTCTCTGTGCCACAATCGACGGTTGCGATGGCGTTTTCCACACTGCCTCTCCGATGACCGACGATCCCG
TAAGTAGACAATTCTATTAATCGGTTGAGTGGTATTAGTATAGTACTCATGTTTTCTTAGTTTTCATTT
TCTAAATTAATGTAACATAATTAGGAGACAATGTTGGAGCCGGCGGTGAACGGAGCCAAGTTCGTGATTG
 ACGCAGCGGCTAAAGCCAAGGT**CAAGCGCGTGGTTTTAC**GTTCATCAATTGGTGCAGTTTACATGAACC
CTAACCGTGACACTCAAGCCATTGTTGACGAAAACTGCTGGAGTGATCTTGATTCTGCAAAAACA**CTA**
AGGTATTGTTTTTTTTATCTATGCTATAAGTTTTCGAGATGCGCTGCTAAGTCTTAACAAAGAGTTTT
CTGCAATAAAATCGAGCATGCGGCTAGAATTAGGTTAAATTTCTCTTTGTTTTATCTCCTTATAGAAT
 TGGTATTGCTACGGGAAGATGTTGGCGGAACAATCGGCATGGGAGACGGCCAAAGCAAAAGGTGTGGAC
TTAGTGGTGCTAAATCCGGTTTTGGTTCTCG**GACCACCGCTCCAGTCAG**CGATCAACGCTAGTCTAGTCT
 CATATTCTCAAGTACCTCACCGGCTCAGCCAAGACCTACGCTAACTTGACTCAGGTCTACGTGGACGTC
 CGTGACGTGGCACTAGGCCATGTTCTGGTCTACGAAGCACCTCCGCCTCAGGCCGTTACATCCTCGCC
 GAGACCGCACTTCACCGCGGAGAGGTTGTTGAGATTCTGGCCAAATCTTCCCGGAGTATCCACTTCCC
 ACCAAGT**AAGTCAAGTTTGGCTCTTTTGAACACTTTGGTCAAAAAATATCAAAGTCAACACGATTTAGT**
TTTAGTCGGTCTAATAAATACAACCTTTGGTTTACAACTATTTCAAGTTTTGTTTTGACACACCACAA
AAATTATGACTTGGAGAATTGAACATATCTATTCAAAAAAATTATAAATATTTAGTTAGGATAAAAGG
GACATGAGTGGTATTTGGTATTATTGTGACTCTTGTCCTATGTCCCATATGTTTTAAAAATGAGCACTT
GTGGTTGTGGTGAGATTGGTGTGTACTAACTCTCACATCACAAAGTCCATGTCATCTGTCACCTACTGC
 TGACGTTGAAATCTTACAAGATCTTATAGTACACGTGTTTGGGTCAAATTCATTTGACAAACACGTAC
 GGGGGTGTGAATGTTTTTTCTTCACCTACTCCAATATTTGGTCACTAGTTTCATGACTTGTGTGTCTCC
 TTTAGTTAGTTTAATAATTAAACGTTACTTCAAAGTGATATACAAGAAATCCTTTTCACATTTTCGTAT
TCTGCTGATTAACAAAAGTATTGTTTGTTTTAATGTTACTAGGTGTTTCGGACGAGAAGAATCCGAGGGC
 TAAGCCATACAAGTTTACTACCCAAAAGATAAAAGACTTAGGCTTGAATTTAAACCCATCAAGCAATC
 TCTTTACGAATCTGTCAAGAGCTTGCAAGAGAAAGGCCATCTTCTCTACCTCAAGATTCGAACCAAAA
 CGAAGTCATCATCGAATCT**TAG**

-3'

Figure B2: CCR2; putative cinnamoyl-CoA reductase At1g80820

The coding sequence is shown in black font, the intron sequences in **blue** font, and the predicted translation start and stop codons are **boxed**. The region amplified by RT-PCR is highlighted in **grey**, and the PCR primers used to amplify it are shown in **bold** font which is double-underlined.

5'-

ATG GCGATCACTTACTTGCTTCCTCTGTTTCTTTCTTATCATCACCTCCTCTGTTTCAGCTAATTT
 CCAAAGAGACGTTGAGATCACTTGGGGTGAT **GGTCGTGGACAGATCAAGAACA**ATGGAGAGCTTCTCAC
 TTTATCTCTAGATAAATCCTCTGGTTCTGGATTCCAATCCAAAAACGAGTACTTGTTTGGTAAAGTCTC
 CATGCAAATGAAGCTTGTCCCTGGAAACTCCGCAGGAACAGTCACAACACTTTAC **GTAAGTTCAACAAA**
ACAATCTCTGTTTTCGTTTTTGCATATTATAAAGTTCTTGTATCTGAAATGGTTTTTTGTATATGAACA
GTTGAAATCACCTGGAACAACATGGGACGAGATAGATTTTCGAGTTTTTAGGGGAATTCAGTGGAGAACC
TTACACACTTCACACAAATGTCTACACAAGGCAAAGGAGACAAAAGAACAACAATTCAAACTCTGGTT
 TGATCCAACAGCTAATTTCCACACTTACACTATTCTCTGGAACCCACAAAGAATCATTTTCACCGTCGA
 TGGAACCTCCGATCAGAGAATTCAAGAACATGGAGTCTCTAGGCACTCTGTTTCCCAAGAACAACCAAT
 GAGAATGTACTCGAGTCTTTGGAACGCTGATGATTGGGCAACGAGAGGTGGTTTGGTCAAAACCGATTG
 GTCTAAAGCTCCTTTCACTGCTTCTTACCGTGGCTTTCAACAAGAAGCTTGTGTTTGGTCAAAACGGCAA
 GTCTTCTTGTCTAATGCCTCGAAACAGGGGACTACTACTGGCTCGTGGTTGTCACAAGAGCTTGACTC
 AACAGCTCAACAAAGGATGAGATGGGTGCAGAGGAATACTACATGATCTATAATTATTGTACGGATGCGAA
 GAGGTTCCCTCAAGGTCTTCCTAAAGAGTGCTTAGCTGCA **TAG**

3'

Figure B3: TCH4; Xyloglucan endotransglycosylase At5g57560

The coding sequence is shown in black font, the intron sequences in blue font, and the predicted translation start and stop codons are boxed. The region amplified by RT-PCR is highlighted in grey, and the PCR primers used to amplify it are shown in bold font which is double-underlined.

[ATG]GAATCCGAAGGAGAAACCGCGGTATGCTTTTTTACTCTTGCTTCATCATTATACTTACCTTTAT
 GAGATCTGATTTCAAATTTTCTGTTGAGGTTTCTAATTTTGGCTTCATTGATTCGACTTGATTTGTAGG
 GAAAGCCGATGAAGAACATTGTTCCGCAGACTTGCCAGATCTGTAGTGACAATGTTGGCAAGACTGTTG
 ATGGAGATCGTTTTGTGGCTTGTGATATTTGTTTCATTCCCAGTTTGTTCGGCCTTGCTACGAGTATGAGA
 GGAAAGATGGGAATCAATCTTGTCTCAGTGCAAAACCAGATACAAGAGGCTCAAAGGTCTCTTTTGA
 TCCTTCTGAAGTATACTGTCTTCATTGTTTCATCGATAGTTTATCAGTATGTTTTGAATTTTGGATCAGA
 TTGGTATTTATAGCAATTTGCTAATTTCTGATTCTAGGTAGTCCTGCTATTCTGCTGATAAAGACGAG
 GATGGCTTAGCTGATGAAGGTACTGTTGAGTTCAACTACCTCAGAAGGAGAAAATTTAGAGCGGATG
 CTTGGTTGGCATCTTACTCGTGGGAAGGGAGGAAAATGGGGGAACCCAGTATGATAAAGAGGTCTCT
 CACAATCATCTTCTCGTCTCACGAGCAGACAAGATGTAAGGCATTGCTGTTTCATTCTTCCCTCTTAAG
 CATTTCGCATCCTCACGCAATTTAGTTTTGGAATCTGATTTTGTCAATTTGCTTATTTACAGACTTCAGGA
 GAGTTTTCTGCTGCCTCACCTGAACGCCTCTCTGTATCTTCTACTATCGCTGGGGGAAAGCGCCTTCCC
 TATTCATCAGATGTCAATCAATCACGTAAATATCCTTTATTTCTAACTCTCTCGCCAACACATATATTT
 GTACCTAGGCTTCTCTTTTATGTCAAACCTCTAAACAATAAAATCTGTTGTTGTCAATTCACGCTGCAGC
 AAATAGAAGGATTGTGGATCCTGTTGGACTCGGGAATGTAGCTTGGAAAGGAGAGAGTTGATGGCTGGAA
 AATGAAGCAAGAGAAGAATACTGGTCTGTGACGACGAGGCTGCTTCTGAAAGAGGTGGAGTAGATAT
 TGATGCCAGCACAGATATCCTAGCAGATGAGGCTCTGCTGTGAGTTCTTGTGTTTGTAAATCTTGTGTTGTT
 CTGTCGTGGTGTACCGAGCGTTTTTCTTATTAAGCAATGTCCTGATACTCATTTTCCAATCTTTATTT
 ATTTGTACAGGAATGACGAAGCGAGGCGAGCCTCTGTCAAGGAAAGTTTCAATTCCTTCATCACGGATCAA
 TCCTTACAGAATGGTTATTATGCTGCGGCTTGTATCCTTTGTCTCTTCTTGCATTACCGTATAACAAA
 CCCAGTGCCAAATGCCTTTGCTCTATGGCTGGTCTCTGTGATATGTGAGATCTGGTTTGCTTATCCTG
 GATTTTGGATCAGTTTCCCAAGTGGTTTCTGTGAACCGTGAAACCTACCTCGACAGGCTTGCTTTAAG
 GTAAGTTCTATTTCCCATTTCTTCTGAAGCAATTACTCAAAGGATTGTTTGCTTATACTGTTTCCCATTT
 TTAATTTGATCAGTTGTCATTTTGGGACAGATATGATCGTGAAGGTGAGCCATCACAGTTAGCTGCTG
 TTGACATTTTCTGAGTACTGTTGACCCCTTGAAGGAGCCACCCCTTGTGACAGCCAACACAGTGCTCT
 CTATTCTGGCTGTTGACTACCCAGTTGACAAGGTGCTGCTGTTATGTTTCTGATGATGGTGCTGCTATGT
 TATCATTTGAATCACTTGCAGAAACATCAGAGTTTGTCTGTAATGGGTACCATTTTGAAGAAATATA
 GCATAGAGCCTCGTGACCAAGAATGGTACTTTGCTGCGAAAATAGATTACTTGAAGGATAAAGTTTCAGA
 CATCATTTGTCAAAGATCGTAGAGCTATGAAGGTAAGTTTGTAGTTTTAGTCATCTAGTCACCCCTCACT
 TTGATTTTGTAGTGTATGCTATATTGACCTTTTATTTTCTTTCAGAGGGAATATGAGGAATTTAAATCCG
 AATCAATGCACTTGTTTCCAAAGCCCTAAATGTCTGAAGAAGGGTGGGTATGCAAGATGGCACACC
 GTGGCCTGGAAATAATACAAGGGACCATCCAGGAATGATCCAGGTAAAGAAATGGTTTTAACTATGGAA
 TCGAGAATGCTCTCTCTTCTCTCTAGAGTTTCATTATTGAAGTACCATTGCTGAATGCAGGTCTTCT
 TAGGGCAAATGGTGGACTTGATGCAGAGGGCAATGAGCTCCCGCGTTTGGTATATGTTTCTCGAGAAA
 AGCGACCAGGATTCCAGCACCACAAAAGGCTGGTGCTATGAATGCACTGGTAAGTTTCTGATCTTGGAA
 TTTTTGACTTCTTTCATTCTGACCAATTTGTTAGTCTAATCTGGGTACTTTTCAAATGAATAGGTGAGAG
 TTTTCAGCAGTTCTTACCAATGGACCTTTCATCTTGAATCTTGATTGTGATCATTACATAAAATAACAGCA
 AAGCCTTAAGAGAAGCAATGTGCTTCTGATGGACCCAAACCTCGGGAAGCAAGTTTGTATGTTTCAGT
 TCCACAAAGATTTGATGGTATCGATAAGAACGATAGATATGCTAATCGTAATACCGTGTTCTTTGATG
 TAAGTCACACTTACCTATACTTGGCTCTAATTTCTTGTCTTTCAAATGCTTTTAGACACGAATATA
 CATTAAACTCAGAGTTTCTTGAAGTTTGTGCTAATTTTCCATGATATGTTTCCAGATTAACTTGAGAG
 GTTTAGATGGGATTCAAGGACCTGTATATGTGCGAATGAGTGTGTTTCAACAGAACAGCATTATACG
 GTTATGAACCTCCAATAAAAGTAAACACAAAGCAAGCTCTTTATCTAAGCTCTGTGGTGGATCAA
 GAAAGAAGAATTCCAAGCTAAGAAAGAGTGGCAAAAAGAAATCAGGCAGGCATACTGACTCAACTG
 TTCCTGTATTCAACCTCGATGACATAGAAGAGGGAGTTGAAGGTACAACCTGTTTTTATTTCTTCTTTGG
 TTTCCGTTATACCCATATGTTGCTGTTTGAATATTGATCCAGGGGAGGGGATTATTTATAGTTGACAG
 TTGTCTAAATAGTTTCCATACTAGGTATCTCATCATGTCTTAACTATTTGGCATTTGTGAAACCTTAGGT
 GCTGGTTTTGATGATGAAAAGGCGCTCTTAATGTGCAAAATGAGCCTGGAGAAAGCGATTTGGACAGTCT
 GCTGTTTTTGTGTTCTTACCTTAATGGAAAATGGTGGTGTCTCTCTTTCAGCAACTCCAGAAAACCTT
 CTCAAAGAGGCTATCCATGTCTTAGTTGTGGTTATGAGGATAAGTCAGATTGGGGAATGGAGGTATAA
 TCTCATTTGAACCTCTACATGAATCTGCATTGTTCTGACATATCCACTTTGGCATTACCTTTGTTTATA
 TTTTCCGCTGTCTTTCTTTCAGATTGGATGGATCTATGGTTCTGTGACAGAAGATATTTCTGACTGGGTTG
 AAAATGCATGCCCGTGGATGGCGATCCATTTACTGCAATGCCAAGCTTCCAGCTTTCAAGGGTTCTGCT
 CCTATCAATCTTTAGATCGTCTGAACCAAGTGCTGAGGTGGGCTTTAGGTTTCAGTTGAGATTCTCTTC
 AGTCGGCATTGTCTATATGGTATGGTTACAATGGGAGGCTAAAAATTTCTTGAGAGGTTTGCGTATGTG
 AACACCACCATCTACCCTATCACCTCCATTCTCTCTCATGTATTTGTACATTTGCCAGCCGTTTGTCTC
 TTCACCAACAGTTTATTATTCTCTCAGTTTTGACACCTCTCTCTGTCTATCTATCTCTATCTCTATCTC
 TATCTCTAGAACAACCTTAATTACGTTCTGTTTAACTGAAACCATGTTGTGTTTGTGCATCTATTTACG
 GTTCCAAATCCTGATCAGCTGGTTCTATTGTTCTCTTTGCGAGATTAGTAACATTGCAAGTATATGGT

TTCTGTCTCTCTTTCTCTCCATTTTCGCCACGGGTATACTAGAAATGAGGTGGAGTGGCGTAGGCATAG
 ACGAATGGTGGAGAAACGAGCAGTTTTGGGTCATTGGTGGAGTATCCGCTCATTTATTCGCTGTGTTTC
 AAGGTATCCTCAAAGTCCTTGCCGGTATTGACACAACTTCACAGTTACCTCAAAAGCTTCAGATGAAG
 ACGGAGACTTTGCTGAGCTCTACTTGTTCAAATGGACAACACTTCTGATTCCGCCAACGACGCTGCTCA
 TTGTAAACTTAGTGGGAGTTGTTGCAGGAGTCTCTTATGCTATCAACAGTGGATACCAATCATGGGGAC
 CACTCTTTGGTAAGTTGTTCTTTGCCTTCTGGGTGATTGTTCACTTGTACCCTTTCCTCAAGGGTTTGA
 TGGGTCGACAGAACCGGACTCCTACCATTGTTGTGGTCTGGTCTGTTCTCTTGGCTTCTATCTTCTCGT
 TGTGTGGGTTAGGATTGATCCCTTCACTAGCCGAGTCACTGGCCCGGACATTCTGGAATGTGGAATCA
 ACTGTTGA

Figure B4: CESA3; cellulose synthase catalytic subunit At5g05170

The coding sequence is shown in black font, the intron sequences in blue font, and the
 predicted translation start and stop codons are boxed. The region amplified by RT-
 PCR is highlighted in grey, and the PCR primers used to amplify it are shown in bold
 font which is double-underlined.

5'-

ATGTTTCTTTCTTATCTTCTTGTGGAGGCTTTTCAGGTGGTTATTGCTACCGTGGTCTCCATAGT
 CTTCTTAGTGTTTCGCGGGTCTAACACTGGTAGGTTTCAGCCACGGCATTAAACCATAACAAACAGCTTTT
 TATTATATTCACTCCGATTCTTGTACCAGCCACGATAGCCACTGCTGTCATAACCACAGGATCAACCAG
 GGGTGGCGCACTCGGAGCGATGGCCGTTGCTCTCATCAGGTGGTTCATTAAAGTGAAATTTTGTAAAACT
 ATAGTCATTTTTGTTTTATGAAAACTTGTTCATTCTCTTTTTTTTTCTCTATTCTATCTTTGATTCT
 TTTACATATTCTAATTCATTTATTTTAAAGAATTAGTGTACCCTGTGTACACTTAATGGTCTTATTAA
 TTCTTTAATGTTTTGTCTTCTAACTTCGTTGTCTATTCCATCACAACCCATGTTTACCTTTTCTTGAAA
 CATCATTAGAAAACTGTCAACGTGATTAATAAGAAGTGGTACAATTTGTTTTTAATACATAAGTAAC
 CTTTGTACGCACTTGTGAGTATATATGTAGACGTAAGATGGGAGCTAAGCCGACTGGCGAAGGAACTTC
 GTCAAGCCCAACCTCTTCTCAAATTCACAGTTTATGGTGGATATGGAGCATTTTGGGAGGAAAGAAATTT
 TTCTGGAACATTTCGGAATAAACCAGGGGGTGGAAATCCGTTTGGAGACATCTCAAATGGCTCGGACC
 AGGGGCCGAGGTGGAGGTGCACCTGGAGGATTAGGAGGGGGCGGAAATCCGTTTGGAAACATCTCAAA
 ATGGTTTCGACACAGGGGCCGAGGTGGAGATGCATCTGCTGCTGGTGGTGCACCTGCCGCTGAAGCTGC
 ACCAGCCGCTGGAGCTGCGCCTGCCGCTGGAGCTGCGCCTGCCGCTGGAGCTGCGCCTGCTGCTGGAGC
 TGCTCCTGCCGCTGGTGGAAGTACACCACCCACATGGTAAAGGAAATAAGTCAAGTTGTTCCAACATGT
 ATATTGTGCATTGATTACATAAGGAAACAAAAGCTTTTTAAAACGTCCTTATGCTCATATGTATTCTCCAA
 GGTCAAAGCTGCTTACACAAGACTATGCTACAATGTTTATTAATTTATAGTATAAATCATATAGCTCGA
 TGAACAAATGGGAACGTATAATGTATAATGTACGGTCGACTCTTAGACCATGTACATTGCACATTTAGT
 CGGCATTGTAGTCTGTAAATCATACTATATCAATTCTTAAGGTTTTTATATACTAAGTAATTGAAAATT
 GAAAATTGTTTTCACTACTTTCAAATTTGTTATCTTTATACCAAAGCACATTGATTATTGAATCTTGA

-3'

Figure B5: GRP6; glycine-rich protein Z11858

The coding sequence is shown in black font, the intron sequences in blue font, and the predicted translation start and stop codons are boxed. The region amplified by RT-PCR is highlighted in grey, and the PCR primers used to amplify it are shown in bold font which is double-underlined.

5'-

ATGACGGCGACTGCGTTTAGGGTCGGCTTGTGGTTGGCCGTTACGGCTTCCTTTCTCTTAACCGCAAC
 AAACGCCAAATCCCCGGCGTTTACAGTGGCGGACCGTGCCAGAATGCACACGCCACTTTCTACGGTGG
 CAGTGACGCCTCCGGCACAATGGG**TATAAATATTC**ACTACCTTACGTCTTACCAAATCCACCATTGTC
GATTTTCATTTCGTACATATACCATGAATTATGATTTCTGACTTCTTCTTTTTTGTGAAGTTCTAACTT
 TTTTGTTCCTCTCTGTTTTTCTTTTTTGGCGCGTGGGGTTTTGCTAGGCGGCGCGTGTGGGTACGGGAAC
 TGTACAGCCAAGGATACGGTGTGAACACGGCGGCGTTGAGCACTGCTTTGTTCAACAACGGATTACAGCT
 GTGGTGCTTGTTTTGGAGATTAAAGTGTACTGATGATCCGAGATGGTGTGT**TCCGGGAAATCCATCTATTC**
TTGTGACGGCGACGAACTTTTGTCCGCCGAATTTTGCTCAGCCGAGTGACGACGGAGGGTGGTGCAATC
 CGCCGCGCGAGCATTTTGTATCTCGCCATGCCTATGTTCTCAAGATCGGTCTATACCGTGCAGGCATTG
TCCCGCTCTCCTATCCGAGGTCTCTCTCTGTTTTTGTGTTTGGTTCGTCGTTTGGTGGTTCGGCTATTAT
 AATTTGGCGAAATCAATAAGAATTTCACTGTTAATAATACGGTGAAGAAATTACACAAAGAACCATATG
 CATTAAATGGATGATTCATGATAGTGACTTTTGCAAATCTAGATTATGTTTAAAGGAGATTAAATATTTG
 AAGGGGAGATAAATGTTTTACGTGTAAACAAATTAGAGGCTTTAGTGTAACAAATAGAGGCTTTA
 GTTTTCGATTATTCGTTATAATATGCTAGAACTACAGAGTTTGAATATAGCACTTTTCATGTCTCATGT
 GAAATTGACGTTTTAAATTTCTTAATCCAATATTCAAAAAAAAAAAAAAAAATCCTTTATAAATCTAAA
 GATTCTTTTTTTAAATAGTATTTTCAATATCTATTTTTTCTTTTAGGTTCTGTTTCTTTAATTA
 ACTTTAAAGATACTTGTACCGACTACCGAACATGTTTTTTGTTTACCTCTAGGCTTGTAGCACTTTT
 AGATAACGGCCTATGTGTTTCAGAGTTCAGAACTGAAACCATCACTCTCGATTATTAGTATTATTTTT
 TGTTTCTTTCTTTCTTTTATACACAATTTAAATACGAATTATTTATATAGTATTCCAATTATCTTTT
 CGGGAAACCAAGCAGGACACATAGACACAGTAACCCAGAGATCCACCTCTCTGTCACTCTCAGTCTC
ACTTGTCTTGTGTTAATAATTGTCTGAATTTCTGTTTCTCTGAAGGGTACCTTCTCGGAAGATAGGA
GGGATAAGATTACAGTAAACGGATTCAGATACTTCAATCTTGTCTGTTAACTAACGTTGCCGGCGCC
GGAGATATTAACGGAGTTAGCGTAAAGGGATCAAAGACAGATTGGGTGAGGATGAGTCGGAACTGGGGA
 CAGAACTGGCAATCCAACGCCGTTCTCATCGCCAATCACTCTCTTTCCGAGTCACCGCCTCTGACCGA
 CGTTCTTCTACCTCATGGAACGTTGCTCCTGCCACGTGGCAGTTTGGTCAGACTTTCTCCGGCAAAAAAC
 TTTTCGAGTCTGAAATC**TGA**

-3'

Figure B6: EXP3; putative expansin At2g37640

The coding sequence is shown in black font, the intron sequences in blue font, and the predicted translation start and stop codons are boxed. The region amplified by RT-PCR is highlighted in grey, and the PCR primers used to amplify it are shown in bold font which is double-underlined.

5'-

TCAGGTTTCTATCTCTCTCGTC AAACACAACGAAAGACATTGAAACTGAGAGA- **ATG**GCTCTTAAGAC
 ATTGCAAGCTCTGATCTTTCTTGGTCTATTTGCCGCTCATGTCTAGCTCAAGCTCCGGCTCCGGCACC
 TATCACGTTTCTCCCTCCGGTAGAGTCTCCTTCTCCAGTTGTTACACCAACTGCAGAACCACCGGCTCC
 CGTTGCTTCACCCCTATTCCAGCCAACGAACCCACTCCGGTTCCAACAACCTCCACCAACCGTCTCACC
 CCCGACCACGTGCCCCACAACCTCCCTGTCGCTTCTCCTCC**TAA** ACCATATGCTTTGGCTCCAGGCC
 CATCAGCTCAACACCAGCTCCGGCCCCGGTCCCTAGAGCAGACCGGCCGGTAGCTGACTCAGCATTGA
 CTAACAAAGCTTTCTTCTTAGCAGACATCATGCGCGAGCCTTCTACGCCGTTTTCGGCTTAAAGAGTGG
 CTTCCGTATTACTCTATGATTCTCTCTCTCACTCTCCTTTGTTTTCTTATCATGATTGGTTTGAG
 AGATCTCTGTGTTTTCCCTAATAACATTCGTCTCTCTTCTTGTGTTGTTCTTTTGGGATCTTTTGA
TATTTGTATAAGTTTGATTGGACCATGGCATTAACCT **CAGGGAAGAAGTTCTGATTGTA** ATTTTCTTC
 ATTATTTTTTTAATTAATAAAGTCTTGTTTAAT

3'

Figure B7: AGP3; arabinogalactan protein At4g40090

The coding sequence is shown in black font and the predicted translation start and stop codons are **boxed**. AGP3 does not contain intron sequences. The region amplified by RT-PCR is highlighted in **grey**, and the PCR primers used to amplify it are shown in **bold** font which is double-underlined.

5'-

ATGGAGATTAACGGGGCACACAAGAGCAACGGAGGAGGAGTGGACGCTATGTTATGCGGCGGAGACAT
CAAGACAAAGAACATGGTGATCAACGCGGAGGATCCTCTCAACTGGGGAGCTGCAGCGGAGCAAAATGAA
AGGTAGCCATTTGGATGAAGTGAAGAGAATGGTTGCTGAGTTTAGGAAGCCAGTTGTGAATCTTGGTGG
TGAGACTCTGACCATTGGACAAGTGGCTGCGATCTCAACTATTGGTAACAGTGTGAAGGTGGAGCTATC
GGAGACAG**CTAGAGCCGGTGTGAATGCTA**GTAGTGATTGGGTTATGGAGAGTATGAACAAAGGCACCTGA
TAGTTATGGTGTTACTACTGGTTTTGGTGCTACTTCTCATCGGAGAACCAAAAACGGTGTCCGACCTTCA
GAAGGAACCTATTAG**GTATTAATCATATCTTTTGTCTCTAATCAGAAACAATTA**AACTTTTAAAT
GTTAGTATATCTTAGGTAGAATACGTGGCTGTTATTAGTTGGATGCAGTATACATATGGAATAGGAA
AAAATGTACGGAGTTAGTTTGTTTAATATTTTCCCTTTCTAGATTTTTTCTCTAATTTGTGATTTTTT
CTTTATCATCCAATTAATGAATTTTCAAAATTAATTTCAAAAAAAATTACATGGTAAAAAA
CAATGAATTTTAAAGTTATTAAAATCACGGAAACAATTTCTATAAAAGTTATGACGTTGCATGGGAAAT
ATACGGGTTCCGGTCAATTTAAGTGGATCGGGTCATATTTTCTTGAGTAATTAAAAGTTAATGATTTAA
TTTAATGAAAAATTAATAACTAATCAACACGAAATTTGAATGTTTTTGTTCGTTACAGATTCTCTTAAC
GCCGGAATATTTCGAAGCACGAAAGAAACAAGCCACACATTGCCACACTCCGCCACAAGAGCCGCCATG
CTTGACGAATCAACACTCT**CTCCAAGGATTTTCCGGTATC**CGATTGAGATTCTCGAAGCAATTACC
AGTTTTCTCAACAACAACATCACTCCATCTCTCCCCCTCCGTGGTACAATCACCGCCTCCGGAGATCTC
GTTCTCTCTCCTACATCGCCGACTTCTCACCGGTCTGCCAATTCCAAAGCTACTGGTCCCAACGGT
GAAGCTTTAACAGCAGAGGAAGCTTTCAAATTAGCAGGAATCAGCTCCGGATTCTTTGATCTCCAGCCT
AAGGAAGGTCTCGCGCTAGTCAATGGCACGGCGGTTGGATCTGGAATGGCGTCAATGGTGTATTTCGAA
ACGAATGTTCTCTCTGTTTTGGCTGAGATTTGTCGGCGGTTTTTCGCAGAGGTGATGAGTGGTAAGCCT
GAGTTCACCGATCATCTCACTCACAGACTTAAACATCATCCCGGTCAAATCGAAGCGGCGCGATAATG
GAGCATATCCTCGACGGAAGCTCGTACATGAAATTAGCTCAGAAGCTTCACGAGATGGATCCGTTACAG
AAACCTAAACAAGATCGTTACGCTCTTCGTACTTCTCCTCAATGGTTAGGTCCCTCAAATCGAAGTGATC
CGTTACGCAACGAAATCGATCGAGCGTGAGATTAACCTCCGTCAACGATAATCCGTTGATCGATGTTTCG
AGGAACAAGGCGATTACGGTGGTAACTTCCAAGGAACACCAATCGGAGTTTCAATGGATAACACGAGA
TTGGCGATAGCAGCGATTGGTAAACTCATGTTTGCTCAATTTCTCAGAGCTTGTGAATGATTTCTACAAC
AATGGTTTACCCTCGAATCTAACCGCTTCGAGGAATCCAAGTTTGGATTATGGATTCAAGGGAGCTGAG
ATTGCAATGGCTTCTTATTGTTTCAGAGCTTCAATACTTAGCTAATCCTGTGACTAGCCATGTTCAATCA
GCAGAGCAACATAACCAAGATGTCAACTCTTTGGGACTAATCTCGTCTCGCAAAACCTTGAAGCTGTT
GATATTCTCAAGCTTATGTCAACAACGTTCCCTCGTTGCGATTGTTCAAGCTGTGGATTTGAGACA'TTG
GAGGAGAATTTGAGACAGACTGTGAAGAACACTGTCTCTCAAGTGGCGAAGAAAGTTCTTACTACTGGA
GTCAATGGTGAGCTTCATCCTTCTCGCTTCTGCGAAAAGGATTTACTCAAAGTTGTAGACCGTGAACAA
GTCTACACATACGCGGATGATCCTTGTAGCGCAACGTACCCGTTGATTTCAGAAGCTGAGACAAGTTATT
GTTGACCATGCTTTGATCAATGGTGAGAGTGAGAAGAATGCAGTGACTTCAATCTTCCATAAGATTGGA
GCTTTTCGAGGAGGAGCTTAAGGCAGTGCTACCGAAAAGAGTGGAAAGCAGCAAGAGCAGCCTACGATAAC
GGAACATCGGCTATCCCGAACAGGATCAAGGAATGTAGGTCTGATCCATTGTATAGATTCTGTGAGGGAA
GAGCTTGGAAACAGAGCTTTTGACCGGAGAGAAAGTGACGTGCGCTGGAGAAGAGTTTCGACAAGGTTTTTC
ACGGCGATTTGTGAAGGTAAAAATCATTGATCCGATGATGGAATGTCTCAACGAGTGGAAACGGAGCTCCC
ATTCCAATATGTTAAGAGTATAGTCTCTGTTTTTTTCTTACCATAAAGTCTTTTTTTTTTTTACATGTC
TGAATAATTTTACCAAATGATTGTCTGTGAAGTGGTTTTATGTCTGTCTAATTTAAATTTGTGTGTAA
ACTCATTGTAAGTTCTCAAATGAACAATTTTCTTTTACAAATTAATGTGTGAATCATACCTTCTTCTT
TTTATCTCAATATCCA

-3'

Figure B8: PAL1; phenylalanine ammonia lyase At2g37040

The coding sequence is shown in black font, the intron sequences in blue font, and the predicted translation start and stop codons are boxed. The region amplified by RT-PCR is highlighted in grey, and the PCR primers used to amplify it are shown in bold font which is double-underlined.

5'-

ATG AACAGAGGAAGCTTATGCCCTAATCCCATCTGTCTCCCTCCTCTTGAGCAATCCATCTCCAAATT
 CTTGTAACCTCTCTTTCTCTTTTCTCTGTGTGGATTCTTTTAAATGTCAATATTAGGGCATTATCCAT
 AAATGTTTCTAGTGATTACTCTGTTTTTATTCTTCAGATTTAGATTTATAGTTGGTGATTACTCTGTTT
 TATTCTGCAATCAGAGTTCAGTGTCTCTGTTTCTAGGATTTGTTTTCATACCACAAGTGATTCTACA
 GTCTTTTACTGTGTAATCATTGTTAGGAATTGAAATGTTTGAATGGAGTTTTCTGACATTGAAAATTG
 GATTAGAACACAGAGTGGAACGTTTAAAGATGGAGATCTTCGAGTGAACAAAGATGGAATCCAGACCGT
 GTCTCTGTCCGAACCAGGAGCTGTAAGTTTGTATTATTCATGAGATCTCACTTCCTTTTCGTACATTATGT
 AACTCCATGATTGAATTTGGATGTTTTTGGTTTTTGCAGCCACCTCCTATTGAGCCATTGGACAACCAA
 TTGAGTTTGGCAGATTTAGAAGTGATCAAAGTCATTGGCAAAGGAAGTAGTGTAATGTCCAGTTGGTC
 AAACACAACTCACTCAACAGTTTTTCGCTCTTAAGGTCGTTGATTCAGATTCTTGTGTTACTTCTTT
 TTCTAGTGTCTTTCTCTCTTGGTTCACAAAGATACATGATATTATTTTCAGGTCATTCAATTGAACA
 CAGAAGAATCAACATGTGCGGCGATTTCTCAGGAGCTGAGAATAAACTTGAGCTCGCAATGTCCATATC
 TTGTCTCATGTTATCAATCTTTCTACCACAACGGTCTTGTTTCAATCATATTGGAATTCATGGATGGTG
 GATCCCTTGAGACTTGTTAAAGAAAGTCGGAAGGTTCTGAAAACATGCTATCTGCCATCTGCAAGC
 GAGTACTCTACGCGAAATCTTAAACATCTCTACCGGTTTTCTATTTTTATCTTCTCTAATAAAACACA
 TAATAAGCTCATTCTTCTCTACTAAACGCAGGTTCTTCGAGGTCTTGTATATTTCATCATGAGAGGC
 GAATCATTCATCGGGACTTAAAGCCTTCAAACCTTGCTAATCAATCATAGAGGTGAAGTCAAGATCACAG
 ACTTTGGTGTGAGCAAGATCTTGACAAGCACAAGTAGTCTTGCTAATTCTTTCTGTTGGGCACATACCCTT
 ATATGTCTGTGAGTCTCCTCCATTACCTCTCAACACTCAATATACATACAACTCAATTTTCAGAGTT
 ACAAGTGGTTTTATACGACTTACTGGTGTGTTATCATGTTTTGCAGCCAGAGAGAATCAGCGGGAGTT
 TGTACAGTAACAAGAGCGATATTGGAGCTTGGGACTGGTTTTGCTCGAATGTGCAACGGGTAAATTC
 CGTATACTCCTCCAGAACACAAGAAAGCATGCGAGTACCGTGTACCGAGCTTGTGGACGCCATTGTTGAAA
 ACCCGCCTCCTTGTGCACCTTCCAATCTCTTTCTCCAGAGTTTTGCTCCTTCATCTCGCAATGTTGAG
 ACAGATTTGACACAGTTGTCATGTCATTTTGTGCTATAACGAGTAGGCATTTGAAATGGTGCTTTAA
 CTTGTGTAGTGTACAAAAAGATCCAAGGGACAGAAAATCAGCAAAGGAGCTTCTGGTGCGTTAATCATA
 TAAGACTCTGAGTCTTTCACCTTGTACTGTCTTGACTACTTTTAACGATCTTTTTTCTGGTTCCATCT
 TGGTGAATAAGGAACACAAGTTCGTAAAGATGTTTGAAGATTCGGATACAAATCTCTCGGCTTACTTCAC
 CGACGCAGGATCTTTGATTCCCCCACTTGCTAAC TAG

-3'

Figure B9: MEK1; protein kinase, homologue of MAP kinase kinase AL049483
 The coding sequence is shown in black font, the intron sequences in blue font, and the predicted translation start and stop codons are boxed. The region amplified by RT-PCR is highlighted in grey, and the PCR primers used to amplify it are shown in bold font which is double-underlined.

5'-

ATGGCCTCTTTCCTTGTCTTAGCATTCTCCCTTGCTTTTGTCTCTCAAACCACCGCAAATTACTTCTA
 CTCTTCCCCCTCCACCACCGGTTAAGCACTACTCCCCCTCCTCCGGTTTACAAGTCTCCCCCACCACCGGT
 TAAGCACTACTCCCCCTCCTCCGGTTTACAAGTCTCCCCCACCACCGGTTAAGCATTACTCCCCCTCCTCC
 GGTTTACAAGTCCCCCACCACCACCGAGTTAGATACTACTCCCCCTCCTCCGGTTTACAAGTCCCCCACCACC
 ACCGGTTAAGCACTACTCGCCTCCTCCGGTTTACAAGTCCCCCACCACCACCGAGTTAAATACTACTCCCC
 TCCTCCGGTTTACAAGTCCCCGCCACCACCGGTTAAGCACTACTCGCCTCCTCCGGTTTACAAGTCTCC
 TCCACCACCGAGTTAAGTACTACTCCCCCTCCTCCAGTTTACAAGTCTCCACCACCACCGGTTCACTACTC
 TCCTCCTCCCGTAGTATACCATTTCCCCCACCACCACCGGTTCACTACTCTCCTCCTCCCGTAGTATATCA
 CTCCCCCACCACCACCGGTTCACTACTCTCCTCCTCCAGTCGTATACCACTCTCCACCACCACCGGTTCA
 CTACTCACCTCCTCCAGTCGTATACCACTCTCCACCACCACCGGTTCACTACTCACCTCCTCCAGTTGT
 ATACCACTCCCCCACCACCACCAAGAAGCACTACGAATACAAATCTCCTCCTCCGGTCCATTACTCTCC
 CCCTACGGTATACCATTTCTCCTCCTCCTCCAGTACCACTACTCACCT**CCACACCAACCCCTACCTTTA**
CAAATCACCACCTCCTCCTCACTAC**TAG**ATTACTTAATCGTCTCTAATG**GTAATTATTATTTCTCATA**
CTTTACAATGCTACACTTCAATCAAATCTAGTAACCTATTATTTCTTATGTTAACATATCTCATATATT
TTTGCAGGAGTCGACGACAAATCTCCTCCTCACAAAGAATCGTTTGGTG

-3'

Figure B.10: EXT1; extensin ATU43627

The coding sequence is shown in black font, the intron sequences in blue font, and the predicted translation start and stop codons are boxed. The region amplified by RT-PCR is highlighted in grey, and the PCR primers used to amplify it are shown in bold font which is double-underlined.

Appendix C

Candidate gene fragments amplified for generation of the RNAi constructs

5'-

ACTACTCTCTTAAGCCCTTTTCATAACCTTGTAACCATTAAAGAGGCTTTGCTCAATTACAAGAAGAAGA
 AAAA**ATG**CTTGTCGACGGGAACTCGTCTGCGTCACCGGAGCCGGCGGCTACATTGCTTCTTGGATCG
 TTAAGTTACTCTTAGAGAGAGGCTACACCGTTAGAGGAACCGTAAGGAACCCAACTGATCCCAAGAACA
 ACCATCTCAGAGAGCTTCAAGGAGCCAAGGAAAGACTCACTCTTCACAGTGCAGATCTTCTCGACTACG
 AAGCTCTCTGTGCCACAATCGACGGTTGCGATGGCGTTTTCCACACTGCCTCTCCGATGACCGACGAGA
 CAATGTTGGAGCCGGCGGTGAACGGAGCCAAGTTCGTGATTGACGCAGCGGCTAAAGCCAAGGTCAAGC
 GCGTGGTTTTTCACGTCATCAATTGGTGCAGTTTACATGAACCCTAACCGTGACACTCAAGCCATTGTTG
 ACGAAAACCTGCTGGAGTGATCTTGATTTCTGCAAAAAACAAGAATTGGTATTGCTACGGGAAGATGTTGG
 CGGAACAATCGGCATGGGAGACGGCCAAAGCAAAAAGGTGTGGACTTAGTGGTGCTAAATCCGGTTTTGG
 TTCTCGGACCACCGCTCCAGTCAGCGATCAACGCTAGTCTAGTCCATATTCTCAAGTACCTCACC GGCT
 CAGCCAAGACCTACGCTAACTTGACTCAGGTCTACGTGGACGTCCGTGACGTGGCACTAGGGCATGTTT
 TGGTCTACGAAGCACCTCCGCTCAGGCCGTTACATCCTCGCCGAGACCGCACTTCACCGCGGAGAGG
 TTGTTGAGATTCTGGCCAAATTTCCCGGAGTATCCACTTCCCACCGTGTTCGGACGAGAAGAATCCGA
 GGGCTAAGCCATACAAGTTTACTACCCAAAAGATAAAAGACTTAGGCTTGGAAATTTAAACCCATCAAGC
 AATCTCTTTACGAATCTGTCAAGAGCTTGCAAGAGAAAGGCCATCTTCCTCTACCTCAAGATTGGAACC
 AAAACGAAGTCATCATCGAATCT**TAG**GACACCGATCCACGACCCTAGAAATCTCAACATACCTACATGA
 AAGCTTATTTCTTAAGTAAATACATACGTTTTGATTTTGACTAAAGTATTGTTAAATCTTAAATCATTAT
 ATATAGCTGATTGTTCTTTCTTTCTTTGGTTGTAATTGAGAATATGTTACGCATATGTATTATACGATA
 ATGGAAGCAATGGTTTTATTATCCGATGTT

-3'

Figure C1: Fragment used for generation of an RNAi construct targeting Cinnamoyl CoA reductase 2

CCR2 cDNA sequence (NM_106730) is shown: the fragment used is highlighted in grey, and the PCR primers used to amplify the fragment are presented in **bold font** which is double underlined. The untranslated region is presented in grey font, the coding sequence in black font, and the predicted translation start and stop codons are **boxed**.

5'-

ACAAACCAATCTAACTCAATACAAGAATATCTACAATCTCTAGAAA**ATG**GCGATCACTTACTTGCTTC
 CTCTGTTTCTTTCTCTTATCATCACCTCCTCTGTTTCAGCTAATTTCCAAAGAGACGTTGAGATCACTT
 GGGGTGATGGTCGTGGACAGATCAAGAACAATGGAGAGCTTCTCACTTTATCTCTAGATAAATCCTCTG
 GTTCTGGATTCCAATCCAAAAACGAGTACTTGTGGTAAAGTCTCCATGCAAATGAAGCTTGTCCCTG
 GAAACTCCGCAGGAACAGTCACAACACTTTACTTTGAAATCACCTGGAACAACATGGGACGAGATAGATT
 TCGAGTTTTAGGGAATTCAAGTGGAGAACCTTACACACTTCACACAAATGTCTACACACAAGGCAAAG
 GAGACAAAGAACAACAATTCAAACCTCTGGTTTGATCCAACAGCTAATTTCCACACTTACACTATTCTCT
 GGAACCCACAAAGAATCATTTTCACCGTCGATGGAACTCCGATCAGAGAATTCAAGAACATGGAGTCTC
 TAGGCACTCTGTTTCCCAAGAACAACCAATGAGAATGTACTCGAGTCTTTGGAACGCTGATGATTGGG
 CAACGAGAGGTGGTTTGGTCAAACCGATTGGTCTAAAGCTCCTTTCACTGCTTCTTACCGTGGCTTTC
 AACAAGAAGCTTGTGTTTGGTCAAACGGCAAGTCTTCTTGTCTAATGCCTCGAAACAGGGGACTACTA
 CTGGCTCGTGGTTGTCACAAGAGCTTGACTCAACAGCTCAACAAAGGATGAGATGGGTGCAGAGGAACT
 ACATGATCTATAATTATTGTACGGATGCGAAGAGGTTCCCTCAAGGTCTTCCTAAAGAGTGCTTAGCTG
 CA**TAG**AGAGAG**TAAAGAGTTGAGAGAGGAACAACATTTATTTTCTCTTCTGGTTATATAAATCTATT**
CAATTTATTTCTAGATCACTTCAATTTTATTTGTTTCTTTTGTAGTATCTCTATAGTTCTGTTAAAGCTT
TAAATTTCTCTTTCTTACAATGCTGCTTTTGTGTT

-3'

Figure C2: Fragment used for generation of an RNAi construct targeting Touch gene 4

TCH4 cDNA sequence (AF051338) is shown: the fragment used is highlighted in grey, and the PCR primers used to amplify the fragment are presented in **bold** font which is double underlined. The untranslated region is presented in grey font, the coding sequence in black font, and the predicted translation start and stop codons are **boxed**.

5'-

GTCCCTATCCAATACACATCTCTCTCTCTTTATTAAC**TCAATG**ACGGCGACTGCGTTTAGGGTCGGC
 TTGTGGTTGGCCGTTACGGCTTCCTTTCTCTTAACCGCAACAAACGCCAAAATCCCCGGCGTTTACAGT
 GGCGGACCGTGGCAGAAATGCACACGCCACTTTCTACGGTGGCAGTGACGCCCTCCGGCACAATGGGCGGC
 GCGTGTGGGTACGGGAACCTTGTACAGCCAAGGATACGGTGTGAACACGGCGGCGTTGAGCACTGCTTTG
 TTCAACAACGGATTACAGCTGTGGTGCTTGTTTTGAGATTAAGTGTACTGATGATCCGAGATGGTGTGTT
 CCGGGAATCCATCTATTCTTGTGACGGCGACGAACTTTTGTCCGCCGAATTTTGCTCAGCCGAGTGAC
 GACGGAGGGTGGTGCAATCCGCCGCGGAGCATTTTGATCTCGCCATGCCATATGTTCTCAAGATCGGT
 CTATACCGTGCAGGCATTGTCCCGTCTCCTATCGCAGGGTACCTTGTTCGGAAGATAGGAGGGATAAGA
 TTCACAGTAAACGGATTACAGATACTCAATCTTGTCTGGTAACTAACGTTGCCGGCGCCGGAGATATT
 AACGGAGTTAGCGTAAAGGGATCAAAGACAGATTGGGTGAGGATGAGTCGGAACCTGGGGACAGAACTGG
 CAATCCAACGCCGTTCTCATCGGCCAATCACTCTTTCCGAGTCACCGCCTCTGACCGACGTTCTTCT
 ACCTCATGGAACGTTGCTCCTGCCACGTGGCAGTTTGGTCAGACTTTCTCCGGCAAAAACTTTCGAGTC
TGAAATCTCAAAAACCCACCGAAAAGATGTTTAAATTTATTTTAAATGCAAGGAGACACAAAC
 AACAAGACAGATGACACATTTCCAGCCCTGGTATTCCCTTTAAATTTCTTGGAAATATCCGCTGGC
 TTGTGGAAAATATTTCCTTTTAAATTTATTTACGCAAAATTTCTTTTATCTTTTGCATTTACGAG
 TGATTTGTTTCTCTCTGCTTAATTTGCTTCCTTAAATTTATTTCTTTGGTGGCAATCTTCCTTTCTGCTAAT
 AATCCAAAGACCTGCTGAACACTGCTGATGGAATGAATGGACCGTGTAATGGGCCATTGGGCCAAGTT
 TTCTTGATATAAAATCTGAAATACTACTAAA

-3'

Figure C3: Fragment used for generation of an RNAi construct targeting Expansin 3

EXP3 cDNA sequence (NM_129320) is shown: the fragment used is highlighted in grey, and the PCR primers used to amplify the fragment are presented in **bold font** which is double underlined. The untranslated region is presented in grey font, the coding sequence in black font, and the predicted translation start and stop codons are **boxed**.

5'-

ATGGAATCCGAAGGAGAAACCGCGGGAAAGCCGATGAAGAACATTGTTCCGCAGACTTGCCAGATCTG
TAGTGACAATGTTGGCAAGACTGTTGATGGAGATCGTTTTGTGGCTTGTGATATTTGTTTCATTCCCAGT
TTGTGCGGCCTTGCTACGAGTATGAGAGGAAAGATGGGAATCAATCTTGTCCTCAGTGCAAAACCAGATA
CAAGAGGCTCAAAGGT**AGTCCTGCTATTTCCTGGTGA**TAAAGACGAGGATGGCTTAGCTGATGAAGGTAC
TGTTGAGTTCAACTACCCCTCAGAAGGAGAAAATTTAGAGCGGATGCTTGGTTGGCATCTTACTCGTGG
GAAGGGAGAGGAAATGGGGGAACCCAGTATGATAAAGAGGTCTCTCA**CAATCATCTTCCTCGTCTCAC**
GAGCAGACAAGATACTTCAGGAGAGTTTTCTGCTGCCTCACCTGAACGCCTCTCTGTATCTTCTACTAT
CGCTGGGGGAAAGCGCCTTCCCTATTTCATCAGATGTCAATCAATCACCAAATAGAAGGATTGTGGATCC
TGTTGGACTCGGAATGTAGCTTGGGAAGGAGAGAGTTGATGGCTGGAAAATGAAGCAAGAGAAGAATAC
TGGTCCTGTGACGACGAGGCTGCTTCTGAAAGAGGTGGAGTAGATATTGATGCCAGCAGATATACCT
AGCAGATGAGGCTCTGCTGAATGACGAAGCGAGGAGCCTCTGTCAAGGAAAGTTCAATTCCTTCATC
ACGGATCAATCCTTACAGAATGGTTATTATGCTGCGGCTTGTTATCCTTTGTCTCTTCTTGCATTACCG
TATAACAAACCCAGTGCCAAATGCCTTTGCTCTATGGCTGGTCTCTGTGATATGTGAGATCTGGTTTTGC
CTTATCCTGGATTTTGGATCAGTTTCCCAAGTGGTTTTCTGTGAACCGTGAAACCTACCTCGACAGGCT
TGCTTTAAGATATGATCGTGAAGGTGAGCCATCACAGTTAGCTGCTGTTGACATTTTCGTGAGTACTGT
TGACCCCTTGAAGGAGCCACCCCTTGTGACAGCCAACACAGTGCTCTCTATTCTGGCTGTTGACTACCC
AGTTGACAAGGTGTCCTGTTATGTTTCTGATGATGGTGCTGCTATGTTATCATTTGAATCACTTGCAGA
AACATCAGAGTTTGTCTGTAATGGGTACCATTTTGAAGAAATATAGCATAGAGCCTCGTGCACCAGA
ATGGTACTTTGCTGCGAAAATAGATTACTTGAAGGATAAAGTTCAGACATCATTTGTCAAAGATCGTAG
AGCTATGAAGAGGGAATATGAGGAATTTAAAATCCGAATCAATGCACTTGTTTTCCAAAGCCCTAAAATG
TCCTGAAGAAGGGTGGGTATGCAAGATGGCACACCGTGGCCTGGAAATAATACAAGGGACCATCCAGG
AATGATCCAGGTCTTCTTAGGGCAAAATGGTGGACTTGATGCAGAGGGCAATGAGCTCCCGCGTTTGGT
ATATGTTTCTCGAGAAAAGCGACCAGGATTCCAGCACCACAAAAGGCTGGTGCTATGAATGCACTGGT
GAGAGTTTTCAGCAGTTCTTACCAATGGACCTTTCATCTTGAATCTTGATTGTGATCATTACATAAATAA
CAGCAAAGCCTTAAGAGAAGCAATGTGCTTCTGATGGACCCAAACCTCGGGAAGCAAGTTTGTATGT
TCAGTTCCACAAAGATTGATGGTATCGATAAGAACGATAGATATGCTAATCGTAATACCGTGTCTCT
TGATATTAACCTTGAGAGGTTTAGATGGGATTCAGGACCTGTATATGTCGGAACCTGGATGTGTTTTCAA
CAGAACAGCATTATACGGTTATGAACCTCCAATAAAGTAAAACACAAGAAGCCAAGCTTTTATCTAA
GCTCTGTGGTGGATCAAGAAAGAAGAATTCCAAAGCTAAGAAAAGAGTCGGACAAAAAGAAATCAGGCAG
GCATACTGACTCAACTGTTCTGTATTCAACCTCGATGACATAGAAGAGGGAGTTGAAGGTGCTGGTTTT
TGATGATGAAAAGGCGCTCTTAATGTGCGAAATGAGCCTGGAGAAGCGATTTGGACAGTCTGCTGTTTT
TGTTGCTTCTACCCTAATGGAAAATGGTGGTGTCTCTCTCAGCAACTCCAGAAAACCTTCTCAAAGA
GGCTATCCATGTCAATTAGTTGTGGTTATGAGGATAAGTCAGATTGGGGAATGGAGATTGGATGGATCTA
TGGTTCTGTGACAGAAGATATTCTGACTGGGTTCAAATGCATGCCCCTGGATGGCGATCCATTTACTG
CATGCCTAAGCTTCCAGCTTTCAAGGGTCTGCTCCTATCAATCTTTCAGATCGTCTGAACCAAGTGCT
GAGGTGGGCTTTAGGTTGAGTTGAGATTCTCTTCAGTCGGCATTGTCTTATATGGTATGGTTACAATGG
GAGGCTAAAATTTCTTGAGAGGTTTGCCTATGTGAACACCACCATCTACCCATCACCTCCATTCCTCT
TCTCATGTATTGTACATTGCCAGCCGTTTGTCTCTTCCCAACCAAGTTTATTATTCTCAGATTAGTAA
CATTGCAAGTATATGGTTTCTGTCTCTCTTCTCTCCATTTTCGCCACGGGTATACTAGAAATGAGGTG
GAGTGGCGTAGGCATAGACGAATGGTGGAGAAACGAGCAGTTTGGGTCATTGGTGGAGTATCCGCTCA
TTTATTTCGCTGTGTTTCAAGGTATCCTCAAAGTCTTGGCGGTATTGACACAACTTCACAGTTACCTC
AAAAGCTTCAGATGAAGACGGAGACTTTGCTGAGCTCTACTTGTTCAAATGGACAACACTTCTGATTCC
GCCAACGACGCTGCTCATTGTAACTTAGTGGGAGTTGTTGCAGGAGTCTCTTATGCTATCAACAGTGG
ATACCAATCATGGGGACCACTCTTGGTAAGTTGTTCTTGGCTTCTGGGTGATTGTTCACTTGTACCC
TTTCTCAAGGGTTTGTGAGGTCGACAGAACCGGACTCTACCATTTGTTGTGGTCTGGTCTGTTCTCT
GGCTTCTATCTTCTCGTTGTTGTGGGTTAGGATTGATCCCTTCACTAGCCGAGTCACTGGCCCGGACAT
TCTGGAATGTGGAATCAACTGT**TGA**

-3'

Figure C4: Fragment used for generation of an RNAi construct targeting Cellulose synthase 3

CESA3 cDNA sequence (AF027174) is shown: the fragment used is highlighted in grey, and the PCR primers used to amplify the fragment are presented in **bold font** which is double underlined. The untranslated region is presented in grey font, the coding sequence in black font, and the predicted translation start and stop codons are boxed.

5'-

ATG CCAGTCGACGTAGCCTCACC GGCCGGAAAAACCGTCTGCGTCACCGGAGCTGGTGGATACATCGC
 TTCTTGGATTGTTAAGATACTTCTCGAGAGAGGTTACACAGTCAAAGGAACCGTACGGAATCCAGATGA
 TCCGAGAACACACATTTGAGAGAACTAGAAGGAGGAAAGGAGAGACTGATTCTGTGCAAAGCAGATCTT
 CAGGACTACGAGGCTCTTAAGGCGGCGATTGATGGTTGCGACGGCGTCTTTCACACGGCTTCTCCTGTC
 ACCGACGATCCGGAACAAATGGTGGAGCCGGCCGTGAATGGAGCCAAGTTTGTGATTAATGCTGCGGCT
 GAGGCCAAGGTCAAGCGCGTGGTCATCACCTCCTCCATTGGTGCCGTCTACATGGACCCGAACCGTGAC
 CCTGAGGCTGTCGTTGACGAAAGTTGTTGGAGTGATCTTGACTTCTGCAAAAACACCAAGAATTGG **TAT**
TGTTACGGCAAGATGGTGGCGGAACAAGCGGCGTGGGAGACAGCAAAGGAGAAAGGTGTTGACTTGGTG
 GTGTTGAATCCGGTGCTGGTTCTTGGACCGCCGTACAGCCGACGATCAACGCCAGTCTTTACCACGTC
 CTCAAATATCTAACC GGCTCGGCTAAGACTTATGCTAATTTGACTCAAGCTTATGTGGATGTTFCGGGAT
 GTCGCGCTGGCTCATGTTCTGGTCTATGAGGCACCTCGGCCTCCGGACGTTATCTCCTAGCCGAGAGT
 GCTCGCCACCGCGGGGAAGTTGTTGAGATTCTGGCTAAGCTATTCCCGGAG **GTATCCTCTTCCGACCAAG**
TGCAAGGACGAGAAGAACCCTAGAGCCAAGCCATACAAATTCAC TAACCAGAAGATTAAGGACTTAGGC
 TTAGAGTTAACTTCCACCAAGCAAAGCTTCTACGACACAGTCAAGAGCTTACAAGAGAAAGGCCATCTT
 GCTCCTCCTCCTCCTCCTCCTT CAGCATCGCAAGAATCCGTGGAAAATGGCATTAAAGATCGGGTCT **TG**
AAAAGCTTATTAAATCCCTCAAGTATCCCCCTTAAGTATCCTTAACCATTTGAAGTTGCTTTTGTGTTGT
 TGTCTCTGGTTATGTGAAACCTCTGTTC AATATGTCICGTCTGGTTATGAACTGTGTACACTCAGTTCT
 TTGGCCAAACCGTTTGATGGATTTTGTAGTCAAGTCTTCATGTTTGATCCTATGTAAATAGATTACACTT
 AAGTAAAAAAACAAAAA AAAAAAAAAAAAAA

-3'

Figure C5: Fragment used for generation of an RNAi construct targeting the Cinnamyl CoA reductase family

CCR1 cDNA sequence (AF320624) is shown: the fragment used is highlighted in grey, and the PCR primers used to amplify the fragment are presented in **bold** font which is double underlined. The untranslated region is presented in grey font, the coding sequence in black font, and the predicted translation start and stop codons are boxed.

Appendix D

Efficient siRNAs predicted by siRNA Scan for the final RNAi constructs

As outlined in Chapter 7, the siRNA Scan tool (Xu *et al*, 2006) was used to optimize the design of the RNAi constructs. The efficient siRNAs predicted for each construct by this tool are detailed in the following figures and tables.

ACACGATCCACGACCCTAGAATCTGATCATACCTACATGAAAAGCTTTATTCTTAAGTAATACATACGTTT
UGUCUAGGUGCUGGGAUCUUAGACUAGUAUGGAUGUACUUUCGAAAUAAGAAUUCAUUAUGUAUGCAAA
 * ** * * * *
 TGATTTTGACTAAAGTATTGTT
 ACUAAAACUGAUUUCAUAAACA

Figure D1: Efficient siRNAs predicted by siRNA Scan for the CCR2 construct. The gene specific sequence is in **bold** font, the mRNA sequence in plain font, and predicted efficient siRNAs are in **red** font. The efficient siRNAs (21 bp) are sometimes overlapping; a red asterisk* indicates the base at which the siRNA begins.

Table D1: List of efficient siRNAs predicted by siRNA Scan for the CCR2 construct

Number	Query sequence	siRNA sequence
1	2-22	GUGCUAGGUGCUGGGAUCUUA
2	6-26	UAGGUGCUGGGAUCUUAGACU
3	7-27	AGGUGCUGGGAUCUUAGACUA
4	10-30	UGCUGGGAUCUUAGACUAGUA
5	21-41	UAGACUAGUAUGGAUGUACUU
6	23-43	GACUAGUAUGGAUGUACUUUU
7	26-46	UAGUAUGGAUGUACUUUUCGA

TATTGTTACGGCAAGATGGTGGCGGAACAAGCGGCGTGGGAGACAGCAAAGGAGAAAGGTGTTGACTTGGT
AUAACA AUGCCGUUCUACCACCGCCUUGUUCGCCGCCACCCUCUGUCGUUUCUUCUCCACAACUGAACCA

GGTGTGAATCCGGTGTGTTCTTGGACCGCGTTACAGCCGACGATCAACGCCAGTCTTTACCACGTCC
CCACAACUAGGCCACGACCAAGAACCUGGAGGCAAUGUCGGCUGCUAGUUGCGGUCAGAAAUGGUGCAGG

TCAAATATCTAACCGGCTCGGCTAAGACTTATGCTAATTTGACTCAAGCTTATGTGGATGTTTCGCGATGTC
AGUUUAUAGAUUGGCCGAGCCGAUUCUGAAUACGAUUAACUGAGUUCGAAUACACCUACAAGCGCUACAG

GCGCTGGCTCATGTTCTGGTCTATGAGGCACCCTCGGCCTCCGGACGTTATCTCCTAGCCGAGAGTGCTCG
CGCGACCGAGUACAAGACCAGAUACUCCGUGGGAGCCGGAGGCCUGCAAUAGAGGAUCGGCUCUCACGAGC

CCACCGCGGGGAAGTTGTTGAGATTCTGGCTAAGCTATTCCCGGAGTATCCTCTTCCGACCAAGT
GGUGGCGCCCCUUAACAACUCUAAGACCUAUUCGAUAAGGGCCUCAUAGGAGAAGGCUGGUUUA

Figure D2: Efficient siRNAs predicted by siRNA Scan for the CCRF construct.
The gene specific sequence is in **bold** font, the mRNA sequence in plain font, and predicted efficient siRNAs are in **red** font. The efficient siRNAs (21 bp) are sometimes overlapping; a red asterisk* indicates the base at which the siRNA begins.

Table D2: List of efficient siRNAs predicted by siRNA Scan for the CCRF construct

Number	Fragment	siRNA sequence
1	114-134	CUGCUAGUUGCGGUCAGAAAU
2	128-148	CAGAAAUUGGUGCAGGAGUUUA
3	133-153	AUGGUGCAGGAGUUUAUAGAU
4	134-154	UGGUGCAGGAGUUUAUAGAU
5	153-173	UUGGCCGAGCCGAUUCUGAAU
6	154-174	UGGCCGAGCCGAUUCUGAAUA
7	157-177	CCGAGCCGAUUCUGAAUACGA
8	159-179	GAGCCGAUUCUGAAUACGAU
9	160-180	AGCCGAUUCUGAAUACGAUUA
10	161-181	GCCGAUUCUGAAUACGAUUA
11	162-182	CCGAUUCUGAAUACGAUUA
12	174-194	ACGAUUAACUGAGUUCGAAU
13	219-239	CCGAGUACAAGACCAGAUACU
14	244-264	GGGAGCCGGAGGCCUGCAAUA
15	246-266	GAGCCGGAGGCCUGCAAUAGA
16	282-302	AGCGGUGGCGCCCUUAACA
17	283-303	GCGGUGGCGCCCUUAACAA
18	288-308	GGCGCCCUUAACAACUCUA
19	289-309	GCGCCCUUAACAACUCUAA
20	291-311	GCCCUUAACAACUCUAAGA
21	302-322	AACUCUAAGACCGAUUCGAUA

TAAAGAGTTGAGAGAGGAACAAGATTTTATTTTCTTTGTGGTTATAAAATTCTATTCATTTTATTGTAGA
 AUUU**CUCAACUCUCUCCUUGUUCUAAAAUA**AAAAAGAAACACCAAUAUUUUAAGAUAAAGUAAAAUAACAUCU
 * * *
TCACGTGAATTTTATTGATTTGTTTTGTAGTATACTCTATAGTTCGTTAAAGTTATAATATTCTCTTTGTT
 AGUGCACUAAAAUAACUAAACAAAACAUCAUUAUGAGAUUGAAGCAAUUUCAAUUUUAAGAGAAACAA

ACAATGTGCTT
 UGUUACACGAA

Figure D3: Efficient siRNAs predicted by siRNA Scan for the TCH4 construct.
 The gene specific sequence is in **bold** font, the mRNA sequence in plain font, and
 predicted efficient siRNAs are in **red** font. The efficient siRNAs (21 bp) are
 sometimes overlapping; a red asterisk * indicates the base at which the siRNA begins.

Table D3: List of efficient siRNAs predicted by siRNA Scan for the TCH4 construct

Number	Fragment	siRNA sequence
1	5-25	CUCAACUCUCUCCUUGUUCUA
2	8-28	AACUCUCUCCUUGUUCUAAAA
3	10-30	CUCUCUCCUUGUUCUAAAAUA

AGTCCTGCTATTCTGGTGATAAAGACGAGGATGGCTTAGCTGATGAAGGTACTGTTGAGTTCAACTACCC
 UC**AGGACGAUAAGGACCACUAUUUCU**GCUCCUACCGAAUCGACUACUCCAUGACAACUCAAGUUGAUGGG
 * * * * *
 TCAGAAGGAGAAAATTT**CAGAGCGGATGCTTGGTTGGCATCTTACTCGTGGGAAGGGAGAGGAAATGGGGG**
 AGUCUCCUCUUUUAAAGUCUCGCC**UACGAACCAACCGUAGAAUGAGCACCCUCCCUCCUUUACCCCC**
 * * * * *
 AACCCAGTATGATAAAGAGGTCTCTCACAATCATCTTCCTCGTCTCA
 UUGGGGUCAUACUAAUUCUCCAGAGAGUGUUACUAGAAAGGAGCAGAGU
 *

Figure D4: Efficient siRNAs predicted by siRNA Scan for the CESA3 construct.
 The gene specific sequence is in **bold** font, the mRNA sequence in plain font, and predicted efficient siRNAs are in **red** font. The efficient siRNAs (21 bp) are sometimes overlapping; a red asterisk* indicates the base at which the siRNA begins.

Table D4: List of efficient siRNAs predicted by siRNA Scan for the CESA3 construct

Number	Fragment	siRNA sequence
1	3-23	AGGACGAUAAGGACCACUAUU
2	6-26	ACGAUAAGGACCACUAUUUCU
3	28-48	CUCCUACCGAAUCGACUACUU
4	47-67	UUCCAUGACAACUCAAGUUGA
5	48-68	UCCAUGACAACUCAAGUUGAU
6	67-87	AUGGGAGUCUCCUCUUUUAA
7	68-88	UGGGAGUCUCCUCUUUUAAA
8	97-117	UACGAACCAACCGUAGAAUGA
9	117-137	AGCACCCUCCCUCCUUUA
10	136-156	UACCCCUUGGGGUCAUACUA
11	137-157	ACCCCUUGGGGUCAUACUAU
12	138-158	CCCCUUGGGGUCAUACUAUU
13	139-159	CCCUUGGGGUCAUACUAUUU
14	160-180	CUCCAGAGAGUGUUAGUAGAA

Figure D5: Efficient siRNAs predicted by siRNA Scan for the EXP3 construct. The gene specific sequence is in **bold** font, the mRNA sequence in plain font, and predicted efficient siRNAs are in **red** font. The efficient siRNAs (21 bp) are sometimes overlapping; a red asterisk * indicates the base at which the siRNA begins.

Number	Fragment	siRNA sequence
1	44-64	ACCUUUCUCUGUGUUUGUUCU
2	47-67	UUCUUCUGUGUUUGUUCUUCU
3	61-81	UUCUUCUCUCUACUCUGUAAA
4	85-105	UCGGGACCCAAAAGGGAAAUU
5	86-106	CGGGACCCAAAAGGGAAUUA
6	87-107	GGGACCCAAAAGGGAAAUUAA
7	89-109	GACCCAAAAGGGAAAUUAAAA
8	91-111	CCCAAAGGGAAAUUAAAAGA
9	120-140	AAGGCCACCGAACACCUUUUA
10	121-141	AGGCCACCGAACACCUUUUAU
11	122-142	GGCCACCGAACACCUUUUAUA
12	123-143	GCCACCGAACACCUUUUAUAA
13	186-206	ACGCUAAAUGCUCACUAAACA
14	187-207	CGCUAAAUGCUCACUAAACAA
15	194-214	UGCUCACUAAACAAAAAGAGA
16	247-267	ACCGUAGAAGCAAGACGAUUA
17	248-268	CCGUAGAAGCAAGACGAUUAU
18	298-318	CUCAGCUUACCUGGCACAUUA

References

- Abe, H., Yamaguchi-Shinozaki, K., Urao, T., Iwasaki, T., Hosokawa, D. & Shinozaki, K.; 1997; "Role of Arabidopsis MYC and MYB homologs in drought-and Absciscic acid-regulated gene expression"; *The Plant Cell*; 9: 1859-1868.
- Abe, H., Urao, T., Ito, T., Seki, M., Shinozaki, K. & Yamaguchi-Shinozaki, K.; 2003; "Arabidopsis AtMYC2 (bHLH) and AtMYB2 (MYB) function as transcriptional activators in abscisic acid signaling"; *The Plant Cell*; 15: 63-78.
- Alvarado M., Zsigmond, L., Kovács, I., Koncz, C. & Szabados, L.; 2004; "Gene trapping with firefly luciferase in *Arabidopsis*. Tagging of stress-responsive genes"; *Plant Physiology*; 134: 18-27.
- Antosiewicz, D., Polisensky, D. & Braam, J.; 1995; "Cellular localization of the Ca²⁺ binding TCH3 protein of *Arabidopsis*"; *Plant Journal*; 8: 623-636.
- Arabidopsis* genome initiative; 2000; "Analysis of the genome sequence of the flowering plant *Arabidopsis thaliana*"; *Nature*; 408: 796-815.
- Baden, S & Latimer, J.; 1992; "An effective system for brushing vegetable transplants for height control"; *HortTechnology*; 2(3): 412-414.
- Baluška, F. & Hasenstein, K.; 1997; "Root cytoskeleton: its role in perception of and response to gravity"; *Planta*; 203: S69-S78.
- Baulcombe, D.; 2002; "RNA silencing"; *Current Biology*; 12(3): R82-R84.
- Bechtold, N., Ellis, J. & Pelletier, G.; 1993; "In planta *Agrobacterium*-mediated gene transfer by infiltration of adult *Arabidopsis thaliana* plants; *C R Academy of Sciences Paris Life Sciences*; 316: 1194-1199.
- Becnel, J., Natarajan, M., Kipp, A. & Braam, J.; 2006; "Developmental expression patterns of Arabidopsis XTH genes reported by transgenes and Genevestigator"; *Plant Molecular Biology*; 61: 451-467.
- Bent, A.; 2000; "*Arabidopsis in planta* transformation. Uses, mechanisms, and prospects for transformation of other species"; *Plant Physiology*; 124: 1540-1547.
- Beyl, C. & Mitchell, C.; 1977; "Characterization of mechanical stress dwarfing in *Chrysanthemum*"; *Journal of the American Society for Horticultural Science*; 102(5): 591-594.
- Beyl, C. & Mitchell, C.; 1983; "Alteration of growth, exudation rate, and endogenous hormone profiles in mechanically dwarfed sunflower"; *Journal of the American Society for Horticultural Science*; 108(2): 257-262.

- Biro, R & Jaffe, M.; 1984; "Thigmomorphogenesis: ethylene evolution and its role in the changes observed in mechanically perturbed bean plants"; *Physiologia Plantarum*; 62: 289-296.
- Blancaflor, E.; 2002; "The cytoskeleton and gravitropism in higher plants"; *Journal of Plant Growth Regulation*; 21: 120-136.
- Bohnert, H., Nelson, D. & Jensen, R.; 1995; "Adaptations to environmental stresses"; *The Plant Cell*; 7: 1099-1111.
- Bouchez, D. & Höfte, H.; 1998; "Functional genomics in plants"; *Plant Physiology*; 118: 725-732.
- Boyer, N.; 1967; "Modifications de la croissance d la tige de Bryone (*Bryonia dioica*) a la suite d' irritations tactiles"; *CR Academy of Sciences Paris*; 264: 2114-2117
- Boyer, N., Chapelle, B. & Gaspar, T.; 1979; "Lithium inhibition of the thigmomorphogenetic response in *Bryonia dioica*"; *Plant Physiology*; 63: 1215-1221.
- Boyes, D., Zayed, A., Ascenzi, R., McCaskill, A., Hoffmann, N., & Davis, K.; 2001; "Growth stage-based phenotypic analysis of *Arabidopsis*: A model for high throughput functional genomics in plants"; *The Plant Cell*; 13: 1499-1510.
- Braam, J. & Davis, R.W.; 1990; "Rain-induced, wind-induced, and touch-induced expression of calmodulin and calmodulin-related genes in *Arabidopsis*"; *Cell*; 60(3): 357-364.
- Braam, J.; 1992; "Regulated expression of the calmodulin-related TCH genes in cultured *Arabidopsis* cells: induction by calcium and heat shock"; *Proceedings of the National Academy of Sciences*; 89: 3213-3216.
- Braam, J., Sistrunk, M., Polisensky, D., Xu, W., Purugganan, M., Antosiewicz, D., Campbell, P. & Johnson, K.; 1996; "Life in a changing world: TCH gene regulation of expression and responses to environmental signals"; *Physiologia Plantarum*; 98: 909-916.
- Braam, J.; 1999; "If walls could talk"; *Current Opinion in Plant Biology*; 2: 521-524.
- Braam, J.; 2005; "In touch: plant responses to mechanical stimuli"; *New Phytologist*; 165: 373-389.
- Bradford, M.; 1976; "A rapid and sensitive method for the quantification of microgram quantities of protein utilizing the principle of protein-dye binding"; *Analytical Biochemistry*; 72: 248-254.
- Brown, K.; 2004; "*The Arabidopsis extensin gene atEXT1: studies on protein function and gene regulation*"; PhD thesis, University of Wales Bangor.

- Campbell, P. & Braam, J.; 1999; "Xyloglucan endotransglycosylases: diversity of genes, enzymes and potential wall-modifying functions"; *Trends in Plant Science*; 4(9): 361-366.
- Cassab, G.; 1998; "Plant cell wall proteins"; *Annual Review of Plant Physiology*; 49: 281-309.
- Chrispeels, M.; 1969; "Synthesis and secretion of hydroxyproline containing macromolecules in carrots"; *Plant Physiology*; 44: 1187-1193
- Cipollini, D.F.; 1997; "Wind-induced mechanical stimulation increases pest resistance in common bean"; *Oecologia*; 111: 84-90.
- Cipollini, D.F.; 1998; "The induction of soluble peroxidase activity in bean leaves by wind-induced mechanical perturbation"; *American Journal of Botany*; 85(11): 1586-1591.
- Cipollini, D.F.; 1999; "Costs to flowering of the production of a mechanically hardened phenotype in *Brassica napus* L."; *International Journal of Plant Science*; 160(4): 735-741.
- Cleland, R. & Karlins, A.; 1967; "A Possible Role of Hydroxyproline-Containing Proteins in the Cessation of Cell Elongation"; *Plant Physiology*; 42: 669-671.
- Cleugh, H.; Miller, J. & Böhm, M.; 1998; "Direct mechanical effects of wind on crops"; *Agroforestry systems*; 41: 85-112.
- Clough, S. & Bent, A.; 1998; "Floral dip: a simplified method for *Agrobacterium*-mediated transformation of *Arabidopsis thaliana*"; *The Plant Journal*; 16(6): 735-743.
- Cosgrove, D.; 1997; "Relaxation in a high-stress environment: The molecular bases of extensible cell walls and cell enlargement"; *The Plant Cell*; 9: 1031-1041.
- Darley, C, Forrester, A & McQueen-Mason, S; 2001; "The molecular basis of plant cell wall extension"; *Plant Molecular Biology*; 47: 179-195.
- Darwin, C.; 1893; *Insectivorous plants*; John Murray, London.
- De Jaegher, G., Boyer, N. & Gaspar, T.; 1985; "Thigmomorphogenesis in *Bryonia dioica*: changes in soluble and wall peroxidases, phenylalanine ammonia-lyase activity, cellulose, lignin content and monomeric constituents"; *Plant Growth Regulation*; 3: 133-148.
- Dean, G., Casson, S. & Lindsey, K.; 2004; "KNAT6 gene of *Arabidopsis* is expressed in roots and is required for correct lateral root formation"; *Plant Molecular Biology*; 54: 71-84.
- Desfeux, C., Clough, S. & Bent, A.; 2000; "Female reproductive tissues are the primary target of *Agrobacterium*-mediated transformation by the *Arabidopsis* floral-dip method"; *Plant Physiology*; 123: 895-904.

Doblin, M., Kurek, I., Jacob-Wilk, D. & Delmer, D.; 2002; "Cellulose Biosynthesis in Plants: from Genes to Rosettes"; *Plant and Cell Physiology*; 43 (12): 1407-1420.

Doyle, J. & Doyle, J.; 1987; "A rapid DNA isolation procedure for small quantities of fresh leaf tissue"; *Phytochemical Bulletin*; 19(1): 11-15.

Elliott, K. & Shirsat, A.H.; 1998; "Promoter regions of the extA extensin gene from *Brassica napus* control activation in response to wounding and tensile stress"; *Plant Molecular Biology*; 37: 675-687.

Ennos, A.R.; 1997; "Wind as an ecological factor"; *Tree*; 12(3): 108-111.

Erner, Y., Biro, R. & Jaffe, M.; 1980; "Thigmomorphogenesis: evidence for a translocatable thigmomorphogenetic factor induced by mechanical perturbation of beans (*Phaseolus vulgaris*); *Physiologia Plantarum*; 50: 21-25.

Erner, Y. & Jaffe, M.; 1982; "Thigmomorphogenesis: the involvement of auxin & abscisic acid in growth retardation due to mechanical perturbation"; *Plant & Cell Physiology*; 23(6): 935-941.

Eulgem, T., Rushton, P., Robatzek, S. & Somssich, I.; 2000; "The WRKY superfamily of plant transcription factors"; *Trends in Plant Sciences*; 5(5): 199-206.

Evans, I., Gatehouse, L., Gatehouse, J., Yarwood, J., Boulter, D. & Croy, R.; 1990; "The extensin gene family in oilseed rape (*Brassica napus* L): characterization of sequences of representative members of the family"; *Molecular & General Genetics*; 223: 273-287.

Feinberg, A. & Vogelstein, B.; 1983; "A technique for radiolabeling DNA restriction endonuclease fragments to high specific activity"; *Analytical Biochemistry*; 132(1): 6-13.

Feldmann, K.; 1991; "T-DNA insertion mutagenesis in *Arabidopsis*: mutational spectrum"; *Plant Journal*; 1: 71-82.

Fasano, J., Massa, G. & Gilroy, S.; 2002; "Ionic signaling in plant responses to gravity and touch"; *Journal of Plant Growth Regulation*; 21: 71-88.

Foster, D. & Boose, E.; 1992; "Patterns of forest damage resulting from catastrophic wind in central New England, USA"; *Journal of Ecology*; 80: 79-98.

Fry, S.; 1986; "Cross-linking of matrix polymers in the growing cell walls of angiosperms"; *Annual Review of Plant Physiology*; 37: 165-186.

Fry, S., Smith, R., Renwick, K., Martin, D., Hodge, S. & Matthews, K.; 1992; "Xyloglucan endotransglycosylase, a new wall-loosening enzyme activity from plants"; *Biochemistry Journal*; 282: 821-828.

- Fukusaki, E., Kawasaki, K., Kajiyama, S., An, C., Suzuki, K., Tanaka, Y. & Kobayashi, A.; 2004; "Flower colour modulations of *Torenia hybrida* by downregulation of chalcone synthase genes with RNA interference"; *Journal of Biotechnology*; 111: 229-240.
- Giridhar, G. & Jaffe, M.; 1988; "Thigmomorphogenesis: XXIII . Promotion of foliar senescence by mechanical perturbation of *Avena sativa* and four other species"; *Physiologia Plantarum*; 74: 473-480.
- Goodman, A. & Ennos, A.R.; 2001; "The effects of mechanical stimulation on the morphology and mechanics of maize roots grown in an aerated nutrient solution"; *International Journal of Plant Science*; 162(4): 691-696.
- Goujon, T., Sibout, R., Eudes, A., Mackay, J. & Jouanin, L.; 2003; "Genes involved in the biosynthesis of lignin precursors in *Arabidopsis thaliana*"; *Plant Physiology & Biochemistry*; 41: 677-687.
- Guo, W. & Shirsat, A.; 2006; "Extensin over-expression in *Arabidopsis* limits pathogen invasiveness"; *Molecular Plant Pathology*; 7 (6): 579-592.
- Haley, A., Russell, A., Wood, N., Allan, A., Knight, M., Campbell, A. & Trewavas, A.; 1995; "Effects of mechanical signalling on plant cell cytosolic calcium"; *Proceedings of the National Academy of Sciences*; 92: 4124-4128.
- Hammerschmidt, R., Nuckles, E. & Kuć, J.; 1982; "Association of enhanced peroxidase activity with induced systemic resistance of cucumber to *Colletotrichum lagenarium*"; *Physiological Plant Pathology*; 20: 73-82.
- Helliwell, C. & Waterhouse, P.; 2003; "Constructs and methods for high-throughput gene silencing in plants"; *Methods*; 30: 289-295.
- Heuchert, J. & Mitchell, C.; 1983; "Inhibition of shoot growth in greenhouse-grown tomato by periodic gyratory shaking"; *Journal of the American Society for Horticultural Science*; 108(5): 795-800.
- Higo, K., Ugawa, Y., Iwamoto, M. & Korenaga, T.; 1999; "Plant cis-acting regulatory DNA elements (PLACE) database: 1999"; *Nucleic acids Research*; 27(1): 297-300.
- Hiwasa, K., Rose, J., Nakano, R., Inaba, A. & Kubo, Y.; 2003; "Differential expression of seven α -expansin genes during growth and ripening of pear fruit"; *Physiologia Plantarum*; 117: 564-572.
- Ichimura, K., Mizoguchi, T., Yoshida, R., Yuasa, T. & Shinozaki, K.; 2000; "Various abiotic stresses rapidly activate *Arabidopsis* MAP kinases ATMPK4 and ATMPK6"; *The Plant Journal*; 24(5): 655-665.
- Iliev, E., Xu, W., Polisensky, D., Oh, M., Torisky, R., Clouse, S & Braam, J; 2002; "Transcriptional and post-transcriptional regulation of *Arabidopsis* TCH4. Expression by diverse stimuli. Roles of cis regions and brassinosteroids"; *Plant Physiology*; 130: 770-783.

Jaffe, M. & Biro, R.; 1979; "Thigmomorphogenesis: The effect of mechanical perturbation on the growth of plants, with special reference to anatomical changes, the role of ethylene, and interaction with other environmental stresses"; IN: Mussell, H. & Staples, R.; *Stress Physiology in crop plants*; Wiley, New York.

Jaffe, M., Leopold, A. & Staples, R.; 2002; "Thigmo responses in plants and fungi"; *American Journal of Botany*; 89(3): 375-382.

Jamet, E., Guzzardi, P. & Salva, I.; 2000; "What do transgenic plants tell us about the regulation and function of cell-wall structural proteins like extensins?"; *Russian Journal of Plant Physiology*; 47(3): 318-326.

Johnson, K., Sistrunk, M., Polisensky, D. & Braam, J.; 1998; "*Arabidopsis thaliana* responses to mechanical stimulation do not require ETR1 or EIN2"; *Plant Physiology*; 116: 643-649.

Jones, R., Coe, L., Montgomery, L. & Mitchell, C.; 1990; "Seismic stress responses of soybean to different photosynthetic photon flux"; *Annals of Botany*; 66: 617-622.

Jones, R. & Mitchell, C.; 1992; "Effects of physical agitation on yield of greenhouse-grown soybean"; *Crop Science*; 32: 404-408.

Jones, R.; 1997; "Mechanisms of environmental stress resistance in plants"; IN: Basra, A & Basra, R (Ed); Harwood Academic Publishers, USA.

Keller, E. & Steffen, K.; 1995; "Increased chilling tolerance & altered carbon metabolism in tomato leaves following application of mechanical stress"; *Physiologia Plantarum*; 93: 519-525.

Knight, M., Campbell, A., Smith, S. & Trewavas, A.; 1991; "Transgenic plant aequorin reports the effects of touch and cold-shock and elicitors on cytoplasmic calcium"; *Nature*; 352: 524-526.

Knight, M., Smith, S. & Trewavas, A.; 1992; "Wind-induced plant motion immediately increases cytosolic calcium"; *Proceedings of the National Academy of Sciences*; 89: 4976-4971.

Ko, Jae-Heung., Kyung-Hwan, H., Park, S. & Yang, J.; 2004; "Plant body weight-induced secondary growth in *Arabidopsis* and its transcription phenotype revealed by whole-transcriptome profiling"; *Plant Physiology*; 135: 1069-1083.

Kraus, E., Kolloffel, C. & Lambers, H.; 1994; "The effect of handling on photosynthesis, transpiration, respiration, and nitrogen and carbohydrate content of populations of *Lolium perenne*"; *Physiologia Plantarum*; 91: 631-638.

Lancashire, P.D., Bleiholder, H., Van der Boom, T., Langeluddeke, P., Stauss, R., Weber, E., and Witzemberger, A.; 1991; "A uniform decimal code for growth stages of crops and weeds"; *Annals of Applied Biology*; 119: 561-601.

Lauvergeat, V., Lacomme, C., Lacombe, E., Lasserre, E., Roby, D. & Grima-Pettenati, J.; 2001; "Two cinnamoyl-CoA reductase (CCR) genes from *Arabidopsis thaliana* are differentially expressed during development and in response to infection with pathogenic bacteria"; *Phytochemistry*; 57: 1187-1195.

Lawton, R.; 1982; "Wind stress and elfin stature in a montane rain forest tree: an adaptive explanation"; *American Journal of Botany*; 69(8): 1224-1230.

Lee, D., Polisensky, D. & Braam, J.; 2005; "Genome wide identification of touch and darkness-regulated *Arabidopsis* genes: a focus on calmodulin-like and XTH genes"; *New Phytologist*; 165: 429-444.

Lescot, M., Déhais, P., Thijs, G., Marchal, K., Moreau, Y., Van de Peer, Y., Rouzé & Rombauts, S.; 2002; "PlantCARE, a database of plant *cis*-acting regulatory elements and a portal to tools for *in silico* analysis of promoter sequences"; *Nucleic Acids Research*; 30 (1): 325-327.

Lev-Yadun, S.; 1994; "Induction of sclereid differentiation in the pith of *Arabidopsis thaliana* (L.) Heynh"; *Journal of Experimental Botany*; 45(281): 1845-1849.

Lev-Yadun, S.; 2002; "The distance to which wound effects influence the structure of secondary xylem of decapitated *Pinus pinea*"; *Journal of Plant Growth Regulation*; 21: 191-196.

Li, R. & Wang, H.; 2004; "*Arabidopsis* FH3/FAR1 gene family and distinct roles of its members in light control of *Arabidopsis* development"; *Plant Physiology*; 136: 4010-4022.

Li, Y., Jones, L. & McQuenn-Mason, S.; 2003; "Expansins and cell growth"; *Current Opinion in Plant Biology*; 6: 603-610.

Logemann, E., Birkenbihl, R., Ülker, B. & Somssich, I.; 2006; "An improved method for preparing *Agrobacterium* cells that simplifies the *Arabidopsis* transformation protocol"; *Plant Methods*; 2: 16-20.

Logemann, J., Schell, J. & Willmitzer, L.; 1987; "Improved method for the isolation of RNA from plant tissues"; *Analytical Biochemistry*; 163: 16-20.

Lu, C. & Huang, Y.; 2005; "A memory-efficient algorithm for multiple sequence alignment with constraints"; *Bioinformatics*; 21(1): 20-30.

Ma, L., Sun, N., Liu, X., Jiao, Y., Zhao, H. & Deng, X.; 2005; "Organ-specific expression of *Arabidopsis* genome during development"; *Plant Physiology*; 138: 80-91.

Maleck, K., Levine, A., Eulgem, T., Morgan, A., Schmid, J., Lawton, K., Dangel, J. & Dietrich, R.; 2000; "The transcriptome of *Arabidopsis thaliana* during systemic acquired resistance"; *Nature Genetics*; 26: 403-410.

- Matthew, L.; 2004; "RNAi for plant functional genomics"; *Comparative and Functional Genomics*; 5: 240-244.
- MBI Fermentas; 2003; "MBI Fermentas Catalogue"; MBI Fermentas, UK.
- McNellis, T. & Deng, X.; 1995; "Light control of seedling morphogenetic pattern"; *The Plant Cell*; 7: 1749-1761.
- Memelink, J., Swords, K., de Kam, R., Schilperoort, R., Hoge, J. & Staehelin, L.; 1993; "Structure and regulation of Tobacco extensin"; *Plant Journal*; 4: 1011-1022.
- Merkouropoulos, G., Barnett, D. & Shirsat, A.H.; 1999; "The *Arabidopsis* extensin gene is developmentally regulated, is induced by wounding, Methyl Jasmonate, Absciscic and Salicylic acid, and codes for a protein with unusual motifs"; *Planta*; 208: 212-219.
- Merkouropoulos, G.; 2000; "*Regulation and analysis of atExt1, an extensin gene from Arabidopsis*"; Ph.D. thesis, University of Wales, Bangor, UK.
- Merkouropoulos, G. & Shirsat, A.H.; 2003; "The unusual *Arabidopsis* extensin gene atEXT1 is expressed throughout plant development and is induced by a variety of biotic and abiotic stresses"; *Planta*; 217: 356-366.
- Mitchell, C., Severson, C., Wott, J. & Hammer, P.; 1975; "Seismomorphogenic regulation of plant growth"; *Journal of the American Society for Horticultural Science*; 100 (2): 161-165.
- Mitchell, C.; 1977; "Influence of mechanical stress on auxin-stimulated growth of excised pea stem sections"; *Physiologia Plantarum*; 41: 129-134.
- Mitchell, C. & Myers, P.; 1995; "Mechanical stress regulation of plant growth and development"; *Horticultural Reviews*; 17: 1-41.
- Mitchell, C.; 1996; "Recent advances in plant response to mechanical stress: Theory and application"; *Hortscience*; 31(1).
- Mittler, R.; 2002; "Oxidative stress, antioxidants and stress tolerance"; *Trends in Plant Science*; 7(9): 405-410.
- Mizoguchi, T, Irie, K, Hirayama, T, Hayashidan, N, Yamaguchi-Shinozaki, K, Matsumoto, K & Shinozaki, K; 1996; "A gene encoding a mitogen-activated protein kinase kinase is induced simultaneously with genes for a mitogen-activated protein kinase and an S6 ribosomal protein kinase by touch, cold and water stress in *Arabidopsis thaliana*"; *Proceedings of the National Academy of Sciences USA*; 93: 765-769.
- Montgomery, J., Bressan, R. & Mitchell, C.; 2004; "Optimizing environmental conditions for mass application of mechano-dwarfing stimuli to *Arabidopsis*"; *Journal of the American Society for Horticultural Science*; 129(3): 339-343.

- Moran, P.J. & Cipollini, D.F.; 1999; "Effect of wind-induced mechanical stress on soluble peroxidase activity and resistance to pests in cucumber"; *Journal of Phytopathology* ; 147: 313-316.
- Morgan, P. & Drew, M.; 1997; "Ethylene & plant responses to stress"; *Physiologia Plantarum*; 100: 620-630.
- Murashige, T. & Skoog, F.; 1962; "A revised medium for rapid growth and bio assays with tobacco tissue cultures"; *Physiologia Plantarum*; 15 (3): 473-497.
- Myers, P., Ackerman, J. & Mitchell, C.; 1993; "Growth and turgor responses of dark-grown soybean seedlings to mechanical perturbation"; *Plant Physiology* (supplement): 102: 156.
- Norrgrén, S.; 2006; "*The role of reactive oxygen species (ROS) in cell wall modification*"; Undergraduate thesis, University of Wales, Bangor.
- Oh, S., Park, S. & Kyung-Hwan, H.; 2003; "Transcriptional regulation of secondary growth in *Arabidopsis thaliana*"; *Journal of Experimental Botany*; 54(393): 2709-2722.
- Oliveira, D., Franco, L., Simoens, C., Seurinck, J., Coppieters, J., Botterman, J. & Van Montagu, M.; 1993; "Inflorescence-specific genes from *Arabidopsis thaliana* encoding glycine-rich proteins"; *Plant Journal*; 3(4):495-507
- Olson, P. & Varner, J.; 1993; "Hydrogen peroxide and lignification"; *The Plant Journal*; 4(5): 887-892.
- Pedreira, J., Sanz, N., Peña, M., Sánchez, M., Queijeiro, E., Revilla, G. & zarra, I.; 2004; "Role of apoplastic ascorbate and hydrogen peroxide in the control of cell growth in pine hypocotyls"; *Plant Cell Physiology*; 45(5): 530-534.
- Pickard, P. & Ding, J.; 1993; "The Mechanosensory Calcium-selective Ion Channel: Key Component of a Plasmalemmal Control Centre?"; *Australian Journal of Plant Physiology*; 20: 439-459.
- Pietrzak, M., Shillito, R., Hohn, T. & Potrykus, I.; 1986; "Expression in plants of two bacterial antibiotic resistance genes after protoplast transformation with a new plant expression vector"; *Nucleic acids Research*; 14(14): 5857-5868.
- Pigliucci, M.; 2002; "Touchy and bushy: Phenotypic plasticity and integration in response to wind stimulation in *Arabidopsis thaliana*"; *International Journal of Plant Science*; 163(3): 399-408.
- Plomion, C., Pionneau, C., Brach, J., Costa, P. & Baillères, H.; 2000; "Compression wood-responsive proteins in developing xylem of maritime pine (*Pinus pinaster* Ait); *Plant Physiology*; 123: 959-969.

- Pritchard, J., Hetherington, P.R., Fry, S. & Tomos, A.D.; 1993; "Xyloglucan endotransglycosylase activity, microfibril orientation and the profiles of cell wall properties along growing regions of maize roots"; *Journal of Experimental Botany*; 44(265): 1281-1289.
- Pruyn, M., Ewers, B. & Telewski, F.; 2000; "Thigmomorphogenesis: changes in the morphology and mechanical properties of two populus hybrids in response to mechanical perturbation"; *Tree Physiology*; 20: 535-540.
- Rentel, M. & Knight, M.; 2004; "Oxidative stress-induced calcium signaling in *Arabidopsis*"; *Plant Physiology*; 135: 1471-1479.
- Retuerto, R. & Woodward, F.I.; 1992; "Effects of wind speed on the growth and biomass allocation of white mustard *Sinapis alba* L."; *Oecologia*; 92(1): 113-123.
- Retuerto, R. & Woodward, F.I.; 2001; "Compensatory responses in growth and fecundity traits of *Sinapis alba* L. following release from wind and density stress"; *International Journal of Plant Science*; 162 (1): 171-179.
- Ridge, I. (Editor); 2002; *Plants*; Oxford University Press, Oxford, UK.
- Ringli, C., Keller, B. & Ryser, U.; 2001; "Glycine-rich proteins as structural components of plant cell walls"; *Cellular & Molecular Life Sciences*; 58: 1430-1441.
- Rozen, S. & Skalecky, H.; 2000; "Primer3 on the WWW for general users and for biologist programmers"; *Methods in Molecular Biology*; 132: 365-386.
- Sack, F.; 1997; "Plastids and gravitropic sensing"; *Planta*; 203: S63-S68.
- Sætrom, P. & Snøve, O.; 2004; "A comparison of siRNA efficacy predictors"; *Biochemical and Biophysical Research Communications*; 321: 247-253.
- Sambrook, J., Fritsch, E. & Maniatis, T.; 1989; *Molecular Cloning: A laboratory manual* (second edition); Cold Spring Harbor Laboratory Press, New York.
- Sánchez, M., Queeijeiro, E., Revilla, G. & Zarra, I.; 1997; "Changes in ascorbic acid levels in apoplastic fluid during growth of pine hypocotyls. Effect on peroxidase activities associated with cell walls"; *Physiologia Plantarum*; 101: 815-820.
- Schindler, U., Beckmann, H. & Cashmore, A.; 1992; "TGA1 and G-box binding factors: two distinct classes of *Arabidopsis* leucine zipper proteins compete for the G-box-like element TGACGTGG"; *Plant Cell*; 4: 1309-1319.
- Schultz, C., Johnson, K., Currie, G. & Bacic, A.; 2000; "The classical arabinogalactan protein gene family of *Arabidopsis*"; *The Plant Cell*; 12: 1751-1767.
- Shepherd, V., Beilby, M. & Shimmen, T.; 2002; "Mechanosensory ion channels in charophyte cells: the response to touch and salinity stress"; *European Biophysical Journal*; 31: 341-355.

- Shirsat, A.H., Bell, A., Spence, J. & Harris, J.; 1996; "The *Brassica napus extA* extensin gene is expressed in regions of the plant subject to tensile stresses"; *Planta*; 199: 618-624.
- Shirsat, A.H., Thomson, H. & Elliott, K.A.; 2003; "The *Brassica napus extA* extensin gene negative regulatory region controls expression in response to mechanical stress"; *Plant, Cell and Environment*; 26: 1647-1655.
- Showalter, A.M.; 2001; "Arabinogalactan-proteins: structure, expression and function"; *Cellular & Molecular Life Sciences*; 58: 1399-1417.
- Sistrunk, M., Antosiewicz, D., Purugganan, M. & Braam, J.; 1994; "*Arabidopsis* TCH3 encodes a novel Ca^{2+} binding protein and shows environmentally induced and tissue-specific regulation"; *The Plant Cell*; 6: 1553-1565.
- Snedden, W. & Fromm, H.; 2001; "Calmodulin as a versatile calcium signal transducer in plants"; *New Phytologist*; 151: 35-66.
- Takahashi, H., Suge, H. & Kato, T.; 1991; "Growth promotion by vibration at 50Hz in rice and cucumber seedlings"; *Plant Cell Physiology*; 32(5): 729-732.
- Thijs, G., Lescot, M., Marchal, K., Rombauts, S., De Moor, B., Rouzé, P. & Moreau, Y.; 2001; "A higher-order background model improves the detection of promoter regulatory elements by Gibbs sampling"; *Bioinformatics*; 17: 1113-1122.
- Thijs, G., Marchal, K., Lescot, M., Rombauts, S., De Moor, B., Rouzé, P. & Moreau, Y.; 2002; "A Gibbs sampling method to detect overrepresented motifs in the upstream regions of co-expressed genes"; *Journal of Computational Biology*; 9(2): 447-464.
- Thordal-Christensen, H., Zhang, Z., Wei, Z. & Collinge, D.; 1997; "Subcellular localization of H_2O_2 in plants. H_2O_2 accumulation in papillae and hypersensitive response during the barley-powdery mildew interaction"; *The Plant Journal*; 11(6): 1187-1194.
- Timell, T.E.; 1986; "*Compression wood in gymnosperms*"; Springer-Verlag, Berlin.
- Travella, S., Klimm, T. & Keller, B.; 2006; "RNA interference-based gene silencing as an efficient tool for functional genomics in hexaploid bread wheat"; *Plant Physiology*; 142: 6-20.
- Trewavas, A. & Knight, M.; 1994; "Mechanical signaling, calcium & plant form"; *Plant Molecular Biology*; 26: 1329-1341.
- Uchida, A. & Yamamoto, K.; 2002; "Effects of mechanical vibration on seed germination of *Arabidopsis thaliana*"; *Plant Cell Physiology*; 43(6): 947-951.
- Ui-Tei, K., Naito, Y., Takahashi, F., Haraguchi, T., Ohki-Hamazaki, H., Juni, A., Ueda, R. & Saigo, K.; 2004; "Guidelines for the selection of highly effective siRNA sequences for mammalian and chick RNA interference"; *Nucleic Acids Research*; 32(3): 936-948.

- Van Der Luit, A., Olivari, C., Haley, A., Knight, M. & Trewavas, A.; 1999; "Distinct calcium signalling pathways regulate calmodulin gene expression in tobacco"; *Plant Physiology*; 121: 705-714.
- Wang, T., Iyer, L., Pancholy, R., Shi, X. & Hall, T.; 2005; "Assessment of penetrance and expressivity of RNAi-mediated silencing of the *Arabidopsis* phytoene desaturase gene"; *New Phytologist*; 165: R1-R10.
- Wayne, R. & Staves, M.; 1996; "A down to earth model of gravisensing or Newton's Law of Gravitation from the apple's perspective"; *Physiologia Plantarum* 98: 917–921
- Wesley, S., Helliwell, C., Smith, N., Wang, M., Rouse, D., Liu, Q., Gooding, P., Singh, S., Abbott, D., Stoutjesdijk, P., Robinson, S., Gleave, A., Green, A. & Waterhouse, P.; 2001; "Construct design for efficient, effective and high-throughput gene silencing in plants"; *The Plant Journal*; 27(6): 581-590.
- Wienecke, K., Glas, R. & Robinson, D.; 1982; "Organelles involved in the synthesis and transport of hydroxyproline-containing glycoproteins in carrot root discs"; *Planta*; 155(1): 58-63.
- Wilson, L. & Fry, J.; 1986; "Extensin – a major cell wall glycoprotein"; *Plant, Cell and Environment*; 9: 239-260.
- Wright, A., Knight, H. & Knight, M.; 2002; "Mechanically stimulated TCH3 gene expression in *Arabidopsis* involves protein phosphorylation and EIN6 downstream of calcium"; *Plant Physiology*; 128: 1402-1409.
- Wu, L., Joshi, C. & Chiang, V.; 2000; "A xylem-specific cellulose synthase gene from aspen (*Populus tremuloides*) is responsive to mechanical stress"; *The Plant Journal*; 22(6): 495-502.
- Xu, W., Campbell, P., Vargheese, A. & Braam, J.; 1995; "The *Arabidopsis* XET-related gene family: environmental and hormonal regulation of expression"; *The Plant Journal*; 9(6): 879-889.
- Xu, P., Zhang, Y., Kang, L., Roossinck, M. & Mysore, K.; 2006; "Computational estimation and experimental verification of off-target silencing during posttranscriptional gene silencing in plants"; *Plant Physiology*; 142: 428-440.
- Yahraus, T., Chandra, S., Legendre, L. & Low, P.; 1995; "Evidence for a mechanically induced oxidative burst"; *Plant Physiology*; 109: 1259-1266.
- Yamaguchi-Shinozaki, K. & Shinozaki, K.; 1993; "The plant hormone abscisic acid mediates the drought-induced expression but not the seed-specific expression of rd22, a gene responsive to dehydration stress in *Arabidopsis thaliana*"; *Molecular & General Genetics*; 238: 17-25.

Zimmerman, J.K; 1994; "Responses of tree species to hurricane winds in subtropical wet forest in Puerto Rico: implications for tropical tree life histories"; *Journal of Ecology*; 82: 911-922.

Electronic References

LION Bioscience AG; <http://www.ba.itb.cnr.it>

MotifSampler; <http://www.esat.kuleuven.ac.be/~thijs/Work/Motifsampler.html>

MusicME; <http://genome.life.nctu.edu.tw/MUSICME/>

Nottingham Arabidopsis Stock Centre (NASC); <http://arabidopsis.info/>

National Centre for Biological Information (NCBI); <http://www.ncbi.nlm.nih.gov>

PLACE; <http://www.dna.affrc.go.jp/PLACE/>

PlantCARE; <http://bioinformatics.psb.ugent.be/webtools/plantcare/html/>

Primer 3; <http://frodo.wi.mit.edu/>

siRNA Scan; <http://bioinfo2.noble.org/RNAiScan.htm>